UNIVERSIDAD DE GRANADA
UNIVERSITÉ HASSAN PREMIER

Programa de doctorado en FÍSICA Y MATEMÁTICAS

APPROXIMATION BY SPLINE FUNCTIONS ON POWELL-SABIN TRIANGULATIONS

Tesis doctoral en cotutela elaborada por

SALAH EDDARGANI

Bajo la dirección de

Dr. D. DOMINGO BARRERA ROSILLO
Dr. D. ABDELLAH LAMNII

Curso académico 2020-2021

Editor: Universidad de Granada. Tesis Doctorales
Autor: Salah Eddargani
ISBN: 978-84-1117-187-8
URI: http://hdl.handle.net/10481/72080

Abstract

Smooth splines on triangulations are the subject of many applications in various fields, among them approximation theory, computer-aided geometric design, entertainment industry, etc. Smooth spline spaces with a lower degree are the classical choice, which is extremely difficult to achieve in arbitrary triangulations. An alternative is to use macro elements of lower degree that split each triangle into a number of macro-triangles. In particular, Powell-Sabin (PS-) split which divides each triangle into six macro-triangles.

In this thesis, we deal with the approximation by quartic PS-splines. Namely, we start by solving a Hermite interpolation problem in the space of C^1 quartic PS-splines and providing several local quasi-interpolation schemes reproducing quartic polynomials and not requiring the resolution of any linear system. The provided schemes are constructed with the help of Marsden's identity. Then, we address the geometric characterization of Powell-Sabin triangulations allowing the construction of bivariate quartic splines of class C^2.

Quasi-interpolation in a space of sextic PS-splines has also been considered. These spline functions are C^2 continuous on the whole domain but fourth-order regularity is required at vertices and C^3 smoothness conditions are imposed across the edges of the refined triangulation and also at the interior point chosen to define the refinement. An algorithm is proposed to define the Powell-Sabin triangles with small area and diameter needed to construct a normalized basis. Quasi-interpolation operators which reproduce sextic polynomials are constructed after deriving Marsden's identity from a more explicit version of the control polynomials introduced some years ago in the literature.

Examining the applicability of PS-splines the numerical quadratures, we have proved that any Gaussian quadrature formula exact on the space of quadratic polynomials defined on a triangle T endowed with a specific PS-refinement integrates also the functions in the space of C^1 quadratic PS-splines defined on T. This extends the existing results in the literature, where the inner split point Z chosen to define the split had to lie on a very specific subset of the T. Now Z can be freely chosen inside T.

Sometimes, when dealing with Digital Elevation Models in engineering, the construction of normalized basis functions could be extremely expensive regarding time and memory needed, which is caused by the treatment of big data. To avoid this problem, we provide quasi-interpolation schemes defined on a uniform triangulation of type-1 endowed with a PS-split. The spline schemes are generated by setting their Bézier ordinates to suitable combinations of the given data values.

Inspiring from bivariate PS-splines theory, we define a family of univariate many knot spline spaces of arbitrary degree defined on an initial partition that is refined by adding a point in each sub-interval. For an arbitrary smoothness r, splines of degrees $2r$ and $2r+1$ are considered by imposing additional regularity when necessary. For an arbitrary degree, a B-spline-like basis is constructed by using the Bernstein-Bézier representation. Blossoming is then used to establish a Marsden's identity from which several quasi-interpolation operators having optimal approximation orders are defined.

Finally, we address the approximation by C^2 cubic splines via two approaches. In the first one, we discuss the construction of C^2 cubic spline quasi-interpolation schemes defined on a refined partition. These schemes are reduced in terms of the degree of freedom compared to those existing in the literature. Namely, we provide a recipe for reducing the degree of freedom by imposing super-smoothing conditions while preserving full smoothness and cubic precision. In addition, we provide subdivision rules by means of blossoming. The derived rules are designed to express the B-spline coefficients associated with a finer partition from those associated with the former one. While in the second approach, we construct a novel normalized B-spline-like representation for C^2 continuous cubic spline space defined on an initial partition refined by inserting two new points inside each sub-interval. Thus, we derive several families of super-

convergent quasi-interpolation operators.

Keywords: Powell-Sabin split, Bernstein-Bézier form, Quasi-interpolation schemes, Hermite interpolation, Marsden's identity, many knot spline spaces, Normalized representation.

Preface

This thesis is the results of my Ph.D. studies carried out at both University Hassan First of Settat and University of Granada in numerical analysis and applied mathematics. Which has been made from January 2018 until September 2021. I gratefully acknowledge the financial support from the University of Granada for the research stay during which parts of this work were carried out. Also, I gratefully acknowledge the scholarship from CNRST (i.e., Centre National pour la Recherche Scientifique et Technique) through the Excellence Scholarship Programme.

First of all, I would like to express my sincere gratitude to my supervisors, Prof. Abdellah Lamnii and Prof. Domingo Barrera Rosillo for their support, encouragement and valuable advice. They have initiated me in spline approximation theory, and they have carefully guided me through the academic world. I am very grateful for the valuable time spent in sharing their expertise and knowledge with me. Finally, I would also like to say how much I appreciate their great availability and their professional and personal qualities.

Also, I would like to thank Professors María José Ibáñez and Mohamed Lamnii for their kindness and for their valuable time and collaboration.

During my thesis I had the pleasure to carry out a research internship at the Institute of Applied Mathematics of Bilbao under the supervision of Prof. Michael Bartoň. I would like to thank him very much for having offered me this opportunity.

Last but not least, I would like to thank my parents and my brothers for their support and encouragements.

Contents

Symbols

Ω	bounded polygonal domain
$\partial\Omega$	boundary of Ω
Δ	triangulation
Δ_{PS}	Powell-Sabin split of Δ
$\|\Delta\|$	mesh size of Δ
$\|T\|$	area of the triangle T
Δ_θ	smallest angle of Δ
$\mathcal{V}$	set of vertices in Δ
$\mathcal{Z}$	set of triangle split points in Δ
$\mathcal{E}$	set of edges in Δ
$\mathcal{E}^*$	set of edges that connect a triangle split point to an edge split point
nv	number of vertices in Δ
nt	number of triangles in Δ
ne	number of edges in Δ
X_n	partition of a bounded interval $[a, b]$ into n sub-intervals
X_n^{ref}	refinement of X_n
$\mathbb{P}_d$	space of polynomials of degree d
S_d^r	space of C^r smooth splines of degree d
$\mathfrak{B}_{\beta,T}^d$	Bernstein polynomial of degree d
b_β	BB-coefficients
b_β^r	De Casteljau ordinates
$\mathbf{B}[p]$	polar form of p
D_u^r	r-th order directional derivative with respect to direction u
$PS-splines$	Powell-Sabin (PS-) splines
$\partial_{a,b}f\,(P)$	The partial derivative $\dfrac{\partial^{a+b}f}{\partial x^a \partial y^b}\,(P)$ of $f\,(x, y)$ at the point P

Resumen: Aproximación mediante funciones spline sobre triangulaciones de tipo Powell-Sabin.

Las funciones spline bivariadas definidas sobre una triangulación han sido consideradas como objetos fundamentales en una gran cantidad de ámbitos, entre los que se encuentran la Teoría de Aproximación, el Diseño Geométrico Asistido por Ordenador y la resolución de problemas relativos a ecuaciones en derivadas parciales.

La utilización de este tipo de funciones exige el cálculo de la dimensión del espacio de funciones spline, lo que es extremadamente difícil, pues depende de la interacción entre Geometría, Combinatoria y Topología.

El estudio de los espacios de funciones spline continuas es simple, pero dar un paso hacia una regularidad de orden más elevado conduce a problemas de difícil solución, que en muchos casos siguen abiertos. Para los espacios polinómicos a trozos de grados suficientemente elevados en relación con la regularidad exigida, la determinación de las correspondientes dimensiones ha sido llevada a cabo por P. Alfeld y L. L. Schumaker en [9, 10]. Sin embargo, el problema general está lejos de ser definitivamente resuelto.

Teniendo en cuenta la utilización de estos espacios en la resolución numérica de diversos problemas de interés práctico, es natural elegir el grado más bajo que permita conseguir funciones spline con la regularidad necesaria. Con este objetivo, la triangulación sobre la cual se define el espacio de funciones spline es refinada, es decir, cada triángulo de la partición es descompuesto en micro-triángulos. Las estructuras refinadas más populares son las de Clough-Tocher y Powell-Sabin.

Dada una triangulación conforme, Δ, de un dominio poligonal del plano, Ω, un refinamiento de Powell-Sabin Δ_{PS} de Δ se obtiene al dividir cada macro-triángulo T_j en seis micro-triángulos de la siguiente forma:

(i) Se elige un punto de ruptura Z_j en el interior de cada triángulo T_j. Si dos triángulos T_i y T_j tienen una arista común, la línea que une los puntos Z_i y Z_j intercepta dicha arista común en un punto interior $R_{i,j}$. En general, se suele elegir cada punto Z como el baricentro de cada triángulo.

(ii) Se une cada punto Z_j con los vértices del triángulo T_j.

(iii) Para todo triángulo T_j de Δ,

- si T_j es adyyacente a un triángulo T_i, se unen Z_j y $R_{i,j}$;
- si T_j es un triángulo de frontera, se une Z_j con un punto arbitrario del lado que yace en la frontera, por ejemplo, el punto medio.

La Figura 1 muestra el resultado del procedimiento anterior descrito para la triangulación dada.

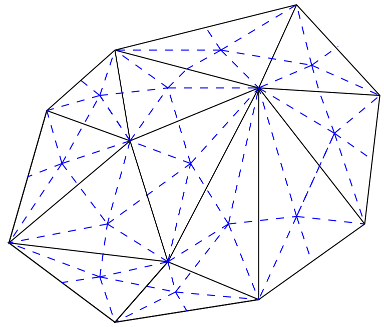

Figura 1: Triangulación de tipo Powell-Sabin.

M. Powell y M. Sabin fueron los primeros autores en estudiar splines sobre triangulaciones dotadas de un refinamiento de tipo Powell-Sabin [18]. Demostraron que una función spline cuadrática de clase $\mathcal{C}^1$ definida sobre una triangulación refinada está unívocamente determinada por sus valores y sus gradientes en los vértices de la triangulación inicial. En [23], P. Dierckx obtuvo mediante un procedimiento puramente geométrico una representación de tales splines cuadráticos de clase $\mathcal{C}^1$ a partir de una base normalizada de B-splines, es decir, formada por funciones que disfrutan de las siguientes propiedades: son de soporte compacto, no negativas y forman una partición convexa de la unidad. Tras la introducción de estos espacios, numerosos autores han dedicado una atención particular a este tipo de funciones spline. M. J. Lai y L. L. Schumaker estudiaron en [30] un espacio spline específico definido añadiendo un condición adicional de regularidad en ciertos vértices y en líneas interiores. El espacio resultante se denomina espacio de super-splines. También se encuentran en la literatura espacios de super-splines cúbicos de clase $\mathcal{C}^1$.

De manera natural, la construcción de splines de clase $\mathcal{C}^2$ ha sido objeto de una intensa investigación [25, 32] y se pretende hacer aportaciones en este ámbito.

Polinomios definidos sobre triángulos

En esta sección recordamos algunos conceptos generales de los polinomios sobre triángulos en su representación de Bernstein-Bézier.

Coordenadas baricéntricas

Las coordenadas baricéntricas son una herramienta elegante para trabajar con puntos en un triángulo. Considera un triángulo T de vértices $V_i := (x_i, y_i)$, $i = 1, 2, 3$, entonces cualquier punto $V = (x, y)$ en T puede ser representado como $V = \sum_{i=1}^{3} \tau_i V_i$, donde las coordenadas (τ_1, τ_2, τ_3) se denominan baricéntricas y cumplen que $1 = \sum_{i=1}^{3} \tau_i$, $\tau_i \geq 0$, $i = 1, 2, 3$.

Estas coordenadas también se llaman coordenadas areales, porque las coordenadas baricéntricas del punto V con respecto al triángulo T son proporcionales a las áreas de los subtriángulos $t_1 \langle V, V_2, V_3\rangle$, $t_2 \langle V, V_3, V_1\rangle$ y $t_3 \langle V, V_1, V_2\rangle$, ver (Figura 2). Precisamente, las coordenadas baricéntricas de V con respecto a T están dadas por

$$\tau_i = \frac{|t_i|}{|T|}, \qquad i = 1, 2, 3.$$

$|A|$ representado el área del triángulo A.

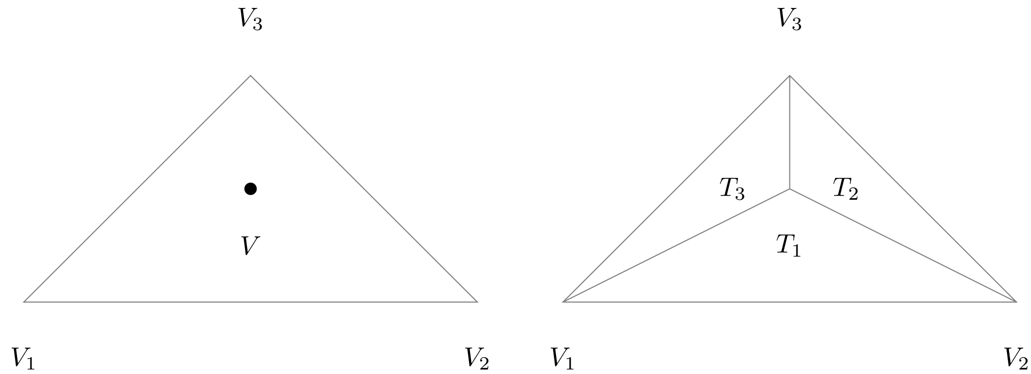

Figura 2: Coordenadas baricéntricas de un punto V respeto del triángulo T.

Representación de Bernstein-Bézier

A lo largo de esta sección consideremos que T es un triángulo fijo. Sean $(\tau_1,\, \tau_2,\, \tau_3)$ las coordenadas baricéntricas de un punto $V \in \mathbb{R}^2$ con respecto a T. La identidad

$$1 = (\tau_1 + \tau_2 + \tau_3)^d = \sum_{|\beta|=d} \frac{d!}{\beta!} \tau^\beta,$$

donde $\beta = (\beta_1, \beta_2, \beta_3) \in \mathbb{N}_0^3$, $|\beta| = \sum_i \beta_i$, $\beta! = \beta_1!\beta_2!\beta_3!$ and $\tau^\beta = \prod_i \tau_i^{\beta_i}$, conduce a los polinomios de Bernstein-Bézier de grado d

$$\mathfrak{B}^d_{\beta,\,T}\,(\tau) := \frac{d!}{\beta!} \tau^\beta$$

Satisfacen las siguientes propiedades:

- Son linealmente independientes.
- Forman una partición de la unidad, es decir

$$1 = \sum_{|\beta|=d} \mathfrak{B}^d_{\beta,\,T}\,(\tau)\,.$$

- Son no negativas.

Como los polinomios de Bernstein-Bézier forman una base del espacio $\mathbb{P}_d$ de polinomios de grado menor o igual que d, toda superficie polinómica $p(V)$ tiene una única representación de Bernstein-Bézier,

$$p\,(V) = b\,(\tau) := \sum_{|\beta|=d} b_\beta\, \mathfrak{B}^d_{\beta,\,T}\,(\tau)\,,$$

Los coeficientes b_β se denominan puntos de Bézier de p y $b\,(\tau)$ se llama representación de Bernstein-Bézier (BB-representación) de p. Los puntos de Bézier determinan la malla de Bézier de $b\,(\tau)$ sobre el triángulo T (ver la Figura 3).

El algoritmo de De Casteljau

La función $b\,(\tau) = \sum_{|\beta|=d} b_\beta\, \mathfrak{B}^d_{\beta,\,T}\,(\tau)$ se puede evaluar fácilmente usando una generalización del algoritmo de De Casteljau univariado.

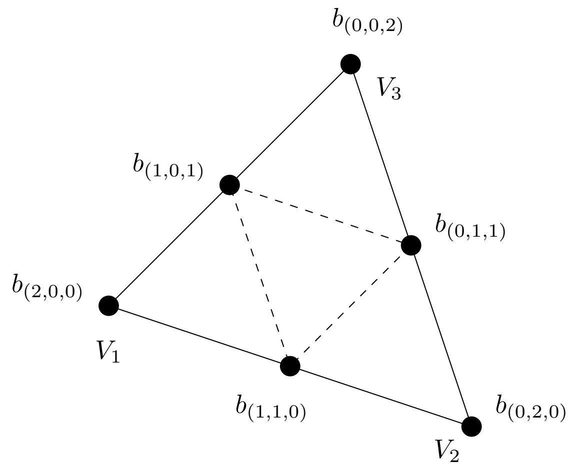

Figura 3: La malla de Bézier de una superficie cuádratica.

La función $b(\tau)$ evaluada en el punto $\tau = (\tau_1, \tau_2, \tau_3)$ tiene como valor

$$p(\tau) = b^d_{(0,0,0)}(\tau),$$

donde

$$\begin{aligned} b^0_\beta(\tau) &= b_\beta(\tau), \quad |\beta| = d, \\ b^r_\beta(\tau) &= \tau_1 b^{r-1}_{\beta-e_1} + \tau_2 b^{r-1}_{\beta-e_2} + \tau_3 b^{r-1}_{\beta-e_3}, \quad |\beta| = d-r, \text{ and } r = 1,\ldots,d. \end{aligned}$$

Los puntos intermedios b^r_β del algoritmo de De Casteljau, en su ordenación canónica, forman un esquema tetraédrico. Si τ yace en un triángulo T, entonces todos los pasos del algoritmo de De Casteljau son combinaciones convexas, lo cual garantiza su estabilidad numérica.

Los splines de tipo Powell-Sabin

Los splines Powell-Sabin son polinomios cuadráticos a trozos con una continuidad global C^1. El espacio lineal de polinomios cuadráticos a trozos sobre Δ se define como sigue

$$S^1_2(\Delta) := \left\{ s \in C^1(\Omega) : \quad s_{|T}\mathbb{P}_2 \text{ for all } T \in \Delta \right\}$$

El siguiente problema de interpolación es considerado: dado un conjunto de triples (f_i, f^x_i, f^y_i), $i = 1,\ldots,nv$, find $s(x,y) \in S^1_2(\Delta)$ tal que,

$$s(V_i) = f_i, \quad \frac{\partial s}{\partial x}(V_i) = f^x_i \text{ and } \frac{\partial s}{\partial y}(V_i) = f^y_i, \tag{1}$$

El número nv indica el número de vértices en Δ. El problema (1) exige la imposición de nueve parámetros para definir el polinomio cuadrático en cada triángulo, mientras que sólo hay seis coeficientes disponibles, vea la Figura (3). A fin de conseguir una solución al problema de interpolación (1), una alternativa es la solución propuesta por Powell y Sabin en [18] se basa en la subdivisión de cada triángulo en seis microtriángulos (PS-split), vea la Figura 1.

Las ordenadas de Bézier en las abscisas $\bullet$ están determinadas por las condiciones de interpolación en los vértices, las ordenadas denotadas por $\circ$ están dadas por las condiciones de conexión C^1 a lo largo de las aristas de subdivisión, vea la Figura 4.

El problema de interpolación (1) es muy útil para construir una base local para $S^1_2(\Delta)$. En [23], P. Dierckx obtuvo mediante un procedimiento puramente geométrico una representación de

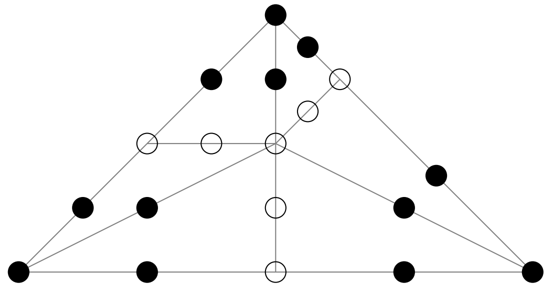

Figura 4: Ordenadas de Bézier de la subdivisión de Powell-Sabin

tales splines cuadráticos de clase $\mathcal{C}^1$ a partir de una base normalizada de B-splines. Así, cualquier spline de Powell- Sabin se puede representar como

$$s(x,y) = \sum_{i=1}^{nv} \sum_{j=1}^{3} c_{i,j} \mathcal{B}_{i,j}(x,y),$$

donde las funciones $\mathcal{B}_{i,j}$ se llaman Powell-Sabin B-splines y $c_{i,j}$ son los coeficientes de la representación. Para obtener las funciones de base $\mathcal{B}_{i,j}$, primero asociamos a cada vértice V_i de la triangulación tres tripletas linealmente independientes $(\alpha_{i,j}, \beta_{i,j}, \gamma_{i,j})$, $j = 1, 2, 3$. El procedimiento propuesto por P. Dierckx [23] para determinar estas tripletas se resume como sigue:

- Para cada vértice V_i de Δ, hallar los correspondientes PS-puntos de dicho vértice. Estos puntos son los puntos de dominio Bézier inmediatamente circundantes de V_i en Δ_{PS}. El propio vértice V_i también se considera un PS-punto.

- Para cada vértice V_i, encontrar un triángulo $t_i \langle Q_{i,1}, Q_{i,2}, Q_{i,3} \rangle$ que contiene todos los PS-puntos correspondientes a V_i. Este triángulo t_i se llama PS-triángulo asociado a V_i. Las coordenadas cartesianas de los vértices $Q_{i,j}$, $j = 1, 2, 3$, se denotan por $(X_{i,j}, Y_{i,j})$.

- Las tres tripletas linealmente independientes $(\alpha_{i,j}, \beta_{i,j}, \gamma_{i,j})$, $j = 1, 2, 3$, se definen como sigue:

  ◇ $\alpha_i = (\alpha_{i,1}, \alpha_{i,2}, \alpha_{i,3})$ son las coordenadas baricéntricas de V_i con respecto a t_i.

  ◇ $\beta_i = (\beta_{i,1}, \beta_{i,2}, \beta_{i,3})$ y $\gamma_i = (\gamma_{i,1}, \gamma_{i,2}, \gamma_{i,3})$ están dadas por

$$\beta_{i,1} = \frac{\begin{vmatrix} 1 & X_{i,2} & X_{i,3} \\ 0 & Y_{i,2} & Y_{i,3} \\ 0 & 1 & 1 \end{vmatrix}}{\begin{vmatrix} X_{i,1} & X_{i,2} & X_{i,3} \\ Y_{i,1} & Y_{i,2} & Y_{i,3} \\ 1 & 1 & 1 \end{vmatrix}}, \quad \beta_{i,2} = \frac{\begin{vmatrix} X_{i,1} & 1 & X_{i,3} \\ Y_{i,1} & 0 & Y_{i,3} \\ 1 & 0 & 1 \end{vmatrix}}{\begin{vmatrix} X_{i,1} & X_{i,2} & X_{i,3} \\ Y_{i,1} & Y_{i,2} & Y_{i,3} \\ 1 & 1 & 1 \end{vmatrix}} \quad \text{y} \quad \beta_{i,3} = \frac{\begin{vmatrix} X_{i,1} & X_{i,2} & 1 \\ Y_{i,1} & Y_{i,3} & 0 \\ 1 & 1 & 0 \end{vmatrix}}{\begin{vmatrix} X_{i,1} & X_{i,2} & X_{i,3} \\ Y_{i,1} & Y_{i,2} & Y_{i,3} \\ 1 & 1 & 1 \end{vmatrix}}$$

$$\gamma_{i,1} = \frac{\begin{vmatrix} 0 & X_{i,2} & X_{i,3} \\ 1 & Y_{i,2} & Y_{i,3} \\ 0 & 1 & 1 \end{vmatrix}}{\begin{vmatrix} X_{i,1} & X_{i,2} & X_{i,3} \\ Y_{i,1} & Y_{i,2} & Y_{i,3} \\ 1 & 1 & 1 \end{vmatrix}}, \quad \gamma_{i,2} = \frac{\begin{vmatrix} X_{i,1} & 0 & X_{i,3} \\ Y_{i,1} & 1 & Y_{i,3} \\ 1 & 0 & 1 \end{vmatrix}}{\begin{vmatrix} X_{i,1} & X_{i,2} & X_{i,3} \\ Y_{i,1} & Y_{i,2} & Y_{i,3} \\ 1 & 1 & 1 \end{vmatrix}} \quad \text{y} \quad \gamma_{i,3} = \frac{\begin{vmatrix} X_{i,1} & X_{i,2} & 0 \\ Y_{i,1} & Y_{i,3} & 1 \\ 1 & 1 & 0 \end{vmatrix}}{\begin{vmatrix} X_{i,1} & X_{i,2} & X_{i,3} \\ Y_{i,1} & Y_{i,2} & Y_{i,3} \\ 1 & 1 & 1 \end{vmatrix}}$$

El B-spline de Powell-Sabin $\mathcal{B}_{i,j}$ se define como la única solución del problema de interpolación (1) con todos los valores $\left(f_k, f_k^x, f_k^y\right)$ nulas excepto para $k = i$, en cuyo caso $(f_i, f_i^x, f_i^y) = (\alpha_{i,j}, \beta_{i,j}, \gamma_{i,j})$.

Descripción de la tesis

El objetivo general de esta tesis es la construcción de espacios de funciones spline sobre particiones de Powell-Sabin, tanto en un sentido clásico como en una situación univariada. Más específicamente, los temas que se abordan son los siguientes.

En primer lugar, se construye una base de B-splines del espacio de splines cuárticos de clase $\mathcal{C}^1$ sobre una partición de Powell-Sabin a partir la resolución de ciertos problemas de interpolación de Hermite. Con ayuda de la identidad de Marsden se definirán operadores de quasi-interpolación exactos sobre el espacio de polinomios cuárticos.

A continuacion, a partir del espacio cuártico de clase $\mathcal{C}^1$ introducido en [32], se construye un subespacio spline reforzando la regularidad en algunas de las aristas interiores de la triangulación refinada, para estudiar bajo qué condiciones geométricas de la triangulación considerada el espacio de super-splines es de clase $\mathcal{C}^2$.

El espacio de splines cuárticos de Powell-Sabin está definido como en [32]:

$$S_4^1\left(\Delta_{\mathrm{PS}}\right) := \left\{s \in \mathcal{C}^1\left(\Omega\right) :\, s_{|t} \in \mathbb{P}_4 \;\; \forall\, t \in \Delta_{\mathrm{PS}}\right\}$$

En [32] se considera un subespacio particular de super splines de $S_4^1\left(\Delta_{\mathrm{PS}}\right)$. Si $\mathcal{V} := \{V_i\}_{i=1}^{nv}$, $\mathcal{Z} := \{Z_i\}_{i=1}^{nt}$, $\mathcal{E} := \{\mathfrak{e}_i\}_{i=1}^{ne}$ y $\mathcal{E}^*$ son, respectivamente, los subconjuntos de vértices en Δ, de puntos de división, de aristas de Δ y de aristas que unen un punto de división Z_i con un punto $R_{i,j}$ y nv, nt y ne representan el número de vértices, triángulos y aristas de Δ, respectivamente, entonces el subespacio

$$S_4^{1,2}(\Delta_{\mathrm{PS}}) := \left\{s \in S_4^1(\Delta_{\mathrm{PS}}) :\, s \in \mathcal{C}^2\left(\mathcal{V} \,\cup\, \mathcal{Z} \,\cup\, \mathcal{E} \,\cup\, \mathcal{E}^*\right)\right\}$$

tiene dimensión $6nv + 3ne$.

En esta memoria se considera el siguiente subespacio de $S_4^{1,2}(\Delta_{\mathrm{PS}})$:

$$S_4^{1,2,3}\left(\Delta_{\mathrm{PS}}\right) := \left\{s \in\, S_4^{1,2}\left(\Delta_{\mathrm{PS}}\right) :\;\, s \in\, \mathcal{C}^3\left(\mathcal{E}^*\right)\right\}$$

Se obtienen condiciones geométricas que caractericen la clase C^2 de las funciones de este espacio.

Seguidamente, se estudian splines de Powell-Sabin de grado 6 imponiendo condiciones adicionales de regularidad en puntos interiores de la triangulación y también en ciertas aristas de la triangulación refinada. Cada spline queda determinado únivocamente por sus valores en los vértices de la triangulación inicial y en los puntos interiores, así como los de sus derivadas parciales hasta el cuarto orden en los vértices.

El espacio de funciones séxticas a trozos sobre la partición Δ_{PS} con continuidad global C^2 será

$$S_6^2\left(\Delta_{\mathrm{PS}}\right) := \left\{s \,\in\, C^2\left(\Omega\right) : s_{|t} \in \mathbb{P}_6 \;\; \forall\, t \,\in\, \Delta_{\mathrm{PS}}\right\}.$$

Se considera el siguiente subespacio de $S_6^2\left(\Delta_{\mathrm{PS}}\right)$:

$$S_6^{2,4,3}\left(\Delta_{\mathrm{PS}}\right) := \left\{s \,\in\, S_6^2\left(\Omega,\, \Delta_{\mathrm{PS}}\right) : s \in\, C^4\left(\mathcal{V}\right),\; s \in\, C^3\left(\mathcal{Z} \cup \mathcal{E}^*\right)\right\}.$$

Se construye una base normalizada de $S_6^{2,4,3}\left(\Delta_{\mathrm{PS}}\right)$ y se establece la identidad de Marsden relativa a $S_6^{2,4,3}\left(\Delta_{\mathrm{PS}}\right)$ y, a partir de ella una familia de operadores de quasi-interpolación.

En [45] se da una contribución relativa a la cuadratura gausiana mediantes splines de Powell-Sabin cuadráticos definidos sobre un único triángulo. La disponibilidad de otras cuadraturas y la generalización de estas reglas para pasar de un solo macro-triángulo a una malla triangular es un problema delicado. En este contexto, se demuestra que una fórmula de cuadratura gausiana óptima de 3-nodos puede ser extendida al espacio de los splines cuadráticos de clase $\mathcal{C}^1$ sobre una triangulación de tipo-1.

En quinto lugar, presentamos esquemas de cuasi interpolación que se definen en una triangulación uniforme de tipo-1 dotada de la partición de Powell-Sabin proporcionada por las baricentras de sus triángulos. A diferencia de la construcción habitual de quasi-interpolantes splines sobre la 6-split, el enfoque adoptada no requiere la construcción de un conjunto de funciones de base apropiadas. En concreto, los quasi-interpolantes se definen sus ordenadas de Bézier en cada triangulo combinaciones adecuadas de los valores dados. Los esquemas propuestos son de clase C^1 y reproducen polinomios cuadráticos.

Tras los resultados sobre aproximación spline en triangulaciones de Powell-Sabin, se utilizan los procedimiento desarrollados para definir una familia de funciones spline univariadas de grado arbitrario definidas sobre una partición dada, que es refinada incluyendo en cada subintervalo un punto interior a semejanza de lo que se hace en el caso bidimensional. Haciendo uso de la representación de Bernstein-Bézier, se construye una base de B-splines que forman una partición convexa de la unidad. Mediante formas polares, se establece una identidad de Marsden a partir de la cual se definan operadores de quasi-interpolación con órdenes de aproximación óptimos.

También, se discute la construcción de esquemas de cuasi-interpolación de splines cúbicos de clase C^2 definidos en una partición refinada. Estos esquemas son reducidos en lo que respecta al grado de libertad en comparación con los que existen en la literatura. En particular, se da una receta para reducir el grado de libertad imponiendo condiciones de super-suavidad a la vez que se preserva la suavidad completa y la precisión cúbica. Por otra parte, se obtienen reglas de subdivisión mediante blossoming. Las reglas derivadas están diseñadas para expresar los coeficientes de los B-spline asociados a una partición más fina a partir de los asociados a la anterior.

Finalmente, como complement de lo antes, se da una nueva representación normalizada tipo B-spline para el espacio de splines cúbicos de clase C^2 definidos sobre una partición inicial refinada mediante la inserción de dos nuevos puntos dentro de cada sub-intervalo. Las funciones base se construyen de forma geométrica son no negativas, soporte compacto y forman una partición convexa de la unidad. Mediante la teoría de los polinomios de control introducida en este memoria, se deriva la identidad de Marsden, a partir de la cual se definen varias familias de quasi-interpolantes super-convergentes.

General introduction

Approximation methods are today a common tool which is, so to say, just a click away from the user. Interpolation and quasi-interpolation are particular and important approximation methods, which are widely used to address the solution of theoretical problems and show their full potential to numerically solve problems that occur in many different branches of science, chemistry, biology, engineering and economics.

Originally, the computation of functions on a computer was a field of application of approximation, but now the approximation methods are very helpful for ordinary and partial linear and non-linear differential equations, integral equations, and more general functional equations since they frequently appear in applications. But in general, the approximation problems that arise in applications are much more difficult than the problems considered in classical theory; the difficulties come mainly from the fact that multivariate approximation, singularities, free boundaries, etc, occur.

When we do not know enough about the type of the function wanted, then it is natural to approximate the function by polynomials, and if we expect that the value of the function varies strongly, we can divide the domain under consideration into small pieces and we obtain an approximation by splines. Therefore, polynomial and spline approximations are very important for applications.

Spline approximation is a reference choice when the approximation of functions or data is crucial, since they are much less affected by the large oscillations that are typical of high degree polynomials, and the frequent overshoots are reduced.

Spline theory in its present form first appeared in two papers by Schoenberg (1946) [1, 2]. Since its introduction, univariate splines approximation has been the subject of thousand research papers and a number of books. Its fast development was largely over by the year 1980. This rapidity is mainly due to their great utility in applications. Indeed, spline functions provide many desirable properties as well as good approximation power. Since they are easy to manipulate and store on a digital computer, univariate splines have become an indispensable tool in a wide variety of application domains.

The univariate spline approximation can be easily extended to two-dimensional case by means of a tensor product representation [3]. Namely, the tensor product splines have been widely recognized as very powerful tools for surface fitting, because of its compact representation, flexibility, easy implementation and the ability to preserve the same nice properties of univariate splines. A definite drawback, however, is that they are restricted to rectangular meshes or domains which can easily be transformed to a rectangle. In addition, shape preservation constraints, such as convexity or monotonicity, are not easy to implement either. Splines defined on triangulations are then considered as an attractive alternative.

The polynomial spline functions defined on triangulations are tools widely used in many different fields, both theoretical and applied. The book by Lai and Schumaker [97] presents an in-depth study of this type of functions, focusing mainly on the theoretical aspects. This kind of spline spaces is useful if a suitable set of basis functions is well constructed and studied. Although this requires the computation of their dimensions, which is extremely difficult, since it depends on an interplay between geometry, combinatorics and topology. Lower bounds to the dimension are given in [5, 6] and upper bounds in [7, 8]. There are some exact results for particular choices of polynomial degree and smoothness [9, 10, 11, 12], and for particular constrained triangulations [13]. Yet, in general and especially for low degree polynomials the problem remains open.

As shown in [14], regularity C^m on an arbitrary triangulation of a polygonal domain is obtained if all derivatives up to order $2m$ at the vertices of the triangles are given. In particular, to get C^1 triangular splines on an arbitrary triangulation the values of the derivatives of order less than or equal to 2 at the vertices and the lowest degree is equal to 5 (see [14, Thm. 2] and the references therein). However, in practice, high smoothness with low degree is the commonly chosen option.

In order to reduce the degree of the spline, it was proposed in [15] to refine each triangle by joining its vertices to an interior point. The Clough-Tocher refinement thus obtained allows to determine a C^1 spline of degree 3 and also a macro-triangle whose nodal parameters yield a C^1 piecewise polynomial of degree 4 (see [54] and the references therein). Introduced more than 50 years ago, C^1 cubic splines on Clough-Tocher partitions are still a subject of interest. For example, in [17] Gaussian quadrature for C^1 cubic Clough-Tocher macro-triangles is studied.

In [18], Powell and Sabin introduced a new refinement with the specific objective of contour plotting, managing to define a C^1 piecewise quadratic function from the values at the nodes of the function to be approximated and its gradient. The first subdivision into six triangles is achieved by selecting an inner point in every triangle and connecting it with similar points in the adjacent triangles as well as with the three vertices. The inner point of a boundary triangle is joined to a point over a boundary edge when no adjacent triangle is available. From this Powell-Sabin (PS) 6-split a PS12-split is easily derived by joining in every triangle the three points lying on the edges of the triangle that the previous construction produces [19].

Powell-Sabin refinement has been extended to trivariate case in [20], where each tetrahedron is divided into 24 sub-tetrahedra. These results have been generalized to multivariate case in [21] and profoundly analyzed by T. Sorokina and Worsey in [22]. Each simplex in $\mathbb{R}^s$ is then divided into $(s+1)!$ smaller sub-simplices. The construction of C^1 smooth quadratic splines over such a refined tessellation is still a challenging task for $s > 2$. This is because certain geometric constraints on the positions of the split points must be fulfilled. These geometric constraints are definitely satisfied if $s = 1, 2$, but it remains an open question whether they can be satisfied for an arbitrary tessellation when $s > 2$.

Application of spline in numerical analysis often requires the use of non-negative basis with local supports. To the best of our knowledge, on an arbitrary triangulation, the only recognized normalized bases are constructed by means of Powell-Sabin refinement. Any surface represented as a linear combination of non-negative, locally supported basis functions that form a partition of the unity, can be locally controlled and edited in a predictable way. The normalized B-spline representation of bivariate C^1 quadratic splines achieved by Dierckx [23] was essential in the development of spline spaces on Powell-Sabin partitions and applications. The method proposed by P. Dierckx is completely geometrical, it is reduced to finding a set of Powell-Sabin triangles that must contain a number of specified points. Linear and quadratic programming problems are the standard methods proposed by many authors in the literature [23, 24, 25, 26] to define such triangles.

The study of spline function spaces on Powell-Sabin partitions obtained by refinement into 6 sub-triangles has attracted great interest in the scientific community since its introduction. The cubic case has been considered in [24, 27, 28, 29]. Spaces of quintic splines have been analyzed in [30] and more recently in [25, 31], among others. In [26] and [29], normalized bases for PS-splines of degree $3r-1$ are defined and super-splines of arbitrary degree are given, respectively. After the latter, the paper [32] was published, where only almost C^2 quartic Powell-Sabin splines are considered.

Quasi-interpolation over Powell-Sabin triangulations for specific spaces have been also studied in depth [31, 33, 50, 35], as well as for a family of spaces [36]. The construction of such operators is based on establishing Marsden's identity. It is a powerful tool that allows to write the monomials in terms of the corresponding B-spline-like functions.

In contrast to classical approximants, spline quasi-interpolants do not require the solution of linear systems, so they are very convenient in practice. In general, a quasi-interpolant for a given function is obtained as a linear combination of some elements of a suitable set of basis functions. In order to ensure both numerical stability and local control of the constructed approximant, these basis functions are required to be positive, to form a convex partition of the unity and to possess a small local support. The coefficients of the linear combination are given by linear functionals depending on the function to be approximated and/or its derivatives. There are many applications of quasi-interpolation operators, in particular, they are used for the numerical computation of integrals or, the numerical solution of integral equations, see e.g. [37, 38, 39, 40].

Recently, a new approach based on polar forms has emerged from the work of Ramshaw [41]. This approach has allowed to revisit the theory of univariate B-splines and has yielded a powerful tool for understanding the relationship between the coefficients and the spline curves. Polar forms provide a rich and robust theory to understand splines. They can be applied to express the values of the coefficients of a spline, the derivatives, the smoothness conditions, etc.

In this thesis, we have used some powerful properties of polar forms in approximation by univariate and bivariate spline functions. In particular, we have devoted some parts of this thesis to the construction of quasi-interpolants (abbreviated as QIs) that have become popular and occupy an advanced position in approximation theory.

Outlined of the thesis

This thesis consists of two parts. In the first part, we deal with bivariate spline functions defined on triangulations endowed with Powell-Sabin splits. We consider various spaces with different degree and smoothness, and their applications to quasi-interpolation and Gaussian quadrature rules. The second part is devoted to deal with univariate splines defined on partition with a Powell-Sabin refinement, which means that a refinement is produced by inserting one split point inside each macro-interval.

The thesis is organized as follows. First, we start by recalling some facts about triangles and triangulations, Bernstein-Bézier form, De Casteljau algorithm and polar forms theory. Thus, we introduce the Powell-Sabin split.

Chapter 2 is divided into two parts. In the first one, we consider a Hermite interpolation problem in spaces of C^1 quartic Powell-Sabin splines. Thus, we construct from Marsden's identity a family of quasi-interpolation operators yielding the optimal approximation power. The second part deals with the characterization of Powell-Sabin triangulations allowing the construction of bivariate quartic splines of class C^2. The result is established by relating the triangle and edge split points provided by the refinement of each triangle. For a triangulation fulfilling the characterization obtained, a normalized representation of the splines in the C^2 space is given.

In Chapter 3, we revise a subspace of $\mathcal{C}^2$ sextic Powell-Sabin splines obtained by imposing additional smoothness requirements at the interior points of the triangulation chosen to construct the sub-triangulation and also across some edges of the refined triangulation. This subspace of super-splines was studied in [42], where it is shown that every spline is uniquely determined by its values at the vertices of the initial triangulation and the interior points and those of its partial derivatives up to the fourth order at the vertices. In addition, the construction of normalized basis reduced to determine a set of small triangles that contain a sets of points. The main idea of existing methods is to minimize the area of a triangle without imposing any condition concerning the diameter of the sought triangles, and somtimes triangles with small areas are obtained but having large diameter. In order to avoid this limitations, we will present an algorithm that aims to produce PS6-triangles with small area and diameter, and compare it with the one proposed in [43]. Thus, quasi-interpolation operators which reproduce sextic polynomials are constructed after deriving Marsden's identity from a more explicit version of the control polynomials introduced some years ago in the literature. Finally, some tests show the good performance of these operators.

The quadrature rule of Stroud and Hammer for cubic polynomials [68] has been recently shown to integrate exactly also C^1 continuous quadratic Powell-Sabin 6-split splines over macro-triangles if the inner split point is the barycenter and the edge split points are the centers of the macro-edges [45]. It has been further shown numerically that if the inner split point is not the barycenter of the macro-triangle, there exist 3-point micro-edge quadratures that admit exact integration of the associated spline space, however, the inner split-point is constrained to lie within a specific sub-region of the macro-triangle. In Chapter 4, we show that for Ceva's variant of the segmentation of the macro-triangle, one can exactly integrate Powell-Sabin splines using a polynomial 3-point micro-edge quadrature for an arbitrary inner split point.

Chapter 5 deals with the construction of quasi-interpolation schemes defined on a uniform triangulation of type-1 endowed with a Powell-Sabin split. In contrast to the usual construction of quasi interpolation splines on the 6-split, the approach described in this chapter does not require the construction of a set of appropriate basis functions. Namely, the spline schemes are generated by setting their Bézier (B-) ordinates to suitable combinations of the given data values. The proposed schemes are C^1 continuous and reproduce quadratic polynomials. Some numerical tests are illustrated to confirm the theoretical results.

In Chapter 6, we define a family of univariate many knot spline spaces of arbitrary degree defined on an initial partition that is refined by adding a point in each sub-interval. For an arbitrary smoothness r, splines of degrees $2r$ and $2r+1$ are considered by imposing additional regularity when necessary. For an arbitrary degree, a B-spline-like basis is constructed by using the Bernstein-Bézier representation. Blossoming is then used to establish a Marsden's identity from which several quasi-interpolation operators having optimal approximation orders are defined.

Chapter 7 is divided into two parts. In the first one, we discuss the construction of C^2 cubic spline quasi-interpolation schemes defined on a refined partition. These schemes are reduced in terms of the degree of freedom compared to those existing in the literature. Namely, we provide a recipe for reducing the degree of freedom by imposing super-smoothing conditions while preserving full smoothness and cubic precision. In addition, we provide subdivision rules by means of blossoming. The derived rules are designed to express the B-spline coefficients associated with a finer partition from those associated with the former one. The second part is devoted to construct a novel normalized B-spline-like representation for C^2-continuous cubic spline space defined on an initial partition refined by inserting two new points inside each sub-interval. The basis functions are compactly supported non-negative functions that are geometrically constructed and form a convex partition of unity. With the help of the control polynomial theory introduced herein, a Marsden's identity is derived, from which several families of super-convergent quasi-interpolation operators are defined.

We conclude with a summary of the contributions, conclusions and proposals for possible future research.

Chapter 1

Preliminaries

In this chapter, we discuss bivariate polynomials on triangles, polar forms, and some results on control polynomials. Given a positive integer d, the dimension of the linear space $\mathbb{P}_d$ of polynomials of total degree less than or equal to d is equal to $\frac{1}{2}(d+1)(d+2)$. Next, we recall some useful results on representing the polynomials in this space.

1.1 Triangulation

In what follows, we briefly review some facts about triangles and triangulations. Consider three non-collinear points $V_i := (x_i, y_i)$, $i = 1, 2, 3$. The convex hull of these points form the triangle $T := \langle V_1, V_3, V_3 \rangle$. The points V_i, $i = 1, 2, 3$, are called the vertices of T, and the three edges of T are denoted by $\langle V_1, V_2 \rangle$, $\langle V_2, V_3 \rangle$ and $\langle V_3, V_1 \rangle$. The signed area of T is given by

$$A(T) = \frac{1}{2} \begin{vmatrix} 1 & 1 & 1 \\ x_1 & x_2 & x_3 \\ y_1 & y_2 & y_3 \end{vmatrix},$$

where, $|.|$ stands for determinant.

Let Ω be a polygonal domain in $\mathbb{R}^2$. A collection of triangles $\Delta := \{T_1, T_2, \ldots, T_n\}$ of triangles is called a triangulation of $\Omega = \cup_{i=1}^{n} T_i$ provided that if a pair of triangles in Δ intersect, then their intersection is either a common vertex or a common edge.

This definition allows quite general triangulations. For example, Δ can be formed by two separate triangles, or it can be formed by two triangles touching each other only at one vertex. In addition, the definition allows triangulations of domains Ω with one or more holes. This kind of triangulations arise often in the finite element method for solving partial differential equations.

1.2 Bernstein-Bézier representation

Consider the non-degenerated triangle T. It is well-known that every point $V := (x, y) \in \mathbb{R}^2$ can be uniquely expressed as

$$V = \sum_{i=1}^{3} \tau_i V_i, \quad \tau_1 + \tau_2 + \tau_3 = 1,$$

where the barycentric coordinates $\tau := (\tau_1, \tau_2, \tau_3)$ with respect to T are the unique solution of system

$$\begin{pmatrix} x_1 & x_2 & x_3 \\ y_1 & y_2 & y_3 \\ 1 & 1 & 1 \end{pmatrix} \begin{pmatrix} \tau_1 \\ \tau_2 \\ \tau_3 \end{pmatrix} = \begin{pmatrix} x \\ y \\ 1 \end{pmatrix}.$$

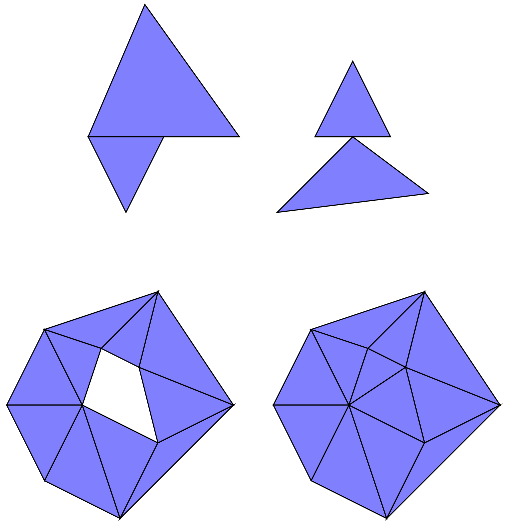

Figure 1.1: Top: examples of two sets of triangles that do not form a triangulation. Bottom: Examples of triangulations: (left) triangulation with a hole, (right) triangulation without any holes.

Any bivariate polynomial $p \in \mathbb{P}_d$ has a unique representation in barycentric coordinates

$$p\,(V) = b\,(\tau) := \sum_{|\beta|=d} b_\beta\, \mathfrak{B}^d_{\beta,\,T}\,(\tau)\,, \tag{1.1}$$

where $\beta := (\beta_1,\, \beta_2,\, \beta_3) \in \mathbb{N}^3$ are multi-indices of length $|\beta| := |\beta_1| + |\beta_2| + |\beta_3|$ and

$$\mathfrak{B}^d_{\beta,\,T}\,(\tau) := \frac{d!}{\beta!}\tau^\beta = \frac{d!}{\beta_1!\,\beta_2!\,\beta_3!}\,\tau_1^{\beta_1}\,\tau_2^{\beta_2}\,\tau_3^{\beta_3}$$

are the Bernstein-Bézier polynomials of degree d with respect to T. The coefficients b_β are called the Bézier (B-) ordinates or Bernstein-Bézier (BB-) coefficients of p with respect to T, and $b\,(\tau)$ is said to be the Bernstein-Bézier (BB-) form or Bernstein-Bézier (BB-) representation of p. It may be represented by associating each coefficient b_β with the domain points ξ_β determined by the barycentric coordinates $\left(\frac{\beta_1}{d},\, \frac{\beta_2}{d},\, \frac{\beta_3}{d}\right)$ with respect to T (see Figure 1.2). The points $(\xi_\beta,\, b_\beta) \in \mathbb{R}^3$ are the control points of the so called B-net for the surface of equation $z = p\,(x, y)$. This surface is tangent at the vertices of T to the linear piecewise function defined by the B-net. The graph of the surface is contained in the convex hull of the control points and p can be easily bounded from them.

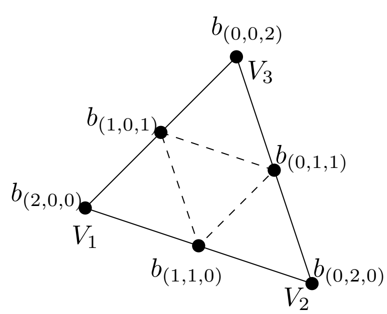

Figure 1.2: Schematic representation of the BB-coefficients of a quadratic bivariate polynomial.

Hereafter, $D_r\,(V_1)$ will denote the *disk of radius* r around the vertex V_1 of a triangle $T =$

$\langle V_1, V_2, V_3\rangle$. It is the subset of domain points ξ_β defined as

$$D_r(V_1) := \{\xi_\beta,\ \beta_1 \geq d-r\}.$$

Figure 1.3 shows the typical plots of some Bernstein-Bézier basis functions of degree 4.

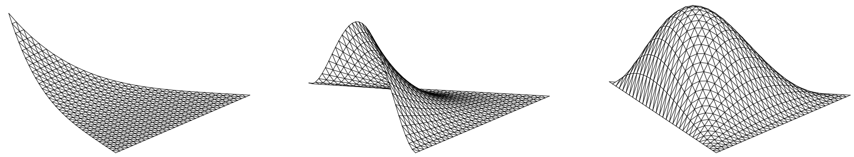

Figure 1.3: The Bernstein-Bézier basis functions $\mathfrak{B}^4_{(4,0,0),T}$, $\mathfrak{B}^4_{(2,2,0),T}$ and $\mathfrak{B}^4_{(2,1,1),T}$ (from left to right).

In general, the evaluation of a polynomial of high degree is computationally expensive and, moreover, is often subjected to numerical instabilities. De Casteljau's algorithm [46] is a recursive procedure reduces the complexity and constitutes an indispensable tool to evaluate a polynomial at a fixed point.

The algorithm is based on the simple recurrence relation

$$\mathfrak{B}^d_{\beta,T}(\tau) = \tau_1\mathfrak{B}^{d-1}_{\beta-e_1,T} + \tau_2\mathfrak{B}^{d-1}_{\beta-e_2,T} + \tau_3\mathfrak{B}^{d-1}_{\beta-e_3,T},$$

where $e_1 = (1,0,0)$, $e_2 = (0,1,0)$ and $e_3 = (0,0,1)$. It is an immediate consequence of the definition of $\mathfrak{B}^d_{\beta,T}$.

Theorem 1.2.1. *The value at $\tau = (\tau_1, \tau_2, \tau_3)$ of the polynomial p in (1.1) is given by*

$$p(\tau) = b^d_{(0,0,0)}(\tau),$$

where

$$\begin{aligned} &b^0_\beta(\tau) = b_\beta(\tau), \quad |\beta| = d,\\ &b^r_\beta(\tau) = \tau_1 b^{r-1}_{\beta-e_1} + \tau_2 b^{r-1}_{\beta-e_2} + \tau_3 b^{r-1}_{\beta-e_3}, \quad |\beta| = d-r, \text{ and } r = 1,\ldots,d. \end{aligned}$$

The intermediate values b^r_β are called De Casteljau ordinates.

The smoothness conditions between adjacent polynomial patches are easily expressed in terms of the BB-coefficients relative to the triangles. Let $\hat{T} := \langle V_4, V_2, V_3\rangle$ be an adjacent triangle to T and $\hat{p}$ a polynomial of total degree d defined on $\hat{T}$. Assume that V_4 has $\hat{\tau} := (\hat{\tau}_1, \hat{\tau}_2, \hat{\tau}_3)$ as vector of barycentric coordinates with respect to T. Then the function defined by assembling p and $\widehat{p}$ is of class C^r across the edge $\langle V_2, V_3\rangle$ if the B-ordinates $\hat{b}_{\beta,\hat{T}}$ of $\hat{p}$ satisfy for $\beta_1 = 0, \ldots, r$ and $\beta_2 + \beta_3 = d-r$ the conditions

$$\hat{b}_{\beta,\hat{T}} = \sum_{|\alpha|=\beta_1} b_{\alpha+\beta_2 e_2+\beta_3 e_3,T}\mathfrak{B}^r_{\alpha,T}(\hat{\tau}), \tag{1.2}$$

The conversion of the Bézier form to a different triangle can be neatly expressed in terms of polar form [41, 47]. In the next section, we briefly review some facts about polar forms or blossoming.

1.3 Polar forms

The construction of spline functions on triangulations greatly benefits from the use of blossoming or polarisation. In the following, we recall some basic properties of the polar forms of a polynomial.

The blossom or polar forms $\mathbf{B}[p_d]$ of a bivariate polynomial $p_d : \mathbb{R}^2 \to \mathbb{R}$ of degree d is the unique function $\mathbf{B}[p_d] : (\mathbb{R}^2)^d \to \mathbb{R}$ satisfying the following properties:

1. $\mathbf{B}[p_d]$ is symmetric, i.e. for any permutation σ of integers $1, \ldots, d$ it holds

$$\mathbf{B}[p_d](A_1, \ldots, A_d) = \mathbf{B}[p_d]\left(A_{\sigma(1)}, \ldots, A_{\sigma(d)}\right).$$

2. $\mathbf{B}[p_d]$ is multi-affine, i.e.

$$\mathbf{B}[p_d](A_1, \ldots, a\,B + b\,C, \ldots, A_d) = a\,\mathbf{B}[p_d](A_1, \ldots, B, \ldots, A_d) + b\,\mathbf{B}[p_d](A_1, \ldots, C, \ldots, A_d)$$

when $a + b = 1$.

3. $\mathbf{B}[p_d]$ is diagonal, i.e. $\mathbf{B}[p_d](A, \ldots, A) = p_d(A)$.

The B-ordinates of p with respect to T in (1.1) can be expressed in terms of polar forms. It holds

$$b_\beta = \mathcal{B}[p](V_1[\beta_1], V_2[\beta_2], V_3[\beta_3]),$$

where $V[\ell]$ means that the point V is repeated ℓ times as an argument of the polar forms, omitting the term $[\ell]$ when $\ell = 1$.

Moreover, the blossom of a product of linear polynomials can be expressed in terms of blossoms of its factors. More precisely, the following result holds [33].

Lemma 1.3.1. *Let π_d be the set of all permutations of integers $1, \ldots, d$, and p_i be polynomials in $\mathbb{P}_1$. Then,*

$$\mathbf{B}\left[\prod_{i=1}^{d} p_i\right](u_1, \ldots, u_d) = \frac{1}{d!} \sum_{\pi \in \pi_d} \prod_{i=1}^{d} p_i\left(u_{\pi(i)}\right).$$

Some results concerning a connection between polar forms and directional derivatives are given here. For every polynomial $p \in \mathbb{P}_d$, the q^{th} directional derivative of p with respect to vectors $\xi_1, \ldots, \xi_q \in \mathbb{R}^2$ is given by

$$D_{\xi_1, \ldots, \xi_q}\, p(u) = \frac{d!}{(d-q)!} \mathbf{B}[p](u[d-q], \xi_1, \ldots, \xi_q). \tag{1.3}$$

Let us recall the following restricted version of Lemma 4.1 given in [33] for further use.

Lemma 1.3.2. *Let d_1 and d_2 be two positive integers, with $d_2 \leq d_1$. Then, for any polynomial $p \in \mathbb{P}_{d_1}$ and any points $V_1, \ldots, V_{d_1 - d_2}$ in $\mathbb{R}^2$, function*

$$q(X) := \mathbf{B}[p](V_1, \ldots, V_{d_1-d_2}, X[d_2]), \tag{1.4}$$

is a polynomial of degree $\leq d_2$. Moreover, for any points $W_1, \ldots, W_{d_2}$ in $\mathbb{R}^2$, it holds

$$\mathbf{B}[q](W_1, \ldots, W_{d_2}) = \mathbf{B}[p](V_1, \ldots, V_{d_1-d_2}, W_1, \ldots, W_{d_2}).$$

Finding suitable transformations between different polynomial or spline bases is useful for solving some interpolation and quasi-interpolation problems coming from applications, particularly Computer Aided Geometric Design. Marsden's identity is a powerful tool that allows writing the monomials in terms of the corresponding B-splines.

In the following, we introduce the notion of control polynomials, which is the main tool to establish Marsden's identity for Powell-Sabin spline spaces. The controlled spline function's behavior at a vertex can be derived from one of the control polynomials at the same vertex. We use the notation $\partial_{a,b} f(P)$ for the partial derivative $\dfrac{\partial^{a+b} f}{\partial x^a \partial y^b}(P)$ of $f(x, y)$ at the point P.

Proposition 1.3.1. *Let d_1 and d_2 be two positive integers, with $d_2 \leq d_1$. Let $p \in \mathbb{P}_{d_1}$ and $V_1 \in \mathbb{R}^2$. For any real number θ, the polynomial q of degree d_2 defined by*

$$q(X) := \mathbf{B}[p]\left(V_1[d_1 - d_2],\, (\theta X + (1-\theta)V_1)[d_2]\right), \tag{1.5}$$

satisfies

$$\partial_{a,b}\, p\,(V_1) \;=\; \frac{1}{\theta^{a+b}}\,\frac{\binom{d_1}{a+b}}{\binom{d_2}{a+b}}\,\partial_{a,b}\, q(V_1)$$

for all $0 \leq a+b \leq d_2$.

Proof. We prove the result by induction on d_2. As blossoming is multi-affine, the polynomial function q can also be written as

$$q\,(X) = \sum_{i=0}^{d_2} \binom{d_2}{i}\,\theta^i\,\left(1-\theta\right)^{d_2-i}\,\mathbf{B}\,[p]\,(V_1[d_1-i],\, X[i])\,.$$

From Lemma 1.3.2, q is a polynomial of degree $\leq d_2$. Define the polynomial q_i of degree i as

$$q_i\,(X) :=\; \mathbf{B}\,[p]\,(V_1[d_1-i],\, X[i])\,,$$

and let $\xi_1 := (1,0)$ and $\xi_2 := (0,1)$.
Since $q_i \in \mathbb{P}_i$, we consider only the case when $a+b \leq i$ to derive the equality

$$\begin{aligned}
\partial_{a,b}\, q_i\,(V_1) \;&=\; \frac{i!}{(i-a-b)!}\,\mathbf{B}\,[q_i]\,(V_1[i-a-b],\, \xi_1[a],\, \xi_2[b]) \\
&=\; \frac{i!}{(i-a-b)!}\mathbf{B}\,[p]\,(V_1[i-a-b],\, \xi_1[a],\, \xi_2[b])\,.
\end{aligned}$$

Then,

$$\begin{aligned}
\partial_{a,b}\, q(V_1) \;&=\; \sum_{i=a+b}^{d_2} \frac{d_2!}{(d_2-i)!\,(i-a-b)!}\,\theta^i\,\left(1-\theta\right)^{d_2-i}\,\mathbf{B}\,[p]\,(V_1[i-a-b],\, \xi_1[a],\, \xi_2[b]) \\
&=\; \sum_{j=0}^{d_2-a-b} \frac{d_2!}{(d_2-a-b)!j!}\,\theta^{j+a+b}\,\left(1-\theta\right)^{d_2-a-b-j}\,\mathbf{B}\,[p]\,(V_1[d_1-a-b],\, \xi_1[a],\, \xi_2[b]) \\
&=\; \theta^{a+b}\,\frac{d_2!}{(d_2-a-b)!}\mathbf{B}\,[p]\,(V_1[d_1-a-b],\, \xi_1[a],\, \xi_2[b])\,,
\end{aligned}$$

and the proof is complete. □

When $\theta := \dfrac{d_1}{d_2}$, q is called control polynomial of degree d_2 at vertex V_1 of polynomial p.

1.4 Powell-Sabin partition

A Powell-Sabin (PS-) 6-split Δ_{PS} of Δ is a refinement of Δ obtained by splitting every triangle of Δ into six micro-triangles in the following way [18]:

1. In each triangle T_j, choose an interior point Z_j such that for every two neighboring triangles T_i and T_j the line joining Z_i and Z_j intersects the common edge. Denote this intersection point $R_{i,j}$ and include it to the list of vertices.

2. For each Z_j, connect it by a line with all vertices of T_j and include Z_j to the list of vertices.

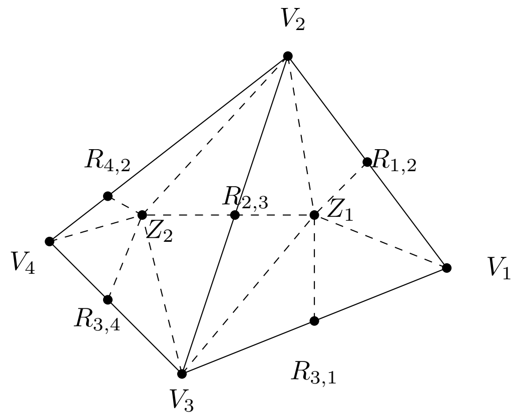

Figure 1.4: PS 6-split of two adjacent triangles: $T\langle V_1, V_2, V_3\rangle$ and $\hat{T}\langle V_4, V_2, V_3\rangle$.

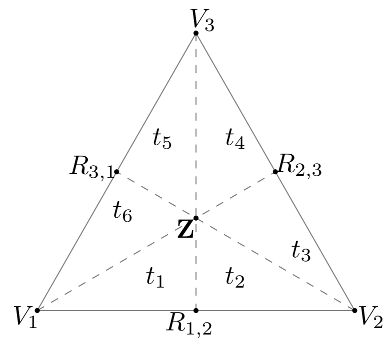

Figure 1.5: Powell-Sabin split of a single triangle $T\langle V_1, V_2, V_3\rangle$.

3. For each edge of the triangle T_j which

   (a) is common to a triangle T_i, join Z_j to $R_{i,j}$

   (b) is an edge of the boundary $\partial\Omega$, join Z_j to an arbitrary interior point on that edge.

An example of a PS 6-split of a triangle is shown in Figure1.4.

Figure 1.5 shows a 6-split of a single triangle, and we assume that the points indicated in the figure have the following barycentric coordinates:

$$V_1 = (1,0,0),\ V_2 = (0,1,0),\ V_3 = (0,0,1),\ Z = (z_1, z_2, z_3),$$
$$R_{12} = (\lambda_{12}, \lambda_{21}, 0),\ R_{23} = (0, \lambda_{23}, \lambda_{32}),\ R_{31} = (\lambda_{13}, 0, \lambda_{31}).$$

Define,

$$S_2^1(\Delta) := \left\{ s \in C^1(\Omega) : \quad s_{|T} \in \mathbb{P}_2 \text{ for all } T \in \Delta \right\}$$

as the linear space of piecewise quadratic polynomials on Δ. The following interpolation problem is considered: given any set of triples (f_i, f_i^x, f_i^y), $i = 1, \ldots, nv$, find $s(x,y) \in S_2^1(\Delta)$ such that,

$$s(V_i) = f_i, \quad \frac{\partial s}{\partial x}(V_i) = f_i^x \text{ and } \frac{\partial s}{\partial y}(V_i) = f_i^y, \tag{1.6}$$

It is clear that such a problem has no solution in general: in fact, problem (1.6) requires the imposition of nine parameters to define the quadratic polynomial on each triangle, while only six coefficients are available (see equation (1.1)).

In order to achieve a solution to the interpolation problem (1.6), one alternative is to interpolate in a different spaces as proposed by Powell and Sabin in [18], based on the subdivision of each triangle into six smaller triangles (PS-split). Hence, the conditions in (1.6) are imposed only on the vertices of the original triangulation, while in the other added nodes only C^1 smoothness conditions of the interpolating function are imposed. More details can be found in [18].

Each element $S_2^1(\Delta_{\mathrm{PS}})$ is uniquely defined by its values and derivatives at the vertices of Δ, thus the functional space $S_2^1(\Delta_{\mathrm{PS}})$ has dimension $3nv$. P. Dierckx [23] presented an elegant geometric method to construct a normalized basis for the spline space $S_2^1(\Delta_{\mathrm{PS}})$. Every Powell-Sabin spline can then be represented as

$$s(x,y) = \sum_{i=1}^{nv} \sum_{j=1}^{3} c_{i,j} \mathcal{B}_{i,j}(x,y),$$

where the functions $\mathcal{B}_{i,j}$ are called Powell-Sabin B-splines and $c_{i,j}$ are the coefficients of the representation. To obtain the basis functions $\mathcal{B}_{i,j}$, we first associate with each vertex V_i in the triangulation three linearly independent triplets $(\alpha_{i,j}, \beta_{i,j}, \gamma_{i,j})$, $j = 1, 2, 3$. The procedure proposed by P. Dierckx [23] to determine these triplets is highlighted as follows:

1. For each vertex V_i in Δ, find the corresponding PS-points of the vertex. These points are the immediately surrounding Bézier domain points of V_i in Δ_{PS}. The vertex V_i itself is also considered a PS-point.

2. For each vertex V_i, find a triangle $t_i \langle Q_{i,1}, Q_{i,2}, Q_{i,3} \rangle$ that contains all the PS-points corresponding to V_i. This triangle t_i is called PS-triangle associated with V_i. The Cartesian coordinates of the vertices $Q_{i,j}$, $j = 1, 2, 3$, are denoted in the rest of this report by $(X_{i,j}, Y_{i,j})$.

3. The three linearly independent triplets $(\alpha_{i,j}, \beta_{i,j}, \gamma_{i,j})$, $j = 1, 2, 3$, are obtained from the PS-triangle t_i corresponding to V_i as follows:

   - $\alpha_i = (\alpha_{i,1}, \alpha_{i,2}, \alpha_{i,3})$ are the barycentric coordinates of V_i with respect to t_i.
   - $\beta_i = (\beta_{i,1}, \beta_{i,2}, \beta_{i,3})$ and $\gamma_i = (\gamma_{i,1}, \gamma_{i,2}, \gamma_{i,3})$ are the unit barycentric directions with respect to t_i, in the x- and y-direction respectively. They can be given as follows:

$$\beta_{i,1} = \frac{\begin{vmatrix} 1 & X_{i,2} & X_{i,3} \\ 0 & Y_{i,2} & Y_{i,3} \\ 0 & 1 & 1 \end{vmatrix}}{\begin{vmatrix} X_{i,1} & X_{i,2} & X_{i,3} \\ Y_{i,1} & Y_{i,2} & Y_{i,3} \\ 1 & 1 & 1 \end{vmatrix}}, \quad \beta_{i,2} = \frac{\begin{vmatrix} X_{i,1} & 1 & X_{i,3} \\ Y_{i,1} & 0 & Y_{i,3} \\ 1 & 0 & 1 \end{vmatrix}}{\begin{vmatrix} X_{i,1} & X_{i,2} & X_{i,3} \\ Y_{i,1} & Y_{i,2} & Y_{i,3} \\ 1 & 1 & 1 \end{vmatrix}} \quad \text{and} \quad \beta_{i,3} = \frac{\begin{vmatrix} X_{i,1} & X_{i,2} & 1 \\ Y_{i,1} & Y_{i,3} & 0 \\ 1 & 1 & 0 \end{vmatrix}}{\begin{vmatrix} X_{i,1} & X_{i,2} & X_{i,3} \\ Y_{i,1} & Y_{i,2} & Y_{i,3} \\ 1 & 1 & 1 \end{vmatrix}}$$

$$\gamma_{i,1} = \frac{\begin{vmatrix} 0 & X_{i,2} & X_{i,3} \\ 1 & Y_{i,2} & Y_{i,3} \\ 0 & 1 & 1 \end{vmatrix}}{\begin{vmatrix} X_{i,1} & X_{i,2} & X_{i,3} \\ Y_{i,1} & Y_{i,2} & Y_{i,3} \\ 1 & 1 & 1 \end{vmatrix}}, \quad \gamma_{i,2} = \frac{\begin{vmatrix} X_{i,1} & 0 & X_{i,3} \\ Y_{i,1} & 1 & Y_{i,3} \\ 1 & 0 & 1 \end{vmatrix}}{\begin{vmatrix} X_{i,1} & X_{i,2} & X_{i,3} \\ Y_{i,1} & Y_{i,2} & Y_{i,3} \\ 1 & 1 & 1 \end{vmatrix}} \quad \text{and} \quad \gamma_{i,3} = \frac{\begin{vmatrix} X_{i,1} & X_{i,2} & 0 \\ Y_{i,1} & Y_{i,3} & 1 \\ 1 & 1 & 0 \end{vmatrix}}{\begin{vmatrix} X_{i,1} & X_{i,2} & X_{i,3} \\ Y_{i,1} & Y_{i,2} & Y_{i,3} \\ 1 & 1 & 1 \end{vmatrix}}$$

The Powell-Sabin B-spline $\mathcal{B}_{i,j}$ is defined as the unique solution of the interpolation problem (1.6) with all $\left(f_k, f_k^x, f_k^y\right) = (0,0,0)$ except for $k = i$, where $(f_i, f_i^x, f_i^y) = (\alpha_{i,j}, \beta_{i,j}, \gamma_{i,j})$.

The Powell-Sabin B-splines fulfil some useful properties in the context of finite element methods. These properties are listed as follows.

- Local support: each Powell-Sabin B-spline $\mathcal{B}_{i,j}$ has a local support. It is zero outside the union of all triangles in Δ that contain the vertex V_i.

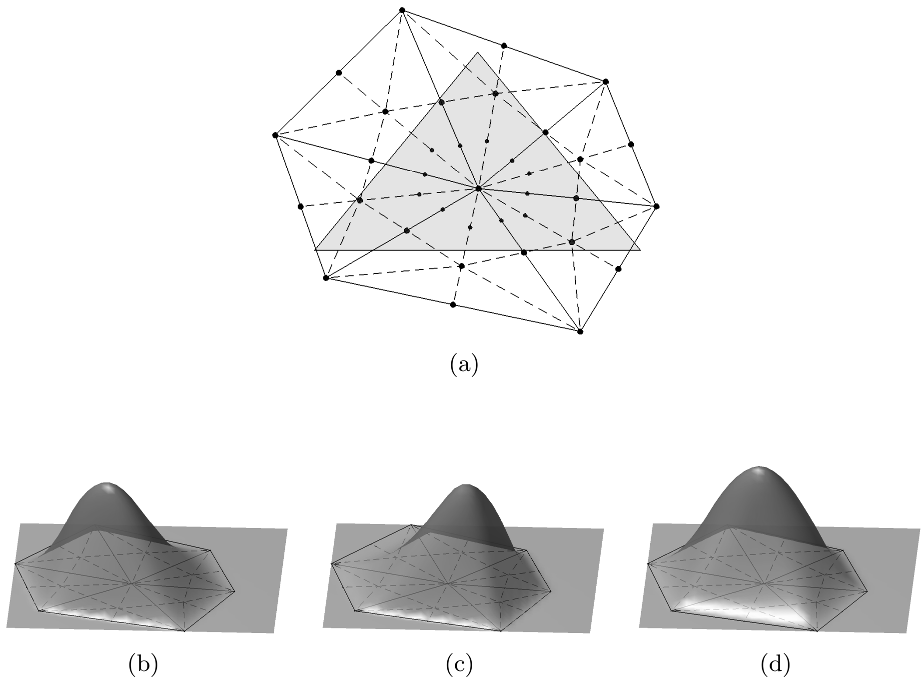

Figure 1.6: (a) A given triangulation with PS-split. (b)-(d) The three Powell-Sabin B-splines $\mathcal{B}_{i,j}$, $j = 1, 2, 3$, corresponding to the central vertex V_i and its PS-triangle.

- Non-negativity and convex partition of unity, i.e.,

$$\mathcal{B}_{i,j}\,(x, y) \geq 0 \text{ and } \sum_{i=1}^{nv}\sum_{j=1}^{3} \mathcal{B}_{i,j}\,(x, y) = 1,$$

  for all $(x, y) \in \Omega$.

- Powell-Sabin control triangles, i.e., defining the Powell-Sabin control points as $\mathbf{c}_{i,j} := (Q_{i,j}, c_{i,j})$, lead to Powell-Sabin control triangles $\mathbf{t}_i\,\langle \mathbf{c}_{i,1}, \mathbf{c}_{i,2}, \mathbf{c}_{i,3}\rangle$, which are tangent to the spline surface $z = s(x, y)$ at the vertices V_i.

- The Powell-Sabin spline basis is stable [48] for the max-norms $\|C\|_\infty = max_{i,j}|c_{i,j}|$ and $\|S\|_{\Omega,\infty} = max_\Omega|s(x, y)|$

  For all choices of the coefficient vector C, it has been proved in [48] that

$$K_\infty\|C\|_\infty \leq \|S\|_{\Omega,\infty} \leq \|C\|_\infty,$$

  where K_∞ depends only on the smallest angle θ_Δ in the triangulation Δ and on the size of the PS-triangles. Moreover, the smaller the PS-triangles the better (the larger) the stability constant.

- Approximation order: Let f be a function in the Sobolev space $\mathbf{W}_p^{k+1} = \left\{ f : \|f\|_{\mathbf{W}_p^{k+1}} < \infty \right\}$ endowed with the usual semi-norm and norm, i.e.,

$$|f|_{\mathbf{W}_p^{k+1}} = \left(\sum_{\alpha+\beta=k+1} \|D_x^\alpha D_y^\beta f(x, y)\|_{\mathbf{L}^p}^p \right)^{1/p} \text{ and } \|f\|_{\mathbf{W}_p^{k+1}} = \left(\sum_{r\leq k} |f|_{\mathbf{W}_p^{r+1}}^p \right)^{1/p}.$$

  For every $0 \leq k \leq 2$ and $0 \leq \alpha + \beta \leq k$, there exists a spline $s_f \in S_2^1\,(\Delta_{\text{PS}})$ such that

$$\|D_x^\alpha D_y^\beta (f - s_f)\|_{\mathbf{L}^p} \,\leq\, K_a\,|\Delta|^{k+1-\alpha-\beta}\,|f|_{\mathbf{W}_p^{k+1}}.$$

  The approximation constant K_a is independent of f and the mesh size $|\Delta|$.

Chapter 2

Approximation by quartic Powell-Sabin splines

Quartic Powell-Sabin splines have not received the same consideration in the literature as quadratic, cubic and quintic splines. C^1 quartic splines have been treated in [32]. Formally the constructed splines are C^1-continuous, although they are of class C^2 everywhere except across some edges of the refinement. They could be very useful in dealing with Digital Elevation Models in engineering as they provide global class approximations that allow important terrain details to be captured without smoothing them out too much and all this achieving the optimal approximation order.

In this chapter, we deal with approximation by quartic PS-splines. It is divided into two parts. The first one is devoted to solving a Hermite interpolation problem in the space of C^1-quartic PS-splines. Hermite interpolation is then easily computed by means of explicit formulas. In order to reach the C^1 continuity, high-dimensional systems of linear equations are not required to be solved, but only such ones of order six. Thus, several local quasi-interpolation schemes reproducing quartic polynomials and not requiring the resolution of any linear system are constructed. The primary tool used is Marsden's identity, established using the notion of control polynomials.

The main objectif of the second part is to characterize the geometry of Powell-Sabin triangulations that allows C^2 class bivariate quartic splines to be defined.

2.1 Quartic Powell-Sabin splines

One of the difficulties of bivariate interpolation (and, in general, multivariate interpolation) is that the insolvency of the problem depends on the geometry of the interpolation nodes. Thus, for insolvent problems it is difficult to express the solution by simple formulas. Chung and Yao's geometric characterization plays a fundamental role (see [49]). In view of such difficulties, splines over triangulations have been developed, in particular Powell-Sabin (PS-) splines.

2.1.1 The PS4-spline space

We are interested in the quartic PS-spline space and we recall some results from [32]. Let Ω be a polygonal domain in $\mathbb{R}^2$ and let $\Delta := \{T_i\}_{i=1}^{nt}$ be a regular triangulation of Ω. Denote by $V_i := (x_i, y_i)^T$, $i = 1, \ldots, nv$, the vertices of the given triangulation, and let Δ_{PS} be a PS-refinement of Δ, which divides each macro triangle $T_j \in \Delta$ into six micro-triangles (see Figure 1.4).

As in [32], the quartic Powell-Sabin spline space is defined as

$$S_4^1(\Delta) := \left\{ s \in \mathcal{C}^1(\Omega) : s_{|t} \in \mathbb{P}_4 \text{ for all } t \in \Delta_{PS} \right\}.$$

Consider the subspace

$$\tilde{S}_4(\Delta_{PS}) := \left\{ s \in S_4^1(\Delta_{PS}) : \, s \in \mathcal{C}^2 \left(\mathcal{V} \cup \mathcal{Z} \cup \mathcal{E} \cup \mathcal{E}^* \right) \right\}.$$

Its dimension is equal to $6nv + 3ne$, and we can consider the following unisolvent Hermite interpolation problem:

$$\begin{array}{rl} \text{Find} & s \in \tilde{S}_4\left(\Delta_{PS}\right) \\ \text{such that} & \partial_{a,b}\, s(V_i) \;=\; f_{i,a,b}\,, \;\; i = 1, \ldots, nv, \;\; a \geq 0, \; b \geq 0, \;\; a + b \leq 2, \\ & \mathbf{D}^a_{w_{i,j}}\, s(R_{ij}) \;=\; g^a_{i,j}, \;\; 0 \leq a \leq 2, \end{array} \tag{2.1}$$

being $w_{i,j}$ unit directions parallel to $\langle Z_k, R_{ij} \rangle$.

2.1.2 Normalized B-spline-like representation

Hereafter, we consider multi-indices $\alpha \in \mathbb{N}^3$ and $\bar{\alpha} \in \mathbb{N}^2$. Each spline $s \in \tilde{S}_4\left(\Delta_{PS}\right)$ can be represented as

$$s \;=\; \sum_{i=1}^{nv} \sum_{|\alpha|=2} c^v_{i,\alpha}\, \mathcal{B}^v_{i,\alpha} \;+\; \sum_{k=1}^{ne} \sum_{|\bar{\alpha}|=2} c^e_{k,\bar{\alpha}}\, \mathcal{B}^e_{k,\bar{\alpha}}, \tag{2.2}$$

where $\mathcal{B}^v_{i,\alpha}$ and $\mathcal{B}^e_{k,\bar{\alpha}}$ are B-splines-like functions with respect to vertices and edges, respectively, such that they are non-negative, have local support, form a partition of unity, and yield a stable basis to $\tilde{S}_4\left(\Delta_{PS}\right)$.

Regarding the vertices, the B-spline-like $\mathcal{B}^v_{i,\alpha}$ is defined as the solution of interpolation problem given by (2.1) with $f_{i,a,b} = \gamma^{a,b}_{i,\alpha}$, the remaining values $f_{k,a,b}$ are equal to zero and all $g^a_k = 0$ except for any k such that V_i is an end point of the edge $\mathfrak{e}_k$, in which case $g^a_k = \beta^a_{k,\bar{\alpha}}$. γ-values and β-values will be specified later.
Without loss of generality, we construct here only $\mathcal{B}^v_{1,\alpha}$. Because of the $\mathcal{C}^2$-smoothness at vertex V_1, the Bézier ordinates in the 2-disk around V_1 are completely determined by the value $\left\{ \gamma^{a,b}_{1,\alpha}, \;\; a \geq 0, b \geq 0, a + b \leq 2 \right\}$. The Bézier ordinates in the 2-disk around Z_1 are computed by defining a quadratic polynomial p^v_2 on the triangle with vertices

$$W_i := \frac{V_i + Z_1}{2}, \quad i = 1, 2, 3. \tag{2.3}$$

The ordinates of this polynomial are

$$\begin{array}{l} b_{2,0,0} = d_7, \quad b_\alpha = 0 \text{ for all } \alpha \in \mathbb{N}^3 \setminus \{(2,0,0)\}\,, |\alpha| = 2, \\ \quad d^v_{18} = \lambda_{12} d^v_7, \quad d^v_{19} = \lambda^2_{12} d^v_7, \quad d^v_{20} = \lambda_{13} d^v_7, \quad d^v_{21} = \lambda^2_{13} d^v_7, \\ \quad d^v_{22} = z_1 d^v_7, \quad d^v_{23} = \lambda_{12} z_1 d^v_7, \quad d^v_{24} = \lambda_{13} z_1 d^v_7, \quad d^v_{25} = z^2_1 d^v_7. \end{array}$$

Note that the B-ordinates d_5, d_{10} and d_{11} can be considered as B-ordinates after subdivision of a quadratic polynomial p^e_2 defined on the edge $\left\langle \frac{V_1 + R_{12}}{2}, \frac{V_2 + R_{12}}{2} \right\rangle$. This polynomial of degree 2 has the value d_5, 0 and 0 as its three B-ordinates. A similar reasoning holds for the B-ordinates d_6, d_{12} and d_{13}:

$$\begin{array}{llll} d^v_{10} = \lambda_{12} d^v_5, & d^v_{11} = \lambda^2_{12} d^v_5, & d^v_{12} = \lambda_{12} d^v_6, & d^v_{13} = \lambda^2_{12} d^v_6, \\ d^v_{14} = \lambda_{13} d^v_9, & d^v_{15} = \lambda^2_{13} d^v_9, & d^v_{16} = \lambda_{13} d^v_8, & d^v_{17} = \lambda^2_{13} d^v_8. \end{array}$$

We define $\beta^0_{k,\bar{\alpha}} = d^v_{11}$, $\beta^1_{k,\bar{\alpha}} = d^v_{13}$ and $\beta^2_{k,\bar{\alpha}} = d^v_{19}$.

Now, consider an edge. The corresponding B-spline-like $\mathcal{B}^e_{k,\bar{\alpha}}$ is defined as the solution of interpolation problem given by (2.1) where all $f_{m,a,b}$ are equal to zero, as well as all g^a_m except

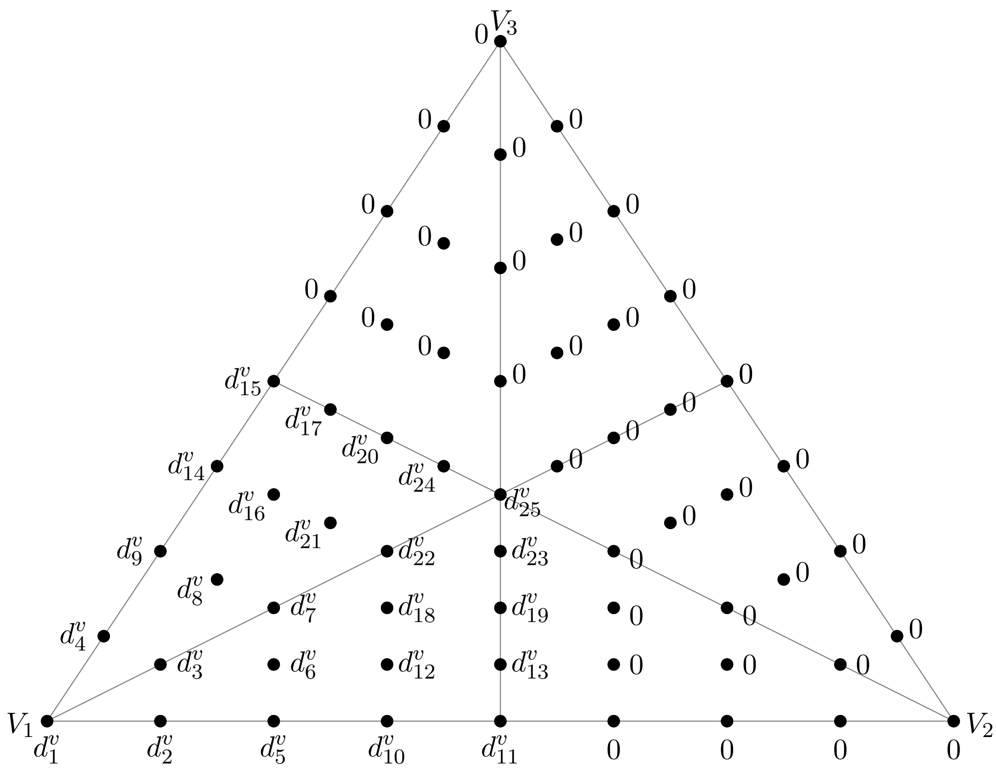

Figure 2.1: B-ordinates of a B-spline with respect to vertex V_1.

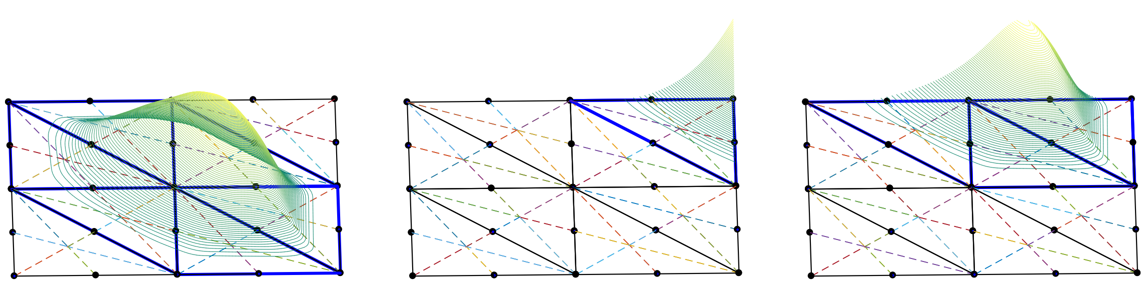

Figure 2.2: A vertex B-spline in a different molecules.

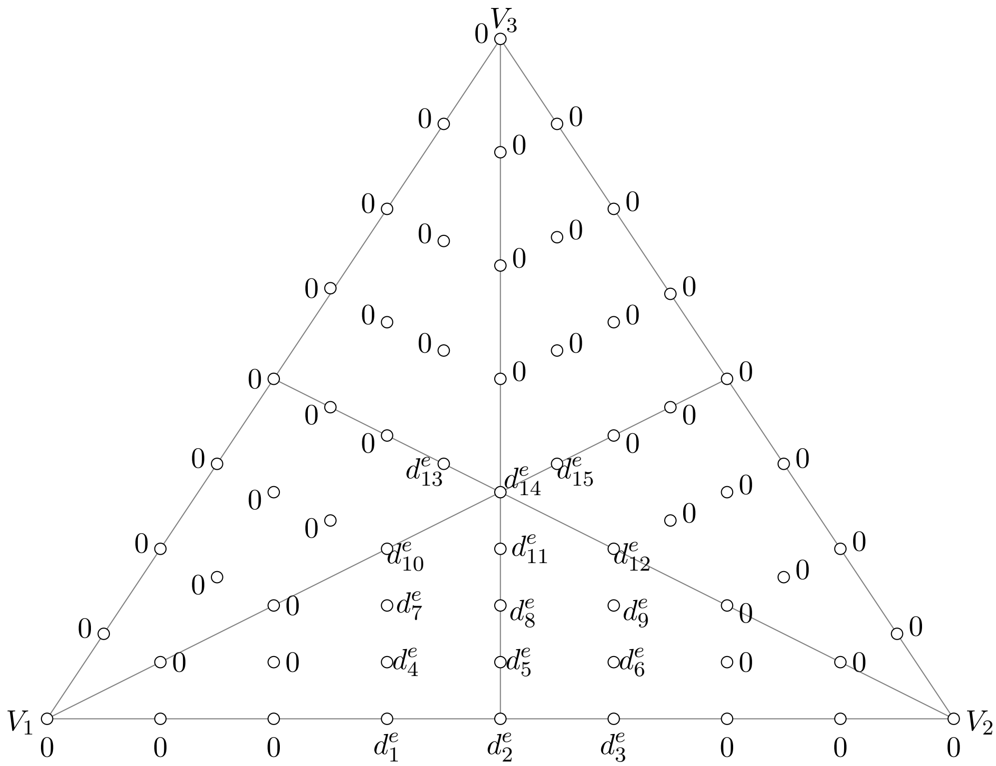

Figure 2.3: B-ordinates of B-spline-like function with respect to $\mathfrak{e}_1 := \langle V_1,\, V_2\rangle$.

for any $m = k$ where $g_k^a = \beta_{k,\bar{\alpha}}^a$. The β-values are given in (2.5).
Using the fact that the spline is $\mathcal{C}^2$-smooth across $\langle Z_1,\, R_{12}\rangle$, then, the B-ordinates d_1, d_2 and d_3 can be regarded as B-ordinates after subdivision of a univariate quadratic polynomial p_2^e defined on the segment $\langle \frac{V_1+R_{12}}{2},\, \frac{V_2+R_{12}}{2}\rangle$. This polynomial is chosen to have 0, $\beta_{k,\bar{\alpha}}^0$ and 0 as its three B-ordinates, for some parameter $\beta_{k,\bar{\alpha}}^0$. The same idea is used to compute d_4, d_5 and d_6, but this time with other parameter noted $\beta_{k,\bar{\alpha}}^1$. By $\mathcal{C}^2$-smoothness around Z_1, the ordinates $d_7, \ldots, d_{15}$ can be determined. To this end, we define a quadratic polynomial over the triangle with the vertices defined in (2.3) in such a way that it has the following B-ordinates:

$$b_{2,0,0} = 0,\; b_{0,2,0} = 0,\; b_{0,0,2} = 0,\; b_{1,1,0} = \beta_{k,\bar{\alpha}}^2,\; b_{0,1,1} = 0,\; b_{1,0,1} = 0.$$

Then, the B-ordinates are given by

$$\begin{aligned}
&d_1^e = \lambda_{21}\,\beta_{k,\bar{\alpha}}^0,\; d_2^e = 2\lambda_{12}\lambda_{21}\,\beta_{k,\bar{\alpha}}^0,\; d_3^e = \lambda_{12}\,\beta_{k,\bar{\alpha}}^0,\; d_4^e = \lambda_{21}\,\beta_{k,\bar{\alpha}}^1,\; d_5^e = 2\lambda_{12}\lambda_{21}\,\beta_{k,\bar{\alpha}}^1,\\
&d_6^e = \lambda_{12}\,\beta_{k,\bar{\alpha}}^1,\; d_7^e = \lambda_{12}\,\beta_{k,\bar{\alpha}}^2,\; d_8^e = 2\lambda_{12}\lambda_{21}\,\beta_{k,\bar{\alpha}}^2,\; d_9^e = \lambda_{12}\,\beta_{k,\bar{\alpha}}^2,\; d_{10}^e = z_2\,\beta_{k,\bar{\alpha}}^2,\\
&d_{11}^e = (z_2\lambda_{12} + z_1\lambda_{21})\,\beta_{k,\bar{\alpha}}^2,\; d_{12}^e = z_1\,\beta_{k,\bar{\alpha}}^2, d_{13}^e = z_2\lambda_{13}\,\beta_{k,\bar{\alpha}}^2,\; d_{14}^e = 2z_1z_2\,\beta_{k,\bar{\alpha}}^2,\; d_{15}^e = z_1\lambda_{23}\,\beta_{k,\bar{\alpha}}^2
\end{aligned}$$

In order to ensure non-negativity, it suffices to impose that all B-ordinates of the B-spline-like $\mathcal{B}_{k,\bar{\alpha}}^e$ are non-negative. This is the case when

$$\beta_{k,\bar{\alpha}}^a \geq 0 \quad \text{for all} \quad a = 0,\, 1,\, 2. \tag{2.4}$$

Then, we need to choose the triplets of parameters $\beta_{k,(2,0)} := \left(\beta_{k,(2,0)}^0,\, \beta_{k,(2,0)}^1,\, \beta_{k,(2,0)}^2\right)$, $\beta_{k,(1,1)} := \left(\beta_{k,(1,1)}^0,\, \beta_{k,(1,1)}^1,\, \beta_{k,(1,1)}^2\right)$ and $\beta_{k,(0,2)} := \left(\beta_{k,(0,2)}^0,\, \beta_{k,(0,2)}^1,\, \beta_{k,(0,2)}^2\right)$ satisfying the condition in (2.4) in order to define three non-negative basis functions related to the edge $\mathfrak{e}_k$. Depending on the type of the edge $\mathfrak{e}_k$, we choose these parameters as follows:

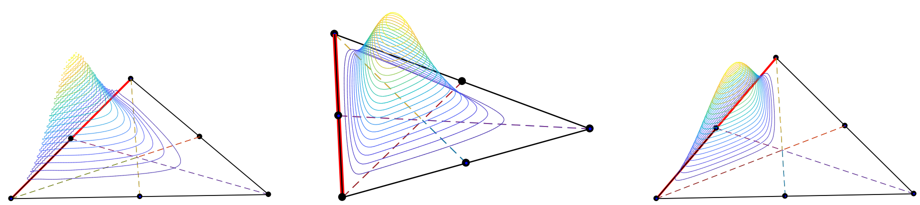

Figure 2.4: The three Edge B-splines with respect to an edge.

- If $\mathfrak{e}_k$ is an interior edge, so that there is another adjacent macro-triangle T' and the line through the split points Z_1 and Z_2 intersects the edge in R_{12}, then

$$\begin{aligned}
\beta_{k,(2,0)} &:= \left(\frac{\|R_{12}-Z_2\|^2}{\|Z_1-Z_2\|^2}, \frac{\|R_{12}-Z_2\|}{\|Z_1-Z_2\|}, 1 \right), \\
\beta_{k,(1,1)} &:= \left(\frac{2\|R_{12}-Z_1\|\|R_{12}-Z_2\|}{\|Z_1-Z_2\|^2}, \frac{\|R_{12}-Z_1\|}{\|Z_1-Z_2\|}, 0 \right), \\
\beta_{k,(0,2)} &:= \left(\frac{\|R_{12}-Z_1\|^2}{\|Z_1-Z_2\|^2}, 0, 0 \right).
\end{aligned} \tag{2.5}$$

- If $\mathfrak{e}_k$ is a boundary edge, then $\beta_{k,(2,0)} := (0,0,1)$, $\beta_{k,(1,1)} := (0,\ 1,\ 0)$ and $\beta_{k,(0,2)} := (1,0,0)$.

Figure 2.4 shows the plots of the three B-splines-like functions with respect to an edge.

2.1.3 A geometric approach to form a convex partition of unity

Now we recall a geometric approach to form a convex partition of unity [32]. Following the same arguments as for quadratic Powell-Sabin B-splines [23], we define the PS4-points and PS4-triangles as follows: for each vertex V_i in Δ, the PS4-points are

$$V_i, \quad S_{i,Z} = \frac{1}{2}(V_i + Z) \quad \text{and} \quad S_{i\ell} = \frac{1}{2}(V_i + R_{i\ell}).$$

For each $V_\ell \in M_{v_i}$ (i.e. the union of all the triangles in Δ having V_i as a vertex) and for each split point Z of T_Z, where V_i is a vertex of T_Z, determine a triangle $t_i\left\langle Q^v_{i,1},\ Q^v_{i,2},\ Q^v_{i,3}\right\rangle$ containing all PS4-points. This triangle is called PS4-triangle.

The following result holds (see [32] and references therein).

Theorem 2.1.1. *The B-splines-like $\mathcal{B}^v_{i,\alpha}$ and $\mathcal{B}^e_{k,\bar\alpha}$ are nonnegative and form a convex partition of unity if the parameters $\gamma^{a,b}_{i,\alpha}$, $i = 1, \ldots, nv, \alpha \in \mathbb{N}^3, |\alpha| = 2,\ a \geq 0,\ b \geq 0,\ a+b \leq 2$, and $\beta^a_{k,\bar\alpha}$, $k = 1, \ldots, n_e, \bar\alpha \in \mathbb{N}^2,\ |\bar\alpha| = 2,\ a = 0, 1, 2,$ defining them are given by $\gamma^{ab}_{i,\alpha} = \partial_{a,b}\, \mathfrak{B}^2_\alpha\,(V_i)$, $\mathfrak{B}^2_\alpha$ being a quadratic Bernstein-Bézier polynomial defined on t_i, and $\beta^a_{k,\bar\alpha}$ being the values given in (2.5).*

Note that each B-spline-like $\mathcal{B}^v_{i,\alpha}$ is related to a quadratic Bernstein basis. Then, the coefficient $c^v_{i,\alpha}$ in (2.2) can be represented schematically as in Figure 2.5 with respect to a PS4-triangle. We can consider this coefficients as B-ordinates of a control polynomial of degree 2 defined on t_i with respect to a vertex V_i. The control or tangent polynomial is noted $T_i(x,y)$ and satisfies

$$\partial_{a,b}\, s\,(V_i) = \left(\frac{2}{4}\right)^{a+b} \frac{12}{(4-a-b)\,(3-a-b)} \partial_{a,b}\, T_i\,(V_i)\,.$$

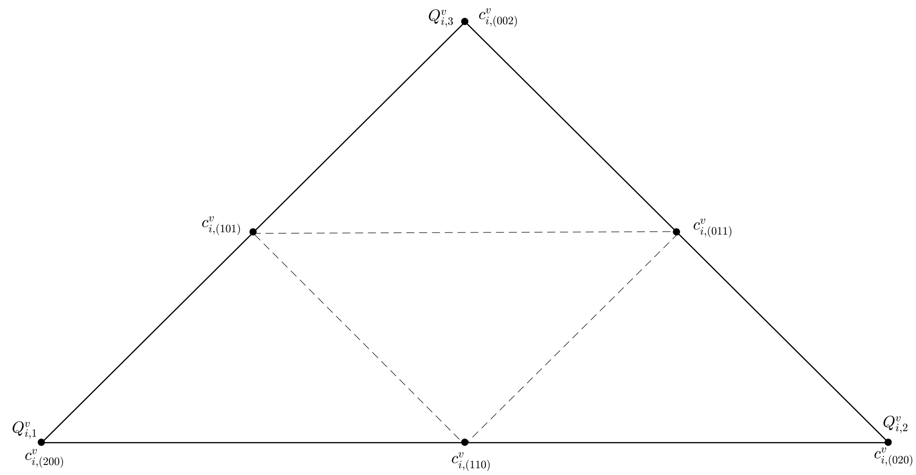

Figure 2.5: Schematic representation of the B-spline coefficients $c^v_{i,\alpha}$, $|\alpha| = 2$ with respect to the PS4-triangle $t_i = (Q^v_{i,1}, Q^v_{i,2}, Q^v_{i,3})$.

2.2 Interpolation with quartic Powell-Sabin splines

This section is devoted to derive explicit expressions for the PS4-spline coefficients in the B-spline representation (2.2) to satisfy the conditions in the interpolation problem given by (2.1).

Firstly, we consider the interpolation problem with respect to partial derivatives at vertices that appear in (2.1). Then, we will deal with conditions regarding directional derivatives at R_{ij} points.

2.2.1 Interpolation at a vertex

As mentioned above, the coefficients $c^v_{i,\alpha}$ can be seen as B-ordinates defined on PS4-triangles. We make use of a function $G_i(P, Q)$ with points $P = (x_p, y_p)$ and $Q = (x_q, y_q)$ as arguments. It is defined as

$$\begin{aligned} G_i(P,Q) = f_i &+ \frac{1}{2}\left((x_p - x_i) + (x_q - x_i)\right) f_{i,1,0} + \frac{1}{2}\left((y_p - y_i) + (y_q - y_i)\right) f_{i,0,1} \\ &+ \frac{1}{3}\left((x_p - x_i)(y_q - y_i) + (x_q - x_i)(y_p - y_i)\right) f_{i,1,1} \\ &+ \frac{1}{3}(x_p - x_i)(x_q - x_i) f_{i,2,0} + \frac{1}{3}(y_p - y_i)(y_q - y_i) f_{i,0,2}. \end{aligned}$$

Then, the following result holds.

Theorem 2.2.1. *If a spline $s \in \tilde{S}_4(\Delta_{PS})$ has B-ordinates*

$$\begin{aligned} c^v_{i,(200)} &= G_i(Q^v_{i,1}, Q^v_{i,1}), & c^v_{i,(110)} &= G_i(Q^v_{i,1}, Q^v_{i,2}), & c^v_{i,(020)} &= G_i(Q^v_{i,2}, Q^v_{i,2}), \\ c^v_{i,(011)} &= G_i(Q^v_{i,2}, Q^v_{i,3}), & c^v_{i,(002)} &= G_i(Q^v_{i,3}, Q^v_{i,3}), & c^v_{i,(101)} &= G_i(Q^v_{i,1}, Q^v_{i,3}), \end{aligned}$$

then, it satisfies the interpolation conditions at vertex V_i given in (2.1).

2.2.2 Interpolation across an edge

Let $\mathcal{T}$ be the triangle with vertices V_1, $S_{12} = \frac{1}{2}(V_1 + R_{12})$ and $S_{1,Z} = \frac{1}{2}(V_1 + Z)$.

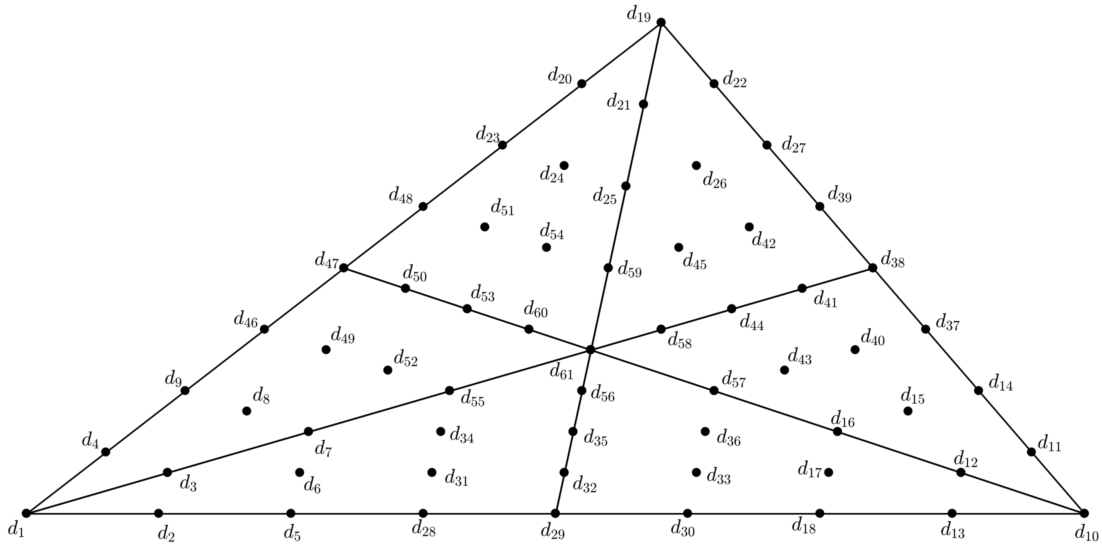

Figure 2.6: Schematic representation of the B-ordinates of PS4-spline.

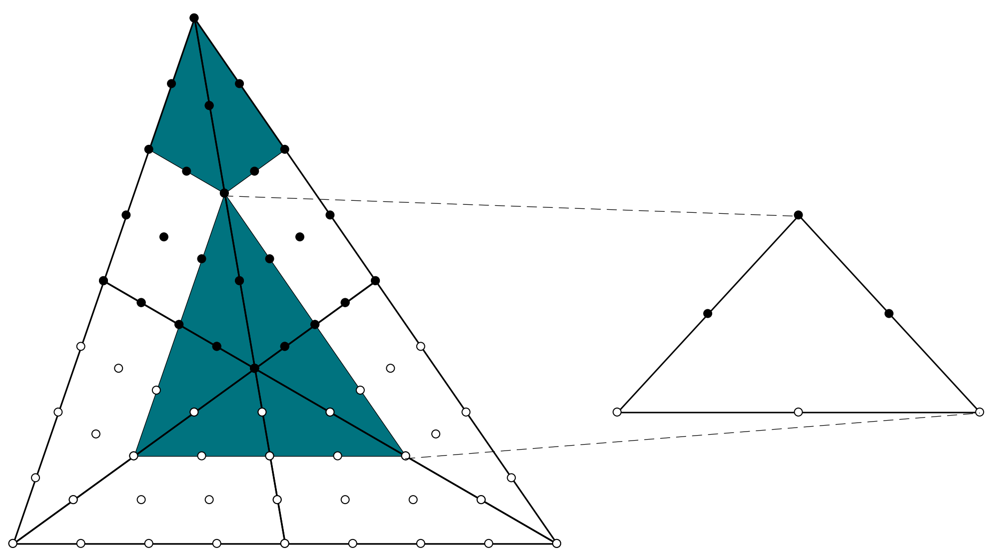

Figure 2.7: B-ordinates of a B-spline-like with respect to a vertex. B-ordinates that are known to be zero are indicated by open bullets ○. The remaining ones are indicated by filled bullets •.

Define the tangent polynomial $T_1(x,y)$ defined on $\mathcal{T}$ by the ordinates $e_{1,\alpha}$, $|\alpha| = 2$ (see Figure 2.8). By blossoming,

$$d_1 = e_{1,(200)} = \mathbf{B}[T]\left(\Gamma^1,\Gamma^1\right), \qquad d_2 = e_{1,(110)} = \mathbf{B}[T]\left(\Gamma^1,\Gamma^2\right), \qquad d_3 = e_{1,(101)} = \mathbf{B}[T]\left(\Gamma^1,\Gamma^3\right),$$
$$d_5 = e_{1,(020)} = \mathbf{B}[T]\left(\Gamma^2,\Gamma^2\right), \qquad d_6 = e_{1,(011)} = \mathbf{B}[T]\left(\Gamma^2,\Gamma^3\right), \qquad d_7 = e_{1,(002)} = \mathbf{B}[T]\left(\Gamma^3,\Gamma^3\right),$$

where $\Gamma^1 = (\Gamma^1_1,\Gamma^1_2,\Gamma^1_3)$, $\Gamma^2 = (\Gamma^2_1,\Gamma^2_2,\Gamma^2_3)$ and $\Gamma^3 = (\Gamma^3_1,\Gamma^3_2,\Gamma^3_3)$ are the barycentric coordinates of V_1, S_{12} and $S_{1,Z}$ with respect to PS4-triangle t_1, respectively. Analogously, the remaining ordinates d_i, $1 \le i \le 27$, are derived.

Let us consider parameters β_1 and β_2 defined as follows:

- If ε_k is a boundary edge, then

$$\beta_1 := c^e_{k,3},\ \beta_2 := c^e_{k,2}.$$

- If ε_k is an interior edge, then

$$\beta_1 := \beta^0_{k,(20)}c^e_{k,1} + \beta^0_{k,(11)}c^e_{k,2} + \beta^0_{k,(02)}c^e_{k,3},\ \beta_2 := \beta^1_{k,(20)}c^e_{k,1} + \beta^1_{k,(11)}c^e_{k,2} + \beta^1_{k,(02)}c^e_{k,3}.$$

By $\mathcal{C}^2$-regularity across $\langle Z\,, R_{12}\rangle$ the B-ordinates $d_{28},\ldots,d_{33}$ can be obtained. For, d_{28}, d_{29} and d_{30}, define $\langle P_1,\, P_2\rangle$, with $P_i = \frac{1}{2}(V_i + R_{12})$, $i = 1,2$, the polynomial function $\hat{P}_1$ with B-ordinates d_5, β_1 and d_{18}. Then,

$$d_{28} = \lambda_{12}\, d_5 \,+\, \lambda_{21}\, \beta_1, \qquad d_{30} = \lambda_{12}\, \beta_1 \,+\, \lambda_{21}\, d_{18}, \qquad d_{29} = \lambda_{12}\, d_{28} \,+\, \lambda_{21}\, d_{30}.$$

Now, for d_{31}, d_{32} and d_{33}, we define on $\left\langle \tilde{P}_1,\, \tilde{P}_2\right\rangle$, with $\tilde{P}_i = \frac{1}{4}(2V_i + Z + R_{12})$, $i = 1,2$, the polynomial $\hat{P}_2$ with B-ordinates d_6, β_2 and d_{17}. Then

$$d_{31} = \lambda_{12}\, d_6 \,+\, \lambda_{21}\, \beta_2, \qquad d_{33} = \lambda_{12}\, \beta_2 \,+\, \lambda_{21}\, d_{17}, \qquad d_{32} = \lambda_{12}\, d_{31} \,+\, \lambda_{21}\, d_{33}.$$

Similar expressions can be obtained for $d_{34},\ldots,d_{45}$. Finally, the B-ordinates $d_{46},\ldots,d_{61}$ can be computed by exploiting the $\mathcal{C}^2$-smoothness at the split point Z. They can be seen as ordinates after subdivision of a quadratic polynomial $\hat{p}$ defined on the triangle defined by the points $P_i = \frac{1}{2}(V_i + Z)$, $i = 1,2,3$. The B- ordinates of this quadratic polynomial $\hat{p}$ are

$$b_{2,0,0} = d_7,\ b_{0,2,0} = d_{16},\ d_{0,0,2} = d_{25},\ b_{1,1,0} = c^e_{3,1},\ b_{1,0,1} = c^e_{2,1},\ d_{0,1,1} = c^e_{1,1}.$$

Therefore,

$$\begin{array}{ll} d_{46} = \lambda_{12}d_7 + \lambda_{21}c^e_{3,1}, & d_{47} = \lambda_{12}d_{46} + \lambda_{21}d_{48}, \\ d_{48} = \lambda_{12}c^e_{3,1} + \lambda_{21}d_{16}, & d_{55} = z_1 d_7 \,+\, z_2 c^e_{3,1} + z_3 c^e_{2,1}, \\ d_{56} = \lambda_{12}d_{55} + \lambda_{21}d_{57}, & d_{57} = z_1 c^e_{3,1} + z_2 d_{16} + z_3 c^e_{1,1}, \\ d_{59} = z_1 c^e_{2,1} \,+\, z_2 c^e_{1,1} + z_3 d_{25}, & d_{61} = z_1 d_{55} + z_2 d_{57} + z_3 d_{59}. \end{array}$$

Similar expressions are obtained for the remaining B-ordinates.

The B-coefficients $c^e_{k,j}$, $j = 1,2,3$, with respect to the edge $\varepsilon_k := \langle V_1,\, V_2\rangle$ have the following expressions:

- If ε_k is a boundary edge, then

$$\begin{aligned} c_{k,1} &= \frac{-d_7\lambda_{12}^2 - d_{16}\lambda_{21}^2 - g^0_{1,2} + 2g^1_{1,2} + g^2_{1,2}}{2\lambda_{12}\lambda_{21}}, \\ c_{k,2} &= \frac{-d_6\lambda_{12}^2 - d_{17}\lambda_{21}^2 + g^0_{1,2} + g^1_{1,2}}{2\lambda_{12}\lambda_{21}}, \\ c_{k,3} &= \frac{-d_5\lambda_{12}^2 - d_{18}\lambda_{21}^2 + g^0_{1,2}}{2\lambda_{12}\lambda_{21}}. \end{aligned} \tag{2.6}$$

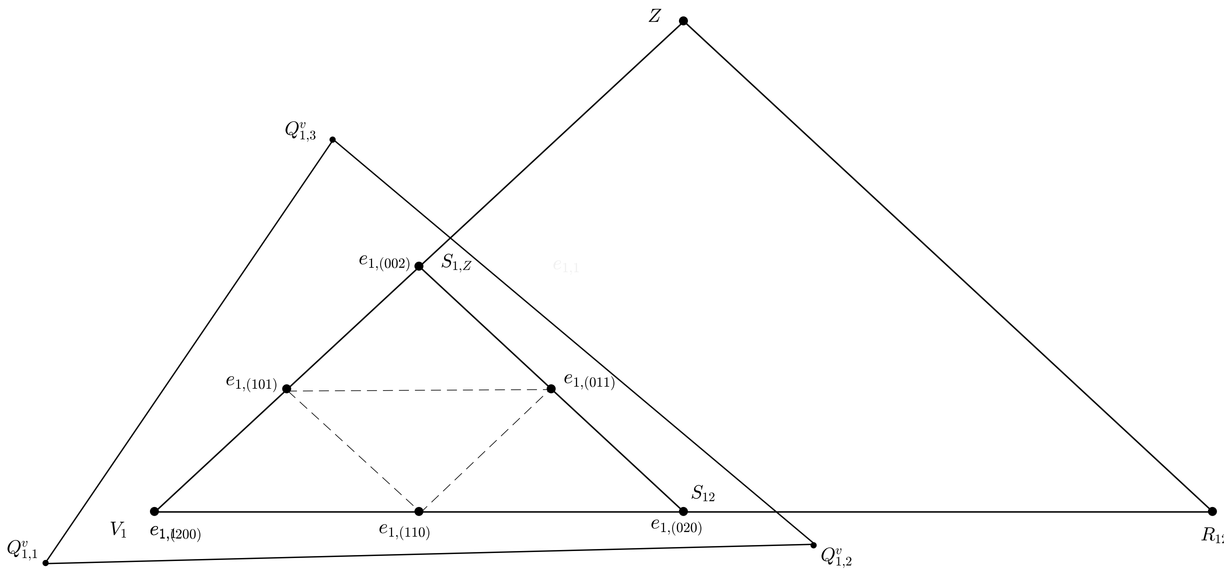

Figure 2.8: A PS4-triangle $t_1 = (Q^v_{1,1}, Q^v_{1,2}, Q^v_{1,3})$ of vertex V_1 containing the PS4-points V_1, S_{12} and $S_{1,Z}$, together with the schematic representation of the Bézier ordinates $e_{1,\alpha}$, $|\alpha| = 2$, of the subdivided tangent polynomial $T_1(x, y)$ onto the triangle with V_1 as vertex.

- If ε_k is an interior edge, then

$$\begin{aligned}
c_{k,1} &= -\frac{d_7\lambda_{12}^2 + d_{16}\lambda_{21}^2 + g^0_{1,2} - 2g^1_{1,2} - g^2_{1,2}}{2\lambda_{12}\lambda_{21}},\\
c_{k,2} &= \frac{\left(d_7\lambda_{12}^2 + d_{16}\lambda_{21}^2 + g^0_{1,2} - 2g^1_{1,2} - g^2_{1,2}\right)\|R_{12} - Z_2\| + \|Z_2 - Z_1\|\left(-d_6\lambda_{12}^2 - d_{17}\lambda_{21}^2 + g^0_{1,2} + g^1_{1,2}\right)}{2\lambda_{12}\lambda_{21}\|R_{12} - Z_1\|},\\
c_{k,3} &= \frac{1}{2\lambda_{12}\lambda_{21}\|R_{12} - Z_1\|^2}\left(-2\|Z_2 - Z_1\|\left(-d_6\lambda_{12}^2 - d_{17}\lambda_{21}^2 + g^0_{1,2} + g^1_{1,2}\right)\|R_{12} - Z_2\|\right.\\
&\quad \left. - \left(d_7\lambda_{12}^2 + d_{16}\lambda_{21}^2 + g^0_{1,2} - 2g^1_{1,2} - g^2_{1,2}\right)\|R_{12} - Z_2\|^2 + \|Z_2 - Z_1\|^2\left(-d_5\lambda_{12}^2 - d_{18}\lambda_{21}^2 + g^0_{1,2}\right)\right).
\end{aligned} \tag{2.7}$$

2.3 Marsden's identity

In order to represent the monomial basis in terms of the B-splines, we use Marsden's identity. Let $Q^v_{i,j}$ be the vertices of PS4-triangle t_i, and define :

$$\begin{aligned}
\tilde{Q}^v_{i,j} &:= 2\,Q^v_{i,j} - V_i, \qquad i = 1, \ldots, nv, j = 1, 2, 3,\\
\tilde{Q}^e_{k,j} &:= 2\,Q^e_{k,j} - R_k, \qquad k = 1, \ldots, ne, j = 1, 2.
\end{aligned}$$

$Q^e_{k,j}$, $j = 1, 2$, belong to a straight line $\left\langle Z, \tilde{Z}\right\rangle$ where Z and $\tilde{Z}$ are the split points of two adjacent macro-triangles.

Theorem 2.3.1. *Let $\mathcal{Q}p$ be the spline defined as*

$$\begin{aligned}
\mathcal{Q}p := &\sum_{i=1}^{nv}\sum_{|\alpha|=2} \mathbf{B}\,[p]\left(V_i[2],\, \tilde{Q}^v_{i,1}[\alpha_1],\, \tilde{Q}^v_{i,2}[\alpha_2],\, \tilde{Q}^v_{i,3}[\alpha_3]\right)\mathcal{B}^v_{i,\alpha}\\
&+ \sum_{k=1}^{ne}\sum_{|\bar{\alpha}|=2} \mathbf{B}\,[p]\left(V_{k,1}, V_{k,2},\, \tilde{Q}^e_{k,1}[\bar{\alpha}_1],\, \tilde{Q}^e_{k,2}[\bar{\alpha}_2]\right)\mathcal{B}^e_{k,\bar{\alpha}}.
\end{aligned}$$

Then, $\mathcal{Q}p = p$ for all $p \in \mathbb{P}_4$.

Proof. It is clear that $\mathcal{Q}p = p$ for all $p \in \mathbb{P}_4$ if and only if

$$\partial_{a,b}\,\mathcal{Q}p\,(V_i) \;=\; \partial_{a,b}\,p\,(V_i)\;, \quad i = 1,\ldots,nv, \quad a \geq 0,\, b \geq 0,\; a+b \leq 2,$$

and

$$\mathbf{D}^a_{w_{i,j}}\,\mathcal{Q}p(R_{ij}) \;=\; \mathbf{D}^a_{w_{i,j}}\,p(R_{ij}), \quad 0 \leq a \leq 2,$$

where $w_{i,j}$ is a unit direction parallel to $\langle Z_k, R_{ij}\rangle$.
Since

$$\mathcal{Q}p\,(V_i) = \sum_{|\alpha|=2} \mathbf{B}\,[p]\left(V_i[2],\,\tilde{Q}^v_{i,1}[\alpha_1],\,\tilde{Q}^v_{i,2}[\alpha_2],\,\tilde{Q}^v_{i,3}[\alpha_3]\right)\,\mathcal{B}^v_{i,\alpha}\,(V_i)\,,$$

define

$$q(X) := \sum_{|\alpha|=2} \mathbf{B}\,[p]\left(V_i[2],\,\tilde{Q}^v_{i,1}[\alpha_1],\,\tilde{Q}^v_{i,2}[\alpha_2],\,\tilde{Q}^v_{i,3}[\alpha_3]\right)\,\mathcal{B}^v_{i,\alpha}(X).$$

Then,

$$\partial_{a,b}q(V_i) = \left(\frac{1}{2}\right)^{a+b}\frac{\binom{4}{a+b}}{\binom{2}{a+b}}\sum_{|\alpha|=2} \mathbf{B}\,[p]\left(V_i[2],\,\tilde{Q}^v_{i,1}[\alpha_1],\,\tilde{Q}^v_{i,2}[\alpha_2],\,\tilde{Q}^v_{i,3}[\alpha_3]\right)\,\mathfrak{B}^2_{t_i,\alpha}(V_i).$$

Let $\tilde{q}(X) := \mathbf{B}\,[p]\left(V_i^2,\,(2X - V_i)^2\right)$. It is a polynomial in $\mathbb{P}_2$. On a PS4-triangle t_i, $\tilde{q}$ can be written as

$$\begin{aligned}
\tilde{q}(X) &= \sum_{|\alpha|=2} \mathbf{B}\,[q]\left(Q^v_{i,1}[\alpha_1],\,Q^v_{i,2}[\alpha_2],\,Q^v_{i,3}[\alpha_3]\right)\,\mathfrak{B}^2_{t_i,\alpha}\,(X)\\
&= \sum_{|\alpha|=2} \mathbf{B}\,[p]\left(V_i[2],\,\tilde{Q}^v_{i,1}[\alpha_1],\,\tilde{Q}^v_{i,2}[\alpha_2],\,\tilde{Q}^v_{i,3}[\alpha_3]\right)\,\mathfrak{B}^2_{t_i,\alpha}\,(X)\,.
\end{aligned}$$

Thus,

$$\partial_{a,b}p\,(V_i) = \left(\frac{1}{2}\right)^{a+b}\frac{\binom{4}{a+b}}{\binom{2}{a+b}}\tilde{q}\,(V_i) = \partial_{a,b}p\,(V_i) = \partial_{a,b}\mathcal{Q}p\,(V_i)\,.$$

Now, it suffices to prove that $\mathbf{D}^a_{w_{ij}}\,\mathcal{Q}p\,(R_{ij}) \;=\; \mathbf{D}^a_{w_{ij}}\,p\,(R_{ij})$, $0 \leq a \leq 2$. For $a = 0$, we have $\mathcal{Q}p(R_{12}) = \Xi_1 + \Xi_2 + q_{1,2}\,(X)$, with

$$\begin{aligned}
\Xi_1 &:= \sum_{|\alpha|=2} \mathbf{B}\,[q]\left(V_1[2],\tilde{Q}^v_{1,1}[\alpha_1],\,\tilde{Q}^v_{1,2}[\alpha_2],\,\tilde{Q}^v_{1,3}[\alpha_3]\right))\mathcal{B}^v_{1,\alpha}\,(R_{12})\,,\\
\Xi_2 &:= \sum_{|\alpha|=2} \mathbf{B}\,[q]\left(V_2[2],\tilde{Q}^v_{2,1}[\alpha_1],\,\tilde{Q}^v_{2,2}[\alpha_2],\,\tilde{Q}^v_{2,3}[\alpha_3]\right)\,\mathcal{B}^v_{2,\alpha}\,(R_{12})\,,\\
q_{1,2}\,(X) &:= \sum_{|\bar{\alpha}|=2} \mathbf{B}\,[p]\left(V_1, V_2,\,\tilde{Q}^e_{1,1}[\bar{\alpha}_1],\,\tilde{Q}^e_{1,2}[\bar{\alpha}_2]\right)\,\mathcal{B}^e_{1,\bar{\alpha}}\,(R_{12})\,.
\end{aligned}$$

For the two first expressions, we have

$$\Xi_1 = \lambda^2_{12}\left(\tilde{q}\,(V_1) + D_{R_{12}-V_1}\tilde{q}\,(V_1) + \frac{1}{2}D^2_{R_{12}-V_1}\tilde{q}\,(V_1)\right) = \lambda^2_{12}\mathbf{B}\,[q]\,(V_1[2], R_{12}[2])\,,$$

and

$$\Xi_2 = \lambda^2_{21}\left(\tilde{q}\,(V_2) + D_{R_{12}-V_2}\tilde{q}\,(V_2) + \frac{1}{2}D^2_{R_{12}-V_2}\tilde{q}\,(V_2)\right) = \lambda^2_{21}\mathbf{B}\,[q]\,(V_2[2], R_{12}[2])\,.$$

Regarding the third term, it holds $\mathcal{B}^e_{1,\bar{\alpha}}(R_{12}) = 2\lambda_{12}\lambda_{21}\,\mathfrak{B}^2_{\bar{\alpha}}(R_{12})$, where $\mathfrak{B}^2_{\bar{\alpha}}$ is the quadratic Bernstein polynomial of order $\bar{\alpha}$ defined over $\langle Q^e_{1,1}\, Q^e_{1,2}\rangle$.
Then,

$$q_{1,2}(R_{12}) = 2\lambda_{12}\lambda_{21} \sum_{|\bar{\alpha}|=2} \mathbf{B}\,[p]\left(V_1, V_2, \tilde{Q}^e_{1,1}[\bar{\alpha}_1], \tilde{Q}^e_{1,2}[\bar{\alpha}_2]\right) \mathfrak{B}^2_{\bar{\alpha}}(R_{12}).$$

Now, let us consider the quadratic bivariate polynomial

$$\tilde{q}_{1,2}(X) := 2\lambda_{12}\lambda_{21}\,\mathbf{B}\,[p]\,(V_1, V_2, (2X - R_{12})[2]).$$

Over the segment $\langle Q^e_{1,1}, Q^e_{1,2}\rangle$, $\tilde{q}_{1,2}$ can be written as

$$\begin{aligned}\tilde{q}_{1,2}(X) &= \sum_{|\bar{\alpha}|=2} \mathbf{B}\,[\tilde{q}_{12}]\left(Q^e_{1,1}[\bar{\alpha}_1]\, Q^e_{1,2}[\bar{\alpha}_2]\right) \mathfrak{B}^2_{\bar{\alpha}}(X) \\ &= 2\lambda_{12}\lambda_{21} \sum_{|\bar{\alpha}|=2} \mathbf{B}\,[p]\left(V_1, V_2, \tilde{Q}^e_{1,1}[\bar{\alpha}_1], \tilde{Q}^e_{1,2}[\bar{\alpha}_2]\right) \mathfrak{B}^2_{\bar{\alpha}}(X).\end{aligned}$$

Then,

$$\tilde{q}_{1,2}(R_{12}) = q_{1,2}(R_{12}) = 2\lambda_{12}\lambda_{21}\mathbf{B}\,[p]\,(V_1, V_2, R_{12}[2]),$$

and the claim for $a = 0$ is complete. When $a = 1$ or $a = 2$, we proceed in the same way. □

2.4 A method for constructing quasi-interpolants based on PS4-splines

In this section, we use Marsden's identity [35, 50] to define such quasi-interpolants in such a way that quartic polynomials are reproduced. They have the form

$$\mathcal{Q}^r f := \sum_{i=1}^{nv} \sum_{|\alpha|=2} \lambda^r_{i,\alpha}(f)\,\mathcal{B}^v_{i,\alpha} + \sum_{k=1}^{ne} \sum_{|\bar{\alpha}|=2} \mu^r_{k,\bar{\alpha}}(f)\,\mathcal{B}^e_{k,\bar{\alpha}}, \tag{2.8}$$

where $\lambda^r_{i,\alpha}$ and $\mu^r_{k,\bar{\alpha}}$ and linear functionals such that

$$\mathcal{Q}^r f = f \quad \text{for all } f \in \mathbb{P}_r,\ r = 0, 1, \ldots, 4. \tag{2.9}$$

We have the following result.

Theorem 2.4.1. *For each $1 \le i \le nv$ and $|\alpha| = 2$ (resp. $1 \le k \le ne$), let $\mathbf{I}^r_{i,\alpha}(f)$ (resp. $\mathbf{J}^r_{k,\bar{\alpha}}(f)$) be the polynomial defined in a neighbourhood of support of $\mathcal{B}^v_{i,\alpha}$ (resp. $\mathcal{B}^e_{k,\bar{\alpha}}$) that interpolates or approximates some scattered data values and derivatives of f and such that for all $p \in \mathbb{P}_r$, it holds*

$$\mathbf{I}^r_{i,\alpha}(p) = p, \left(\text{ resp } \mathbf{J}^r_{k,\bar{\alpha}}(p) = p\right).$$

Then,

$$\begin{aligned}\mathcal{Q}^r f(x,y) := &\sum_{i=1}^{nv} \sum_{|\alpha|=2} \mathbf{B}[\mathbf{I}^r_{i,\alpha}(f)]\left(V_i[2], \tilde{Q}^v_{i,1}[\alpha_1], \tilde{Q}^v_{i,2}[\alpha_2], \tilde{Q}^v_{i,3}[\alpha_3]\right) \mathcal{B}^v_{i,\alpha}(x,y) \\ &+ \sum_{k=1}^{ne} \sum_{|\bar{\alpha}|=2} \mathbf{B}[\mathbf{J}^r_{k,\bar{\alpha}}(f)]\left(V_{k,1}, V_{k,2}, \tilde{Q}^e_{k,1}[\bar{\alpha}_1], \tilde{Q}^e_{k,2}[\bar{\alpha}_2]\right) \mathcal{B}^e_{k,\bar{\alpha}}(x,y).\end{aligned}$$

is a quasi-interpolant of the form (2.8) which satisfies (2.9).

Proof. Let $p_r \in \mathbb{P}_r$. By the exactness of $\mathbf{I}^r_{i,\alpha}$ on $\mathbb{P}_r$, we have

$$\mathbf{B}[\mathbf{I}^r_{i,\alpha}(p_r)]\left(V_i[2],\, \tilde{Q}^v_{i,1}[\alpha_1],\, \tilde{Q}^v_{i,2}[\alpha_2],\, \tilde{Q}^v_{i,3}[\alpha_3]\right) = \mathbf{B}[p_r]\left(V_i[2],\, \tilde{Q}^v_{i,1}[\alpha_1],\, \tilde{Q}^v_{i,2}[\alpha_2],\, \tilde{Q}^v_{i,3}[\alpha_3]\right)$$

for all $i = 1, \ldots, n_v$, and $|\alpha| = 2$. By the exactness of $\mathbf{J}^r_{k,\bar{\alpha}}$ on $\mathbb{P}_r$, we have also

$$\mathbf{B}[\mathbf{J}^r_{k,\bar{\alpha}}(p_r)]\left(V_{k,1}, V_{k,2},\, \tilde{Q}^e_{k,1}[\bar{\alpha}_1],\, \tilde{Q}^e_{k,2}[\bar{\alpha}_2]\right) = \mathbf{B}[p_r]\left(V_{k,1}, V_{k,2},\, \tilde{Q}^e_{k,1}[\bar{\alpha}_1],\, \tilde{Q}^e_{k,2}[\bar{\alpha}_2]\right)$$

for all $k = 1, \ldots, n_e$, and $|\bar{\alpha}| = 2$. Then, from Theorem 2.3.1, it follows that

$$\mathcal{Q}^r f(x,y) = f, \text{ for all } f \in \mathbb{P}_r,\ r = 0, 1, 2, 3, 4.$$

□

2.4.1 Quasi-interpolation based on Taylor approximation

We will use Taylor approximation to define differential quasi-interpolants in $\tilde{S}_4$.

Let $f \in C^4(\Omega)$ and $L^j_i := \left(L^j_{i,x},\, L^j_{i,y}\right)$, $i = 1, \ldots, nv$, $j = 1, \ldots, 6$, be some fixed points lying in the union of all triangles in Δ having V_i as a vertex. Let us suppose that they form an unisolvent scheme in $\mathbb{P}_4$. Let p^j_i be the Taylor polynomial of f of degree 4 at L^j_i, i.e.,

$$p^j_i(x,y) = \sum_{0 \le k+\ell \le 4} \frac{1}{k!\ell!} \partial_{k,\ell} f\left(L^j_i\right)\left(x - L^j_{i,x}\right)^k \left(y - L^j_{i,y}\right)^\ell. \tag{2.10}$$

For $\bar{\alpha} \in \mathbb{N}^2$ with $|\bar{\alpha}| = 2$, let $p_{k,\bar{\alpha}}$ be the Taylor polynomial of degree 4 at the point $L_{k,\bar{\alpha}}$ in the support of $\mathcal{B}^e_{k,\bar{\alpha}}$. Define

$$\begin{aligned}\mathcal{Q}^4 f := &\sum_{i=1}^{nv} \sum_{|\beta|=2} \mathbf{B}\left[p^j_i\right]\left(V_i[2], \tilde{Q}^v_{i,1}[\beta_1], \tilde{Q}^v_{i,2}[\beta_2], \tilde{Q}^v_{i,3}[\beta_3]\right) \mathcal{B}^v_{i,\beta} \\ &+ \sum_{k=1}^{ne} \sum_{|\bar{\alpha}|=2} \mathbf{B}\left[p_{k,\bar{\alpha}}\right]\left(V_{k,1}, V_{k,2}, \tilde{\mathcal{Q}}^e_{k,1}[\bar{\alpha}_1],\, \tilde{\mathcal{Q}}^e_{k,2}[\bar{\alpha}_2]\right) \mathcal{B}^e_{k,\bar{\alpha}}.\end{aligned} \tag{2.11}$$

Theorem 2.4.2. *Let $\mathcal{Q}^4 f$ be defined by (2.11) and (2.10). Then, the quasi-interpolation operator $\mathcal{Q}^4 : C^4(\Omega) \to \tilde{S}_4(\Delta_{PS})$ is exact on $\mathbb{P}_4$, i.e. $\mathcal{Q}^4(p) = p$ for all $p \in \mathbb{P}_4$.*

Next, we will consider a relation between polar forms and differentiation to be used to construct a quasi-interpolant to solve the main Hermite interpolation problem in this paper. Some results concerning a connection between polar forms and directional derivatives are given here (for more details see [47] and references therein). For every polynomial $p \in \mathbb{P}_n$, the q^{th} directional derivative of p with respect to vectors $\xi_1, \ldots, \xi_q \in \mathbb{R}^2$ is given by

$$D_{\xi_1,\ldots,\xi_q}\, p(u) = \frac{n!}{(n-q)!} \mathbf{B}[p]\left(u[n-q], \xi_1, \ldots, \xi_q\right).$$

Proposition 2.4.1. *Let u, v_1 and v_2 be three points in $\mathbb{R}^2$. Then for each $p \in \mathbb{P}_4$, we have*

$$\mathbf{B}[p](u, u, v_1, v_2) = \frac{1}{12} D_{\xi_1 \xi_2}\, p(u) + \frac{1}{4} D_{\xi_1}\, p(u) + \frac{1}{4} D_{\xi_2}\, p(u) + p(u),$$

where $\xi_i := v_i - u$, $i = 1, 2$.

From Proposition 2.4.1, we introduce the functional

$$\mathcal{F}\left[f\right]\left(u,u,v_1,v_2\right) = \frac{1}{12}D_{\xi_1\xi_2}\,f\left(u\right)+\frac{1}{4}D_{\xi_1}\,f\left(u\right)+\frac{1}{4}D_{\xi_2}\,f\left(u\right)+f\left(u\right) \tag{2.12}$$

to define a quartic Powell-Sabin quasi-interpolation operator.

Theorem 2.4.3. *Let us define the coefficients*

$$\lambda^4_{i,\alpha}\left(f\right) := \mathcal{F}\left[f\right]\left(V_i[2],\,\tilde{Q}^v_{i,1}[\alpha_1],\tilde{Q}^v_{i,2}[\alpha_2],\tilde{Q}^v_{i,3}[\alpha_3]\right),\ |\alpha|=2,\ i=1,\ldots,nv,$$

$$\mu^4_{k,\bar{\alpha}}\left(f\right) := \mathcal{F}\left[f\right]\left(V_{k,1},V_{k,2},\tilde{Q}^e_{k,1}[\bar{\alpha}_1],\tilde{Q}^e_{k,2}[\bar{\alpha}_2]\right),\ |\bar{\alpha}|=2,\ k=1,\ldots,ne,\ \varepsilon_k:=\langle V_{k,1},\,V_{k,2}\rangle\,.$$

Then, the corresponding operator $\mathcal{Q}^4$ defined in (2.8) is exact on $\mathbb{P}_4$.

Proof. From Propositions (2.4.1) and (2.12), it is clear that

$$\mathcal{F}[f]\left(V_i[2],\,\tilde{Q}^v_{i,1}[\alpha_1],\tilde{Q}^v_{i,2}[\alpha_2],\tilde{Q}^v_{i,3}[\alpha_3]\right) = \mathbf{B}[\mathbf{I}^4_{i,\alpha}(f)]\left(V_i[2],\,\tilde{Q}^v_{i,1}[\alpha_1],\tilde{Q}^v_{i,2}[\alpha_2],\tilde{Q}^v_{i,3}[\alpha_3]\right),$$

$$\mathcal{F}[f]\left(V_{k,1},V_{k,2},\tilde{Q}^e_{k,1}[\bar{\alpha}_1],\tilde{Q}^e_{k,2}[\bar{\alpha}_2]\right) = \mathbf{B}[\mathbf{J}^4_{k,\bar{\alpha}}(f)]\left(V_{k,1},V_{k,2},\tilde{Q}^e_{k,1}[\bar{\alpha}_1],\tilde{Q}^e_{k,2}[\bar{\alpha}_2]\right).$$

From Theorem 2.4.1, it follows that $\mathcal{Q}^4 p = p$ for all $p\in\mathbb{P}_4$. □

We will use again the notation $f_{i,a,b}=\partial_{a,b}f\left(V_i\right)$ and $D^a_{w_{i,j}}\,f\left(R_{ij}\right)=g^a_{i,j}$ introduced before and consider the values $f_{i,a,b},\ i=1,\ldots,nv,\ a,\,b\geq 0,\ a+b\leq 2$, at vertices and $g^a_{i,j},\ 0\leq a\leq 2$, for edges. Let us consider two points $P_i:=(p_{i,1},p_{i,2}),\ \ i=1,2$, in $\mathbb{R}^2$, and define vectors as

$$\xi_j = 2(P_j-V_i),\ j=1,2.$$

Then, the first two terms in expression (2.12) for functional $\mathcal{F}$ can be expressed as

$$\frac{1}{4}\,D_{\xi_j}\,f\left(V_i\right)=\frac{1}{2}\left(\left(p_{j,1}-x_i\right)f_{i,1,0}+\left(p_{j,2}-y_i\right)f_{i,0,1}\right),$$

$$\frac{1}{12}\,D_{\xi_j,\xi_k}\,f\left(V_i\right)=\frac{1}{3}\left(\left(\left(p_{j,1}-x_i\right)\left(p_{k,2}-y_i\right)+\left(p_{k,1}-x_i\right)\left(p_{j,2}-y_i\right)\right)f_{i,1,1}\right.$$
$$\left.+\left(p_{j,1}-x_i\right)\left(p_{k,1}-x_i\right)f_{i,2,0}+\left(p_{j,2}-y_i\right)\left(p_{k,2}-y_i\right)f_{i,0,2}\right).$$

Note that $\tilde{Q}^v_{i,j}-V_i=2\left(Q^v_{i,j}-V_i\right)$.
In order to interpolate the given data across each edge, let us consider the following notations and, without loss generality, the edge $\varepsilon_k:=\langle V_1,V_2\rangle$.

- If ε_k is a boundary edge, let

$$\mathcal{L}_{k,(0,2)}f := \frac{1}{2\lambda_{12}\lambda_{21}}\left(g^0_{1,2}-\lambda^2_{12}\mathcal{F}\left[f\right]\left(V_1,R_{12},R_{12}\right)\lambda^2_{21}\mathcal{F}\left[f\right]\left(V_2,R_{12},R_{12}\right)\right),$$

$$\mathcal{L}_{k,(1,1)}f := \frac{1}{2\lambda_{12}\lambda_{21}}\left(g^1_{1,2}+g^0_{1,2}-\lambda^2_{12}\mathcal{F}\left[f\right]\left(V_1,R_{12},Z\right)-\lambda^2_{21}\mathcal{F}\left[f\right]\left(V_2,R_{12},Z\right)\right),$$

$$\mathcal{L}_{k,(2,0)}f := \frac{1}{2\lambda_{12}\lambda_{21}}\left(g^2_{1,2}+g^1_{1,2}-2g^0_{1,2}-\lambda^2_{12}\mathcal{F}\left[f\right]\left(V_1,Z,Z\right)-\lambda^2_{21}\mathcal{F}\left[f\right]\left(V_2,Z,Z\right)\right).$$

- If ε_k is an interior edge, let

$$\mathcal{L}_{k,(2,0)}f = -\frac{\mathcal{F}\left[f\right]\left(V_1,Z,Z\right)\lambda^2_{12}+\mathcal{F}\left[f\right]\left(V_2,Z,Z\right)\lambda^2_{21}+g^0_{1,2}-2g^1_{1,2}-g^2_{1,2}}{2\lambda_{12}\lambda_{21}},$$

$$\mathcal{L}_{k,(1,1)}f = \frac{1}{2\lambda_{12}\lambda_{21}\left\|R_{12}-Z_1\right\|}\left(\left(\mathcal{F}\left[f\right]\left(V_1,Z,Z\right)\lambda^2_{12}+\mathcal{F}\left[f\right]\left(V_2,Z,Z\right)\lambda^2_{21}+g^0_{1,2}-2g^1_{1,2}-g^2_{1,2}\right)\times\right.$$
$$\left.\left\|R_{12}-Z_2\right\|+\left\|Z_2-Z_1\right\|\left(-\mathcal{F}[f]\left(V_1,R_{12},Z\right)\lambda^2_{12}-\mathcal{F}\left[f\right]\left(V_2,R_{12},Z\right)\lambda^2_{21}+g^0_{1,2}+g^1_{1,2}\right)\right),$$

$$\mathcal{L}_{k,(0,2)}f = \frac{1}{2\lambda_{12}\lambda_{21}\left\|R_{12}-Z_1\right\|^2}\left(-2\left\|Z_2-Z_1\right\|\left(-\mathcal{F}\left[f\right]\left(V_1,R_{12},Z\right)\lambda^2_{12}-\mathcal{F}\left[f\right]\left(V_2,R_{12},Z\right)\lambda^2_{21}\right.\right.$$
$$\left.+g^0_{1,2}+g^1_{1,2}\right)\left\|R_{12}-Z_2\right\|-\left(\mathcal{F}\left[f\right]\left(V_1,Z,Z\right)\lambda^2_{12}+\mathcal{F}\left[f\right]\left(V_2,Z,Z\right)\lambda^2_{21}+g^0_{1,2}-2g^1_{1,2}-g^2_{1,2}\right)\times$$
$$\left.\left\|R_{12}-Z_2\right\|^2+\left\|Z_2-Z_1\right\|\|^2\left(-\mathcal{F}\left[f\right]\left(V_1,R_{12},R_{12}\right)\lambda^2_{12}-\mathcal{F}\left[f\right]\left(V_2,R_{12},R_{12}\right)\lambda^2_{21}+g^0_{1,2}\right)\right).$$

Using the above notations and definitions, we get a new quasi-interpolant that allows us to solve the Hermite interpolation problem given by (2.1).

Theorem 2.4.4. *Let us define,*

$$\lambda^4_{i,\alpha}(f) := \mathcal{F}[f]\left(V_i[2],\, \tilde{Q}^v_{i,1}[\alpha_1], \tilde{Q}^v_{i,2}[\alpha_2], \tilde{Q}^v_{i,3}[\alpha_3]\right),\ |\alpha| = 2,\ i = 1,\, \ldots,\, nv,$$
$$\mu^4_{k,\bar{\alpha}}(f) := \mathcal{L}_{k,\bar{\alpha}} f,\ k = 1,\, \ldots,\, n_e,\ \varepsilon_k = \langle V_{k,1},\, V_{k,2}\rangle\,.$$

Then, the following quasi-interpolant provides the unique element in $\tilde{S}_4$ which interpolates the data in (2.1):

$$\mathcal{QH}^4 := \sum_{i=1}^{nv} \sum_{|\alpha|=2} \lambda^4_{i,\alpha}(f)\,\mathcal{B}^v_{i,\alpha} + \sum_{k=1}^{ne} \sum_{|\bar{\alpha}|=2} \mu^4_{k,\bar{\alpha}}(f)\,\mathcal{B}^e_{k,\bar{\alpha}}.$$

Proof. There exists a unique spline $s \in \tilde{S}_4(\Omega, \Delta_{\mathrm{PS}})$ satisfying conditions (2.1). We can compute in a stable way the BB-coefficients $c^v_{i,\alpha}$ and $c^e_{k,\bar{\alpha}}$ in representation (2.2). From Theorem 2.2.1, we have

$$c^v_{i,\alpha} = \mathcal{F}[f]\left(V_i, V_i, \tilde{Q}^v_{i,1}[\alpha_1], \tilde{Q}^v_{i,2}[\alpha_2], \tilde{Q}^v_{i,3}[\alpha_3]\right).$$

Consider again the edge $\varepsilon_k = \langle V_1,\, V_2\rangle$. From equations (2.6)-(2.7), we calculate the functionls $\mathcal{L}_{k,(2,0)}f$, $\mathcal{L}_{k,(1,1)}f$ and $\mathcal{L}_{k,(0,2)}f$. For example, if ε_k is a boundary edge, then

$$c_{k,3} = \frac{-d_5\lambda^2_{12} - d_{18}\lambda^2_{21} + g^0_{1,2}}{2\lambda_{12}\lambda_{21}},$$

where, $d_5 = \mathcal{F}[f](V_1, R_{12}, R_{12})$ and $d_{18} = \mathcal{F}[f](V_2, R_{12}, R_{12})$. The other coefficients are obtained in the same way, which completes the proof. □

2.4.2 Quasi-interpolation based on point values

For each vertex V_i, consider a $\mathbb{P}_4$-unisolvent set $\left\{Z^\ell_{i,\alpha},\ \ \ell = 1,\, \ldots,\, 15\right\}$ of points in $\mathbb{R}^2$ (i.e. satisfying the Geometric Configuration, see [49]). The fifteen points are chosen in a neighbourhood of the union M_{v_i} of all triangles in Δ having V_i as a vertex. Then, there exists a unique polynomial that interpolates the value $f\left(Z^\ell_{i,\alpha}\right)$ at at every point $Z^\ell_{i,\alpha}$, $1 \le i \le 15$, and it can be written as

$$\mathcal{I}_{i,\alpha}\, f \;=\; \sum_{\ell=1}^{15} f\left(Z^\ell_{i,\alpha}\right) L^\ell_{i,\alpha},$$

where the fundamental polynomial $L^\ell_{i,\alpha}$ fulfills the conditions $L^\ell_{i,\alpha}\left(Z^k_{i,\alpha}\right) = \delta_{k,\ell}$, $k,\ \ell = 1, \ldots, 15$, and δ stands for the Kroneckers's delta. Moreover, let $W^\ell_{k,\bar{\alpha}}$, $\ell = 1, \ldots, 5$, be five distinct points in the line $\langle Q^e_{k,1},\, Q^e_{k,2}\rangle$ with respect to the edge $\mathfrak{e}_k$, and $L^\ell_{k,\bar{\alpha}}$ be the corresponding fundamental polynomials. Then the unique polynomial of degree 4 that interpolates f at points $\left\{W^\ell_{k,\bar{\alpha}}\right\}_{\ell=1}^5$ is given by

$$\mathcal{J}_{k,\bar{\alpha}}\, f\,(x,y) \;=\; \sum_{\ell=1}^{5} f\left(W^\ell_{k,\bar{\alpha}}\right) L^\ell_{k,\bar{\alpha}}(x,y)\,.$$

The following result follows from Theorem 2.4.1.

Proposition 2.4.2. *The quasi-interpolation operator $\mathcal{Q}^5$ having the form (2.8) with*

$$\lambda^5_{i,\alpha} f \;=\; \sum_{\ell=1}^{15} f(Z^\ell_{i,\alpha})\,\mathbf{B}\left[L^\ell_{i,\alpha}\right]\left(V_i^[2],\, \tilde{Q}^v_{i,1}[\alpha_1],\, \tilde{Q}^v_{i,2}[\alpha_2],\, \tilde{Q}^v_{i,3}[\alpha_3]\right)$$

and

$$\mu^5_{k,\bar{\alpha}} f = \sum_{\ell=1}^{5} f(W^\ell_{i,\bar{\alpha}})\, \mathbf{B}\left[L^\ell_{i,\bar{\alpha}}\right]\left(V_{k,1},\, V_{k,2},\, \tilde{Q}^e_{k,1}[\bar{\alpha}_1],\, \tilde{Q}^e_{k,2}[\bar{\alpha}_2]\right)$$

is exact on $\mathbb{P}_4$.

From Lemma 1.3.1, we easily compute $\mathbf{B}\left[L^\ell_{i,\alpha}\right]\left(V_i[2], \tilde{Q}^v_{i,1}[\alpha_1], \tilde{Q}^v_{i,2}[\alpha_2], \tilde{Q}^v_{i,3}[\alpha_3]\right)$ and $\mathbf{B}\left[L^\ell_{i,\bar{\alpha}}\right]\left(V_{k,1}, V_{k,\right.$ Recall that the fundamental polynomials $L^\ell_{i,\alpha}$ associated with points $Z^\ell_{i,\alpha}$, $l = 1, \ldots, 15$, can be written as

$$L^\ell_{i,\alpha}(x,y) = \frac{R^{\ell,1}_{i,\alpha}(x,y)\, R^{\ell,2}_{i,\alpha}(x,y)\, R^{\ell,3}_{i,\alpha}(x,y)\, R^{\ell,4}_{i,\alpha}(x,y)}{R^{\ell,1}_{i,\alpha}(Z^\ell_{i,\alpha})\, R^{\ell,2}_{i,\alpha}(Z^\ell_{i,\alpha})\, R^{\ell,3}_{i,\alpha}(Z^\ell_{i,\alpha})\, R^{\ell,4}_{i,\alpha}(Z^\ell_{i,\alpha})},$$

where $R^{\ell,n}_{i,\alpha}$,$n = 1,2,3,4$, are four lines containing $Z^j_{i,\alpha}$, $j = 1, \ldots, 15$, with $j \neq \ell$.

Next, we propose a way to minimize the number of needed point evaluations with respect to a vertex (see Figure 2.9).

Proposition 2.4.3. *For each* $i = 1, \ldots, nv$*, assume that the points* $Z^\ell_{i,\alpha}$*,* $\ell = 1, \ldots, 15$*, satisfy the GC condition and that the points* $Z^\ell_{i,\alpha}$*,* $\ell = 1, \ldots, 5$*, are collinear with* V_i *and* $Q^v_{i,n}$*,* $n = 1,2,3$*. Then, it holds*

$$\mathbf{B}\left[L^\ell_{i,\alpha}\right]\left(V_i[2], \tilde{Q}^v_{i,1}[\alpha_1], \tilde{Q}^v_{i,2}[\alpha_2], \tilde{Q}^v_{i,3}[\alpha_3]\right) = 0, \quad \ell = 6, \ldots, 15. \tag{2.13}$$

Proof. For each $i = 1, \ldots, nv$ and $\alpha \in \{(2,0,0),(0,2,0),(0,0,2)\}$, assume that $Z^\ell_{i,\alpha}$, $\ell = 1, \ldots, 15$, is a unisolvent set. If $Z^\ell_{i,\alpha}$, $\ell = 1, \ldots, 5$, are collinear with V_i and $Q^v_{i,n}$, $n = 1,2,3$, then for $\ell = 6, \ldots, 15$, one of the lines $R^{\ell,j}_{i.\alpha}$, $j = 1,2,3,4$, is the line $\langle V_i, Q^v_{l,\alpha}\rangle$, where $Q^v_{\ell,(2,0,0)} = Q^v_{\ell,1}$, $Q^v_{\ell,(0,2,0)} = Q^v_{\ell,2}$ and $Q^v_{\ell,(0,0,2)} = Q^v_{\ell,3}$. Then, (2.13) follows from Lemma 1.3.1. □

We can choose the interpolation points as indicated in the following result.

Theorem 2.4.5. *For each* $i = 1, \ldots, nv$*, let* $Z_{i,\alpha} = \left\{Z^\ell_{i,\alpha}, \ell = 1, \ldots, 15\right\}$ *be the set defined as follows for indices* k*,* m*,* n *such that* $k + m + n = 4$*:*

$$Z^\ell_{i,\alpha} = \begin{cases} \frac{1}{4}\left(kV_i + mQ^v_{i,1} + nA_{i,1}\right), & \textit{if } \alpha = (2,0,0), \\ \frac{1}{4}\left(kV_i + mQ^v_{i,2} + nA_{i,2}\right), & \textit{if } \alpha = (0,2,0), \\ \frac{1}{4}\left(kV_i + mQ^v_{i,3} + nA_{i,3}\right), & \textit{if } \alpha = (0,0,2), \\ \frac{1}{4}\left(kV_i + mQ^v_{i,1} + nQ^v_{i,2}\right), & \textit{if } \alpha = (1,1,0), \\ \frac{1}{4}\left(kV_i + mQ^v_{i,1} + nQ^v_{i,3}\right), & \textit{if } \alpha = (1,0,1), \\ \frac{1}{4}\left(kV_i + mQ^v_{i,2} + nQ^v_{i,3}\right), & \textit{if } \alpha = (0,1,1), \end{cases}$$

where $A_{i,j}$,$j = 1,2,3$*, are three auxiliary points such that* V_i*,* $Q^v_{i,j}$ *and* $A_{i,j}$ *are distinct points. Then,* $Z_{i,\alpha}$ *satisfies the GC condition and the condition in Proposition 2.4.3.*

The functionals $\lambda_{i,\alpha}$ have been computed by using the softawate *Mathematica* and the first

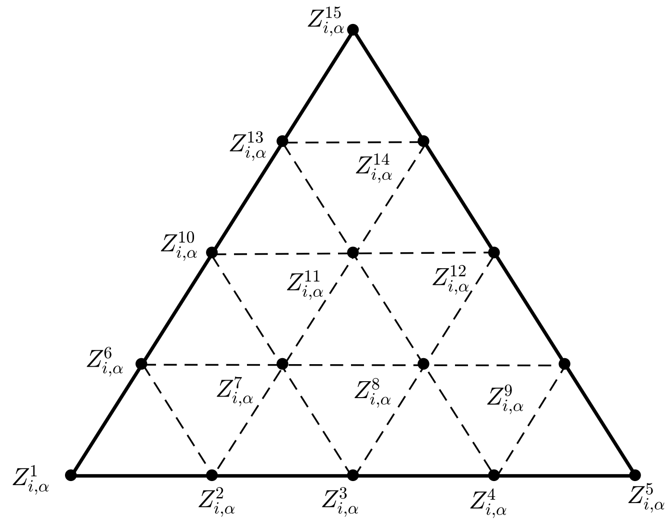

Figure 2.9: Position of interpolation points.

two of them are given by the following expressions:

$$\begin{aligned}
\lambda_{i,(2,0,0)} &= \frac{74}{9} f(V_i) + \frac{35}{9} f(\mathcal{Q}_{i,1}) - \frac{272}{9} f\left(\frac{3V_i+\mathcal{Q}_{i,1}}{4}\right) + \frac{116}{3} f\left(\frac{2V_i+2\mathcal{Q}_{i,1}}{4}\right) \\
&\quad - \frac{176}{9} f\left(\frac{V_i+3\mathcal{Q}_{i,1}}{4}\right), \\
\lambda_{i,(1,1,0)} &= \frac{74}{9} f(V_i) - \frac{155}{4} f(\mathcal{Q}_{i,1}) - \frac{136}{9} f\left(\frac{3V_i+\mathcal{Q}_{i,1}}{4}\right) - \frac{136}{9} f\left(\frac{3V_i+\mathcal{Q}_{i,2}}{4}\right) \\
&\quad + \frac{58}{3} f\left(\frac{2V_i+2\mathcal{Q}_{i,1}}{4}\right) + \frac{58}{3} f\left(\frac{2V_i+2\mathcal{Q}_{i,2}}{4}\right) - \frac{88}{9} f\left(\frac{V_i+3\mathcal{Q}_{i,1}}{4}\right) \\
&\quad - \frac{88}{9} f\left(\frac{V_i+3\mathcal{Q}_{i,2}}{4}\right) + \frac{16}{9} f\left(\frac{\mathcal{Q}_{i,1}+3\mathcal{Q}_{i,2}}{4}\right) + \frac{16}{9} f\left(\frac{\mathcal{Q}_{i,2}+3\mathcal{Q}_{i,1}}{4}\right) \\
&\quad - 4 f\left(\frac{2\mathcal{Q}_{i,1}+2\mathcal{Q}_{i,2}}{4}\right) - \frac{88}{9} f\left(\frac{V_i+3\mathcal{Q}_{i,1}}{4}\right) + 32 f\left(\frac{2V_i+\mathcal{Q}_{i,1}+\mathcal{Q}_{i,2}}{4}\right) \\
&\quad - \frac{32}{3} f\left(\frac{V_i+2\mathcal{Q}_{i,1}+\mathcal{Q}_{i,2}}{4}\right) - \frac{16}{3} f\left(\frac{V_i+\mathcal{Q}_{i,1}+2\mathcal{Q}_{i,2}}{4}\right).
\end{aligned}$$

The other ones have similar structures. Analogously, for each edge $\mathfrak{e}_k$, we choose 5 collinear points in the lines $\left\langle Q_{k,1}^e, Q_{k,2}^e \right\rangle$.

2.4.3 Discrete quasi-interpolants by polarization

Polarisation can be use to define a quasi-interpolant whose coefficients are linear combinations of point values. The polarisation identity

$$\mathbf{B}(p)(u_1,u_2,u_3,u_4) = \frac{1}{24} \sum_{\substack{s\subseteq\{1,2,3,4\}\\ k=|s|}} (-1)^{4-k}\, k^4\, p\left(\frac{1}{k}\sum_{i\in s} u_i\right)$$

has 15 terms and allows to define an operator $\mathcal{M}$ as follows:

$$\mathcal{M}[f](u_1,u_2,u_3,u_4) = \frac{1}{24} \sum_{\substack{s\subseteq\{1,2,3,4\}\\ k=|s|}} (-1)^{4-k}\, k^4\, f\left(\frac{1}{k}\sum_{i\in s} u_i\right).$$

From Marsden's identity, we have the following result.

Theorem 2.4.6. *The quasi-interpolation operator defined as*

$$\mathcal{Q}f := \sum_{i=1}^{nv} \sum_{|\alpha|=2} \lambda_{i,\alpha}(f)\, \mathcal{B}^v_{i,\alpha} + \sum_{k=1}^{ne} \sum_{|\bar{\alpha}|=2} \mu_{k,\bar{\alpha}}(f)\, \mathcal{B}^e_{k,\bar{\alpha}},$$

with $\lambda_{i,\alpha}(f) = \mathcal{M}[f]\left(V_i[2], \tilde{Q}^v_{i,1}[\alpha_1], \tilde{Q}^v_{i,2}[\alpha_2], \tilde{Q}^v_{i,3}[\alpha_3]\right)$ *and* $\mu_{k,\bar{\alpha}}(f) = \mathcal{M}[f](V_{k,1}, V_{k,2}, \tilde{Q}^e_{k,1}[\bar{\alpha}_1], \tilde{Q}^e_{k,2}[\bar{\alpha}_2])$, *is exact on* $\mathbb{P}_4$.

2.5 Numerical tests

This section aims to test the approximation power of the proposed quasi-interpolation operators. To this end, their performance will be examined using the well-known Franke and Nielson's functions [51, 52], given respectively by

$$\begin{aligned} f_1(x,y) &= 0.75e^{-\frac{1}{4}\left((9x-2)^2+(9y-2)^2\right)} + 0.75e^{-\frac{1}{49}(9x+1)^2-\frac{1}{10}(9y+1)} \\ &\quad + 0.5e^{-\frac{1}{4}\left((9x-7)^2+(9y-3)^2\right)} + 0.2e^{-(9x-4)^2-(9y-7)^2} \end{aligned}$$

and

$$f_2(x,y) = \frac{y}{2}\cos^4\left(4\left(x^2+y-1\right)\right),$$

whose plots appear in Figure 2.10.

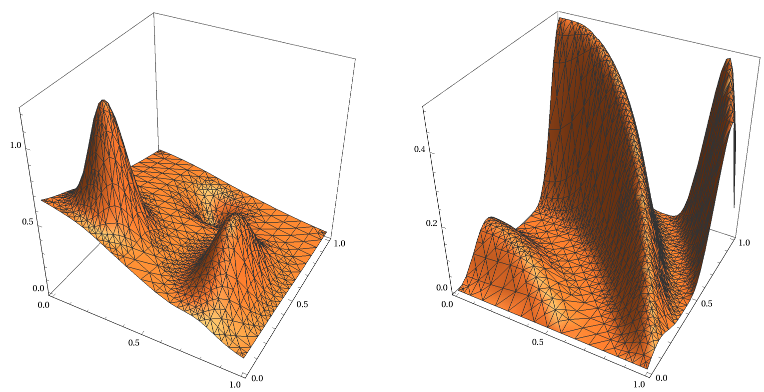

Figure 2.10: Plots of the tests functions: Franke (left) and Nielson (right).

We consider the domain $\Omega = [0,1]\times[0,1]$. The tests are carried out for a sequence of uniform meshes Δ_n with vertices (ih, jh), $i, j = 0, \ldots, n$, where $h := \dfrac{1}{n}$.

The quasi-interpolation error is estimated as $\max_{v\in\Omega} |f(v) - \mathcal{Q}f(v)|$.

The estimated errors and experimental decay for the functions f_1 and f_2 are shown in Tables 2.1 and 2.2, respectively. They confirm the theoretical results.

Figure 2.11 shows the three meshes used to define quasi-interpolants for the test functions f_1 and f_2. Figure 2.12 shows the plots of the splines $\mathcal{Q}f_1$ and $\mathcal{Q}f_2$ for the finer mesh (i.e. $n = 6$).

The considered splines are C^1-continuous, although they are of class C^2 everywhere except across some edges of the refinement. In the next section, we will deal with the characterization of Powell-Sabin triangulations allowing the construction of C^2 continuous quartic splines.

2.6 Full C^2 quartic Powell-Sabin splines

The construction of C^2 PS-splines needs to consider a degree equal to five. In [25], normalized bases are constructed for these spaces, and polar forms are used in [31] to construct discrete

n	nv	QI Theorem 2.4.3	Decay exp	QI Proposition 2.4.2	Decay exp
3	16	0.20	$---$	0.24	$---$
4	25	0.052	4.68	0.096	3.18
5	30	0.018	4.75	0.040	3.92
6	49	0.007	5.18	0.020	3.80
7	64	0.003	5.49	0.010	4.49
8	81	0.00151	5.14	0.0052	4.89

Table 2.1: Estimated errors for Franke's function and numerical convergence order with $n = 3, \ldots, 8$.

n	nv	QI Theorem 2.4.3	Decay exp	QI Proposition 2.4.2	Decay exp
5	30	0.0413	$---$	0.1210	$---$
6	49	0.0207	3.97	0.0612	3.73
7	64	0.0105	4.49	0.0324	4.11
8	81	0.0057	5.19	0.0166	5.02

Table 2.2: Estimated errors for Nielson's function and numerical convergence order with $n = 5, \ldots, 8$.

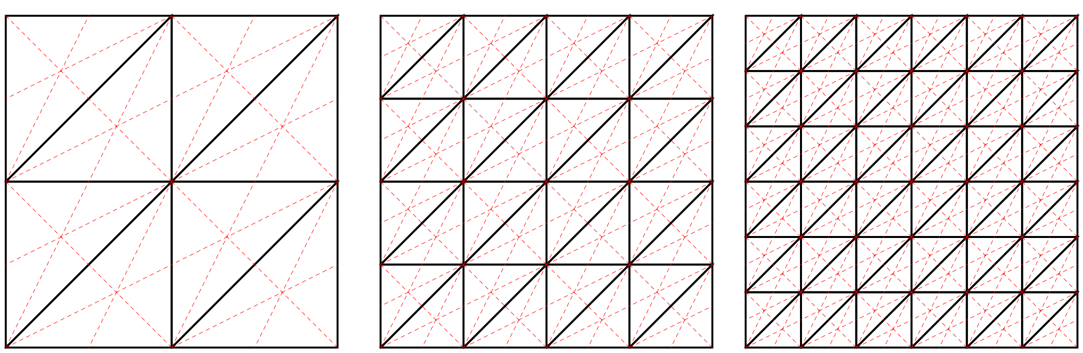

Figure 2.11: Meshes for $n = 2, 4, 6$ (from left to right).

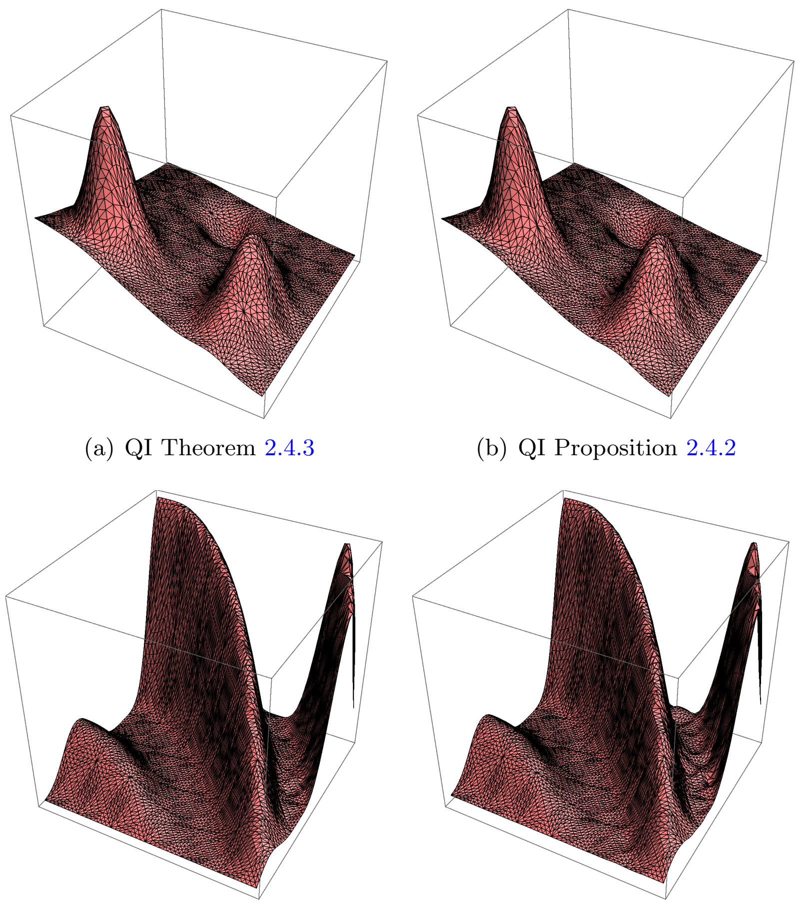

(a) QI Theorem 2.4.3 (b) QI Proposition 2.4.2

(c) QI Theorem 2.4.3 (d) QI Proposition 2.4.2

Figure 2.12: Quasi-interpolants for Franke's function (top) and Nielson's function (bottom).

and differential quasi-interpolants reproducing quintic polynomials. Interpolation with quintic PS-splines are addressed in [53].

The construction of C^2 quartic PS-splines has only been studied very recently, using the idea proposed in [27, 98] to deal with the cubic case, namely to impose additional smoothness conditions at the nodes or inside each triangle.

In [32], this strategy is adopted to construct PS-splines that are almost C^2 continuous. Actually, the resulting functions are only C^1 continuous, although they are of class C^2 except across some edges of the refinement.

In some sense, the characterization obtained here can be seen as a continuation of the work [57]. Indeed, in [57] C^2 quartic splines on a modified Morgan-Scott refinement is discussed. The linear functionals involved in the Hermite interpolation problems in [57] and in this paper are the same, only the refinements are different. Unfortunately, the space developed in [57] is only defined under specific geometrical conditions. When the three inner points used to define the refinement collapse, this space is not defined, and this is the starting point for the work done in this paper. The construction of C^2 quartic splines over refined triangulations with modified Morgan-Scott split is also studied in [58] (see [59] in the case of C^1 quadratic splines). The authors in [58], first, they analysed the construction of C^2 quartic splines on a single macro-triangle endowed with a modified Morgan-Scott split. Then, they examined the problem of how to join the local C^2 interpolating splines on macro-triangles to a quartic spline that is C^2 continuous everywhere. Unfortunately, this results in a global system of linear equations, whose solvability, in general, is very difficult to analyse theoretically. This is because, the linear system depends on the positions of the triangle split points and the edge split points that determine the modified Morgan-Scott split. The relationship between the triangle split points and the edge split points involved in [57] can be viewed as a special case where this linear system has a unique solution.

Several families of PS-super splines of arbitrary degree (and corresponding regularity) have been introduced in the literature [26, 42], and also quasi-interpolation operators based on PS-splines of arbitrary class r and degree $3r-1$ have been defined [36].

The main objective of this section is to characterize the geometry of Powell-Sabin triangulations that allows C^2 class bivariate quartic splines to be defined.

In [32], a normalized basis of the subspace

$$S_4^{1,2}\left(\Delta_{\mathrm{PS}}\right) := \left\{ s \in S_4^1\left(\Delta_{\mathrm{PS}}\right) : \ s \in \ C^2\left(\mathcal{V} \cup \mathcal{Z} \cup \mathcal{E} \cup \mathcal{E}^*\right)\right\}.$$

of $S_4^1\left(\Delta_{\mathrm{PS}}\right)$ is constructed. Its dimension is equal to $6nv + 3ne$. The splines in this subspace are C^2 continuous everywhere except across the edges that connect the split points and the vertices.

We consider the following subspace of $S_4^{1,2}\left(\Delta_{\mathrm{PS}}\right)$:

$$S_4^{1,2,3}\left(\Delta_{\mathrm{PS}}\right) := \left\{ s \in \ S_4^{1,2}\left(\Delta_{\mathrm{PS}}\right) : s \in \ C^3\left(\mathcal{E}^*\right)\right\}. \tag{2.14}$$

Here, $C^3\left(\mathcal{E}^*\right)$ means that for any edge $\mathfrak{e} \in \mathcal{E}^*$ the polynomials over the two micro-triangles sharing $\mathfrak{e}$ have common derivatives up to order three along $\mathfrak{e}$. Splines in $S_4^{1,2,3}\left(\Delta_{\mathrm{PS}}\right)$ are C^3 continuous at the set of edge split points and C^2 at the set of triangle split points.

This is not a classical super spline space because additional continuity has been imposed across certain, but not all, interior edges of Δ_{PS}.

A spline $s \in S_4^{1,2,3}\left(\Delta_{\mathrm{PS}}\right)$ can be defined by means of the following Hermite interpolation problem.

Theorem 2.6.1. *There exists a unique spline $s \in S_4^{1,2,3}\left(\Delta_{PS}\right)$ solving the interpolation problem*

$$\begin{aligned} D_x^a D_y^b\, s\left(V_i\right) &= f_i^{a,b}, \ \ i = 1, \ldots, nv, \ a \geq 0, \, b \geq 0, \ a+b \leq 2, \\ D^2_{\omega_{m,n,q}} s\left(R_{m,n}\right) &= g_{m,n} \quad \textit{for all } \ R_{m,n} \in \mathcal{R}, \quad R_{m,n} \in \left\langle V_m, V_n\right\rangle, \end{aligned} \tag{2.15}$$

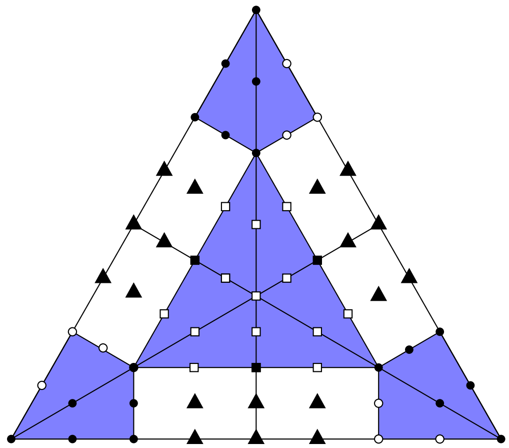

Figure 2.13: The subset $\mathcal{D}_{4,T}$ relative to a macro-triangle T of Δ_{PS}. The B-ordinates of the restriction to T of a spline $s \in S_4^{1,2,3}(\Delta_{\mathrm{PS}})$ are determined for the specified subsets of domain points from the interpolation conditions at the vertices and the regularity of s.

for given values $f_i^{a,b}$ *and* $g_{m,n}$, $\omega_{m,n,q}$ *being a unit direction parallel to* $\langle R_{m,n}, Z_q\rangle$, *where* Z_q *is the triangle split point of a triangle* T_q *having* $\langle V_m, V_n\rangle$ *as an edge.*

Proof. The proof will be done on a single macro-triangle. Its extension to the whole triangulation is deduced from Theorem 1 in [32]. To prove the insolvency of the interpolation problem on a macro-triangle T, we only need to determine the BB-coefficients on T of a spline s satisfying (2.15). For the sake of simplicity, and without loss of generality, consider a single macro-triangle $T\langle V_1, V_2, V_3\rangle$. On each micro-triangle in T, the spline s is a quartic polynomial (see Figure 2.13). We will show how the BB-coefficients of s are uniquely determined by conditions (2.15) and the smoothness requirements.

Since the spline s is C^2 continuous at vertices V_i, $i = 1, 2, 3$, then the values and derivatives up to order 2 at each vertex in (2.15) are uniquely determined by the BB-coefficients relative to the domain points lying in the disks of radius 2 associated with the vertices of T, i.e. the subsets each consisting of the nine domain points lying in each of the coloured neighbouring regions of the vertices shown in Figure 2.13, and which are represented by the symbols $\bullet$ and $\circ$.

To deal with C^2 smoothness at triangle split point Z, we define the triangle with vertices

$$W_i := \frac{V_i + Z}{2}, \ \ i = 1, 2, 3. \tag{2.16}$$

The BB-coefficients relative to the domain points in this triangle are computed by our construction. Also the BB-coefficients marked with $\blacksquare$ are determined from the second derivative of s in the specified direction given in (2.15), to give six independent constraints that yield a quadratic polynomial p_2 in $\tilde{T}\langle W_1, W_2, W_3\rangle$ from which the BB-coefficients related to the domain points ordinates indicated by $\square$ in Figure 2.13 are determined.

The remaining BB-coefficients, indicated by $\blacktriangle$, and placed in the 0th and 1st rows parallel to edge $\langle V_i, V_j\rangle$ are computed from C^3 smoothness conditions along $\langle R_{i,j}, Z\rangle$. For $\ell = 0$, let b_k^0, $k = 1, \ldots, 7$, be the seven central BB-coefficients placed on 0th row parallel to edge $\langle V_i, V_j\rangle$. They can be considered as the BB-coefficients of the univariate cubic polynomial p_3^0 defined on the segment $\left[\hat{W}_{i,j}^0, \tilde{W}_{i,j}^0\right]$ with

$$\hat{W}_{i,j}^0 := \frac{3}{4}V_i + \frac{1}{4}R_{i,j} \quad \text{and} \quad \tilde{W}_{i,j}^0 := \frac{3}{4}V_j + \frac{1}{4}R_{i,j}$$

having BB-coefficients b_1^0, b_2^0, b_6^0 and b_7^0 (see Figure 2.14). After subdivision, b_3^0, b_4^0 and b_5^0 result. This construction ensures that the spline is C^3 at $R_{i,j}$. To determine the BB-coefficients b_k^1,

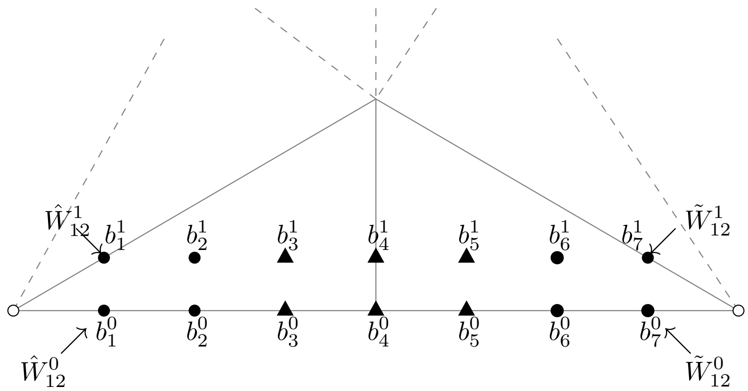

Figure 2.14: The seven central BB-coefficients placed on ℓth ($\ell = 0, 1$) row parallel to edge $\langle V_1, V_2 \rangle$.

$k = 1, \ldots, 7$, associated with the domain points lying on the 1st row parallel to edge $\langle V_i, V_j \rangle$, a similar approach is applied, by considering the points

$$\hat{W}^1_{i,j} := \frac{3}{4} V_i + \frac{1}{4} Z \quad \text{and} \quad \tilde{W}^1_{i,j} := \frac{3}{4} V_j + \frac{1}{4} Z,$$

and the polynomial p^1_3 defined on $\left[\hat{W}^1_{i,j}, \tilde{W}^1_{i,j}\right]$ with BB-coefficients b^1_1, b^1_2, b^1_6 and b^1_7. The BB-coefficients b^ℓ_1, b^ℓ_2, b^ℓ_6 and b^ℓ_7, $\ell = 0, 1$, have been already determined by the interpolation conditions (2.15) at V_i and V_j. This construction ensures that the spline is C^3 across the edge $\langle R_{i,j}, Z \rangle$.

The construction above is carried out on a the macro-triangle T. The rest of the proof runs as in [32, Thm. 1].

□

In what follows, we divide the work into two parts. In the first one, we discuss the space of quartic Powell-Sabin splines on a single macro-triangle T, wherein we investigate the necessary and sufficient conditions to achieve global C^2 smoothness on T. The second part is devoted to extend the results obtained for a macro-triangle to the whole triangulation.

2.6.1 The Powell-Sabin space on a single triangle

As mentioned earlier, we are looking for geometrical conditions ensuring that $S^{1,2,3}_4(\Delta_{\rm PS})$ becomes of C^2 continuity. To do that, we start by analysing the Powell-Sabin space relative to a single triangle by defining an appropriate basis for it, then, we will generalize the obtained results on the whole triangulation.

Consider the macro-triangle $T \langle V_1, V_2, V_3 \rangle$, with $V_1 = (x_1, y_1)$, $V_2 = (x_2, y_2)$ and $V_3 = (x_3, y_3)$ (see Figure 1.5). The barycentric coordinates of the vertices V_1, V_2 and V_3 w.r.t. T are $(1, 0, 0)$, $(0, 1, 0)$ and $(0, 0, 1)$, respectively. Suppose that the barycentric coordinates of $Z = (x_z, y_z)$ are (z_1, z_2, z_3), and let $(\lambda_{1,2}, \lambda_{2,1}, 0)$, $(0, \lambda_{2,3}, \lambda_{3,2})$ and $(\lambda_{1,3}, 0, \lambda_{3,1})$ be coordinates of $R_{1,2} = (x_{1,2}, y_{1,2})$, $R_{2,3} = (x_{2,3}, y_{2,3})$ and $R_{3,1} = (x_{3,1}, y_{3,1})$, respectively. Moreover, we can write

$$R_{1,2} = \tau_{1,1} V_2 + \tau_{2,1} R_{2,3} + \tau_{3,1} Z, \; R_{2,3} = \tau_{1,2} V_3 + \tau_{2,2} R_{3,1} + \tau_{3,2} Z, \; R_{3,1} = \tau_{1,3} V_1 + \tau_{2,3} R_{1,2} + \tau_{3,3} Z,$$

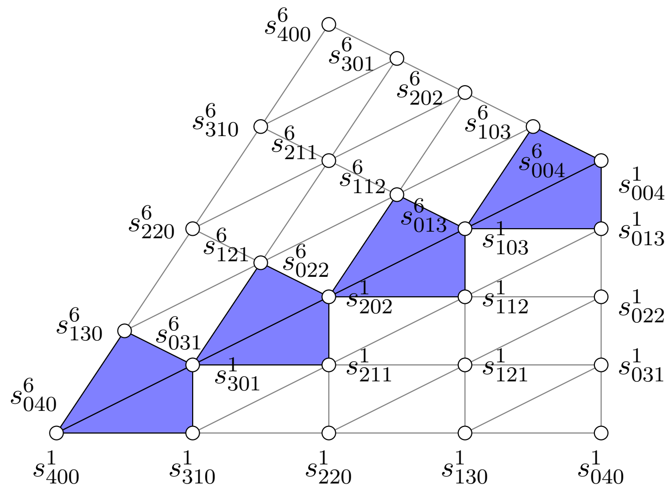

Figure 2.15: The B-ordinates relative to micro-triangles t^1 and t^6 sharing vertex V_1 are shown. The other follow cyclically. The control net triangles involved in the C^1 continuity conditions between s^1 and s^6 are shown in blue.

where

$$\begin{aligned}
(\tau_{1,1},\ \tau_{2,1},\ \tau_{3,1}) &:= \left(\frac{\lambda_{1,2}z_3+\lambda_{3,2}\left(\lambda_{2,1}+z_1-1\right)}{\lambda_{3,2}z_1}, -\frac{\lambda_{1,2}z_3}{\lambda_{3,2}z_1}, \frac{\lambda_{1,2}}{z_1}\right),\\
(\tau_{1,2},\ \tau_{2,2},\ \tau_{3,2}) &:= \left(\frac{-z_3\lambda_{2,3}+\lambda_{3,2}z_2-\lambda_{31}\left(z_2-\lambda_{2,3}\right)}{\lambda_{1,3}z_2}, -\frac{\lambda_{2,3}z_1}{\lambda_{1,3}z_2}, \frac{\lambda_{2,3}}{z_2}\right),\\
(\tau_{1,3},\ \tau_{2,3},\ \tau_{3,3}) &:= \left(\frac{\lambda_{3,1}\left(z_2-\lambda_{2,1}\right)}{\lambda_{2,1}z_3}+1, -\frac{\lambda_{3,1}z_2}{\lambda_{2,1}z_3}, \frac{\lambda_{3,1}}{z_3}\right).
\end{aligned} \tag{2.17}$$

Let us suppose that T is decomposed into the following micro-triangles t^ℓ, $\ell = 1, \ldots, 6$:

$$t^1\left\langle V_1, R_{1,2}, Z\right\rangle, t^2\left\langle R_{1,2}, V_2, Z\right\rangle, t^3\left\langle V_2, R_{2,3}, Z\right\rangle, t^4\left\langle R_{2,3}, V_3, Z\right\rangle, t^5\left\langle V_3, R_{3,1}, Z\right\rangle, t^6\left\langle R_{3,1}, V_1, Z\right\rangle.$$

Let s^ℓ be the restriction of s to t^ℓ, and $s^\ell_{i,j,k}$, $i+j+k=4$, be its BB-coefficients.

The continuity of s on T is easily expressed in terms of the BB-coefficients. For instance, the continuity across the micro-edge $\langle Z, V_1\rangle$ is equivalent to the fulfillment of conditions

$$s^1_{4-j,0,j} = s^6_{0,4-j,j},\ j = 0, \ldots, 4.$$

The conditions yielding the continuity across $\langle Z, R_{1,2}\rangle$, $\langle Z, V_2\rangle$, $\langle Z, R_{2,3}\rangle$, $\langle Z, V_3\rangle$ and $\langle Z, R_{3,1}\rangle$ are similar and involve the BB-coefficients of $\left\{s^1, s^2\right\}$, $\left\{s^2, s^3\right\}$, $\left\{s^3, s^4\right\}$, $\left\{s^4, s^5\right\}$ and $\left\{s^5, s^6\right\}$, respectively (see Figure 2.15).

We also recall that the C^1 continuity of s across $\langle Z, V_1\rangle$ is expressed as

$$s^6_{1,3-j,j} = \tau_{1,3}s^1_{4-j,0,j} + \tau_{2,3}s^1_{3-j,1,j} + \tau_{3,3}s^1_{3-j,0,j+1}, \quad j = 0, 1, 2, 3,$$

where the barycentric coordinates $(\tau_{1,3},\ \tau_{2,3},\ \tau_{3,3})$ of $R_{3,1}$ with respect to $t^1\left\langle V_1,\ R_{1,2},\ Z\right\rangle$ are given in (4.2). Similar expressions are obtained for the C^1 continuity across the micro-edges $\langle Z, R_{1,2}\rangle$, $\langle Z, V_2\rangle$, $\langle Z, R_{2,3}\rangle$, $\langle Z, V_3\rangle$ and $\langle Z, R_{3,1}\rangle$ that use the barycentric coordinates of V_2, $R_{2,3}$, V_3, $R_{3,1}$ and V_1 w.r.t. t^1, t^2, t^3, t^4 and t^5, respectively.

Definition 2.6.2. *Let $\mathcal{C}_1$, $\mathcal{C}_2$ and $\mathcal{C}_3$ be the unique solutions given by Theorem 2.6.1 associated with the interpolation data $f_i^{a,b} = 0$, $i = 1,2,3$, $a, b \geq 0$, $a + b \leq 2$, and*

$$g_{1,2} = \frac{24\lambda_{1,2}\lambda_{2,1}}{\|Z - R_{1,2}\|^2}, \quad g_{2,3} = g_{3,1} = 0,$$
$$g_{2,3} = \frac{24\lambda_{2,3}\lambda_{3,2}}{\|Z - R_{2,3}\|^2}, \quad g_{1,2} = g_{3,1} = 0,$$
$$g_{3,1} = \frac{24\lambda_{3,1}\lambda_{1,3}}{\|Z - R_{3,1}\|^2}, \quad g_{1,2} = g_{2,3} = 0,$$

respectively. We call $\mathcal{C}_\ell$, $\ell = 1,2,3$, the blending functions of the first kind relative to V_ℓ.

The $f-$values yielding the blending functions above are all equal to zero. New blending functions results when all $g-$values are zero.

Definition 2.6.3. *Let $\mathcal{D}_1$ be the unique solution given by Theorem 2.6.1 associated with the values $g_{1,2} = g_{2,3} = g_{3,1} = 0$, $f_2^{a,b} = f_3^{a,b} = 0$ for $a, b \geq 0$ and $a + b \leq 2$, $f_1^{0,0} = 0$, and*

$$\begin{aligned}
f_1^{1,0} &= \frac{4}{F_1}\left(y_1 - y_z\right), \\
f_1^{0,1} &= -\frac{4}{F_1}\left(x_1 - x_z\right), \\
f_1^{2,0} &= \frac{12}{F_1^2}\left(y_1 - y_z\right)\left(\lambda_{1,2}y_1 + \left(1 + \lambda_{2,1}\right)y_z - 2y_{1,2}\right), \\
f_1^{1,1} &= \frac{12}{F_1^2}\left(-x_2\left(\lambda_{1,2}\left(y_z - y_1\right) - 2y_z + y_1 + y_{1.2}\right)\right. \\
&\quad \left. + x_1\left(-\lambda_{1,2}y_1 - \lambda_{2,1}y_z + y_r\right) + x_r\left(y_1 - y_z\right)\right), \\
f_1^{0,2} &= \frac{12}{F_1^2}\left(x_1 - x_z\right)\left(\lambda_{1,2}x_1 + \left(1 + \lambda_{2,1}\right)x_z - 2x_{1,2}\right),
\end{aligned}$$

with

$$F_1 := x_z\left(y_{1,2} - y_1\right) + x_1\left(y_z - y_r\right) + x_{1,2}\left(y_1 - y_z\right).$$

We call $\mathcal{D}_1$ the blending function of the second kind relative to V_1.

For vertices V_2 and V_3, the blending functions of the second kind $\mathcal{D}_2$ and $\mathcal{D}_3$ are defined respectively as solutions of the Hermite interpolation problem in Theorem 2.6.1 with the following datasets:

1. $g_{1,2} = g_{2,3} = g_{3,1} = 0$, $f_1^{a,b} = f_3^{a,b} = 0$ for $a, b \geq 0$ and $a + b \leq 2$, $f_2^{0,0} = 0$, and

$$\begin{aligned}
f_2^{1,0} &= \frac{4}{F_2}\left(y_2 - y_z\right), \\
f_2^{0,1} &= -\frac{4}{F_2}\left(x_2 - x_z\right), \\
f_2^{2,0} &= \frac{12}{F_2^2}\left(y_2 - y_z\right)\left(\lambda_{1,2}y_2 + \left(1 + \lambda_{2,1}\right)y_z - 2y_{2,3}\right), \\
f_2^{1,1} &= \frac{12}{F_2^2}\left(-x_z\left(\lambda_{1,2}\left(y_z - y_2\right) - 2y_z + y_2 + y_{2,3}\right)\right. \\
&\quad \left. + x_2\left(-\lambda_{1,2}y_2 - \lambda_{2,1}y_z + y_{2,3}\right) + x_{2,3}\left(y_2 - y_z\right)\right), \\
f_2^{0,2} &= \frac{12}{F_2^2}\left(x_2 - x_z\right)\left(\lambda_{1,2}x_2 + \left(1 + \lambda_{2,1}\right)x_z - 2x_{2,3}\right),
\end{aligned}$$

with $F_2 := x_z\left(y_{2,3} - y_2\right) + x_2\left(y_z - y_{2,3}\right) + x_{2,3}\left(y_2 - y_z\right).$

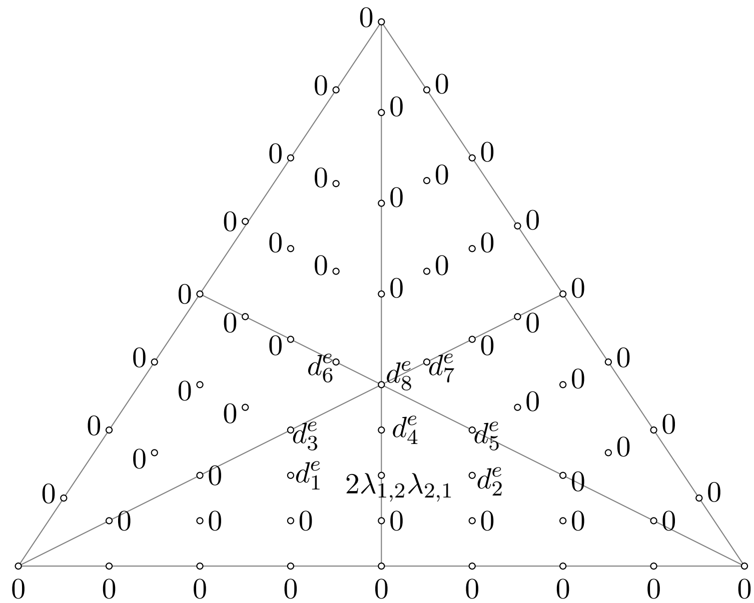

Figure 2.16: Bernstein-Bézier coefficients of blending function $\mathcal{C}_1$.

2. $g_{1,2} = g_{2,3} = g_{3,1} = 0$, $f_1^{a,b} = f_2^{a,b} = 0$ for $a, b \geq 0$ and $a + b \leq 2$, $f_3^{0,0} = 0$, and

$$
\begin{aligned}
f_3^{1,0} &= \frac{4}{F_3}\left(y_3 - y_z\right), \\
f_3^{0,1} &= -\frac{4}{F_3}\left(x_3 - x_z\right), \\
f_3^{2,0} &= \frac{12}{F_3^2}\left(y_3 - y_z\right)\left(\lambda_{1,2} y_3 + \left(1 + \lambda_{2,1}\right) y_z - 2 y_{3,1}\right), \\
f_3^{1,1} &= \frac{12}{F_3^2}\left(-x_z\left(\lambda_{1,2}\left(y_z - y_3\right) - 2y_z + y_3 + y_{3,1}\right)\right. \\
&\quad \left. + x_3\left(-\lambda_{1,2} y_3 - \lambda_{2,1} y_z + y_{3,1}\right) + x_{3,1}\left(y_3 - y_z\right)\right), \\
f_3^{0,2} &= \frac{12}{F_3^2}\left(x_3 - x_z\right)\left(\lambda_{1,2} x_3 + \left(1 + \lambda_{2,1}\right) x_z - 2 x_{3,1}\right),
\end{aligned}
$$

with $F_2 := x_z\left(y_{3,1} - y_3\right) + x_3\left(y_z - y_{3.1}\right) + x_{3,1}\left(y_3 - y_z\right)$.

On each micro-triangle t^ℓ, $\ell = 1, \ldots, 6$, the splines $\mathcal{C}_1$ and $\mathcal{D}_1$, are quartic polynomials that can be represented according to (1.1). The corresponding BB-coefficients are schematically represented in Figures 2.16 and 2.17, respectively. They are given by

$$d_1^e = \lambda_{2,1},\ d_2^e = \lambda_{1,2},\ d_3^e = z_2,\ d_4^e = \lambda_{1,2} z_2 + \lambda_{2,1} z_1,\ d_5^e = z_1,\ d_6^e = \lambda_{1,3} z_2,\ d_7^e = z_1 \lambda_{2,3},\ d_8^e = 2 z_1 z_2,$$

and

$$d_1^v = 1,\ d_2^v = \lambda_{1,2},\ d_3^v = \lambda_{1,2}^2,\ d_4^v = \lambda_{1,2}^3,\ d_5^v = \tau_{2,3},\ d_6^v = \tau_{2,3}\,\lambda_{1,3},\quad d_7^v = \tau_{2,3}\,\lambda_{1,3}^2,\ d_8^v = \tau_{2,3}\,\lambda_{1,3}^3.$$

Figure 2.18 shows the typical plots of blending functions.

$S_4^{1,2,3}(T)$ is a linear space with dimension equal to 21 and its subspace $\mathbb{P}_4$ has dimension 15, so we can think of extending a basis for $\mathbb{P}_4$ to one for $S_4^{1,2,3}(T)$.

Proposition 2.6.4. *It holds that*

$$S_4^{1,2,3}(T) = \mathbb{P}_4 \oplus \operatorname{span}\left\{\mathcal{D}_1, \mathcal{D}_2, \mathcal{D}_3, \mathcal{C}_1, \mathcal{C}_2, \mathcal{C}_3\right\}.$$

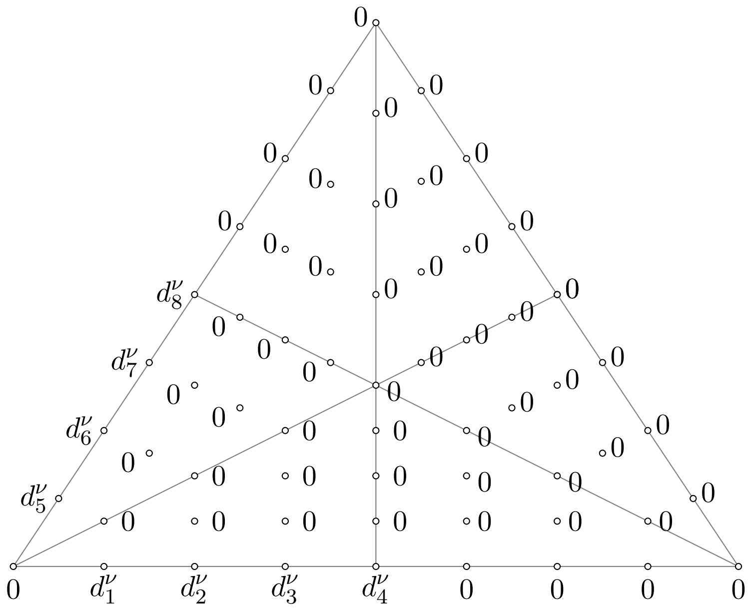

Figure 2.17: Bernstein-Bézier coefficients of blending function $\mathcal{D}_1$.

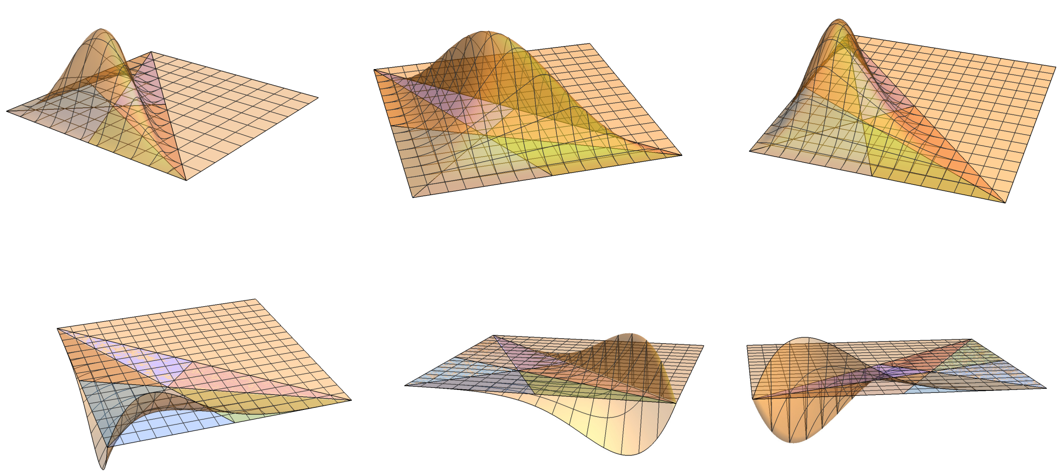

Figure 2.18: (Top) Blending functions $\mathcal{C}_i$ and (bottom) $\mathcal{D}_i$.

Proof. As all functions $\mathcal{D}_\ell$ and $\mathcal{C}_\ell$ are in $S_4^{1,2,3}(T)$, it only remains to show that no non-trivial linear combination of those functions is in $\mathbb{P}_4$. Assume that there exist non-zero coefficients d_i and c_i such that

$$P := d_1\,\mathcal{D}_1 \;+\; d_2\,\mathcal{D}_2 \;+\; d_3\,\mathcal{D}_3 \;+\; c_1\,\mathcal{C}_1 \;+\; c_2\,\mathcal{C}_2 \;+\; c_3\,\mathcal{C}_3 \;\in\; \mathbb{P}_4.$$

Then, in particular, P is of C^4 continuity across $\langle Z, R_{1,2}\rangle$, $\langle Z, R_{2,3}\rangle$ and $\langle Z, R_{3,1}\rangle$, so that

$$\begin{aligned}
0 &= \frac{d_1\lambda_{1,2}^3}{\lambda_{2,1}^4} + \frac{d_2 z_3\lambda_{1,2}}{z_1\lambda_{2,1}\lambda_{3,2}},\\
0 &= \frac{\lambda_{2,3}\left(d_3 z_1\lambda_{3,2}^3 + d_2 z_2\lambda_{1,3}\lambda_{2,3}^2\right)}{z_2\lambda_{1,3}\lambda_{3,2}^4},\\
0 &= -\frac{d_1 z_2\lambda_{1,3}^3 + d_3 z_3\lambda_{2,1}\lambda_{3,1}^2}{z_3\lambda_{2,1}\lambda_{3,1}^3}.
\end{aligned}$$

The determinant of this system of linear equations is equal to

$$\frac{(1-\lambda_{2,1})\,(1-\lambda_{3,2})}{\lambda_{2,1}^4\lambda_{3,1}^3\lambda_{3,2}^4}\left(a\;\lambda_{3,2}^2 + b\;\lambda_{3,2} + c\right),$$

where

$$\begin{aligned}
a &:= -2\lambda_{3,1}^2\lambda_{2,1}^2 + 2\lambda_{3,1}\lambda_{2,1}^2 - \lambda_{2,1}^2 + 2\lambda_{3,1}^2\lambda_{2,1} - \lambda_{3,1}^2,\\
b &:= 2\lambda_{2,1}^2\lambda_{3,1}^2 - 4\lambda_{2,1}\lambda_{3,1}^2 + 2\lambda_{3,1}^2,\\
c &: -\lambda_{2,1}^2\lambda_{3,1}^2 + 2\lambda_{2,1}\lambda_{3,1}^2 - \lambda_{3,1}^2.
\end{aligned}$$

The discriminant of equation $a\;\lambda_{3,2}^2 + b\;\lambda_{3,2} + c = 0$ is given by

$$\Delta = -4\,(1-\lambda_{2,1})^{\,2}\lambda_{2,1}^2\,(1-\lambda_{3,1})^{\,2}\lambda_{3,1}^2,$$

so that it is negative. Therefore, the unique solution is $d_1 = d_2 = d_3 = 0$.

Taking into account the latter, the polynomial function P can be rewritten as

$$P = c_1\,\mathcal{C}_1 \;+\; c_2\,\mathcal{C}_2 \;+\; c_3\,\mathcal{C}_3.$$

The C^4 smoothness of $\mathcal{C}_\ell$ across $\langle V_1, Z\rangle$, $\langle V_2, Z\rangle$ and $\langle V_3, Z\rangle$ yields

$$\begin{aligned}
0 &= \frac{2\lambda_{3,1}^3\left(z_3\left(\lambda_{3,1}\left(c_2 z_2 + c_3\left(-z_2+z_3+1\right)\right) - 2c_3 z_3\right) + c_1 z_2\left(4z_3 - \left(-3z_2+z_3+3\right)\lambda_{3,1}\right)\right)}{z_3^4},\\
0 &= \frac{1}{z_1^4}\left(-2\lambda_{1,2}^3\left(-c_1 z_1\left(\left(z_2+2z_3-2\right)\lambda_{2,1} + z_2\right) + z_3\left(c_2\left(\left(z_2+4z_3-4\right)\lambda_{2,1} + 3z_2\right) - c_3 z_1\lambda_{1,2}\right)\right)\right),\\
0 &= \frac{1}{z_2^4}\left(-2\lambda_{2,3}^3\left(c_1 z_1 z_2\lambda_{2,3} + c_3 z_1\left(-3z_3\lambda_{2,3} + 4z_2\lambda_{3,2}\right) + c_2 z_2\left(z_3 - \left(2z_2+z_3\right)\lambda_{3,2}\right)\right)\right).
\end{aligned}$$

This linear system has the following determinant

$$\frac{32\,(\lambda_{2,1}-1)^{\,3}\lambda_{3,1}^3\,(\lambda_{3,2}-1)^{\,3}}{z_2^3 z_3^3\,(z_2+z_3-1)^{\,3}}\left(\bar{a} + \bar{b}\lambda_{2,1}\right),$$

where,

$$\begin{aligned}
\bar{a} &:= z_2\left(-2\lambda_{3,1} + z_3\left(-\lambda_{3,1}\right) + 2z_2\lambda_{3,1} + 3z_3\right)\left(2z_3\lambda_{3,2} + 3z_2\lambda_{3,2} - 2z_3\right),\\
\bar{b} &:= -2z_3 z_2^2\lambda_{3,1} - 5z_3^2 z_2\lambda_{3,1} + 8z_3 z_2\lambda_{3,1} - 3\left(z_3-1\right)z_3\left(\lambda_{3,2}-1\right)\left(\left(z_3+2\right)\lambda_{3,1} - 3z_3\right)\\
&\quad - 3z_3^2 z_2 + 3z_2^3\lambda_{3,1}\lambda_{3,2} + 5z_3 z_2^2\lambda_{3,2} + 3\left(3z_3-4\right)z_2^2\lambda_{3,1}\lambda_{3,2} + z_3\left(17z_3-14\right)z_2\lambda_{3,2}\\
&\quad - 12z_3 z_2\lambda_{3,1}\lambda_{3,2} + 9z_2\lambda_{3,1}\lambda_{3,2}.
\end{aligned}$$

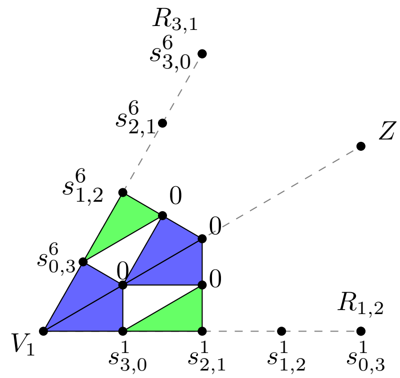

Figure 2.19: BB-coefficients involved in the C^1 and C^2 continuity conditions between the restrictions of the spline to the micro-triangles t^1 and t^6.

The determinant is equal to zero if and only if $\lambda_{2,1} = -\frac{\bar{a}}{\bar{b}}$. Since $\lambda_{2,1}$ is in $(0, 1)$, the value of $\frac{\bar{a}}{\bar{b}}$ must be in $(-1, 0)$ for all possible values of parameters z_2, z_3, $\lambda_{3,2}$ and $\lambda_{3,1}$, which is not true (for instance, for $z_2 = 0.802$, $z_3 = 0.493$, $\lambda_{3,2} = 0.293$ and $\lambda_{3,1} = 0.45$ it holds $\frac{\bar{a}}{\bar{b}} = 1.07038 \notin (-1, 0)$). Then, it follows that $c_1 = c_2 = c_3 = 0$. The proof is complete. □

In general, the functions in $S_4^{1,2,3}(T)$ are not in $C^2(T)$ [32]. Therefore, it is reasonable to study under which conditions on the Powell-Sabin refinement of T the splines in $S_4^{1,2,3}(T)$ are C^2 continuous.

In order to achieve completely C^2 quartic Powell-Sabin splines, the blending functions need to be C^2 continuous across the micro-edges $\langle Z, V_1\rangle$, $\langle Z, V_2\rangle$ and $\langle Z, V_3\rangle$. We start by analyzing under what conditions the C^2 continuity of blending functions $\mathcal{D}_i,\ i = 1, 2, 3$, is achieved. Then we will extract the relations between the first kind blending functions under the achieved configuration so that the spline becomes C^2 continuous.

In Figure 2.19, a schematic representation of BB-coeficients involved in the C^2 smoothness across the edge $\langle Z, V_1\rangle$ is done.

Proposition 2.6.5. *Blending functions of the second kind are C^2 continuous on $T\langle V_1, V_2, V_3\rangle$ if and only if*

$$\lambda_{2,1} = \frac{z_2}{1 - z_3},\ \lambda_{3,1} = \frac{z_3}{1 - z_2},\ \lambda_{3,2} = \frac{z_3}{1 - z_1}.$$

Proof. Consider $\mathcal{D}_1$ and the structure shown in Figure 2.19. It is a C^2 continuous function across $\langle V_1\,, Z\rangle$ if and only if

$$s^6_{1,2} = \tau^2_{2,3}\, s^1_{2,1} + 2\,\tau_{2,3}\,\tau_{1,3}\, s^1_{3,0}.$$

Note that $s^6_{1,2} = \tau_{2,3}\lambda_{1,3}\, s^1_{3,0}$ and $s^1_{2,1} = \lambda_{1,2}\, s^1_{3,0}$. That gives

$$\tau_{2,3} = \frac{\lambda_{1,3} - 2\tau_{1,3}}{\lambda_{1,2}}, \tag{2.18}$$

Analogously, $\mathcal{D}_2$ and $\mathcal{D}_3$ are C^2 continuous functions across $\langle V_2,\ Z\rangle$ and $\langle V_3,\ Z\rangle$, respectively, if and only if

$$\tau_{2,2} = \frac{\lambda_{3,2} - 2\tau_{1,2}}{\lambda_{3,1}} \quad \text{and} \quad \tau_{2,3} = \frac{\lambda_{1,3} - 2\tau_{1,3}}{\lambda_{1,2}}. \tag{2.19}$$

Equations (2.18) and (2.19) can be reformulated as

$$\begin{aligned}
\frac{\lambda_{3,1}z_2 + \lambda_{2,1}\left(\lambda_{3,1}\left(z_2+z_3-2\right)+z_3\right)}{\lambda_{1,2}\lambda_{2,1}z_3} &= 0, \\
\frac{\lambda_{3,2}\left(\lambda_{2,1}+\left(\lambda_{2,1}-2\right)z_2\right)-\left(\lambda_{2,1}+\lambda_{3,2}-1\right)z_3}{\lambda_{2,3}\lambda_{3,2}z_1} &= 0, \\
\frac{\lambda_{3,1}z_2 + \lambda_{2,1}\left(\lambda_{3,1}\left(z_2+z_3-2\right)+z_3\right)}{\lambda_{1,2}\lambda_{2,1}z_3} &= 0.
\end{aligned} \tag{2.20}$$

The unique solution of (2.20) provides the values in the claim.

□

Conditions in Proposition 2.6.5 can be geometrically interpreted as follows.

Proposition 2.6.6. *Functions $\mathcal{D}_i$, $i=1,2,3$, are C^2 continuous if and only if the points in each of subsets $\{V_1, Z, R_{2,3}\}$, $\{V_2, Z, R_{3,1}\}$ and $\{V_3, Z, R_{1,2}\}$ are collinear.*

Proof. First, let us prove that the conditions are necessary. Without loss of generality, let us consider the third of the subsets. We have to prove that V_3, Z and $R_{1,2}$ are collinear. By Proposition 2.6.5, the barycentric coordinates of $R_{1,2}$ w.r.t. T are

$$(\lambda_{1,2},\lambda_{2,1},0) = (1-\lambda_{2,1},\lambda_{2,1}) = \left(\frac{1-z_2-z_3}{1-z_3},\frac{z_2}{1-z_3},0\right) = \left(\frac{z_1}{1-z_3},\frac{z_2}{1-z_3},0\right).$$

Then,

$$R_{1,2} = \frac{z_1}{1-z_3}V_1 + \frac{z_2}{1-z_3}V_2.$$

Moreover, $Z = z_1V_1 + z_2V_2 + z_3V_3$. Taking into account the Cartesian coordinates of Z and the vertices, we get

$$R_{1,2} - Z = \frac{z_3}{1-z_3}\left(z_1x_1 + z_2x_2 + \left(z_3-1\right)x_3, z_1y_1 + z_2y_2 + \left(z_3-1\right)y_3\right).$$

Therefore, the slope of the straight line determined by Z and $R_{1,2}$ is equal to

$$m_{1,2} := \frac{z_1y_1 + z_2y_2 + \left(z_3-1\right)y_3}{z_1x_1 + z_2x_2 + \left(z_3-1\right)x_3}.$$

On the other hand, the straight line determined by Z and V_3 has the direction of vector

$$Z - V_3 = z_1V_1 + z_2V_2 + \left(z_3-1\right)V_3 = \left(z_1x_1 + z_2x_2 + \left(z_3-1\right)x_3, z_1y_1 + z_2y_2 + \left(z_3-1\right)y_3\right),$$

so that its slope is also equal to $m_{1,2}$. Consequently, both the straight lines defined by $\{Z, R_{1,2}\}$ and $\{Z, V_3\}$ have the same slope and pass through the Z point, and V_3, Z and $R_{1,2}$ are collinear.

Conversely, suppose that V_3, Z and $R_{1,2}$ are collinear. As proved above, the slope of the straight line determined by V_3 and Z is equal to $m_{1,2}$, so that its equation is $y = m_{1,2}x + n_{1,2}$, where $n_{1,2}$ is computed by imposing that the line passes through V_3 to get

$$n_{1,2} = \frac{y_3\left(z_1x_1 + z_2y_2\right) - x_3\left(z_1y_1 + z_2y_2\right)}{z_1x_1 + z_2x_2 + \left(z_3-1\right)x_3}.$$

Since $R_{1,2} = \lambda_{1,2}V_1 + \lambda_{2,1}V_2$ can be written in Cartesian coordinates as

$$\left(\lambda_{1,2}x_1 + \lambda_{2,1}x_2, \lambda_{1,2}y_1 + \lambda_{2,1}y_2\right) = \left(\lambda_{1,2}x_1 + \left(1-\lambda_{1,2}\right)x_2, \lambda_{1,2}y_1 + \left(1-\lambda_{1,2}\right)y_2\right),$$

it must be fulfilled that

$$m_{1,2}\left(\lambda_{1,2}x_1 + \left(1-\lambda_{1,2}\right)x_2\right) + n_{1,2} = \lambda_{1,2}y_1 + \left(1-\lambda_{1,2}\right)y_2.$$

A straightforward calculation gives

$$\lambda_{1,2} = \frac{z_1}{1 - z_3}.$$

The proof is complete.

□

Once C^2 continuity of blending functions of the second kind has been characterized, we need now to get C^2 continuity for the spline on T. To this end, we should derive the C^2 smoothness relations between the three blending functions of the first kind which are defined on a split triangle that meets the conditions in Proposition 2.6.5.

Theorem 2.6.7. *Assume that the PS-split T_{PS} of T meets the conditions in Proposition 2.6.5. Then, the spline $s = p_4 + \sum_{i=1}^{3} (d_i \mathcal{D}_i + c_i \mathcal{C}_i), p_4 \in \mathbb{P}_4(T)$, in $S_4^{1,2,3}(T)$ is fully C^2 continuous on T if and only if*

$$c_1 z_2 = c_3 z_3, \quad c_2 z_3 = c_1 z_1, \quad c_3 z_1 = c_2 z_2. \tag{2.21}$$

Proof. The C^2-smoothness conditions across the edge $\langle V_1, Z\rangle$ gives the equality

$$0 = \tau_{3,3}^2 (c_1 z_2 + c_3 z_3) + 2\tau_{3,3}\tau_{2,3} c_1 \lambda_{2,1}.$$

Substituting $\tau_{3,3}$, $\tau_{2,3}$ and $\lambda_{2,1}$ respectively by their values $\frac{1}{1-z_2}$, $\frac{1-z_3}{1-z_2}$, and $\frac{z_2}{1-z_3}$, we get

$$c_1 z_2 = c_3 z_3.$$

The other two conditions are derived similarly.

□

Under the hypothesis in Proposition 2.6.5, the general solution of system (2.21) depends on one parameter $\alpha \in \mathbb{R}$ and can be written as $(c_1, c_2, c_3) = \alpha (z_3, z_1, z_2)$, so that any C^2 continuous spline $s \in S_4^{1,2,3}(T)$ can be expressed as

$$s = p_4 + \sum_{i=1}^{3} d_i \mathcal{D}_i + \alpha \mathcal{B}^t,$$

where $\mathcal{B}^t := z_3 \mathcal{C}_1 + z_1 \mathcal{C}_2 + z_2 \mathcal{C}_3$ is a $C^2(T)$ continuous function associated to triangle T which will be called blending function of the third kind. The condition imposed on the Powell-Sabin refinement of T results in a lower dimension to $S_4^{1,2,3}(T)$, 19 instead of 21.

The B-ordinates of $\mathcal{B}^t$ are given by

$$\begin{array}{llll}
d_1 = z_3 \lambda_{2,1}, & d_5 = 2z_1 \lambda_{2,3} \lambda_{3,2}, & d_9 = z_2 \lambda_{3,1}, & d_{13} = 2z_1 (\lambda_{2,3} z_3 + \lambda_{3,2} z_2), \\
d_2 = 2z_3 \lambda_{1,2} \lambda_{2,1}, & d_6 = z_1 \lambda_{2,3}, & d_{10} = 2z_3 z_2, & d_{14} = 2z_1 z_2, \\
d_3 = z_3 \lambda_{1,2}, & d_7 = z_2 \lambda_{1,3}, & d_{11} = 2z_3 (\lambda_{1,2} z_2 + \lambda_{2,1} z_1), & d_{15} = 2z_2 (\lambda_{1,3} z_3 + \lambda_{3,1} z_1), \\
d_4 = z_1 \lambda_{3,2}, & d_8 = 2z_2 \lambda_{1,3} \lambda_{3,1}, & d_{12} = 2z_1 z_3, & d_{16} = 6z_1 z_2 z_3.
\end{array}$$

They are shown in Figure 2.20. The typical plot of a function $\mathcal{B}^t$ is shown in Figure 2.21.

We have just proved that every spline $s \in S_4^{1,2,3}(T)$ is C^2 continuous on a triangle T for which its PS-split meets the condition in Proposition 2.6.5. When the refinement of T satisfies the conditions of Proposition 2.6.5, the dimension of $S_4^{1,2,3}(T)$ diminishes from 21 to 19, since three B-splines of the first kind give rise to a single B-spline of the third kind, $\mathcal{B}^t$.

Now, it remains to prove that the spline s is also C^2 continuous over the whole triangulation Δ if the split point of each macro-element of Δ satisfies the conditions in Proposition 2.6.5 and the edge split points produced on common sides of two triangles coincide, i.e. if the opposite vertices of each pair of triangles sharing an edge are aligned with the corresponding triangle split points. Denote by $\widetilde{\Delta}_{\mathrm{PS}}$ this kind of triangulation. Figure 2.22 shows a triangulation satisfying these requirements.

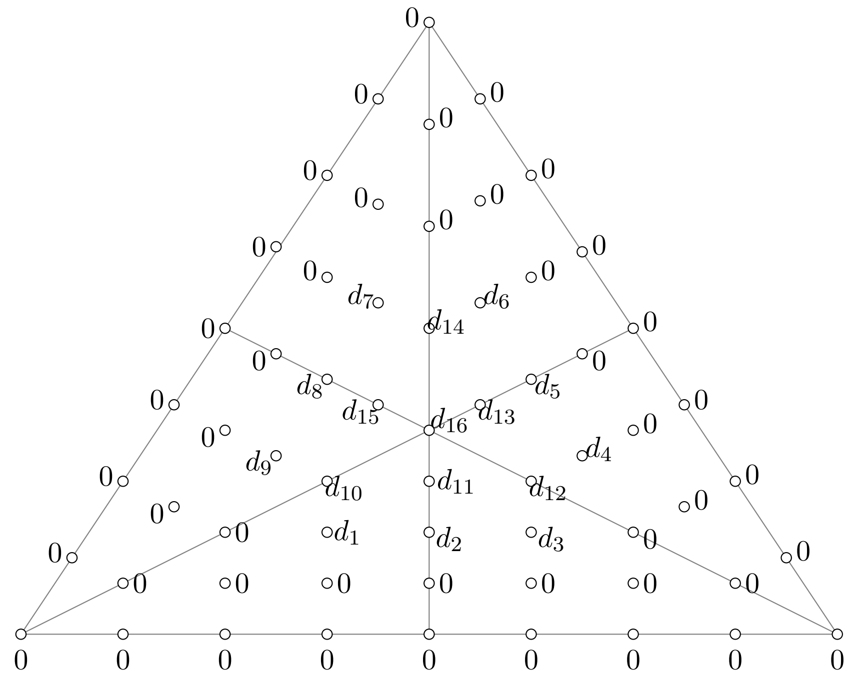

Figure 2.20: B-ordinates of a reduced B-spline.

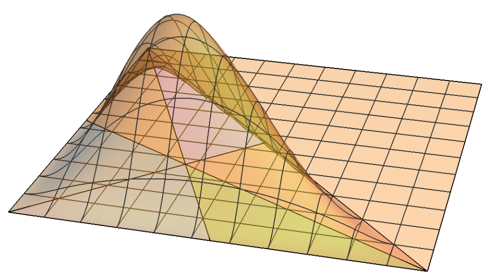

Figure 2.21: Blending function $\mathcal{B}^t$.

2.6.2 The Powell-Sabin space on the whole triangulation

This section aims to prove that each quartic spline space over $\widetilde{\Delta}_{\rm PS}$ is C^2 continuous everywhere and C^3 at the edge split points. To this end, we will provide a general representation of $S_4^{1,2,3}(\Delta_{\rm PS})$ over an arbitrary PS-split $\Delta_{\rm PS}$ of Δ, and then we will prove that the provided representation is totally C^2 continuous over $\widetilde{\Delta}_{\rm PS}$. Moreover, the B-spline-like functions to be constructed in this section will enjoy the usual properties required when dealing with the construction of bases of spline function spaces. They will be non-negative, locally supported and form a unit partition. Furthermore, any spline represented in these bases have a meaningful geometric interpretation, can be locally controlled and evaluated in a stable way.

Since the dimension of $S_4^{1,2,3}(\Delta_{\rm PS})$ equals $6nv + ne$, then such a representation will be obtained by defining six B-spline-like functions $\mathcal{B}^v_{i,\alpha}$, $|\alpha| = 2$ associated with each vertex and another one, $\mathcal{B}^e_\ell$, for each edge. The B-spline-likes $\mathcal{B}^v_{i,\alpha}$ and $\mathcal{B}^e_\ell$ are called B-spline-likes with respect to vertices and edges, respectively. The procedure to construct them follows the technique in [27, 25, 32, 42, 55].

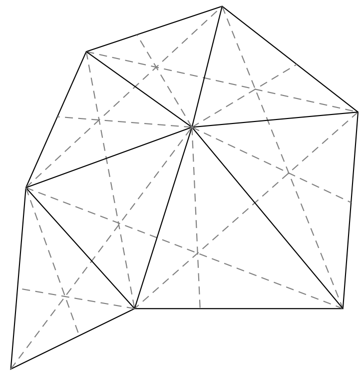

Figure 2.22: Powell-Sabin triangulation satisfying conditions in Proposition 2.6.5.

B-spline-like function with respect to vertex

We outline the construction of $\mathcal{B}^v_{i,\alpha}$ in the spirit of [32]. For every vertex V_i, let $M_i := \cup_{T\in\Delta, V_i\in T} T$ be the molecule relative to V_i, i.e. the union of all triangles in Δ containing V_i. For all vertex V_ℓ lying on the boundary of M_i and for all $T_j \subset M_i$, let

$$S_{i,\ell} := \frac{1}{2}(V_i + R_{i,\ell}) \quad \text{and} \quad L_{i,j} := \frac{1}{2}(V_i + Z_j),$$

Points V_i, $S_{i,\ell}$ and $L_{i,j}$ are said to be PS4-points associated with V_i. Let $t_i := (Q_{i,1}, Q_{i,2}, Q_{i,3})$ be a triangle containing the PS4-points of V_i. It will be called PS4-triangle. Denote by $\mathfrak{B}^2_{t_i,\alpha}$, $|\alpha| = 2$, the Bernstein polynomials of degree 2 with respect to t_i, and define the values

$$\gamma^{a,b}_{i,\alpha} := \frac{12}{(4-a-b)(3-a-b)} \left(\frac{1}{2}\right)^{a+b} \partial^a_x \partial^b_y \mathfrak{B}^2_{t_i,\alpha}(V_i) \text{ for all } a \geq 0, b \geq 0, 0 \leq a+b \leq 2. \quad (2.22)$$

They are used to define the B-spline-like $\mathcal{B}^v_{i,\alpha}$ as follows.

Without loss of generality, consider the vertex V_1. $\mathcal{B}^v_{1,\alpha}$ is defined as the unique solution of the Hermite interpolation problem (2.15) with all f- and g-values equal to zero except $f^{a,b}_1 = \gamma^{a,b}_{1,\alpha}$, $g_{1,2} = \beta^\alpha_{1,2}$ and $g_{3,1} = \beta^\alpha_{3,1}$, where the β-values are chosen as follows.

Let $T\,\langle V_1, V_2, V_3\rangle$ be a triangle included in the molecule M_1. In each of the six micro-triangles of T, $\mathcal{B}^v_{1,\alpha}$ is a quartic polynomial. The B-ordinates in its Bernstein-Bézier representation are shown in Figure 2.23. Many of them are null. The non-zero B-ordinates are determined from the given data and the smoothness conditions. Note that

$$\beta^\alpha_{1,2} = \frac{12}{\|Z - R_{1,2}\|^2}\left(d^v_{11} - 2d^v_{13} + d^v_{19}\right) \quad \text{and} \quad \beta^\alpha_{3,1} = \frac{12}{\|Z - R_{3,1}\|^2}\left(d^v_{15} - 2d^v_{17} + d^v_{20}\right).$$

The B-ordinates $d^v_1, \ldots, d^v_9$ are computed from the chosen parameters $\gamma^{a,b}_{1,\alpha}$, $a \geq 0, b \geq 0, 0 \leq a+b \leq 2$. The ordinates $d^v_{18}, \ldots,\ d^v_{25}$ are computed from $\mathcal{C}^2$ smoothness at the triangle split point Z. Let p_2 be the quadratic polynomial defined on the triangle $\langle W_1, W_2, W_3\rangle$ with vertices $W_i = \dfrac{1}{2}(V_i + Z)$ in such a way that all B-ordinates are equal to zero except $b_{2,0,0} = d^v_7$. Then, by subdivision, the following relationships result:

$$\begin{array}{llll} d^v_{18} = \lambda_{12}\, d^v_7, & d^v_{19} = \lambda^2_{12}\, d^v_7, & d^v_{20} = \lambda^2_{13}\, d^v_7, & d^v_{21} = \lambda_{13}\, d^v_7, \\ d^v_{22} = z_1\, d^v_7, & d^v_{23} = \lambda_{12} z_1\, d^v_7, & d^v_{24} = \lambda_{13} z_1\, d^v_7, & d^v_{25} = z^2_1\, d^v_7. \end{array}$$

The B-ordinates $d^v_{10}, \ldots, d^v_{17}$ are computed from $\mathcal{C}^3$-smoothness across $\langle R_{1,2}, Z\rangle$ and $\langle R_{3,1}, Z\rangle$. Let us define the univariate cubic polynomials, p^0_3 and p^1_3, on the lines $\left\langle \dfrac{3V_1 + R_{1,2}}{4}, \dfrac{3V_2 + R_{1,2}}{4} \right\rangle$

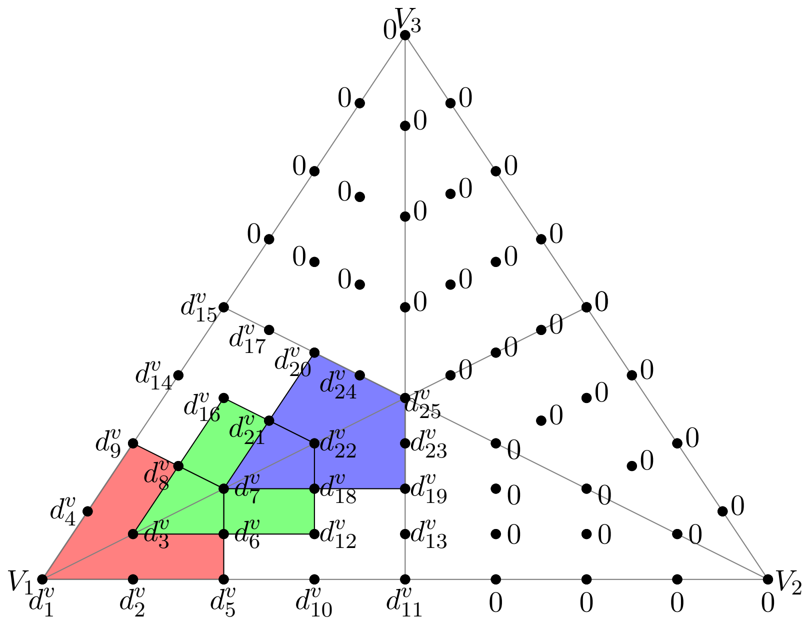

Figure 2.23: B-ordinates of a B-spline-like with respect to vertex V_1.

and $\left\langle \dfrac{2V_1 + R_{1,2} + Z}{4}, \dfrac{2V_2 + R_{1,2} + Z}{4} \right\rangle$, respectively, having B-ordinates

$$b^0_{3,0} = d_2^v, \qquad b^0_{2,1} = \frac{d_5^v - \lambda_{1,2} d_2^v}{\lambda_{2,1}} =: \tilde{d}_5^v, \qquad b^0_{1,2} = 0, \qquad b^0_{0,3} = 0,$$

and

$$b^1_{3,0} = d_3^v, \qquad b^1_{2,1} = \frac{d_6^v - \lambda_{1,2} d_3^v}{\lambda_{2,1}} =: \tilde{d}_6^v, \qquad b^1_{1,2} = 0, \qquad b^1_{0,3} = 0.$$

Then, after subdivision,

$$d_{10}^v = \lambda_{1,2}^2 d_2^v + 2\lambda_{1,2}\lambda_{2,1}\tilde{d}_5^v, \qquad d_{11}^v = \lambda_{1,2}^3 d_2^v + 2\lambda_{1,2}^2\lambda_{2,1}\tilde{d}_5^v$$

and

$$d_{12}^v = \lambda_{1,2}^2 d_3^v + 2\lambda_{1,2}\lambda_{2,1}\tilde{d}_6^v, \qquad d_{13}^v = \lambda_{1,2}^3 d_3^v + 2\lambda_{1,2}^2\lambda_{2,1}\tilde{d}_6^v.$$

Similarly,

$$d_{14}^v = \lambda_{1,3}^2 d_4^v + 2\lambda_{1,3}\lambda_{3,1}\tilde{d}_9^v, \qquad d_{15}^v = \lambda_{1,3}^3 d_4^v + 2\lambda_{1,3}^2\lambda_{3,1}\tilde{d}_9^v,$$

and

$$d_{16}^v = \lambda_{1,3}^2 d_3^v + 2\lambda_{1,3}\lambda_{3,1}\tilde{d}_8^v, \qquad d_{17}^v = \lambda_{1,3}^3 d_3^v + 2\lambda_{1,3}^2\lambda_{3,1}\tilde{d}_8^v,$$

where $\tilde{d}_8^v := \dfrac{d_8^v - \lambda_{1,3} d_3^v}{\lambda_{3,1}}$ and $\tilde{d}_9^v := \dfrac{d_9^v - \lambda_{1,3} d_4^v}{\lambda_{3,1}}$.

The restriction of $\mathcal{B}_{1,\alpha}^v$ on T can be written in terms of $\mathcal{D}_i$, $i = 1, 2, 3$, and $\mathcal{B}^t$. Then, $\mathcal{B}_{1,\alpha}^v$ is C^2 continuous on T, if and only if T_{PS} meets the conditions in Proposition 2.6.5. In what follows, we will confirm this result.

The BB-coefficients involved in C^2 continuity conditions between the restrictions of $\mathcal{B}_{1,\alpha}^v$ to the micro-triangles t^1 and t^6 are divided into three categories. The BB-coefficients lying in the area in light red color satisfy the C^2 smoothness because they are computed from the derivative values up to order two of $\mathcal{B}_{1,\alpha}^v$. The BB-coefficients lying in the area in blue color also satisfy the C^2 smoothness. By construction, they are computed throughout the values of a

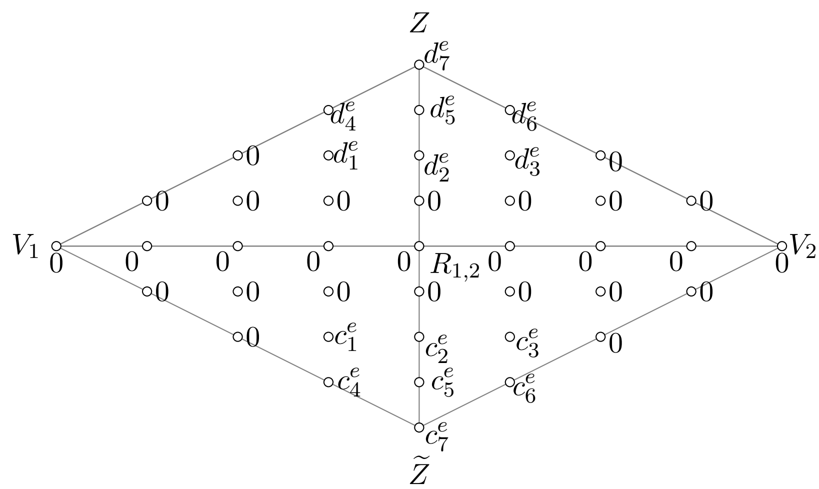

Figure 2.24: B-ordinates of a B-spline-like $\mathcal{B}_1^e$ on the four micro triangles that have $\langle V_1,\, R_{1,2}\rangle$ or $\langle V_2,\, R_{1,2}\rangle$ as an edge.

quadratic polynomial defined on the triangle with vertices W_i in (2.16). It remains to check the C^2 smoothness conditions between the BB-coefficients lying in the area in green color. Using equation (1.2), the remaining C^2 condition between the BB-coefficients lying in the area in green color is given by

$$d_{16}^v = \tau_{2,3}^2 d_{12}^v + 2\tau_{2,3}\tau_{3,3} d_{18}^v + \tau_{3,3}^2 d_{22}^v + 2\tau_{3,3}\tau_{1,3} d_7^v + \tau_{1,3}^2 d_3^v + 2\tau_{1,3}\tau_{2,3} d_6^v.$$

By substituting the relevant BB-coefficients by their values, it is verified that the condition is fulfilled. By Theorem 2.6.1, it follows that $\mathcal{B}_{1,\alpha}^v$ is globally C^2 continuous over $\widetilde{\Delta}_{\mathrm{PS}}$.

B-spline-like function with respect to edge

Let $T\langle V_1,\, V_2,\, V_3\rangle$ and $\widetilde{T}\langle V_1,\, V_2,\, V_4\rangle$ be two triangles sharing the common edge $\mathfrak{e}_1 = \langle V_1,\, V_2\rangle$. Let $\mathcal{B}_1^e$ be the B-spline-like with respect to the edge $\mathfrak{e}_1$. It is defined as the unique solution of the Hermite interpolation problem (2.15) with all f- and g-values equal to zero except $g_{1,2} = \beta_{1,2}$. For the sake of simplicity, we chose $\omega_{m,n,q} = \dfrac{Z - R_{1,2}}{\|Z - R_{1,2}\|}$ (see Theorem 2.6.1). The β-values can be chosen as in Definition 2.6.2. For instance we consider an arbitrary value for $\beta_{1,2}$.

Let $\widetilde{Z}$ be the inner spilt point of $\widetilde{T}$. The BB-coefficients of $\mathcal{B}_1^e$ on T are computed in a similar way to those of $\mathcal{C}_1$. Now we deal only with the BB-coefficients associated with the domain points located in the four micro-triangles that have $\langle V_1,\, R_{1,2}\rangle$ or $\langle V_2,\, R_{1,2}\rangle$ as an edge. They are schematically presented in Figure 2.24. In order to prove that $\mathcal{B}_1^e$ is C^2 continuous across $\langle V_1,\, V_2\rangle$, we need to provide the value of d_1^e, d_2^e, d_3^e, c_1^e, c_2^e and c_3^e. The first ones are

$$d_2^e = \frac{\beta_{1,2}}{12}\|Z - R_{1,2}\|^2, \quad d_1^e = \frac{\beta_{1,2}}{24\lambda_{1,2}}\|Z - R_{1,2}\|^2, \quad d_3^e = \frac{\beta_{1,2}}{24\lambda_{2,1}}\|Z - R_{1,2}\|^2.$$

If $R_{1,2} = \lambda\, Z + (1-\lambda)\,\widetilde{Z}$, then, for the remaining ones we have

$$c_2^e = \left(\frac{\lambda}{1-\lambda}\right)^2 \frac{\beta_{1,2}}{12}\|Z-R_{1,2}\|^2, \quad c_1^e = \left(\frac{\lambda}{1-\lambda}\right)^2 \frac{\beta_{1,2}}{24\lambda_{1,2}}\|Z-R_{1,2}\|^2, \quad c_3^e = \left(\frac{\lambda}{1-\lambda}\right)^2 \frac{\beta_{1,2}}{24\lambda_{2,1}}\|Z-R_{1,2}\|^2.$$

The C^2 smoothness conditions across $\langle V_1,\, V_2\rangle$ are

$$c_1^e = \left(\frac{\lambda}{1-\lambda}\right)^2 d_1^e, \quad c_2^e = \left(\frac{\lambda}{1-\lambda}\right)^2 d_2^e \quad \text{and} \quad c_3^e = \left(\frac{\lambda}{1-\lambda}\right)^2 d_3^e.$$

The conditions are all fulfilled, which confirms that $\mathcal{B}_1^e$ is C^2 continuous across $\langle V_1, V_2\rangle$.

The value of $\beta_{1,2}$ must be fixed in order to ensure that the B-splines form a partition of unity. To this end, it suffices to chose $\beta_{1,2} = \dfrac{24\lambda_{1,2}\lambda_{2,1}}{\|Z - R_{1,2}\|^2}$.

The blending function of the third kind $\mathcal{B}^t$ associated with T is written as a convex combination of B-spline-like functions with respect to the edges of T with a suitable choice of coefficients which guarantees that it is C^2 continuous on T. Indeed, if we chose $g_{2,3} = \beta_{2,3} = \dfrac{24\lambda_{2,3}\lambda_{3,2}}{\|Z - R_{2,3}\|^2}$ and $g_{3,1} = \beta_{3,1} = \dfrac{24\lambda_{3,1}\lambda_{1,3}}{\|Z - R_{3,1}\|^2}$ for the other two edges, then $\mathcal{B}^t = z_3\mathcal{B}_1^e + z_1\mathcal{B}_2^e + z_2\mathcal{B}_3^e$, and the C^2 smoothness is ensured.

Hence, it is stated that the B-spline-like functions with respect to the vertices and the blending functions of the third kind are all C^2 everywhere. Furthermore, each quartic spline defined on $\tilde{\Delta}_{\mathrm{PS}}$ is C^2 continuous everywhere and C^3 at the edge split points, so that it would be appropriate to write $S_4^{2,3}\left(\tilde{\Delta}_{\mathrm{PS}}\right)$ for the spline space. Its dimension is reduced to $6nv + nt$ because of the conditions imposed on $\tilde{\Delta}_{\mathrm{PS}}$, which on a single triangle give way to a blending function on the third kind $\mathcal{B}^t$ instead of three B-spline-likes with respect to edges.

2.7 Conclusions and discussions

This chapter was divided into two parts. The considered splines in the first part are C^1-continuous, although they are of class C^2 everywhere except across some edges of the refinement. In the second part, we dealt with the characterization of Powell-Sabin triangulations allowing the construction of C^2 continuous quartic splines. Indeed, we have proved that under certain geometrical conditions regarding the triangle and edge split points associated with an arbitrary triangulation of a polygonal domain Ω, the space of almost $C^2(\Omega)$ continuous Powell-Sabin splines introduced in [32] becomes a subspace of a $C^2(\Omega)$. This has been done by constructing for an arbitrary triangle T endowed with a Powell-Sabin refinement a specific basis and deriving the conditions that must be verified for the global regularity to be C^2 instead of C^1. For a triangulation whose triangles satisfy those conditions, the dimension of the corresponding space of C^2 quartic splines is reduced.

Except in exceptional cases (including type-1 and criss-cross triangulations), the sub-triangulation obtained by connecting the opposite vertices of each pair of triangles sharing an edge of the triangulation does not satisfy the conditions in Proposition 2.6.5, which characterizes C^2 continuity. In some cases it will be possible, resulting in a Powell-Sabin sub-triangulation such that for each triangle the interior edges intersect at a point, as shown in Figure 2.22. In other cases, Morgan-Scott sub-triangulations will be obtained, which easily give rise to modified Morgan-Scott sub-triangulations [57]. In other cases, mixed sub-triangulations will appear, as Figure 2.25 shows.

It has been proved that, when the triangulation fulfills the conditions of Proposition 2.6.5, it is possible to construct C^2 quartic splines. If a Morgan-Scott sub-triangulation is obtained, then it is also possible to construct such splines on the corresponding modified Morgan-Scott sub-triangulation (see [57]). Otherwise, a mixed refinement will result. The work in progress deals with the geometrical construction of a B-spline-like basis for the space of quartic splines that can be defined over this sub-triangulation in order to get a normalized B-spline-like representation, whose coefficients will be expressed in terms of polar forms.

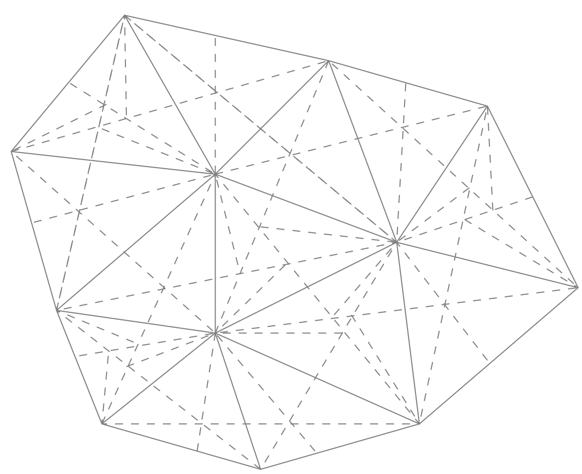

Figure 2.25: Example of a mixed triangulation arising when the procedure to get a Powell-Sabin sub-triangulation allowing C^2-quartic splines is applied.

Chapter 3

Quasi-interpolation in a space of C^2 sextic super-splines over Powell-Sabin triangulations

The application of splines in various fields requires efficient algorithms for constructing locally supported bases for the spline spaces. The B-spline representation of bivariate C^1 quadratic splines achieved by Dierckx [23] was essential in the development of spline spaces on PS partitions and applications. The method proposed by P. Dierckx is completely geometrical, it is reduced to finding a set of PS2-triangles that must contain a number of specified points. Linear and quadratic programming problems are the standard methods proposed by many authors in the literature [23, 24, 25, 26]. The main idea of both methods is to minimize the area of a triangle without imposing any condition concerning the diameter of the sought triangles. Moreover, the quadratic problem only provides local maxima. In order to avoid this limitation, we will present an algorithm that aims to produce PS6-triangles with small area and diameter, and compare it with the one proposed in [43].

The study of spline function spaces on Powell-Sabin partitions obtained by refinement into 6 sub-triangles has attracted great interest in the scientific community since its introduction. The cubic case has been considered in [24, 27, 28, 29]. Spaces of quintic splines have been analyzed in [30] and more recently in [25, 31], among others. In [26] and [29], normalized bases for PS-splines of degree $3r-1$ are defined and super-splines of arbitrary degree are given, respectively. After the later, the paper [32] was published, where only almost C^2 quartic Powell-Sabin splines are considered.

Quasi-interpolation over Powell-Sabin triangulations for specific spaces has been also studied in depth [33, 31, 35, 50], as well as for a family of spaces [36]. The construction of such operators is based on establishing Marsden's identity. It is a powerful tool that allows to write the monomials in terms of the corresponding B-splines. In this view, we will establish a general Marsden's identity in subspace of sextic super-splines from an easy approach based on a version of the control polynomials different from the one used in [26].

In this chapter, we revise a subspace of $\mathcal{C}^2$ sextic PS6 splines obtained by imposing additional smoothness requirements at the interior points of the triangulation chosen to construct the sub-triangulation and also across some edges of the refined triangulation. This subspace of super-splines was studied in [42], where it is shown that every spline is uniquely determined by its values at the vertices of the initial triangulation and the interior points and those of its partial derivatives up to the fourth order at the vertices.

3.1 Explicit construction of a B-spline basis for a subspace of Powell-Sabin super splines

Let Ω be a polygonal domain in $\mathbb{R}^2$, and let Δ be a regular triangulation of Ω. Let Δ_{PS} be the Powell-Sabin 6-split of Δ.

The space of sextic piecewise polynomials on Δ_{PS} with global C^2-continuity is defined as

$$S_6^2\left(\Delta_{\text{PS}}\right) := \left\{ s \in C^2\left(\Omega\right) : s_{|t} \in \mathbb{P}_6 \;\text{ for all } t \in \Delta_{\text{PS}} \right\}.$$

We now consider a particular super spline subspace of $S_6^2\left(\Omega,\, \Delta_{\text{PS}}\right)$ introduced in [42]. As usual $\mathcal{V}$, $\mathcal{Z}$, $\mathcal{E}^*$, nv and nt are respectively the subsets of vertices in Δ, split points in Δ_{PS}, edges in Δ_{PS} that connect a split point Z_i to a point $R_{i,j}$, the number of vertices and triangles in Δ. As given in [42], the space of PS super-splines is defined as

$$S_6^{2,4,3}\left(\Delta_{\text{PS}}\right) := \left\{ s \in S_6^2\left(\Delta_{\text{PS}}\right) : s \in C^4\left(\mathcal{V}\right),\; s \in C^3\left(\mathcal{Z} \cup \mathcal{E}^*\right) \right\}.$$

Each $C^2\left(\Omega\right)$-function s is of class C^4 at any vertex in $\mathcal{V}$ and of class C^3 at any split point in $\mathcal{Z}$ and across any edge in $\mathcal{E}^*$. In [42], by using minimal determining sets it was proved that for given values $f_i^{a,b}$, $i = 1, \ldots, nv$, and g_k, $k = 1, \ldots, nt$, there exists a unique PS6 spline $s \in S_6^{2,4,3}\left(\Delta_{PS}\right)$ such that

$$\partial_{a,b}\, s\left(V_i\right) = f_i^{a,b},\; 0 \le a + b \le 4, \quad \text{and} \quad s\left(Z_k\right) = g_k. \tag{3.1}$$

Therefore, the dimension of the space $S_6^{2,4,3}\left(\Delta_{\text{PS}}\right)$ is equal to $15nv + nt$.

A procedure for the construction of a normalized basis for the space $S_6^{2,4,3}\left(\Delta_{\text{PS}}\right)$ is then based on the solution of the above Hermite interpolation problem for appropriate values $f_i^{a,b}$ and g_k (see [42]). Non-negative and locally supported basis functions $\mathcal{B}_{i,j}^v$ and $\mathcal{B}_k^t$ with respect to vertices and triangles, respectively, that form a partition of unity are defined, and any $s \in S_6^{2,4,3}\left(\Delta_{\text{PS}}\right)$ can be represented as

$$s = \sum_{i=1}^{nv} \sum_{j=1}^{15} c_{i,j}^v\, \mathcal{B}_{i,j}^v + \sum_{k=1}^{nt} c_k^t\, \mathcal{B}_k^t. \tag{3.2}$$

In what follows, we give a fully elaborate construction of such a normalized basis [25, 26, 42]. For every vertex V_i, let $M_i := \cup_{T \in \Delta, V_i \in T}\, T$ be the molecule of vertex V_i, i.e. the union of all triangles in Δ containing V_i. For all vertices V_ℓ, $\ell \in \Lambda_i$, (where Λ_i is the set of indices for the vertices that form an edge in Δ with V_i) lying on the boundary of M_i, let

$$S_{i,\ell} := \frac{1}{3} V_i + \frac{2}{3} V_\ell.$$

The points V_i and $S_{i,\ell}$, $\ell \in \Lambda_i$, are said to be PS6-points associated with the vertex V_i. Let $t_i = \langle Q_{i,1},\, Q_{i,2},\, Q_{i,3} \rangle$ be a triangle containing the PS6-points of V_i. It will be called PS6-triangle. Denote by $\mathfrak{B}^4_{t_i,mn\ell}$, $m + n + \ell = 4$, the Bernstein polynomials of degree 4 with respect to t_i, and define, for all $0 \le a + b \le 4$, the values

$$\begin{aligned}
&\alpha_{i,1}^{a,b} := C_{a,b}\; \partial_{a,b} \mathfrak{B}^4_{t_i,400}(V_i),\;\; \alpha_{i,2}^{a,b} := C_{a,b}\, \partial_{a,b}\, \mathfrak{B}^4_{t_i,310}(V_i),\;\; \alpha_{i,3}^{a,b} := C_{a,b} \partial_{a,b}\, \mathfrak{B}^4_{t_i,220}(V_i),\\
&\alpha_{i,4}^{a,b} := C_{a,b}\; \partial_{a,b} \mathfrak{B}^4_{t_i,130}(V_i),\;\; \alpha_{i,5}^{a,b} := C_{a,b}\, \partial_{a,b}\, \mathfrak{B}^4_{t_i,040}(V_i),\;\; \alpha_{i,6}^{a,b} := C_{a,b} \partial_{a,b}\, \mathfrak{B}^4_{t_i,031}(V_i),\\
&\alpha_{i,7}^{a,b} := C_{a,b}\; \partial_{a,b} \mathfrak{B}^4_{t_i,022}(V_i),\;\; \alpha_{i,8}^{a,b} := C_{a,b}\, \partial_{a,b}\, \mathfrak{B}^4_{t_i,013}(V_i),\;\; \alpha_{i,9}^{a,b} := C_{a,b} \partial_{a,b}\, \mathfrak{B}^4_{t_i,004}(V_i),\\
&\alpha_{i,10}^{a,b} := C_{a,b}\; \partial_{a,b} \mathfrak{B}^4_{t_i,103}(V_i),\;\; \alpha_{i,11}^{a,b} := C_{a,b}\, \partial_{a,b}\, \mathfrak{B}^4_{t_i,202}(V_i),\;\; \alpha_{i,12}^{a,b} := C_{a,b} \partial_{a,b}\, \mathfrak{B}^4_{t_i,301}(V_i),\\
&\alpha_{i,13}^{a,b} := C_{a,b}\, \partial_{a,b}\, \mathfrak{B}^4_{t_i,211}(V_i),\;\; \alpha_{i,14}^{a,b} := C_{a,b} \partial_{a,b}\, \mathfrak{B}^4_{t_i,121}(V_i),\;\; \alpha_{i,15}^{a,b} := C_{a,b} \partial_{a,b}\, \mathfrak{B}^4_{t_i,112}(V_i),
\end{aligned} \tag{3.3}$$

with $C_{a,b} := \dfrac{30}{\left(6 - a - b\right)\left(5 - a - b\right)} \left(\dfrac{2}{3}\right)^{a+b}$.

They are used to define the B-spline-like functions $\mathcal{B}_{i,j}^v$ and $\mathcal{B}_k^t$ as follows.

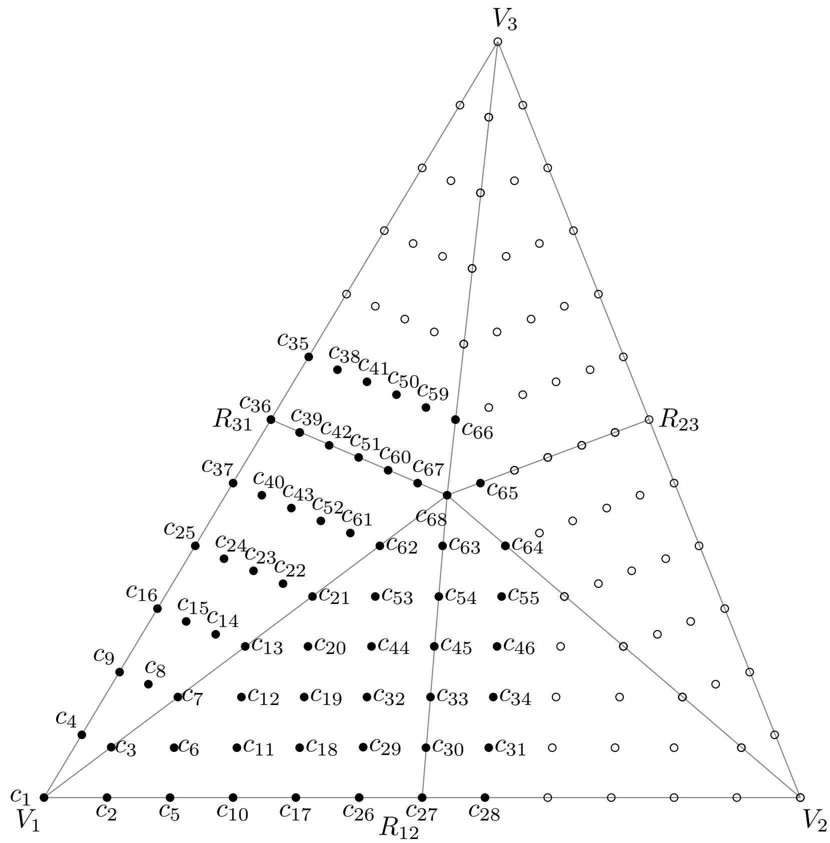

Figure 3.1: Representation of the Bézier ordinates of a B-spline relative to a vertex. The B-coefficients that are known to be zero are indicated by open $\circ$.

3.1.1 Vertex B-spline-like

Every B-spline-like $\mathcal{B}^v_{i,j}$, $1 \le j \le 15$, relative to the vertex V_i is defined as the unique solution of a particular Hermite interpolation with conditions given by (3.1). Firstly, all $f^{a,b}_\ell$ are equal to zero except for $\ell = i$, and $f^{a,b}_i = \alpha^{a,b}_{i,j}$. Moreover, if V_i is a vertex of a triangle $T_k := \langle V_1, V_2, V_3 \rangle$, then g_k is equal to a value $\beta^k_{i,j}$ to be precise later and the remaining $g-$values are all equal to zero. The spline defined in this way is zero outside the molecule M_i of vertex V_i. Next, we shall compute the BB-coefficients of $\mathcal{B}^v_{i,j}$ relative to the triangles determining its support. For the sake of simplicity, we compute only the BB-coefficients of the B-spline $\mathcal{B}^v_{1,j}$ relative to the vertex V_1 of a triangle T_k. The corresponding Bézier ordinates are schematically represented in Figure 3.1.

From the definition of $\mathcal{B}^v_{1,j}$, many BB-coefficients are equal to zero. Figure 1.4 shows the refinement of T_k and we assume that the points indicated in the figure have the following barycentric coordinates:

$$V_1 = (1,0,0),\ V_2 = (0,1,0),\ V_3 = (0,0,1),\ Z = (z_1, z_2, z_3),$$
$$R_{12} = (\lambda_{12}, \lambda_{21}, 0),\ R_{23} = (0, \lambda_{23}, \lambda_{32}),\ R_{31} = (\lambda_{13}, 0, \lambda_{31}).$$

Because of the C^4-smoothness of the spline at V_1, the ordinates $c_1, c_2, \ldots, c_{25}$ are uniquely determined by the values $\alpha^{a,b}_{1,j}$, $0 \le a+b \le 4$. The ordinates $c_{26}, \ldots, c_{34}$ are obtained by the C^3-smoothness across the edge $\langle R_{12}, Z \rangle$.

Let us define three univariate cubic polynomial functions p^0_3, p^1_3 and p^2_3 on the segments $\langle \frac{V_1+R_{12}}{2}, \frac{V_2+R_{12}}{2} \rangle$, $\langle \frac{3V_1+2R_{12}+Z}{6}, \frac{3V_2+2R_{12}+Z}{6} \rangle$ and $\langle \frac{3V_1+R_{12}+2Z}{6}, \frac{3V_2+R_{12}+2Z}{6} \rangle$, respectively. Before subdivision, their BB-coefficients were

$$\begin{aligned} b_{30}^0 &= c_{10}, & b_{21}^0 &= \hat{c}_{17}, & b_{12}^0 &= 0, & b_{03}^0 &= 0,\\ b_{30}^1 &= c_{11}, & b_{21}^1 &= \hat{c}_{18}, & b_{12}^1 &= 0, & b_{03}^1 &= 0,\\ b_{30}^2 &= c_{12}, & b_{21}^2 &= \hat{c}_{19}, & b_{12}^2 &= 0, & b_{03}^2 &= 0,\end{aligned}$$

respectively, where

$$\hat{c}_{17} = \frac{c_{17} - \lambda_{12}c_{10}}{\lambda_{21}}, \quad \hat{c}_{18} = \frac{c_{18} - \lambda_{12}c_{11}}{\lambda_{21}}, \quad \hat{c}_{19} = \frac{c_{19} - \lambda_{12}c_{12}}{\lambda_{21}}.$$

Therefore, we get

$$\begin{aligned} c_{26} &= \lambda_{12}(c_{17} + \lambda_{21}\hat{c}_{17}), & c_{27} &= \lambda_{12}^2(c_{17} + 2\lambda_{21}\hat{c}_{17}), & c_{28} &= \lambda_{12}^2\hat{c}_{17},\\ c_{29} &= \lambda_{12}(c_{18} + \lambda_{21}\hat{c}_{18}), & c_{30} &= \lambda_{12}^2(c_{18} + 2\lambda_{21}\hat{c}_{18}), & c_{31} &= \lambda_{12}^2\hat{c}_{18},\\ c_{32} &= \lambda_{12}(c_{19} + \lambda_{21}\hat{c}_{19}), & c_{33} &= \lambda_{12}^2(c_{19} + 2\lambda_{21}\hat{c}_{19}), & c_{34} &= \lambda_{12}^2\hat{c}_{19}.\end{aligned}$$

The values $c_{35}, \ldots, c_{43}$ are determined using a similar method. They are given by the following expressions:

$$\begin{aligned} c_{37} &= \lambda_{13}(c_{25} + \lambda_{31}\hat{c}_{25}), & c_{36} &= \lambda_{13}^2(c_{25} + 2\lambda_{31}\hat{c}_{25}), & c_{35} &= \lambda_{13}^2\hat{c}_{25},\\ c_{40} &= \lambda_{13}(c_{24} + \lambda_{31}\hat{c}_{24}), & c_{39} &= \lambda_{13}^2(c_{24} + 2\lambda_{31}\hat{c}_{24}), & c_{38} &= \lambda_{13}^2\hat{c}_{24},\\ c_{43} &= \lambda_{13}(c_{23} + \lambda_{31}\hat{c}_{23}), & c_{42} &= \lambda_{13}^2(c_{23} + 2\lambda_{31}\hat{c}_{23}), & c_{41} &= \lambda_{13}^2\hat{c}_{23},\end{aligned}$$

with

$$\hat{c}_{25} = \frac{c_{25} - \lambda_{13}c_{16}}{\lambda_{31}}, \quad \hat{c}_{24} = \frac{c_{24} - \lambda_{13}c_{15}}{\lambda_{31}}, \quad \hat{c}_{23} = \frac{c_{23} - \lambda_{13}c_{14}}{\lambda_{31}}.$$

The remaining Bézier ordinates must be chosen in such a way that the B-spline is $\mathcal{C}^3$-continuous at the split point Z. Therefore, let us first define the points

$$W_i := \frac{V_i + Z}{2}, \; i = 1, 2, 3, \tag{3.4}$$

and let $p_3 \in \mathbb{P}_3$ be the polynomial of degree 3 defined over the triangle $T\langle W_1, W_2, W_3\rangle$ with ordinates

$$b_{300} = c_{13},\; b_{210} = \hat{c}_{20},\; b_{201} = \hat{c}_{22},\; b_{120} = b_{030} = b_{021} = b_{012} = b_{003} = b_{102} = b_{111} = 0,$$

where

$$\hat{c}_{20} = \frac{c_{20} - \lambda_{12}c_{13}}{\lambda_{21}}, \qquad \hat{c}_{22} = \frac{c_{22} - \lambda_{13}c_{13}}{\lambda_{31}}. \tag{3.5}$$

Following a method analogous to that used in [25] for the quintic splines, we get

$$\begin{aligned} &c_{44} = \lambda_{12}^2c_{13} + 2\lambda_{12}\lambda_{21}\hat{c}_{20},\; c_{45} = 12\lambda^3c_{13} + 3\lambda_{12}^2\lambda_{21}\hat{c}_{20},\; c_{46} = \lambda_{12}^2\hat{c}_{20},\\ &c_{47} = 0,\; c_{48} = 0,\; c_{49} = 0,\; c_{50} = \lambda_{13}^2\hat{c}_{22},\; c_{51} = \lambda_{13}^3c_{13} + 3\lambda_{13}^2\lambda_{31}\hat{c}_{22},\\ &c_{52} = \lambda_{13}^2c_{13} + 2\lambda_{13}\lambda_{31}\hat{c}_{22},\; c_{53} = z_1\lambda_{12}c_{13} + (z_2\lambda_{12} + z_1\lambda_{21})\hat{c}_{20} + z_3\lambda_{12}\hat{c}_{22},\\ &c_{54} = z_1\lambda_{12}^2c_{13} + (z_2\lambda_{12}^2 + z_1\lambda_{12}\lambda_{21})\hat{c}_{20} + z_3\lambda_{12}^2\hat{c}_{22},\; c_{55} = \lambda_{12}z_1\hat{c}_{20},\\ &c_{56} = 0,\; c_{57} = 0,\; c_{58} = 0,\; c_{59} = \lambda_{13}z_1\hat{c}_{22},\; c_{60} = z_1\lambda_{13}^2c_{13} + z_2\lambda_{13}^2\hat{c}_{20} + (z_3\lambda_{13}^2 + 2z_1\lambda_{13}\lambda_{31})\hat{c}_{22},\\ &c_{61} = z_1\lambda_{13}c_{13} + z_2\lambda_{13}\hat{c}_{20} + (z_3\lambda_{13} + z_1\lambda_{31})\hat{c}_{22},\; c_{62} = z_1^2c_{13} + 2z_1z_2\hat{c}_{20} + 2z_1z_3\hat{c}_{22},\\ &c_{63} = z_1^2\lambda_{12}c_{13} + (2z_1z_2\lambda_{12} + z_1^2\lambda_{21})\hat{c}_{20} + 2z_1z_3\lambda_{12}\hat{c}_{22},\; c_{64} = z_1^2\hat{c}_{20} + 2z_1z_3\hat{c}_{22},\\ &c_{65} = z_1^2\lambda_{23}\hat{c}_{20} + z_1^2\lambda_{32}\hat{c}_{22},\; c_{66} = z_1^2\hat{c}_{22},\; c_{67} = z_1^2\lambda_{13}c_{13} + 2z_1z_2\lambda_{13}\hat{c}_{20} + (2z_1z_3\lambda_{13} + z_1^2\lambda_{31})\hat{c}_{22},\\ &c_{68} = z_1^3c_{13} + 3z_1^2z_2\hat{c}_{20} + 3z_1^2z_3\hat{c}_{22}.\end{aligned}$$

The choice $\beta_{1,j}^k = c_{68}$ provides the values needed to completely define the B-spline $\mathcal{B}_{1,j}^v$.

Figure 3.2 shows typical plots of the fifteen C^2 sextic B-splines associated with a vertex of the triangulation.

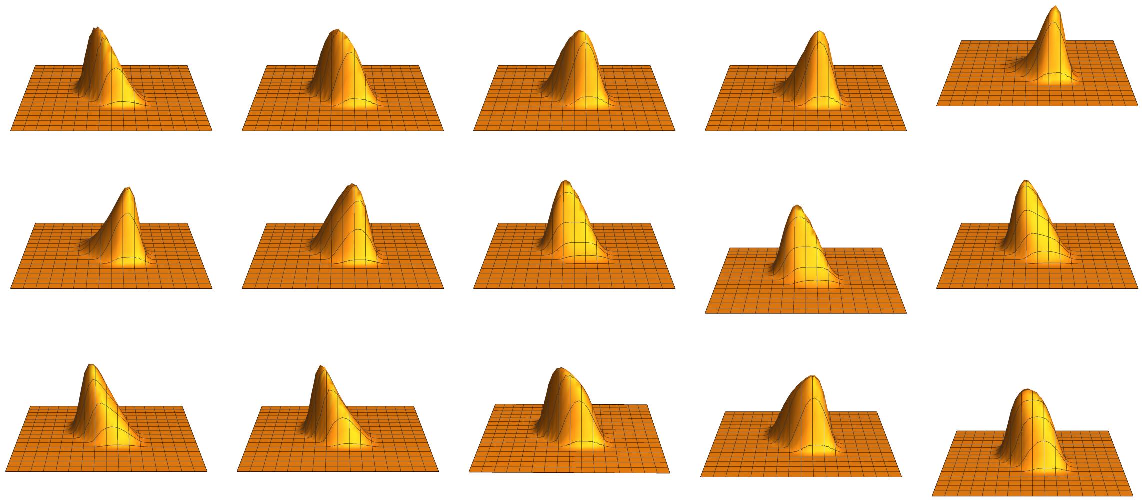

Figure 3.2: B-splines relative to a vertex.

3.1.2 Triangle B-spline-like

For the sake of simplicity, we denote by b_ℓ the B-ordinates with respect to a triangle (see Figure 3.3). The B-spline-like $\mathcal{B}_k^t$ with respect to the triangle T_k is defined as the spline satisfying conditions (3.1) with all $f_i^{a,b}$ equal to zero, $g_k = \beta_k$ and the remaining $g-$values equal to zero. It vanishes outside T_k. In order to specify the value of β_k, we look at the Bernstein-Bézier representation of the B-spline $\mathcal{B}_k^t$. We consider again the macro-triangle $T_k = \langle V_1, V_2, V_3\rangle$, as above.

Let us define again a polynomial $p_3 \in \mathbb{P}_3$ of degree 3 defined on the triangle $T\langle W_1, W_2, W_3\rangle$, where W_i are defined in (3.4), and having the following B-ordinates:

$$b_{300} = b_{210} = b_{201} = b_{120} = b_{030} = b_{021} = b_{012} = b_{003} = b_{102} = 0,\ b_{111} = 1.$$

Also as in the above subsection, we get

$$\begin{aligned}
&b_1 = \lambda_{21}z_3,\ b_2 = 2\lambda_{12}\lambda_{21}z_3,\ b_3 = \lambda_{12}z_3,\ b_4 = \lambda_{32}z_1,\ b_5 = 2\lambda_{23}\lambda_{32}z_1,\ b_6 = \lambda_{23}z_1,\\
&b_7 = \lambda_{13}z_2,\ b_8 = 2\lambda_{13}\lambda_{31}z_2,\ b_9 = \lambda_{31}z_2,\ b_{10} = 2z_2z_3,\ b_{11} = 2z_3(\lambda_{12}z_2 + \lambda_{21}z_1),\\
&b_{12} = 2z_1z_3,\ b_{13} = 2z_1(\lambda_{23}z_3 + \lambda_{32}z_2),\ b_{14} = 2z_2z_1,\ b_{15} = 2z_2(\lambda_{31}z_1 + \lambda_{13}z_3),\ b_{16} = 6z_1z_2z_3.
\end{aligned} \tag{3.6}$$

From the construction, it is clear that all the Bézier ordinates are nonnegative. Then, the B-spline-like $\mathcal{B}_k^t$ is nonnegative. We can choose $\beta_k = 6z_1z_2z_3$.

For each vertex V_i and each triangle T_k, we define points $Q_{i,\beta} := (X_{i,\beta}, Y_{i,\beta})$, with $\beta := (\beta_1, \beta_2, \beta_3)$, $|\beta| := \beta_1 + \beta_2 + \beta_3 = 4$, and $Q_k^t := \left(X_k^t, Y_k^t\right)$ in such a way that the reproduction of the monomials x and y holds, i.e.

$$\sum_{i=1}^{nv} \sum_{|\beta|=4} X_{i,\beta}\,\mathcal{B}_{i,\beta}^v(x,y) + \sum_{k=1}^{nt} X_k^t\,\mathcal{B}_k^t(x,y) = x, \tag{3.7}$$

$$\sum_{i=1}^{nv} \sum_{|\beta|=4} Y_{i,\beta}\,\mathcal{B}_{i,\beta}^v(x,y) + \sum_{k=1}^{nt} Y_k^t\,\mathcal{B}_k^t(x,y) = y. \tag{3.8}$$

Proposition 3.1.1. *Let $Q_{i,(4,0,0)}$, $Q_{i,(0,4,0)}$ and $Q_{i,(0,0,4)}$ be the three vertices of a triangle t_i. If the remaining points are defined by*

$$Q_{i,\beta} := \frac{1}{4}(\beta_1 Q_{i,(4,0,0)} + \beta_2 Q_{i,(0,4,0)} + \beta_3 Q_{i,(0,0,4)})$$

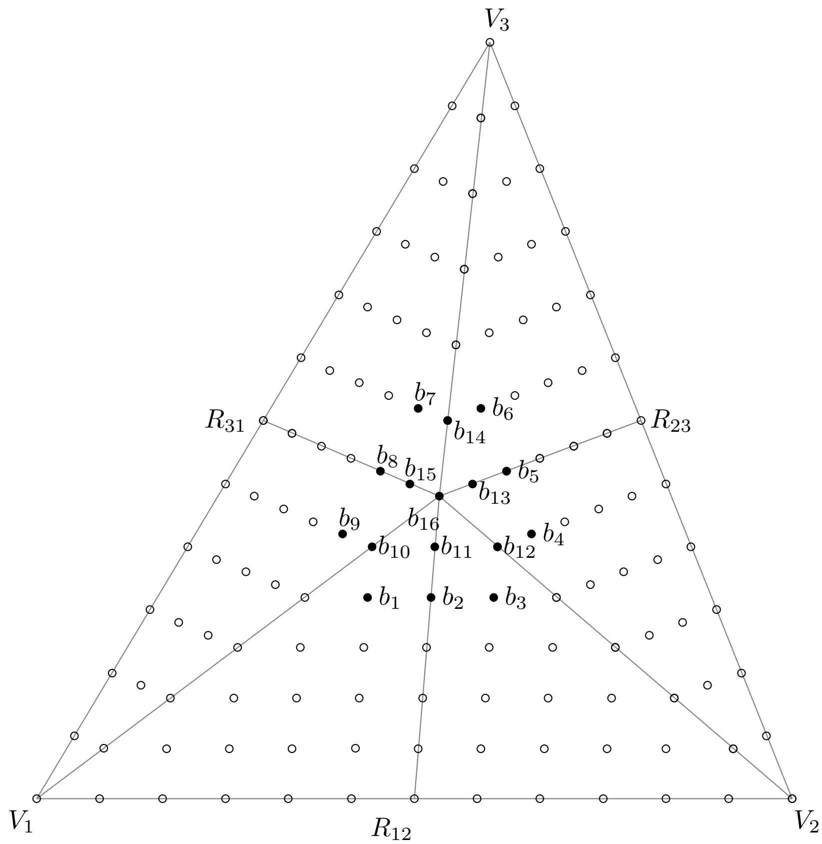

Figure 3.3: Schematic representation of the Bézier ordinates of a B-spline with respect to a triangle. The B-coefficients that are known to be zero are indicated by an open $\circ$.

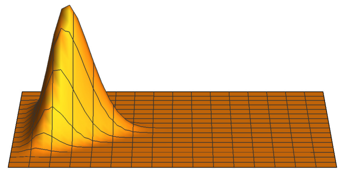

Figure 3.4: B-spline relative to a triangle.

and

$$Q_k^t = \frac{V_1 + V_2 + V_3}{6} + \frac{Z_k}{2},$$

then (3.7) and (3.8) hold.

Proof. For all $(x, y) \in t_i$, we have

$$x = \sum_{|\beta|=4} \mathbf{B}\,[x] \left(Q_{i,(4,0,0)}^{\beta_1}, Q_{i,(0,4,0)}^{\beta_2}, Q_{i,(0,0,4)}^{\beta_3} \right) \mathfrak{B}_{t_i,\beta}^4 (x, y)\,. \tag{3.9}$$

Using (3.3) and (3.9), we get (3.7). Now, to prove (3.8), we need to show that

$$\sum_{i=1}^{3} \sum_{|\beta|=4} X_{i,\beta}\, \mathcal{B}_{i,\beta}^v (x, y) \; + \; X_k^t\, \mathcal{B}_k^t (x, y) = z_1 x_1 + z_2 x_2 + z_3 x_3. \tag{3.10}$$

Recall that, in the construction of B-splines in the above section, the value of a PS6-spline at a split point Z is computed through a particular cubic polynomial evaluated at the split point. We consider again the macro-triangle $T_k = \langle V_1, V_2, V_3 \rangle$. The two cubic polynomials corresponding to the two PS6 splines in the equations (3.7) and (3.8) are denoted by $p_{x,3}(\tau)$ and $p_{y,3}(\tau)$. They are defined on the triangle with the vertices given in (3.4). The Bézier ordinates of $p_{x,3}$ are given by the following expressions:

$$\begin{aligned}
b_{300}^x &= \frac{1}{2}x_1 + \frac{1}{2}(z_1 x_1 + z_2 x_2 + z_3 x_3), \; b_{210}^x = \frac{2}{3}b_{300}^x + \frac{1}{3}b_{030}^x, \; b_{201}^x = \frac{2}{3}b_{300}^x + \frac{1}{3}b_{003}^x,\\
b_{030}^x &= \frac{1}{2}x_2 + \frac{1}{2}(z_1 x_1 + z_2 x_2 + z_3 x_3), \; b_{120}^x = \frac{1}{3}b_{300}^x + \frac{2}{3}b_{030}^x, \; b_{021}^x = \frac{2}{3}b_{030}^x + \frac{1}{3}b_{003}^x,\\
b_{003}^x &= \frac{1}{2}x_3 + \frac{1}{2}(z_1 x_1 + z_2 x_2 + z_3 x_3), \; b_{102}^x = \frac{1}{3}b_{300}^x + \frac{2}{3}b_{003}^x, \; b_{012}^x = \frac{1}{3}b_{030}^x + \frac{2}{3}b_{003}^x.
\end{aligned}$$

By the definition of Q_k^t, it holds

$$b_{111} = X_k^t = \frac{1}{3}(b_{300}^x + b_{030}^x + b_{003}^x).$$

Therefore, it is clear that $p_{x,3}(\tau) = \tau_1 b_{300}^x + \tau_2 b_{030}^x + \tau_3 b_{003}^x$, and (3.10) follows. Hence, (3.7) is proved. Equality (3.8) can be proved in a similar way.

□

Figure 3.4 shows the plot of the C^2 sextic B-spline associated with a triangle of the triangulation Δ_{PS}.

3.2 Nearly optimal PS6 triangles

The construction of a normalized PS6 basis of $S_6^{2,4,3}(\Omega,\, \Delta_{\text{PS}})$ is reduced to finding a set of PS6 triangles that must contain a number of specified points. The set of PS6 triangles is not uniquely defined for a given refinement [62]. One possibility for their construction is to calculate triangles of minimal area, the so-called optimal PS triangles introduced by P. Dierckx [23]. Computationally, this problem leads to a quadratic programming problem. From a practical point of view, other choices may be more appropriate. An alternative (and easier to implement) solution is given in [62], where the sides of the PS triangle are obtained by connecting neighbouring PS-points in a suitable way. This technique was adopted and improved in [43]. A particular choice of the PS6 triangles can also simplify the treatment of boundary conditions [61]. For quasi-interpolation (see [50]) the corners of each PS6 triangle are preferred to be chosen on edges of the triangulation.

We will recall the standard method proposed in literature [23, 24, 25, 26] to construct PS6 triangles, and then we will introduce a novel procedure.

3.2.1 Quadratic programming problem

Consider points $Q_{i,j} = (X_{i,j},\, Y_{i,j}),\ j = 1,2,3$, yielding a PS6-triangle relative to the vertex $V_i = (x_i,\, y_i)$ and triplets $\left(\Gamma_{i,j},\, \Gamma^x_{i,j},\, \Gamma^y_{i,j}\right)$, $j = 1,2,3$, satisfying the following equality:

$$\begin{pmatrix} \Gamma_{i,1} & \Gamma_{i,2} & \Gamma_{i,3} \\ \Gamma^x_{i,1} & \Gamma^x_{i,2} & \Gamma^x_{i,3} \\ \Gamma^y_{i,1} & \Gamma^y_{i,2} & \Gamma^y_{i,3} \end{pmatrix} \begin{pmatrix} X_{i,1} & Y_{i,1} & 1 \\ X_{i,2} & Y_{i,2} & 1 \\ X_{i,3} & Y_{i,3} & 1 \end{pmatrix} = \begin{pmatrix} x_i & y_i & 1 \\ 1 & 0 & 0 \\ 0 & 1 & 0 \end{pmatrix}. \tag{3.11}$$

The area of the PS6 triangle being

$$\begin{vmatrix} X_{i,1} & Y_{i,1} & 1 \\ X_{i,2} & Y_{i,2} & 1 \\ X_{i,3} & Y_{i,3} & 1 \end{vmatrix} = \begin{vmatrix} \Gamma_{i,1} & \Gamma_{i,2} & \Gamma_{i,3} \\ \Gamma^x_{i,1} & \Gamma^x_{i,2} & \Gamma^x_{i,3} \\ \Gamma^y_{i,1} & \Gamma^y_{i,2} & \Gamma^y_{i,3} \end{vmatrix}^{-1} = \frac{1}{\Gamma^x_{i,1}\Gamma^y_{i,2} - \Gamma^y_{i,1}\Gamma^x_{i,2}},$$

then, maximize the objective function $\Gamma^x_{i,1}\Gamma^y_{i,2} - \Gamma^y_{i,1}\Gamma^x_{i,2}$ is one approach to obtain a triangle of smallest area. Additional constraints are needed to get a PS6 triangle containing all PS6-points with respect to V_i.

The classical construction due to Dierckx is then summarized in the next result.

Proposition 3.2.1. *The construction of an optimal PS6 triangle t_i with respect to vertex V_i is equivalent to the following quadratic programming problem: find triplets $\left(\Gamma_{i,j},\, \Gamma^x_{i,j},\, \Gamma^y_{i,j}\right)$, $j = 1,2,3$, maximizing the objective function $\Gamma^x_{i,1}\Gamma^y_{i,2} - \Gamma^y_{i,1}\Gamma^x_{i,2}$ subject to the constraints*

$$\begin{aligned} \Gamma_{i,1} + \Gamma_{i,2} + \Gamma_{i,3} &= 1 \\ \Gamma^x_{i,1} + \Gamma^x_{i,2} + \Gamma^x_{i,3} &= 0 \\ \Gamma^y_{i,1} + \Gamma^y_{i,2} + \Gamma^y_{i,3} &= 0 \end{aligned}$$

and

$$\begin{aligned} &\Gamma_{i,j} \geq 0, \\ &L_{i\ell,j} = \Gamma_{i,1} + \frac{2}{3}\left(\Gamma^x_{i,j}\,(x_\ell - x_i) + \Gamma^y_{i,j}\,(y_\ell - y_i)\right) \geq 0, \end{aligned}$$

with $j = 1,2,3$ and for all vertices $V_\ell = (x_\ell,\, y_\ell)$ lying on the boundary of the molecule M_i of V_i, where $(\Gamma_{i,1},\, \Gamma_{i,2},\, \Gamma_{i,3})$ and $(L_{i\ell,1},\, L_{i\ell,2},\, L_{i\ell,3})$ are the barycentric coordinates with respect to PS6-triangle t_i of the PS6 points V_i and $S_{i\ell}$, respectively.

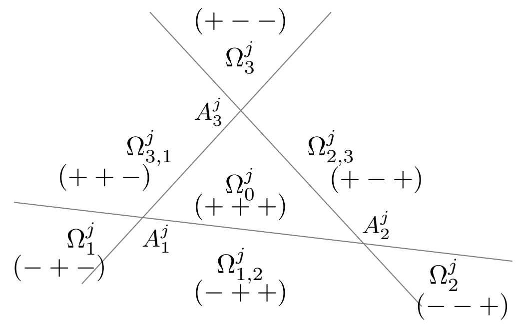

Figure 3.5: The seven regions determined by the triangle T_j, with associated signs
.

The objective function of the optimization problem can be written as $\max x^T A\, x$, where

$$x^T := \left(\Gamma_{i,1}, \Gamma_{i,2}, \Gamma_{i,1}^x, \Gamma_{i,2}^x, \Gamma_{i,1}^y, \Gamma_{i,2}^y\right) \quad \text{and} \quad A = \begin{pmatrix} 0 & 0 & 0 & 0 & 0 & 0 \\ 0 & 0 & 0 & 0 & 0 & 0 \\ 0 & 0 & 0 & 0 & 0 & -1 \\ 0 & 0 & 0 & 0 & 1 & 0 \\ 0 & 0 & 0 & 1 & 0 & 0 \\ 0 & 0 & -1 & 0 & 0 & 0 \end{pmatrix}.$$

The eigenvalues of the matrix A are -1, -1, 1, 1, 0 and 0, so that A is indefinite. As pointed out in [23], *"since the Hessian matrix of the objective function is not negative (semi-) definite, appropriate software can only find a local maximum"*. Therefore, we cannot guarantee that the quadratic optimization problem has a unique solution, which leads to a scenario of local solutions.

The technique for determining PS6 triangles is not unique. An option for construct them is to calculate a triangle with minimal area. Although the quadratic program of P. Dierckx [23] produces excellent results, it can also produce PS6-triangle with quite large diameters. Therefore, in order to overcome the limitation of the above optimization problem, namely, the appearance of pre-degenerated triangles, i.e. triangles with minimal area and long diameters, which impact negatively the quality of the approximation, we propose an algorithm yielding a PS6 triangle with a diameter as small as possible.

3.2.2 Algorithm for determining a triangle containing a set of points

Given a triangle T, let $\{\Omega_i\}_{i=0}^6$ be the interiors of the seven regions obtained by extending the edges of T indefinitely (see Figure 3.5). Then, for each fixed $0 \le i \le 6$, the barycentric coordinates of all the points in Ω_i have constant signs. In particular, a point lies in the interior of T if and only if its barycentric coordinates are positive.

The algorithm proposed here to define a triangle containing the points A_i, $1 \le i \le n$, starts from an initial triangle and builds step by step triangles so that the triangle $T_j := \left\langle A_1^j,\, A_2^j,\, A_3^j \right\rangle$, $j \ge 2$, obtained at the j^{th} step of the algorithm contains the points $A_1, \ldots, A_{j-1}$. Denote by Ω_k^j, $k = 0, 1, 2, 3$, and $\Omega_{k,k+1}^j$, $k = 1, 2, 3$, the seven regions obtained by dividing the plan through T_j (see Figure 3.5).

More precisely, the procedure described in Algorithm 1 is carried out to determine a triangle from the previous one.

Figure 3.10 shows the PS6 triangles produced by the algorithm when applied to the PS6 points close to those used in [43]. They have two or three edges in common with the convex hull of the PS6 points.

Next, we give a result needed to determine triangles having nearly minimal area.

Algorithm 1 DETERMINING THE TRIANGLE T_{j+1} FROM T_j

Require: compute the barycentric coordinates of A_j with respect to T_j and select the region where A_j is located.

if $A_j \in \Omega_0^j$ **then**

A_j is in T_j, do $T_{j+1} \leftarrow T_j$ and move to the next point A_{j+1}

else if $A_j \in \Omega_{3,1}^j$ **then**

1. Let I and J be the intersections of the line passing through A_j and parallel to that passing through $\left\{A_3^j, A_1^j\right\}$ with the lines passing through $\left\{A_2^j, A_1^j\right\}$ and $\left\{A_2^j, A_3^j\right\}$, respectively, and let T_{j+1}^1 be the triangle with vertices A_2^j, I and J.
2. Let L be the line passing through A_j and orthogonal to bisector of angle spanned by the lines $\left\langle A_2^j, A_1^j\right\rangle$ and $\left\langle A_2^j, A_3^j\right\rangle$. Let I and J be the intersections of L with the lines defined by $\left\{A_2^j, A_1^j\right\}$ and $\left\{A_2^j, A_3^j\right\}$, and define as T_{j+1}^2 the triangle with vertices A_2^j, I and J.
3. Define T_{j+1} as the triangle of minimum area among T_{j+1}^1 and T_{j+1}^2.

The same process is used if A_j belongs to $\Omega_{1,2}^j$ or $\Omega_{2,3}^j$.

else if $A_j \in \Omega_3^j$ **then**

$T_{j+1} = \left\langle A_1^j, A_2^j, A_j\right\rangle$.

The same procedure is applied if $A_j \in \Omega_1^j$ or $A_j \in \Omega_2^j$

end if

Lemma 3.2.2. *Let a, A_1, A_2, A_3 and A_4 be five points in $\mathbb{R}^2$. If $a \in T_{ijk} := \langle A_i, A_j, A_k\rangle$ for $i, j, k = 1, 2, 3, 4$ and $i \neq j \neq k$, then, a is in the triangle obtained by applying the algorithm using T_{ijk} and A_ℓ, $\ell \neq i \neq j \neq k$.*

Proof. For the sake of simplicity, consider only one of the four different triangles which can be obtained from four points. Let $T_{134} := \langle A_1, A_3, A_4\rangle$ be a triangle containing a. By applying the algorithm proposed here to T_{134} and A_2, we can distinguish the following scenarios:

- If $A_2 \in T_{134}$, then, the resulting triangle will be T_{134} itself.
- If $A_2 \notin T_{134}$, then the obtained triangle will contain T_{134}.

In both cases the resulting triangle will contain T_{134}, so will contain also a. The proof is complete. □

From Lemma 3.2.2, at step j in the algorithm, we use the four triangles obtained by a permutation of the vertices of T_j and A_j, and we choose the triangle of small diameter among the four ones.

Figure 3.6 shows the PS6-triangles provided by the proposed algorithm for the considered triangulation. It can be noticed that the resulting triangles pass through at least three PS6-points. They have near minimal areas and smaller diameters.

As said before, the quadratic optimization problem proposed by P. Dierckx [23] can produce PS6-triangles with quite large diameters, and the algorithm proposed here aims to avoid this problem even though the resulting triangles have no minimal areas. Figure 3.7 shows the results provided by Dierckx's method and the algorithm for minimizing the diameter when a near degenerate vertex is considered.

Figure 3.8 shows the results obtained when the time of execution of both algorithms is examined. The time required by Dierckx' algorithm is more than 30 times longer than that required by the proposed algorithm.

Other algorithms for determining PS triangles have also been described in the literature. As said before, in [43], after Proposition 1, the authors outline an algorithm that produces PS

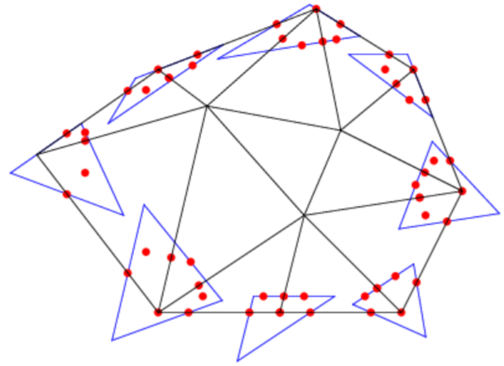

Figure 3.6: A triangulation of a polygonal domain along with the PS6-triangles obtained by the proposed algorithm.

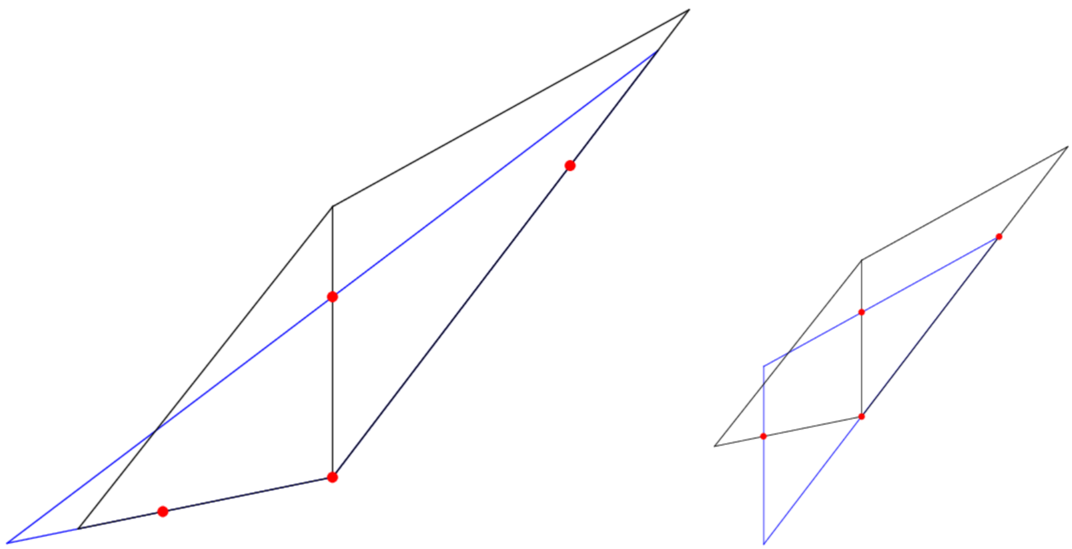

Figure 3.7: PS6 triangles associated with a near degenerate vertex obtained by quadratic programming (left) and the proposed algorithm (right). The area of the triangle provided by the Dierckx's method is equal to 0.2344 cm^2 and the diameter is equal to 12.7857 cm. The area and the diameter of the second one are 0.25 cm^2 and 7.9907 cm, respectively.

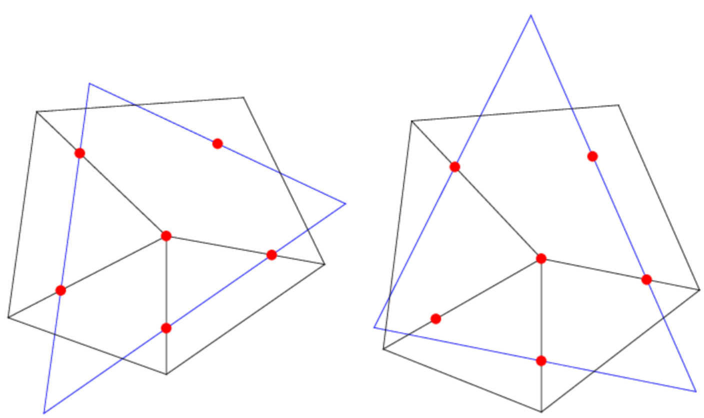

Figure 3.8: Results produced by the proposed algorithm (left) and Dierckx's algorithm (right).

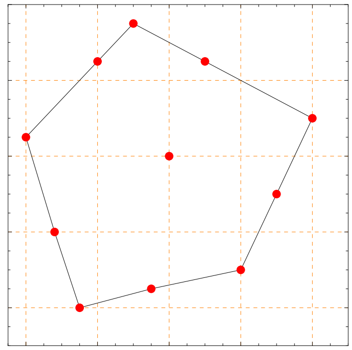

Figure 3.9: PS points close to those of the ones in [43].

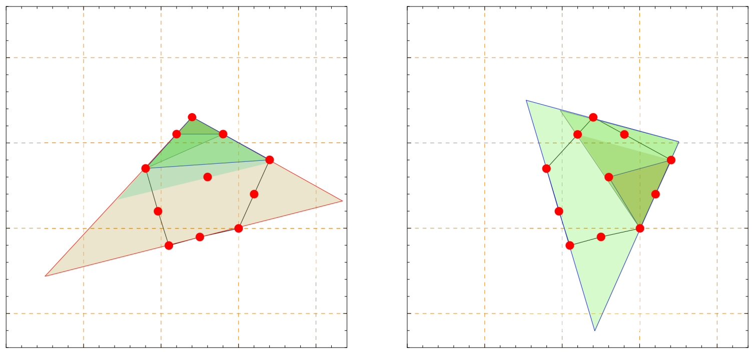

Figure 3.10: Results produced by the proposed algorithm applied to a set of PS6 points close to the points indicated in Figure 3.9.

triangles sharing two or three edges with the convex hull of the PS points. Next, we compare it the proposed algorithm.

To do that, we consider PS points like those in Figure 1 in [43]. They are represented in Figure 3.9.

Algorithm 1 provides the PS6 triangles shown in Figure 3.10. Each of them is produced from a choice of an initial triangle. On the left side, we show those obtained after three steps starting from the small dark triangle. We see that these PS triangles share two or three sides with the convex hull of the PS points. On the right side, we show two other PS triangles produced by the algorithm after four steps. They also share two or three sides with the convex hull. The results provided by the algorithm in [43] and Algorithm 1 are similar, although the latter one does not need to compute the convex hull of the PS points.

3.3 Quasi-interpolation schemes with optimal approximation order

In this section, we give proof of Marsden's identity for the space $S_6^{2,4,3}(\Delta_{\mathrm{PS}})$, expressing any super spline s in this space as a linear combination of the normalized sextic Powell-Sabin B-splines defined above. The coefficients in that combination are given in terms of the polar forms of s. Therefore, Proposition 1.3.1 facilitates the establishment of Marsden's identity in comparison with other existing methods (e.g. matrix inverse [24]).

Here, we use the same notation as in Subsection **??**. Let $Q_{i,j}$, $j = 1, 2, 3$, be the vertices of a PS6 triangle t_i w.r.t V_i. Define

$$\tilde{Q}_{i,j} := -\frac{1}{2}V_i + \frac{3}{2}Q_{i,j}, \quad i = 1, \dots, nv, \quad j = 1, 2, 3.$$

We have the following result.

Corollary 3.3.1. *For any* $p \in \mathbb{P}_6$ *it holds*

$$p = \sum_{i=1}^{nv} \sum_{|\beta|=4} \mathbf{B}\,[p] \left(V_i[2], \tilde{Q}_{i,1}[\beta_1], \tilde{Q}_{i,2}[\beta_2], \tilde{Q}_{i,3}[\beta_3] \right) \mathcal{B}^v_{i,\beta} + \sum_{k=1}^{nt} \mathbf{B}\,[p]\,(Z_k[3], V_{k1}, V_{k2}, V_{k3})\, \mathcal{B}^t_k, \tag{3.12}$$

where V_{k1}, V_{k2} *and* V_{k3} *are the vertices of the macro triangle containing* Z_k.

Proof. Define

$$s = \sum_{i=1}^{nv} \sum_{|\beta|=4} \mathbf{B}\,[p] \left(V_i[2], \tilde{Q}_{i,1}[\beta_1], \tilde{Q}_{i,2}[\beta_2], \tilde{Q}_{i,3}[\beta_3] \right) \mathcal{B}_{i,\beta}[v] + \sum_{k=1}^{nt} \mathbf{B}\,[p]\,(Z_k[3], V_{k1}, V_{k2}, V_{k3})\, \mathcal{B}^t_k.$$

We will prove that

$$\partial_{a,b} s\,(V_i) \;=\; \partial_{a,b} p(V_i),\;\; i = 1, \ldots, nv,\;\; 0 \le a+b \le 4,$$

and

$$s\,(Z_k) \;=\; p\,(Z_k)\,,\;\; k = 1, \ldots, nt,$$

from which the equality $s = p$ will follow.

It is clear that

$$s\,(V_i) = \sum_{|\beta|=4} \mathbf{B}\,[p] \left(V_i[2], \tilde{Q}_{i,1}[\beta_1], \tilde{Q}_{i,2}[\beta_2], \tilde{Q}_{i,3}[\beta_3] \right) \mathcal{B}^v_{i,\beta}\,(V_i)\,.$$

Define

$$q_{vi}\,(X) := \sum_{|\beta|=4} \mathbf{B}\,[p] \left(V_i[2], \tilde{Q}_{i,1}[\beta_1], \tilde{Q}_{i,2}[\beta_2], \tilde{Q}_{i,3}[\beta_3] \right) \mathcal{B}^v_{i,\beta}\,(X)\,.$$

From (3.3), for all $0 \le a+b \le 4$ it holds

$$\begin{aligned}
&\partial_{a,b} q_{vi}\,(X) \\
&= \frac{30}{(6-a-b)\,(5-a-b)} \left(\frac{4}{6}\right)^{a+b} \partial_{a,b} \sum_{|\beta|=4} \mathbf{B}\,[p] \left(V_i[2], \tilde{Q}_{i,1}[\beta_1], \tilde{Q}_{i,2}[\beta_2], \tilde{Q}_{i,3}[\beta_3] \right) \mathfrak{B}^4_{t_i,\beta}\,(X) \\
&= \frac{6!}{(6-a-b)!\,(a+b)!} \frac{(a+b)!\,(4-a-b)!}{4!} \left(\frac{4}{6}\right)^{a+b} \times \\
&\partial_{a,b} \sum_{|\beta|=4} \mathbf{B}\,[p] \left(V_i[2], \tilde{Q}_{i,1}[\beta_1], \tilde{Q}_{i,2}[\beta_2], \tilde{Q}_{i,3}[\beta_3] \right) \mathfrak{B}^4_{t_i,\beta}\,(X)\,.
\end{aligned}$$

Now, we use the notion of control polynomial developed in [Lemma 1.3.1, Chapter 1]. Let

$$\tilde{q}_{vi} := \mathbf{B}\,[p] \left(V_i[2], \left(\frac{-1}{2} V_i + \frac{3}{2} X \right) [4] \right)$$

be the control polynomial of degree 4 of p at the vertex V_i. We can write $\tilde{q}_{vi}$ on the PS-triangle t_i as

$$\tilde{q}_{vi}\,(X) \;=\; \sum_{|\beta|=4} \mathbf{B}\,[\tilde{q}_{vi}]\,(Q_{i,1}[\beta_1], Q_{i,2}[\beta_2], Q_{i,3}[\beta_3])\, \mathfrak{B}^4_{t_i,\beta}\,(X)\,.$$

According to Lemma 1.3.2,

$$\tilde{q}_{vi}\,(X) = \sum_{|\beta|=4} \mathbf{B}\,[p] \left(V_i[2], \tilde{Q}_{i,1}[\beta_1], \tilde{Q}_{i,2}[\beta_2], \tilde{Q}_{i,3}[\beta_3] \right) \mathfrak{B}^4_{t_i,\beta}\,(X)\,.$$

Using Proposition 1.3.1, we deduce that

$$\partial_{a,b}p\left(V_i\right)=\frac{30}{\left(6-a-b\right)\left(5-a-b\right)}\left(\frac{4}{6}\right)^{a+b}\partial_{a,b}\tilde{q}_{vi}\left(V_i\right)=\partial_{a,b}q_{vi}\left(V_i\right)=\partial_{a,b}s\left(V_i\right).$$

Now, it suffices to prove that $s\left(Z_k\right)=p\left(Z_k\right)$. Without loss of generality, we shall prove the equality only for one triangle in Δ. Let $T=\langle V_1,V_2,V_3\rangle$ be a triangle in Δ with split point Z_1. Then

$$\begin{aligned}
s\left(Z_1\right) = &\sum_{|\beta|=4}\mathbf{B}\left[p\right]\left(V_1[2],\tilde{Q}_{1,1}[\beta_1],\tilde{Q}_{1,2}[\beta_2],\tilde{Q}_{1,3}[\beta_3]\right)\mathcal{B}^v_{1,\beta}\left(Z_1\right)\\
&+\sum_{|\beta|=4}\mathbf{B}[p](V_2[2],\tilde{Q}_{2,1}[\beta_1],\tilde{Q}_{2,2}[\beta_2],\tilde{Q}_{2,3}[\beta_3])\,\mathcal{B}^v_{2,\beta}(Z_1)\\
&+\sum_{|\beta|=4}\mathbf{B}\left[p\right]\left(V_3[2],\tilde{Q}_{3,1}[\beta_1],\tilde{Q}_{3,2}[\beta_2],\tilde{Q}_{3,3}[\beta_3]\right)\mathcal{B}^v_{3,\beta}\left(Z_1\right)+\mathbf{B}\left[p\right]\left(Z_1[3],V_1,V_2,V_3\right)\mathcal{B}^t_k\left(Z_1\right).
\end{aligned}$$

From Section 3, we have

$$\begin{aligned}
&\sum_{|\beta|=4}\mathbf{B}\left[p\right]\left(V_1[2],\tilde{Q}_{1,1}[\beta_1],\tilde{Q}_{1,2}[\beta_2],\tilde{Q}_{1,3}[\beta_3]\right)\mathcal{B}^v_{1,\beta}\left(Z_1\right)\\
&=c_{68}\\
&=z_1^3c_{13}+3z_1^2z_2\,\tilde{c}_{20}+3z_1^2z_3\tilde{c}_{22}\\
&=z_1^3\mathbf{B}\left[p\right]\left(V_1^3,Z_1^3\right)+3z_1^2z_2\mathbf{B}\left[p\right]\left(V_1^2,V_2,Z_1^3\right)+3z_1^2z_3\mathbf{B}\left[p\right]\left(V_1^2,V_3,Z_1^3\right).
\end{aligned}$$

Similarly,

$$\begin{aligned}
&\sum_{|\beta|=4}\mathbf{B}\left[p\right]\left(V_2[2],\tilde{Q}_{2,1}[\beta_1],\tilde{Q}_{2,2}[\beta_2],\tilde{Q}_{2,3}[\beta_3]\right)\mathcal{B}^v_{2,\beta}\left(Z_1\right)\\
&=z_2^3\mathbf{B}\left[p\right](V_2^3,Z_1^3)+3z_2^2z_1\mathbf{B}\left[p\right](V_2^2,V_1,Z_1^3)+3z_2^2z_3\mathbf{B}\left[p\right](V_2^2,V_3,Z_1^3),\\
&\sum_{|\beta|=4}\mathbf{B}\left[p\right]\left(V_3[2],\tilde{Q}_{3,1}[\beta_1],\tilde{Q}_{3,2}[\beta_2],\tilde{Q}_{3,3}[\beta_3]\right)\mathcal{B}^v_{3,\beta}\left(Z_1\right)\\
&=z_3^3\mathbf{B}\left[p\right]\left(V_3^3,Z_1^3\right)+3z_3^2z_1\mathbf{B}\left[p\right]\left(V_3^2,V_1,Z_1^3\right)+3z_3^2z_2\mathbf{B}\left[p\right]\left(V_3^2,V_2,Z_1^3\right),
\end{aligned}$$

and

$$\mathbf{B}\left[p\right]\left(Z_1[3],V_1,V_2,V_3\right)\mathcal{B}^t_k\left(Z_1\right)=6z_1z_2z_3\mathbf{B}\left[p\right]\left(Z_1^3,V_1,V_2,V_3\right).$$

By taking into account the multi-affine property of the polar form, the claim follows. □

Now, we state the following result, whose proof follows the idea used in [35] in dealing with quadratic Powell-Sabin splines.

Theorem 3.3.2. *For any super spline $s\in S_6^{2,4,3}\left(\Omega,\,\Delta_{PS}\right)$, it holds*

$$s=\sum_{i=1}^{nv}\sum_{|\beta|=4}\mathbf{B}\left[s_i\right]\left(V_i[2],\tilde{Q}_{i,1}[\beta_1],\tilde{Q}_{i,2}[\beta_2],\tilde{Q}_{i,3}[\beta_3]\right)\mathcal{B}^v_{i,\beta}+\sum_{k=1}^{nt}\mathbf{B}\left[\tilde{s}_k\right]\left(Z_k[3],V_{k1},V_{k2},V_{k3}\right)\mathcal{B}^t_k,$$

where $s_i:=s_{|\mathsf{t}_i}$ stands for the restriction of s to the triangle t_i in Δ_{PS} and $\tilde{s}_k$ is the restriction of s to a triangle $\mathsf{t}_k=\langle V_{k1},V_{k2},V_{k3}\rangle$ containing Z_k.

Proof. Consider a spline s in $S_6^{2,4,3}\left(\Delta_{\mathrm{PS}}\right)$. Let t_i be a triangle in Δ_{PS} having V_i as a vertex. Let s_i be the restriction of s to t_i, i.e. the sextic polynomial such that

$$\partial_{a,b}s\left(V_i\right)\;=\;\partial_{a,b}s_i\left(V_i\right),\quad s\left(Z_k\right)=\tilde{s}_k\left(Z_k\right),\;\;0\leq a+b\leq 4.$$

Let p_i be the restriction of s on $\mathbf{t}_i$. From Corollary 3.3.1, it is clear that for all $(x,y)\in\Omega$ and $r=1,\dots,n_v$ it holds

$$p_r=\sum_{i=1}^{nv}\sum_{|\beta|=4}\mathbf{B}\left[p_r\right]\left(V_i[2],\tilde{Q}_{i,1}[\beta_1],\tilde{Q}_{i,2}[\beta_2],\tilde{Q}_{i,3}[\beta_3]\right)\mathcal{B}^v_{i,\beta}+\sum_{k=1}^{nt}\mathbf{B}\left[p_r\right]\left(Z_k[3],V_{k1},V_{k2},V_{k3}\right)\mathcal{B}^t_k.$$

Then,

$$p_r\left(V_r\right)=\sum_{|\beta|=4}\mathbf{B}\left[p_r\right]\left(V_r[2],\tilde{Q}_{r,1}[\beta_1],\tilde{Q}_{r,2}[\beta_2],\tilde{Q}_{r,3}[\beta_3]\right)\mathcal{B}^v_{r,\beta}\left(V_r\right).$$

Therefore,

$$p_r\left(V_r\right)=\sum_{|\beta|=4}\mathbf{B}\left[s_r\right]\left(V_r[2],\tilde{Q}_{r,1}[\beta_1],\tilde{Q}_{r,2}[\beta_2],\tilde{Q}_{r,3}[\beta_3]\right)\mathcal{B}^v_{r,\beta}\left(V_r\right).$$

Define,

$$\begin{aligned}q\left(x,y\right):=&\sum_{i=1}^{nv}\sum_{|\beta|=4}\mathbf{B}\left[s_i\right]\left(V_i[2],\tilde{Q}_{i,1}[\beta_1],\tilde{Q}_{i,2}[\beta_2],\tilde{Q}_{i,3}[\beta_3]\right)\mathcal{B}^v_{i,\beta}\left(x,y\right)\\&+\sum_{k=1}^{nt}\mathbf{B}\left[s_k\right]\left(Z_k[3],V_{k1},V_{k2},V_{k3}\right)\mathcal{B}^t_k\left(x,y\right).\end{aligned}$$

It holds

$$q\left(V_r\right)=\sum_{|\beta|=4}\mathbf{B}\left[s_r\right]\left(V_r[2],\tilde{Q}^{[}_{r,1}\beta_1],\tilde{Q}_{r,2}[\beta_2],\tilde{Q}_{r,3}[\beta_3]\right)\mathcal{B}^v_{r,\beta}\left(V_r\right).$$

Then, for all $r=1,\dots,n_v$, we get

$$q(V_r)=p_r(V_r)=s_r(V_r)=s(V_r).$$

Similarly, we obtain

$$\partial_{a,b}q(V_r)=\partial_{a,b}p_r(V_r)=\partial_{a,b}s_r(V_r)=\partial_{a,b}s(V_r),\;\;1\le a+b\le 4,$$

and

$$q(Z_k)=p_k(Z_k)=\tilde{s}_k(Z_k)=s(Z_k).$$

Since every element in $S_6^{2,4,3}\left(\Delta_{\mathrm{PS}}\right)$ is uniquely determined by its values and derivative values up to order four at the vertices of Δ, then the claim follows and the proof is completed. □

Marsden's identity is a useful tool for constructing quasi-interpolants to enough regular functions (see [35] and references therein for details). We will use it to define differential quasi-interpolants in $S_6^{2,4,3}\left(\Delta_{\mathrm{PS}}\right)$. Only an outline of the construction is given here.

Lef $f\in C^6\left(\Omega\right)$ and $L_i^j:=\left(L^j_{i,x},\,L^j_{i,y}\right)$, $i=1,\dots,nv$, $j=1,\dots,15$, be some fixed points lying in the union of all triangles in Δ having V_i as vertex. Let us suppose that they form an unisolvent scheme in $\mathbb{P}_6\left(\mathbb{R}^2\right)$, and let p_i^j be the Taylor polynomial of f of degree 6 at L_i^j, i.e.

$$p_i^j\left(x,y\right)=\sum_{0\le k+\ell\le 6}\frac{1}{k!\ell!}\partial_{k,\ell}f\left(L_i^j\right)\left(x-L^j_{i,x}\right)^k\left(y-L^j_{i,y}\right)^\ell.\tag{3.13}$$

Let p_k be the Taylor polynomial of degree 6 at the point L_k in the support of $\mathcal{B}^t_k$.

Define

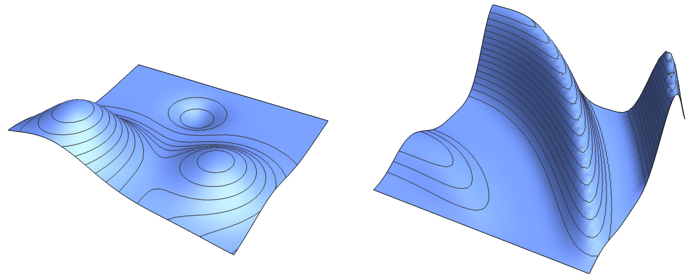

Figure 3.11: Plots of the tests functions: Franke (left) and Nielson (right).

$$\mathcal{Q}f\,(x,y) = \sum_{i=1}^{nv} \sum_{|\beta|=4} \mathbf{B}\left[p_i^j\right] \left(V_i[2], \tilde{Q}_{i,1}[\beta_1], \tilde{Q}_{i,2}[\beta_2], \tilde{Q}_{i,3}[\beta_3]\right) \mathcal{B}^v_{i,\beta}\,(x,y) + \sum_{k=1}^{nt} \mathbf{B}\,[p_k]\,(Z_k[3], V_{k1}, V_{k2}, V_{k3})\; \mathcal{B}^t_k\,(x,y)\,. \tag{3.14}$$

Let $\mathcal{Q}f$ be a quasi-interpolant defined by (3.14) and (3.13). Then, the quasi-interpolation operator $\mathcal{Q} : C^6\,(\Omega) \to S_6^{2,4,3}\,(\Omega,\,\Delta_{\mathrm{PS}})$ defined such that $\mathcal{Q}\,(f) := \mathcal{Q}f$ is exact on $\mathbb{P}_6$, i.e. $\mathcal{Q}\,(p) = p$ for all $p \in \mathbb{P}_6$.

Moreover, if each L_i^j belongs to a triangle τ_i^j in Δ_{PS} with V_i as a vertex, then $\mathcal{Q}\,(s) = s$ for any spline $s \in S_6^{2,4,3}\,(\Delta_{\mathrm{PS}})$.

3.3.1 Numerical tests

The aim of this subsection is to test the approximation power of the proposed quasi-interpolation operator. To this end, we will test its performance using the well-known Franke and Nielson's functions [51, 52] (see [Section 2.5, Chapter 2]). Whose plots appear in Figure 3.11.

Let us consider the domain $\Omega = [0,1] \times [0,1]$. The test is carried out for a sequence of uniform mesh Δ_n associated with the vertices (ih, jh), $i, j = 0, , n$, where $h := \dfrac{1}{n}$. For each triangulation, we have to compute the B-splines $\mathcal{B}^v_{i,j}$ and $\mathcal{B}^t_k$ with respect to vertices and split points respectively, and the corresponding points PS6-triangles according to the minimal area procedure described in this work.

The quasi-interpolation error is estimated as

$$\max_{\ell,k=1,\ldots,50} |f\,(x_\ell, y_k) - \mathcal{Q}f\,(x_\ell, y_k)|\,,$$

where x_i and y_j are equally spaced points in $[0,1]$. The numerical convergence order (NCO) is given by the rate

$$\mathrm{NCO} := \log_2\left(\frac{E(2n)}{E(n)}\right),$$

where $E\,(m)$ stands for the estimated error associated with Δ_m.

The estimated errors and NCOs for the functions f_1 and f_2 are shown in Table 3.1. They confirm the theoretical results.

Figure 3.12 shows two of the meshes used to define quasi-interpolants for the test functions f_1 and f_2.

Figure 3.13 shows the plots of the splines $\mathcal{Q}f_1$ and $\mathcal{Q}f_2$ for the two above meshes.

		Franke's function		Nielson's function	
n	nv	Estimated error	NCO	Estimated error	NCO
2	9	1.07×10^{-1}	–	1.50×10^{-2}	–
4	25	8.47×10^{-4}	6.98	1.71×10^{-4}	7.08
8	81	7.05×10^{-6}	6.81	1.09×10^{-6}	7.20

Table 3.1: Estimated errors for Franke's and Nielson's functions and NCOs with $n = 2^m$, $1 \leq m \leq 3$.

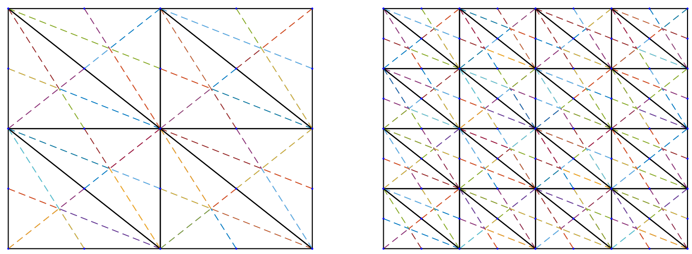

Figure 3.12: Meshes for $n = 2^m$, $1 \leq m \leq 2$.

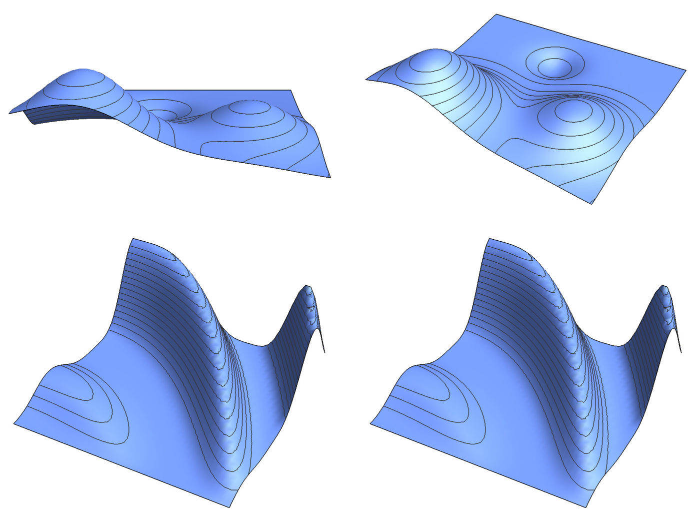

Figure 3.13: Quasi-interpolants for Franke's function (top) and Nielson's function (bottom).

3.4 Conclusion

In this chapter, a fully carried out construction of a normalized basis of the space $S_6^{2,4,3}(\Delta_{\mathrm{PS}})$ introduced in [42] has been given and an algorithm has been proposed and compared with two others in the literature. Also, an efficient manner to establish Marsden's identity has been detailed from which quasi-interpolation operators with optimal approximation order are defined. Some tests show the good performance of these operators.

Chapter 4

Gaussian rules on 6-split

M. Bartoň and J. Kosinka have recently presented an optimal Gaussian quadrature for $\mathcal{C}^1$ quadratic Powell-Sabin 6-split macro-triangles [45]. Quadratic polynomials on triangles can be integrate exactly by using a 3-point formula, so that the number of nodes is optimal. On the other hand, on a single macro-triangle T the space $S_2^1(T)$ of C^1 quadratic Powell-Sabin 6-split splines has dimension equal to 9, so that it is quite natural to ask whether the quadrature formula exact for quadratic polynomials is also exact on $S_2^1(T)$. In the above-mentioned paper, the authors set up a non-standard basis to $S_2^1(T)$ in such a way that any of its basis functions is integrated exactly by the quadrature formula exact on the space $\mathbb{P}_2(T)$ of quadratic polynomials on T.

Unfortunately, the existence of these quadrature rules depends on the choice of the inner split point. More precisely, the authors have shown that the inner split point cannot be arbitrarily placed inside the triangle but must be located inside a specific locus $\mathcal{R}$ (see Figure 4.1).

In order to avoid this limitation, we have studied the existence of micro-edges quadrature rules in the context of a specific configuration. This configuration allows us to confirm that micro-edge quadrature rules exist for an arbitrary choice of the inner split point.

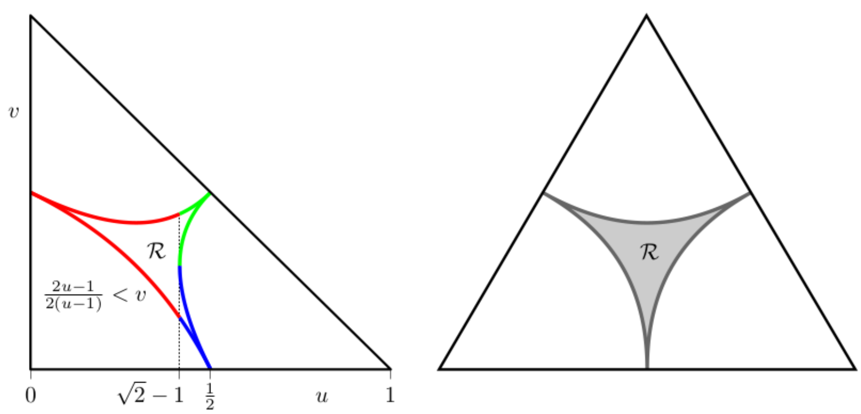

Figure 4.1: Two visualisations of the region $\mathcal{R}$ of all admissible inner split-points ensuring the existence of a micro-edge quadrature for PS-splines [45, Fig. 7, page 247].

4.1 Powell-Sabin 6-split

Sea Δ a triangulation with vertices $\mathcal{V} := \{V_i\}_{1\leq i\leq nv}$. Let Δ_{PS} be the Powell-Sabin 6-split of Δ. It is well known that there exists a unique spline $s \in S_2^1(\Delta_{\mathrm{PS}})$ such that [18]

$$D_x^a\, D_y^b\; s\,(V_i) \;= f_i^{a,b},\; i=1,\ldots,nv,\;\; a,b\geq 0 \text{ and } a+b\leq 1, \tag{4.1}$$

for given f-values. That is, given function values and partial derivatives at each vertex of the original triangulation Δ, the Hermite interpolation problem (4.1) has a unique solution in $S_2^1(\Delta_{\mathrm{PS}})$ and from that one can also conclude that the dimension of $S_2^1(\Delta_{\mathrm{PS}})$ equals to $3\,nv$.

4.2 Splines on a macro-triangle

We now consider the case of a single triangle T with vertices V_1, V_2 and V_3 to deal with $S_2^1(T)$. Let $R_{2,3}$, $R_{3,1}$ and $R_{1,2}$ denote points interior to the edges opposite to the vertices V_1, V_2 and V_3, respectively.

Definition 4.2.1 (C-refinement). *We say that the macro-triangle T is endowed with a C-refinement if the linear segments $\langle V_1, R_{2,3}\rangle$, $\langle V_2, R_{3,1}\rangle$ and $\langle V_3, R_{1,2}\rangle$ intersect at a point.*

Chosen a point Z interior to the triangle T, a C-refinement results if $R_{2,3}$, $R_{1,3}$ and $R_{1,2}$ are taken, respectively, as the intersections of the lines defined by Z and the vertices V_1, V_2 and V_3 with the the opposite edges. Note that, if on each edge of a triangulation an interior point is chosen and it turns out that all the triangles are equipped with C-refinements, this does not imply that the resulting sub-triangulation of Δ is of Powell-Sabin type.

C-refinements are characterized by the well known Ceva's Theorem, proved by Giovanni Ceva in 1678 (see [63]) and much earlier, in the 11th century, by Al-Mutaman ibn Hūd (see [64, p. 9]). However, to establish the main contribution in this paper, Ceva's Theorem will be characterized in terms of barycentric coordinates. For this aim, let us suppose that $V_1 = (x_1, y_1)$, $V_2 = (x_2, y_2)$ and $V_3 = (x_3, y_3)$. The barycentric coordinates of vertices V_1, V_2 and V_3 with respect to T are $(1,0,0)$, $(0,1,0)$ and $(0,0,1)$, respectively. Suppose that those of $Z = (x_z, y_z)$ are (z_1, z_2, z_3), and let $(\lambda_{1,2}, \lambda_{2,1}, 0)$, $(0, \lambda_{2,3}, \lambda_{3,2})$ and $(\lambda_{1,3}, 0, \lambda_{3,1})$ be the barycentric coordinates of $R_{1,2} = (x_{1,2}, y_{1,2})$, $R_{2,3} = (x_{2,3}, y_{2,3})$ and $R_{3,1} = (x_{3,1}, y_{3,1})$, respectively. It is straightforward to prove that

$$\begin{aligned}
R_{1,2} \;&=\; \tau_{1,1}\, V_2 \;+\; \tau_{2,1}\, R_{2,3} \;+\; \tau_{3,1}\, Z,\\
R_{2,3} \;&=\; \tau_{1,2}\, V_3 \;+\; \tau_{2,2}\, R_{3,1} \;+\; \tau_{3,2}\, Z,\\
R_{3,1} \;&=\; \tau_{1,3}\, V_1 \;+\; \tau_{2,3}\, R_{1,2} \;+\; \tau_{3,3}\, Z,
\end{aligned}$$

where

$$\begin{aligned}
(\tau_{1,1},\, \tau_{2,1},\, \tau_{3,1}) \;&:=\; \left(\frac{\lambda_{1,2}z_3 - \lambda_{3,2}\,(1-\lambda_{2,1}-z_1)}{\lambda_{3,2}z_1}, -\frac{\lambda_{1,2}z_3}{\lambda_{3,2}z_1}, \frac{\lambda_{1,2}}{z_1}\right),\\
(\tau_{1,2},\, \tau_{2,2},\, \tau_{3,2}) \;&:=\; \left(\frac{-z_3\lambda_{2,3} + \lambda_{3,2}z_2 - \lambda_{31}\,(z_2-\lambda_{2,3})}{\lambda_{1,3}z_2}, -\frac{\lambda_{2,3}z_1}{\lambda_{1,3}z_2}, \frac{\lambda_{2,3}}{z_2}\right),\\
(\tau_{1,3},\, \tau_{2,3},\, \tau_{3,3}) \;&:=\; \left(\frac{\lambda_{3,1}\,(z_2-\lambda_{2,1})}{\lambda_{2,1}z_3}+1, -\frac{\lambda_{3,1}z_2}{\lambda_{2,1}z_3}, \frac{\lambda_{3,1}}{z_3}\right).
\end{aligned} \tag{4.2}$$

Then the following result holds.

Proposition 4.2.2. *The macro-triangle T is endowed of a C-refinement if and only if*

$$\lambda_{2,1} = \frac{z_2}{1-z_3}, \quad \lambda_{3,2} = \frac{z_3}{1-z_1} \;\text{ and } \lambda_{1,3} = \frac{z_1}{1-z_2}.$$

Proof. We prove first the necessity of the condition. Suppose that V_3, Z and $R_{1,2}$ are collinear. The slope of the straight line determined by V_3 and Z is equal to

$$m_{1,2} = \frac{z_1 y_1 + z_2 y_2 + (z_3 - 1)\, y_3}{z_1 x_1 + z_2 x_2 + (z_3 - 1)\, x_3}.$$

Its Cartesian equation is $y = m_{1,2}x + n_{1,2}$, where $n_{1,2}$ is computed by imposing that the line passes through V_3 to get

$$n_{1,2} = \frac{y_3\,(z_1 x_1 + z_2 y_2) - x_3\,(z_1 y_1 + z_2 y_2)}{z_1 x_1 + z_2 x_2 + (z_3 - 1)\, x_3}.$$

Since $R_{1,2} = \lambda_{1,2} V_1 + \lambda_{2,1} V_2$ can be written in Cartesian coordinates a

$$(\lambda_{1,2} x_1 + \lambda_{2,1} x_2, \lambda_{1,2} y_1 + \lambda_{2,1} y_2) = (\lambda_{1,2} x_1 + (1 - \lambda_{1,2})\, x_2, \lambda_{1,2} y_1 + (1 - \lambda_{1,2})\, y_2)\,,$$

it must be fulfilled that

$$m_{1,2}\,(\lambda_{1,2} x_1 + (1 - \lambda_{1,2})\, x_2) + n_{1,2} = \lambda_{1,2} y_1 + (1 - \lambda_{1,2})\, y_2.$$

A straightforward calculation gives

$$\lambda_{1,2} = \frac{z_1}{1 - z_{1,3}}.$$

We turn now to the sufficiency. By hypothesis, the barycentric coordinates of $R_{1,2}$ with respect to T are

$$(\lambda_{1,2}, \lambda_{2,1}, 0) = (1 - \lambda_{2,1}, \lambda_{2,1}, 0) = \left(\frac{1 - z_2 - z_3}{1 - z_3}, \frac{z_2}{1 - z_3}, 0 \right) = \left(\frac{z_1}{1 - z_3}, \frac{z_2}{1 - z_3}, 0 \right).$$

Then,

$$R_{1,2} = \frac{z_1}{1 - z_3} V_1 + \frac{z_2}{1 - z_3} V_2.$$

Moreover, $Z = z_1 V_1 + z_2 V_2 + z_3 V_3$. Taking into account the Cartesian coordinates of Z and the vertices, we get

$$R_{1,2} - Z = \frac{z_3}{1 - z_3}\,(z_1 x_1 + z_2 x_2 + (z_3 - 1)\, x_3, z_1 y_1 + z_2 y_2 + (z_3 - 1)\, y_3)\,.$$

Therefore, the slope of the straight line determined by Z and $R_{1,2}$ is equal to $m_{1,2}$. On the other hand, the straight line determined by Z and V_3 has the direction of vector

$$Z - V_3 = z_1 V_1 + z_2 V_2 + (z_3 - 1)\, V_3 = (z_1 x_1 + z_2 x_2 + (z_3 - 1)\, x_3, z_1 y_1 + z_2 y_2 + (z_3 - 1)\, y_3)\,,$$

so that its slope is also equal to $m_{1,2}$. Consequently, both the straight lines defined by $\{Z, R_{1,2}\}$ and $\{Z, V_3\}$ have the same slope and pass through the Z point, so V_3, Z and $R_{1,2}$ are collinear. □

The rest of this section is will divided into two parts. The first one deals with the case where Z is the barycenter, while the other situation is addressed in the second part.

4.2.1 Case where the inner split point is the barycenter

Let $\mathcal{C}_1$, $\mathcal{C}_2$ and $\mathcal{C}_3$ be the solutions of the following Hermite interpolation problems: for $i = 1, 2, 3$,

$$\mathcal{C}_i\,(V_j) = 0, \quad D_x\,\mathcal{C}_i\,(V_j) = \delta_{i,j}\beta_j, \quad D_y\,\mathcal{C}_i\,(V_j) = \delta_{i,j}\gamma_j,\ j = 1, 2, 3,$$

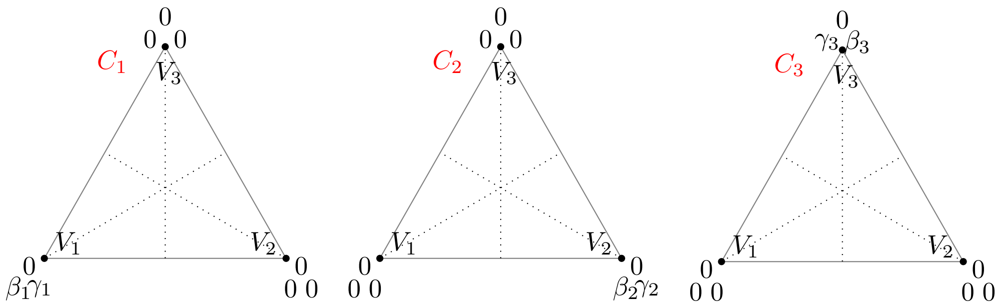

Figure 4.2: Functions $\mathcal{C}_i$ are uniquely determined by their values and their first-order partial derivatives at the vertices of the macro-triangle. For each of them, next to each vertex, the value at that vertex (top) and those of the first-order partial derivatives (from left to right) are arranged in a triangular structure.

where δ stands for the Kronecker delta function, $\beta_j := \beta_j(a_j)$ and $\gamma_j := \gamma_j(a_j)$ are defined as

$$\beta_1 := \frac{4a_1}{|T|}(2y_1 - y_2 - y_3), \qquad \beta_2 := \frac{4a_2}{|T|}(-y_1 + 2y_2 - y_3), \quad \beta_3 := \frac{4a_3}{|T|}(-y_1 - y_2 + 2y_3),$$

$$\gamma_1 := \frac{4a_1}{|T|}(-2x_1 + x_2 + x_3), \quad \gamma_2 := \frac{4a_2}{|T|}(x_1 - 2x_2 + x_3), \qquad \gamma_3 := \frac{4a_3}{|T|}(x_1 + x_2 - 2x_3),$$

$|T|$ stands for the area of T, and a_1, a_2 and a_3 are free parameters (see Fig. 4.2).

Note that function $\mathcal{C}_i$ depends on β_i and γ_i, hence on a_i, so that the notation $\mathcal{C}_{i,a_i}$ would be required. However, where there is no doubt, any reference to such dependence can be omitted.

These functions have been defined in order to extend a basis of the sub-space $\mathbb{P}_2$ of $S_2^1(T)$ to a basis of the whole space. More precisely, we have the following result.

Lemma 4.2.3. *Let T be a macro-triangle endowed with a C-refinement. Then,*

$$S_2^1(T) = \mathbb{P}_2 \bigoplus \operatorname{span}\{\mathcal{C}_1, \mathcal{C}_2, \mathcal{C}_3\}.$$

Proof. As functions $\mathcal{C}_i$ are in $S_2^1(T)$, it only remains to show that no non-trivial linear combination of those functions is in $\mathbb{P}_2$.

Assume that there exist non-zero real coefficients d_i such that

$$P := d_1\,\mathcal{C}_1 \,+\, d_2\,\mathcal{C}_2 \,+\, d_3\,\mathcal{C}_3 \,\in\, \mathbb{P}_2.$$

Then, in particular, P is of $\mathcal{C}^2$ continuity across $\langle Z, R_{1,2}\rangle$, $\langle Z, R_{2,3}\rangle$ and $\langle Z, R_{3,1}\rangle$, from which it follows that

$$2(a_1d_1 + a_2d_2) = 0, \quad 2(a_2d_2 + a_3d_3) = 0, \quad 2(a_1d_1 + a_3d_3) = 0.$$

Therefore $d_1 = d_2 = d_3 = 0$. The proof is complete. □

On each micro-triangle of T, the splines $\mathcal{C}_i$, $i = 1, 2, 3$, are quadratic polynomials that can written in terms of the corresponding Bernstein polynomials according to (1.1). The B-ordinates are schematically represented in Figure 4.3. Figure 4.4 shows typical plots of $\mathcal{C}_1$, $\mathcal{C}_2$ and $\mathcal{C}_3$, which are said to be *blending functions.*

$\mathcal{C}_1$ is a function depending of parameters β_1 and γ_1, which must be chosen so that $\int_T \mathcal{C}_1 = 0$, i.e.

$$\frac{6}{A(T)}\left(\frac{3}{2}\lambda_{2,1}z_3 + \frac{1}{2}\lambda_{1,2}z_3 - \frac{1}{2}\lambda_{1,3}z_2 + \frac{3}{2}\lambda_{3,1}z_2\right) = 0,$$

and also in such a way that $\mathcal{C}_1$ vanishes across $\langle V_1,\, Z\rangle$, $\langle V_2,\, Z\rangle$ and $\langle V_3,\, Z\rangle$. Similar constraints are needed to determine (β_2, γ_2) and (β_3, γ_3) for $\mathcal{C}_2$ and $\mathcal{C}_3$, respectively.

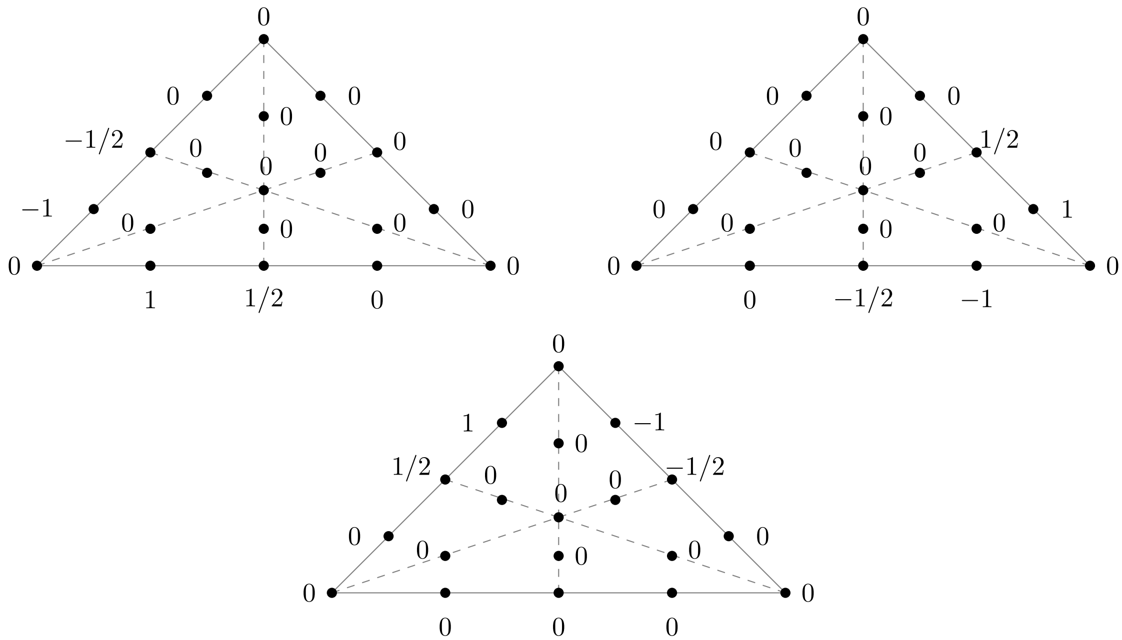

Figure 4.3: From left to right and from top to bottom, schematic representation of B-ordinates of $\mathcal{C}_{i,1}$, $i = 1, 2, 3$.

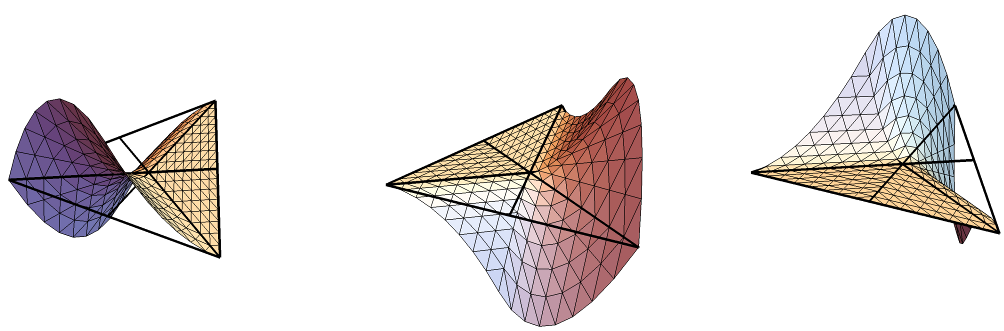

Figure 4.4: From left to right, the graphs of blending functions $\mathcal{C}_{1,1}$, $\mathcal{C}_{2,1}$ and $\mathcal{C}_{3,1}$.

4.2.2 Case where the inner split point is different from the barycenter

In this subsection, we address the general case, where the Z is not the barycenter, i.e. the barycentric coordinates (z_1, z_2, z_3) of Z are different from $(1/3, 1/3, 1/3)$. To this end, we shall use the blending functions $\mathcal{C}_i$, with appropriate parameters a_i, to build suitable blending functions in this case.

Definition 4.2.4. *When Z is not the barycenter, the modified blending functions $\mathcal{D}_i$ are defined as*

$$\mathcal{D}_1 = \mathcal{C}_{1,a_1^1} + \mathcal{C}_{3,a_3^1}, \qquad \mathcal{D}_2 = \mathcal{C}_{1,a_1^2} + \mathcal{C}_{2,a_2^2}, \qquad \mathcal{D}_3 = \mathcal{C}_{1,a_1^3} + \mathcal{C}_{2,a_2^3} + \mathcal{C}_{3,a_3^3}$$

where

$$\begin{aligned} a_1^1 &= (1 - z_2)\,(z_2 - z_1)\,, & a_3^1 &= z_2^2 - z_3^2, \\ a_1^2 &= \frac{(1 - z_2)\,(z_3 - z_1)}{z_3 - 1}, & a_2^2 &= z_2 - z_3, \\ a_1^3 &= (1 - z_2)\left(3 - \frac{1 - z_2}{1 - z_1} - \frac{z_2 + 1}{1 - z_3}\right), & a_2^3 &= a_3^3 = z_2 - z_3. \end{aligned}$$

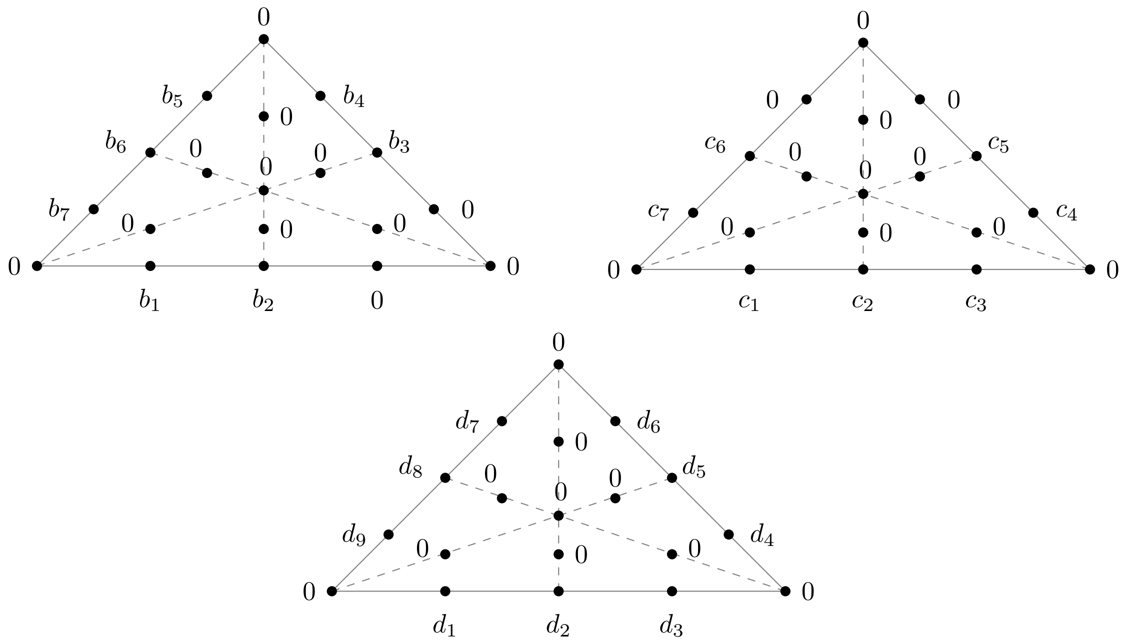

Figure 4.5: Schematic representation of B-ordinates of $\mathcal{D}_i$, $i = 1, 2, 3$.

Also $\mathcal{D}_1$, $\mathcal{D}_2$ and $\mathcal{D}_3$ can be represented on every micro-triangle of T from (1.1). Their non-zero B-ordinates b_ℓ, c_ℓ and d_ℓ, respectively, are schematically represented in Fig. 4.5 along with the remaining ones. The non-zero B-ordinates of $\mathcal{D}_1$ are

$$b_1 = (1-z_2)(z_2-z_1)\,,\ b_2 = \frac{z_1(1-z_2)(z_2-z_1)}{1-z_3},\ b_3 = \frac{(1-z_2)(z_3-z_2)z_3}{1-z_1},$$
$$b_4 = (1-z_2)(z_3-z_2)\,,\ b_5 = z_2^2 - z_3^2,\ b_6 = \frac{(z_3-z_1)(1-2z_2-z_1z_3)}{z_2-1},\ b_7 = (z_3-1)(z_2-z_1)\,.$$

Those of $\mathcal{D}_2$ are

$$c_1 = \frac{(1-z_2)(z_3-z_1)}{z_3-1},\ c_2 = \frac{(z_1-z_2)(1-z_1z_2-2z_3)}{(1-z_3)^2},\ c_3 = \frac{z_3^2-z_2^2}{1-z_3},\ c_4 = z_2 - z_3,$$
$$c_5 = \frac{z_2(z_2-z_3)}{1-z_1},\ c_6 = z_2 + \left(\frac{2z_3}{z_2-1}+3\right)z_3 - 1,\ c_7 = z_3 - z_1.$$

Finally, the non-zero BB-coefficients of $\mathcal{D}_3$ are

$$d_1 = (1-z_2)\left(3 - \frac{1-z_2}{1-z_1} - \frac{z_2+1}{1-z_3}\right),$$
$$d_2 = \frac{(z_1-z_2)\left(z_2^3 - 2z_2^2 + 3z_2 + (2z_2-3)z_3^2 + 3(z_2-1)^2 z_3 - 1\right)}{(1-z_3)^2(1-z_1)},$$
$$d_3 = \frac{z_3^2-z_2^2}{1-z_3},\ d_4 = z_2 - z_3,\ d_5 = \frac{(z_2-z_3)\left(z_2^2+(2z_2-1)z_3\right)}{(1-z_1)^2},\ d_6 = \frac{(1-z_2)(z_3-z_2)}{1-z_1},$$
$$d_7 = z_2 - z_3,\ d_8 = \frac{(z_3-z_1)\left(z_2^2+3(z_3-1)z_2+2(z_3-1)z_3+1\right)}{(z_2-1)(z_2+z_3)},\ d_9 = 2z_2 + 3z_3 + \frac{1-z_2^2}{1-z_1} - 3.$$

It is clear that the blending functions $\mathcal{D}_i$, $i = 1, 2, 3$, vanish across $\langle V_1, Z\rangle$, $\langle V_2, Z\rangle$ and $\langle V_3, Z\rangle$. Moreover, $\displaystyle\int_T \mathcal{D}_i = 0$.

Figure 4.6 shows typical plots of $\mathcal{D}_1$, $\mathcal{D}_2$ and $\mathcal{D}_3$.

From Lemma 4.2.3, the following result holds, whose proof is trivial.

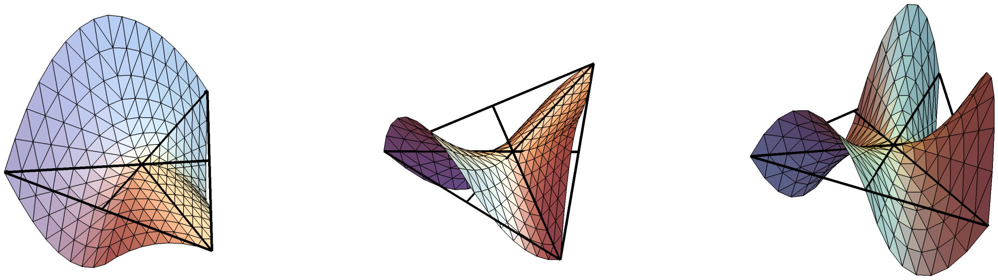

Figure 4.6: From left to right, the graphs of blending functions $\mathcal{D}_1$, $\mathcal{D}_2$ and $\mathcal{D}_3$.

Lemma 4.2.5. *Let T be a macro-triangle endowed with a C-refinement. Then,*

$$S_2^1(T) = \mathbb{P}_2 \bigoplus \operatorname{span}\{\mathcal{D}_1,\, \mathcal{D}_2,\, \mathcal{D}_3\}.$$

In this scenario, every spline $s \in S_2^1(T)$ will be expressed as follows:

$$s = p_2 + \sum_{i=1}^{3} \delta_i \mathcal{D}_i, \quad p_2 \in \mathbb{P}_2(T).$$

Since p_2 is a polynomial function, then, it can be written in Bernstein-Bézier representation (1.1):

$$p_2 = \pi_1 \mathfrak{B}_{(2,0,0),T} + \pi_2 \mathfrak{B}_{(0,2,0),T} + \pi_3 \mathfrak{B}_{(0,0,2),T} + \pi_4 \mathfrak{B}_{(1,1,0),T} + \pi_5 \mathfrak{B}_{(0,1,1),T} + \pi_6 \mathfrak{B}_{(1,0,1),T}.$$

Then $s(V_i) = f_i^{0,0}$, $i = 1, 2, 3$, if and only if $\pi_i = f_i^{0,0}$.
The remaining interpolation conditions in (4.1) are satisfied if and only if

$$\begin{pmatrix}
\frac{2(y_3-y_1)}{|T|} & 0 & \frac{2(y_1-y_2)}{|T|} & \beta_1\left(a_1^1\right) & 0 & \beta_3\left(a_3^1\right) \\
\frac{2(y_2-y_3)}{|T|} & \frac{2(y_1-y_2)}{|T|} & 0 & \beta_1\left(a_1^2\right) & \beta_2\left(a_2^2\right) & 0 \\
0 & \frac{2(y_3-y_1)}{|T|} & \frac{2(y_2-y_3)}{|T|} & \beta_1\left(a_1^3\right) & \beta_{2\left(a_2^3\right)} & \beta_3\left(a_3^3\right) \\
\frac{2(x_1-x_3)}{|T|} & 0 & \frac{2(x_2-x_1)}{|T|} & \gamma_1\left(a_1^1\right) & 0 & \gamma_3\left(a_3^1\right) \\
\frac{2(x_3-x_2)}{|T|} & \frac{2(x_2-x_1)}{|T|} & 0 & \gamma_1\left(a_1^2\right) & \gamma_2\left(a_2^2\right) & 0 \\
0 & \frac{2(x_1-x_3)}{|T|} & \frac{2(x_3-x_2)}{|T|} & \gamma_1\left(a_1^3\right) & \gamma_2\left(a_2^3\right) & \gamma_3\left(a_3^3\right)
\end{pmatrix}
\begin{pmatrix} \pi_4 \\ \pi_5 \\ \pi_6 \\ \delta_1 \\ \delta_2 \\ \delta_3 \end{pmatrix}$$

$$= \begin{pmatrix}
f_1^{1,0} - \frac{2(y_2-y_3)}{|T|} f_1^{0,0} \\
f_2^{1,0} - \frac{2(y_3-y_1)}{|T|} f_2^{0,0} \\
f_3^{1,0} - \frac{2(y_1-y_2)}{|T|} f_3^{0,0} \\
f_1^{0,1} - \frac{2(x_3-x_2)}{|T|} f_1^{0,0} \\
f_2^{0,1} - \frac{2(x_1-x_3)}{|T|} f_2^{0,0} \\
f_3^{0,1} - \frac{2(x_2-x_1)}{|T|} f_3^{0,0}
\end{pmatrix}.$$

4.3 Gaussian quadrature rules on a Powell-Sabin 6-split

A quadrature rule is referred to as an m-point rule when m evaluations of a function f are sufficient to approximate its weighted integral over a triangle T, and in this case

$$\int_T \omega\, f = \sum_{i=1}^{m} \omega_i\, f(t_i) + R_m(f) =: \mathcal{Q}\,[f]\,, \tag{4.3}$$

where ω and $R_m(f)$ are a fixed non-negative weight function defined over T and the error term of the rule, respectively. In particular, the error term is required to be zero for a predefined space $\mathcal{L}$, i.e., $R_m(f) = 0$ for all f in $\mathcal{L}$. Thus, if m is the minimal number of nodes t_i, we refer to the rule as a Gaussian quadrature rule.

In what follows we deal with Gaussian quadrature rules for the family of C^1 continuous splines on a C-refined macro-triangle T, having Z as triangle split point. As stated [65, 66, 67], there exists a quadrature rule

$$\mathcal{Q}\,[f] = \sum_{i=1}^{3} \omega_i\, f(t_i) \simeq \int_T \omega\, f \tag{4.4}$$

that is exact for each function f in $S_2^1\,(T)$.

Once again, we distinguish the two different cases: Z is the barycenter of T or different from it. We start by the first case, i.e., $z_1 = z_2 = z_3 = 1/3$. Each spline $s \in S_2^1\,(T)$ can be written as $s = p_2 + \sum_{i=1}^{3} c_i\,\mathcal{C}_i$. Then, the rule $\mathcal{Q}$ in (4.4) exact for quadratic polynomials is also exact for splines in $S_2^1\,(T)$ if and only if

$$\mathcal{Q}\left[\sum_{i=1}^{3} c_i\,\mathcal{C}_i\right] = 0 = \sum_{i=1}^{3} c_i \int_T \mathcal{C}_i.$$

Hammer-Stroud's micro/macro edge rules [67] are the best known quadrature rules exact for quadratic polynomials. Their weights and the barycentric coordinates of their nodes are given next:

$$\begin{aligned}
\mathcal{Q}^{\text{micro}}:&\quad t_1 = \left(\frac{2}{3}, \frac{1}{6}, \frac{1}{6}\right), \quad t_2 = \left(\frac{1}{6}, \frac{2}{3}, \frac{1}{6}\right), \quad t_3 = \left(\frac{1}{6}, \frac{1}{6}, \frac{2}{3}\right), \quad \omega_1 = \omega_2 = \omega_3 = 1/3,\\
\mathcal{Q}^{\text{macro}}:&\quad t_1 = \left(\frac{1}{2}, \frac{1}{2}, 0\right), \quad t_2 = \left(0, \frac{1}{2}, \frac{1}{2}\right), \quad t_3 = \left(\frac{1}{2}, 0, \frac{1}{2}\right), \quad \omega_1 = \omega_2 = \omega_3 = 1/3.
\end{aligned}$$

Theorem 4.3.1. *Let Z be the barycenter of a C-refined triangle T. Then, the quadrature rules $\mathcal{Q}^{micro}$ and $\mathcal{Q}^{macro}$ are exact on $S_2^1\,(T)$.*

Proof. Since

$$\mathcal{Q}^{\text{micro}}\,[\mathcal{C}_i] = \mathcal{Q}^{\text{macro}}\,[\mathcal{C}_i] = 0 = \int_T \mathcal{C}_i$$

for all blending function, the claim follows. □

We now move on to the more general case of an arbitrary inner split point. The use of Lemma 4.2.5 allows to deduce that any formula with nodes on the micro-edges joining the vertices of the C-refined triangle T to the point Z that exactly integrates the quadratic polynomials defined on T will also integrate the splines in $S_2^1\,(T)$. What are these Gaussian micro-edge quadrature formulae $\widetilde{\mathcal{Q}}$?

Given weights ω_ℓ, $\ell = 1, 2, 3$, and nodes written as

$$\tilde{t}_\ell := \xi_\ell V_\ell + (1 - \xi_\ell)\, Z,\ 0 < \xi_\ell < 1, \tag{4.5}$$

let us supppose that the quadrature formula

$$\widetilde{\mathcal{Q}}\,[f] = \sum_{\ell=1}^{3} \omega_\ell f\left(\widetilde{t}_\ell\right) \tag{4.6}$$

is exact on $\mathbb{P}_2\,(T)$. Then, by Lemma 4.2.5 and taking into account that for $i = 1, 2, 3$ it holds $\int_T \mathcal{D}_i \; = 0$ and $\mathcal{D}_i\left(\widetilde{t}_\ell\right) = 0$, $\ell = 1, 2, 3$, it is straightforward to conclude that (4.6) is also exact on $S_2^1\,(T)$. The weights ω_ℓ and coefficients ξ_ℓ that give rise to the nodes in (4.5) are determined by solving the 6×6 non-linear system

$$\widetilde{\mathcal{Q}}\,[\mathfrak{B}_{\beta,T}] = \int_T \mathfrak{B}_{\beta,T}\,, |\beta| = 2,$$

that express the exactness of $\widetilde{\mathcal{Q}}$ on $\mathbb{P}_2\,(T)$. It is solved numerically by means of the Newton-Raphson method starting from the values $\omega_1^0 = \omega_2^0 = \omega_3^0 = \dfrac{1}{3}$ and $\xi_1^0 = \xi_2^0 = \xi_3^0 = \dfrac{1}{2}$. Table 4.1 shows the results obtained for different choices of the split point.

(z_1, z_2, z_3)	ℓ	ξ_ℓ	w_ℓ
$(1/3, 1/4, 5/12)$	1	0.46446056322990814	0.36054364215704887
	2	0.4387496113528982	0.4761874546578383
	3	0.7716689650652734	0.16326890318511286
$(1/4, 1/3, 5/12)$	1	0.43874961135289886	0.4761874546578379
	2	0.4644605632299088	0.36054364215704865
	3	0.7716689650652715	0.16326890318511347
$(1/12, 12/17, 43/204)$	1	0.4395544547879028	0.4928765282876286
	2	0.00001901531735184312	−0.38429852259550384
	3	0.21527237814336092	0.8914219943078752
$(7/25, 8/25, 2/5)$	1	0.446539495674249	0.43359783418726155
	2	0.4661563118231906	0.3725344915619362
	3	0.68985609875553	0.1938676742508022

Table 4.1: For different split points, weights and parameters defining micro-edge nodes of Gaussian quadrature rules exact on $S_2^1\,(T)$.

Theorem 4.3.2. *Let Z be an arbitrary internal point of T and let $S_2^1\,(T)$ by the C-refinement of Tinduced by Z. Then, any polynomial micro-edge quadrature integrates exactly also $S_2^1\,(T)$.*

4.4 Conclusion

In this chapter, we have proved that any Gaussian quadrature formula exact on the space of quadratic polynomials defined on a triangle T endowed with a C-refinement integrates also the functions in the space of C^1 quadratic splines defined on T. This extend the results in [45], where the inner split point Z had to lie on a very specific subset of the T. Now Z can be freely chosen inside T.

Chapter 5

Explicit quasi-interpolating splines on 6-split

Following the idea used in [69], a new procedure was introduced in [71] and [73] based on the definition of the Bernstein-Bézier (BB-) coefficients of the spline on each triangle in the uniform partition. They are set directly from specific point values in a neighbourhood of the triangle so that C^1 continuity is achieved, in addition to the reproduction of the polynomials of a specific degree.

The aim of the method addressed in [73] is to construct C^1 quartic splines on a type-1 triangulation in such a way that the cubic polynomials are reproduced. Simple rules to produce the BB-coefficients of the quasi-interpolant on each triangle of the partition are provided. The values of the quasi-interpolated function at the domain points of order four relative each triangle of the triangulation are assumed to be known. For a triangle $T \langle v_1, v_2, v_3 \rangle$ with barycentric coordinates $(\lambda_1, \lambda_2, \lambda_3)$, they are of the form $\dfrac{1}{3}\left(iv_1 + jv_2 + kv_3\right)$,with i, j, k non negative integers such that $i + j + k = 3$. The splines obtained from these rules interpolate the point values at vertices.

In [75] a general study of this problem is carried out in order to determine all possible rules for defining BB-coefficients giving C^1 continuity and exactness on the space of polynomials of total degree equal to three. It is shown that there exists a multi-parametric family of rules, having nineteen degrees of freedom, and then the reduction of the number of evaluations needed to compute the BB-coefficients is addressed. Moreover, it is proved that there exists a family of rules based on evaluation at vertices and midpoints of edges of triangles depending on only three parameters. The resulting quasi-interpolating splines also interpolate the point values at vertices. Both in [73] and [75] the used rules have symmetries, so the computational cost is reduced.

A similar methodology is used in [76] to construct C^1 cubic quasi-interpolants that reproduce quadratic polynomials when the values at the vertices and midpoints are known. In this case, quasi-interpolants do not interpolate the data values at vertices. Moreover, different rules correspond to different domain points. There are no symmetries applicable. However, there exists only one solution, i.e. a set of rules that allow the objectives to be met: C^1 continuity and reproduction of the quadratic polynomials.

It would be natural, therefore, to construct C^1 quadratic quasi-interpolants in the same way, reproducing polynomials of degree 1 at most, but this is not possible. Only constants can be reproduced. Consequently, we propose to construct quadratic quasi-interpolants on a type 1 triangulation endowed with a Powell-Sabin refinement [**?**] to achieve the optimal approximation order.

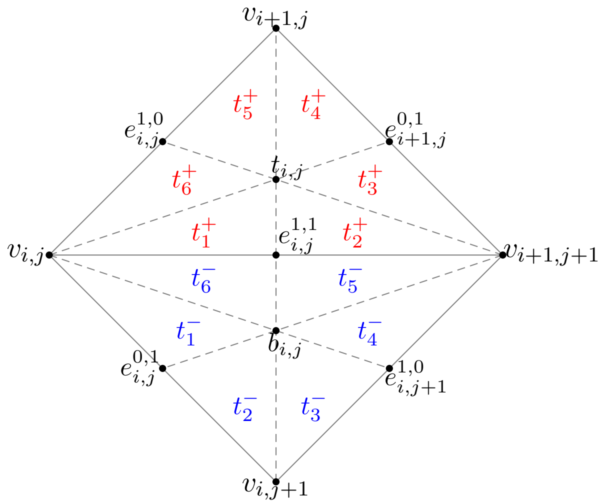

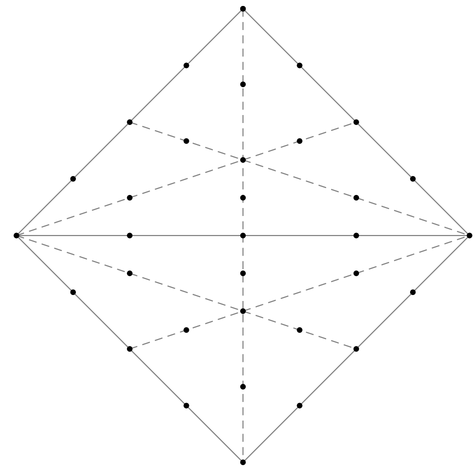

Figure 5.1: 6-split of $T_{i,j}$ and $B_{i,j}$ (left) and domain points associated with the quadratic polynomials on the micro-triangles (right).

5.1 Bernstein-Bézier form of quadratic splines on type-I triangulation

For $h > 0$, the vectors $e_1 := (h, h)$ and $e_2 := (h, -h)$ define the lattice $\mathcal{V} = \{v_{i,j}, i, j \in \mathbb{Z}\}$, where $v_{i,j} := ie_1 + je_2$. These vertices define the faces of the lattice, that can be decomposed into the triangles $T_{i,j}\ \langle v_{i,j}, v_{i+1,j+1}, v_{i+1,j}\rangle$ and $B_{i,j}\ \langle v_{i,j}, v_{i+1,j+1}, v_{i,j+1}\rangle$, so that a type-1 triangulation is obtained, namely $\Delta := \bigcup_{i,j\in\mathbb{Z}} (T_{i,j} \cup B_{i,j})$. In general, these triangles will be referred to as macro-triangles and any one of them will be represented by the capital letter T, without specifying what type it is.

Let $\mathcal{E}$ be the set of edges in Δ and consider the barycenters $t_{i,j} := \frac{1}{3}(v_{i,j} + v_{i+1,j+1} + v_{i+1,j})$ and $b_{i,j} := \frac{1}{3}(v_{i,j} + v_{i+1,j+1} + v_{i,j+1})$ of $T_{i,j}$ and $B_{i,j}$, respectively. Let Δ_{PS} denote the Powell-Sabin (6-) split of Δ obtained in joining the opposite vertices of every two macro-triangles sharing an edge. Edge split points result, which are the mid-point of the edges in $\mathcal{E}$. More specifically, those corresponding to the three edges emanating from the vertex with directions e_1, e_2 and $e_3 := e_1 + e_2$ can be written as $e_{i,j}^{k,\ell} := \frac{1}{2}(v_{i,j} + v_{i+k,j+\ell})$, with $k, \ell \in \{0, 1\}$ and $k + \ell \neq 0$ [18].

Each one of the macro-triangles is divided into the six small triangles: for $T_{i,j}$ they are

$$\begin{aligned}
t_1^+ &= \left\langle v_{i,j},\, e_{i,j}^{1,1},\, t_{i,j}\right\rangle, & t_2^+ &= \left\langle e_{i,j}^{1,1},\, v_{i+1,j+1},\, t_{i,j}\right\rangle, & t_3^+ &= \left\langle v_{i+1,j+1},\, e_{i+1,j}^{0,1},\, t_{i,j}\right\rangle,\\
t_4^+ &= \left\langle e_{i+1,j}^{0,1},\, v_{i+1,j},\, t_{i,j}\right\rangle, & t_5^+ &= \left\langle v_{i+1,j},\, e_{i,j}^{1,0},\, t_{i,j}\right\rangle, & t_6^+ &= \left\langle e_{i,j}^{1,0},\, v_{i,j},\, t_{i,j}\right\rangle,
\end{aligned}$$

and

$$\begin{aligned}
t_1^- &= \left\langle v_{i,j},\, e_{i,j}^{0,1},\, b_{i,j}\right\rangle, & t_2^- &= \left\langle e_{i,j}^{0,1},\, v_{i,j+1},\, b_{i,j}\right\rangle, & t_3^- &= \left\langle v_{i,j+1},\, e_{i,j+1}^{1,0},\, b_{i,j}\right\rangle,\\
t_4^- &= \left\langle e_{i,j+1}^{1,0},\, v_{i+1,j+1},\, b_{i,j}\right\rangle, & t_5^- &= \left\langle v_{i+1,j+1},\, e_{i,j}^{1,1}, b_{i,j}\right\rangle, & t_6^- &= \left\langle e_{i,j}^{1,1},\, v_{i,j},\, b_{i,j}\right\rangle,
\end{aligned}$$

for $B_{i,j}$. They are shown in Figure 5.1(left). In general, the lower case letter t will be used to represent any of the micro-triangles of Δ_{PS}. To lighten the notation, any reference to the subscripts of the macro-triangle has been avoided.

For every vertex $v_{i,j} \in \mathcal{V}$ there are twelve edges emanating from $v_{i,j}$ in six independent directions, so that Δ_{PS} can be considered as a six directional triangulation.

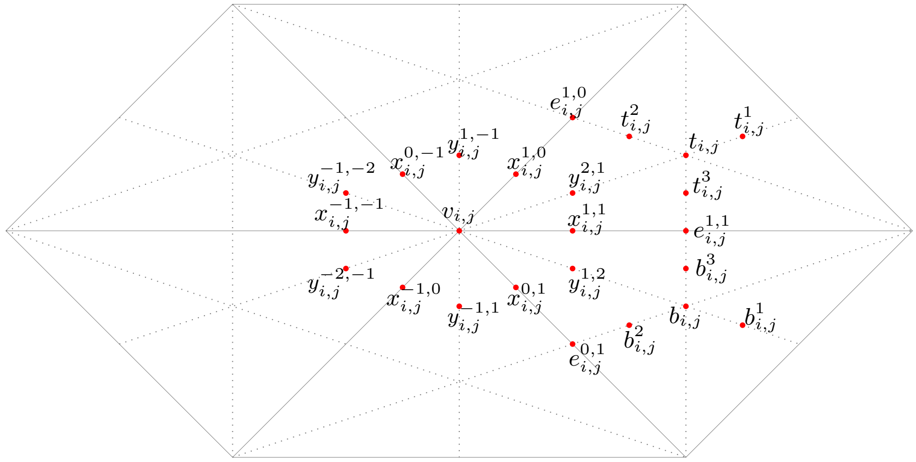

Figure 5.2: Domain points forming the subset $D_{i,j}$ corresponding to $v_{i,j}$.

In this chapter, we consider the space of C^1 quadratic splines on Δ_{PS} defined by

$$S_2^1(\Delta_{\mathrm{PS}}) := \left\{ s \in C^1\left(\mathbb{R}^2\right) : s_{|t} \in \mathbb{P}_2 \quad \text{for all } t \in \Delta_{\mathrm{PS}} \right\},$$

where $\mathbb{P}_2$ denotes the linear space of quadratic polynomials. Since the restriction $p = s_{|t}$ of $s \in S_2^1(\Delta_{\mathrm{PS}})$ to a triangle $t\langle V_1, V_2, V_3\rangle \in \Delta_{\mathrm{PS}}$ is a quadratic polynomial function, it can be represented using the quadratic Bernstein polynomials defined on t. Using the multi-index notations $\beta := (\beta_1, \beta_2, \beta_3) \in \mathbb{N}_0^3$, $|\beta| := \beta_1 + \beta_2 + \beta_3$, and $\beta! := \beta_1!\beta_2!\beta_3!$, at any point $P \in t$ they are given by

$$\mathfrak{B}_{\beta,t}(P) := \frac{2}{\beta!}\tau^\beta = \frac{2}{\beta_1!\beta_2!\beta_3!}\tau_1^{\beta_1}\tau_2^{\beta_2}\tau_3^{\beta_3},$$

where the triplet (τ_1, τ_2, τ_3) provides the barycentric coordinates of P with respect to t, that is to say, the conditions $P = \sum_{i=1}^{3} \tau_i V_i$ and $\sum_{i=1}^{3} \tau_i = 1$ are satisfied. The coordinates τ_1, τ_2 and τ_3 are non-negative whenever P belongs to t.

Every polynomial $p \in \mathbb{P}_2$ can be expressed in terms of the quadratic Bernstein polynomials $\mathfrak{B}_{\beta,t}$, $|\beta| = 2$, i.e. there exist values $b_{\beta,t}$ such that

$$p(x, y) = p(\tau) = \sum_{|\beta|=2} b_{\beta,t}\, \mathfrak{B}_{\beta,t}(\tau).$$

They are called Bézier (B-) ordinates or Bernstein-Bézier (BB-) coefficients of p, and are naturally linked to the domain points $\xi_{\beta,t}$ determined by the barycentric coordinates $\left(\frac{\beta_1}{2}, \frac{\beta_2}{2}, \frac{\beta_3}{2}\right)$ with respect to t.

On each micro-triangle, an element $s \in S_2^1(\Delta_{\mathrm{PS}})$ is uniquely determined by six BB-coefficients, associated with the corresponding domain points. Figure 5.1(right) shows the domain points lying in the micro-triangles of two macro-triangles sharing an edge. When all macro-triangles are taken into account, a subset of domain points is obtained, which we will note $\mathcal{D}$. To determine s, it is necessary to give the BB-coefficients associated with all the points of $\mathcal{D}$. As the triangulation is uniform, following the approach in [72, 73, 75, 77], it is sufficient to establish a partition $\{D_{i,j}, i, j \in \mathbb{Z}\}$ of $\mathcal{D}$ and provide the BB-coefficients linked to the domain points in $D_{i,j}$. Figure 5.2 shows the proposed subset $D_{i,j}$. It is associated to the vertex $v_{i,j}$, so all its points adopt the subscripts of $v_{i,j}$.

Figure 5.3 shows the domain points lying in the hexagon $H_{i,j}$ determined by the triangles sharing the vertex $v_{i,j}$. Each of them is associated with one of the vertices in $H_{i,j}$, and shows its subscripts.

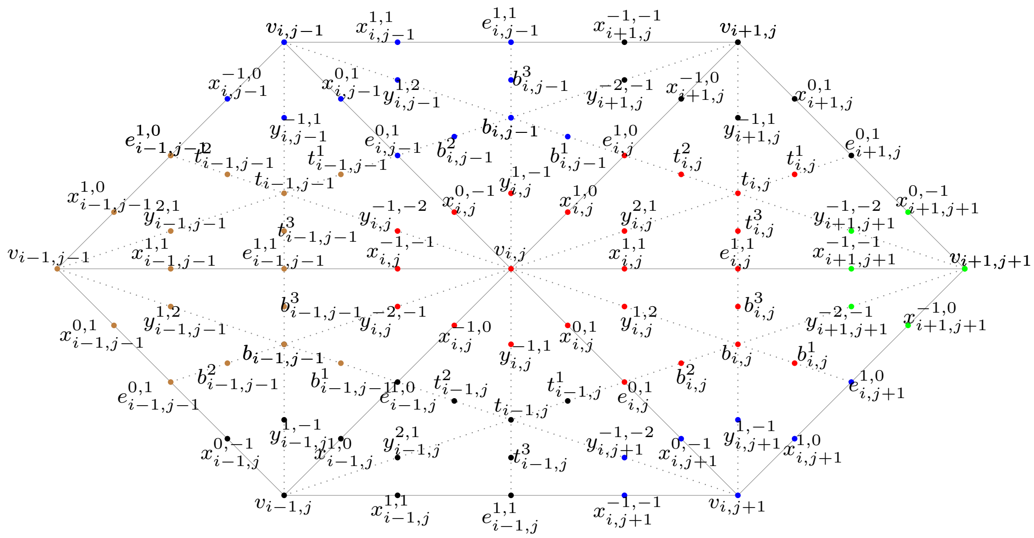

Figure 5.3: BB-coefficientes in the $H_{i,j}$, which are linked to $v_{i,j}$ and to the six vertices determining the hexagon.

5.2 Quasi-interpolation from point values at vertices and middle points

Here we aim to construct a quasi-interpolation operator $\mathcal{Q} : C\left(\mathbb{R}^2\right) \longrightarrow S_2^1\left(\Delta_{\mathrm{PS}}\right)$ exact on $\mathbb{P}_2$, that is to say, such that $\mathcal{Q}f = f$ for all $f \in \mathbb{P}_2$. The quasi-interpolant $\mathcal{Q}f \in S_2^1\left(\Delta_{\mathrm{PS}}\right)$ of f will be defined from the values of f at the vertices and the midpoints of the edges by directly setting its BB-coefficients for all micro-triangles, and then the values at these points are supposed to be known.

The restriction of $\mathcal{Q}f$ to any micro-triangle t will be a linear combination of the Bernstein polynomials $\mathfrak{B}_{\beta,t}$ with B-ordinates depending on the values of f at the vertices and mid-points in a neighbourhood of t. For instance, for the micro-triangle t_1^+ of $T_{i,j}$, we have

$$\begin{aligned}\mathcal{Q}f_{|t_1^+} &= c\left(v_{i,j}\right)\mathfrak{B}_{(2,0,0),t_1^+} + c\left(x_{i,j}^{1,1}\right)\mathfrak{B}_{(1,1,0),t_1^+} + c\left(y_{i,j}^{2,1}\right)\mathfrak{B}_{(1,0,1),t_1^+}\\ &\quad + c\left(e_{i,j}^{1,1}\right)\mathfrak{B}_{(0,2,0),t_1^+} + c\left(t_{i,j}^{3}\right)\mathfrak{B}_{(0,1,1),t_1^+} + c\left(t_{i,j}\right)\mathfrak{B}_{(0,0,2),t_1^+},\end{aligned}$$

where $c(p)$ stands for the B-ordinate associated with the domain point p (see Figure 5.4). Similar expressions are obtained for the restrictions of $\mathcal{Q}f$ to the other five micro-triangles of $T_{i,j}$ and to those of $B_{i,j}$.

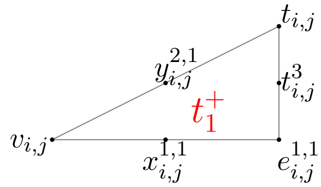

Figure 5.4: The micro-triangle t_1^+ of $T_{i,j}$ and associated domain points.

To define the BB-coefficients involved in the definition of $\mathcal{Q}f$, let $\Xi_{i,j}$ the subset of $\mathbb{R}^2$ formed

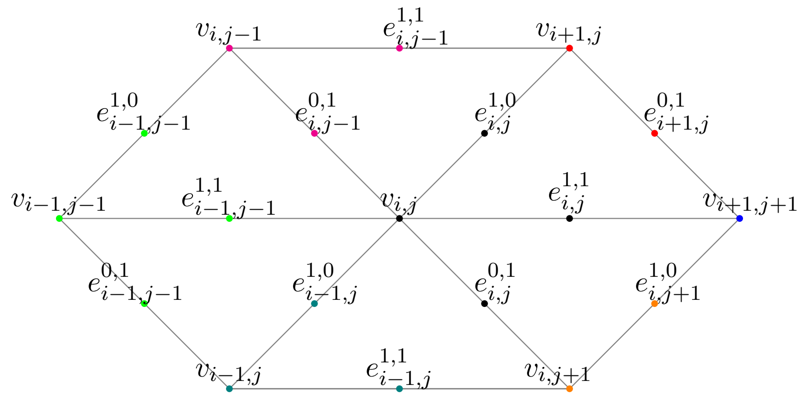

Figure 5.5: The subset $\Xi_{i,j}$. The values of f at the domain points in $\Xi_{i,j}$ are used to determine the BB-coefficients of the restrictions of $\mathcal{Q}f$ to the micro-triangles in Δ_{PS}.

by the vertices and midpoints that are in the hexagon $H_{i,j}$, i.e.

$$\begin{aligned}\Xi_{i,j} := \Big\{ & v_{i,j}, e^{1,1}_{i,j}, e^{1,0}_{i,j}, e^{0,1}_{i,j-1}, e^{1,1}_{i-1,j-1}, e^{1,0}_{i-1,j}, e^{0,1}_{i,j}, v_{i+1,j+1}, e^{0,1}_{i+1,j}, v_{i+1,j} \\ & e^{1,1}_{i,j-1}, v_{i,j-1}, e^{1,0}_{i-1,j-1}, v_{i-1,j-1}, e^{0,1}_{i-1,j-1}, v_{i-1,j}, e^{1,1}_{i-1,j}, v_{i,j+1}, e^{1,0}_{i,j+1} \Big\}.\end{aligned}$$

It is shown in Figure 5.5. The definition of $\Xi_{i,j}$ shows the ordering of its points. Firstly, the vertex, then the midpoints around the vertex and finally the twelve remaining points.

The BB-coefficient $c\,(p)$ of a domain point p will be a linear combination of values of f at these nineteen points. The coefficients form the mask $\mathcal{M}\,(p)$. It is ordered in the same way as $\Xi_{i,j}$. Therefore,

$$c(p) = M\,(p) \cdot f\,(\Xi_{i,j}) = \sum_{\ell=1}^{19} M\,(p)_\ell\, f\,(\Xi_{i,j})_\ell\,,$$

where $M\,(p)_\ell$ and $f\,(\Xi_{i,j})_\ell$ denote the ℓ-th entries of $M\,(p)$ and $f\,(\Xi_{i,j})$, respectively. Note that $f\,(\Xi_{i,j}) := \{f\,(p) : p \in \Xi_{i,j}\}$.

To define the quasi-interpolant $\mathcal{Q}f$ it is necessary to use masks which produce functions of class C^1 and which give rise to operators exact on $\mathbb{P}_2$.

Definition 5.2.1. *To determine the B-ordinate of $\mathcal{Q}f$ associated with a domain point, identify the set $D_{i,j}$ to which it belongs. Then,*

1. *Apply*

$$M\,(v_{i,j}) = \left(\frac{1}{2}, 0, 0, \frac{2}{3}, -\frac{2}{3}, \frac{2}{3}, 0, 0, 0, 0, 0, -\frac{1}{6}, 0, \frac{1}{6}, 0, -\frac{1}{6}, 0, 0, 0\right)$$

for vertex $v_{i,j}$.

2. *For $x-$points, apply the following masks:*

$$M\left(x_{i,j}^{1,1}\right)=\left(1,0,0,1,-2,1,0,0,0,0,0,-\frac{1}{4},0,\frac{1}{2},0,-\frac{1}{4},0,0,0\right),$$

$$M\left(x_{i,j}^{-1,-1}\right)=\left(0,0,0,\frac{1}{3},\frac{2}{3},\frac{1}{3},0,0,0,0,0,-\frac{1}{12},0,-\frac{1}{6},0,-\frac{1}{12},0,0,0\right),$$

$$M\left(x_{i,j}^{1,0}\right)=\left(\frac{3}{4},0,0,\frac{4}{3},-\frac{4}{3},\frac{1}{3},0,0,0,0,0,-\frac{1}{3},0,\frac{1}{3},0,-\frac{1}{12},0,0,0\right),$$

$$M\left(x_{i,j}^{0,-1}\right)=\left(\frac{1}{4},0,0,1,0,0,0,0,0,0,0,-\frac{1}{4},0,0,0,0,0,0,0\right),$$

$$M\left(x_{i,j}^{-1,0}\right)=\left(\frac{1}{4},0,0,0,0,1,0,0,0,0,0,0,0,0,0,-\frac{1}{4},0,0,0\right),$$

$$M\left(x_{i,j}^{0,1}\right)=\left(\frac{3}{4},0,0,\frac{1}{3},-\frac{4}{3},\frac{4}{3},0,0,0,0,0,-\frac{1}{12},0,\frac{1}{3},0,-\frac{1}{3},0,0,0\right).$$

3. *For $y-$points, use the following masks:*

$$M\left(y_{i,j}^{1,-1}\right)=\left(\frac{1}{2},0,0,\frac{4}{3},-\frac{2}{3},0,0,0,0,0,0,-\frac{1}{3},0,\frac{1}{6},0,0,0,0,0\right),$$

$$M\left(y_{i,j}^{-1,1}\right)=\left(\frac{1}{2},0,0,0,-\frac{2}{3},\frac{4}{3},0,0,0,0,0,0,0,\frac{1}{6},0,-\frac{1}{3},0,0,0\right),$$

$$M\left(y_{i,j}^{2,1}\right)=\left(1,0,0,\frac{4}{3},-2,\frac{2}{3},0,0,0,0,0,-\frac{1}{3},0,\frac{1}{2},0,-\frac{1}{6},0,0,0\right),$$

$$M\left(y_{i,j}^{-1,-2}\right)=\left(0,0,0,\frac{2}{3},\frac{2}{3},0,0,0,0,0,0,-\frac{1}{6},0,-\frac{1}{6},0,0,0,0,0\right),$$

$$M\left(y_{i,j}^{-2,-1}\right)=\left(0,0,0,0,\frac{2}{3},\frac{2}{3},0,0,0,0,0,0,0,-\frac{1}{6},0,-\frac{1}{6},0,0,0\right),$$

$$M\left(y_{i,j}^{1,2}\right)=\left(1,0,0,\frac{2}{3},-2,\frac{4}{3},0,0,0,0,0,-\frac{1}{6},0,\frac{1}{2},0,-\frac{1}{3},0,0,0\right).$$

4. *For midpoints, apply the masks*

$$M\left(e_{i,j}^{1,1}\right)=\left(\frac{5}{12},\frac{1}{3},0,\frac{1}{2},-1,\frac{1}{2},0,0,\frac{1}{6},-\frac{1}{24},0,-\frac{1}{8},0,\frac{1}{4},0,-\frac{1}{8},0,-\frac{1}{24},\frac{1}{6}\right),$$

$$M\left(e_{i,j}^{1,0}\right)=\left(\frac{1}{4},0,\frac{1}{2},\frac{2}{3},-\frac{2}{3},\frac{1}{6},0,0,0,\frac{1}{8},0,-\frac{1}{6},0,\frac{1}{6},0,-\frac{1}{24},0,0,0\right),$$

$$M\left(e_{i,j}^{0,1}\right)=\left(\frac{1}{4},0,0,\frac{1}{6},-\frac{2}{3},\frac{2}{3},\frac{1}{2},0,0,0,0,-\frac{1}{24},0,\frac{1}{6},0,-\frac{1}{6},0,\frac{1}{8},0\right),$$

5. *For the barycenters, apply the masks*

$$M\left(t_{i,j}\right)=\left(\frac{1}{6},\frac{2}{9},\frac{4}{9},\frac{4}{9},-\frac{2}{3},\frac{2}{9},0,0,\frac{2}{9},\frac{1}{9},-\frac{2}{9},-\frac{1}{18},0,\frac{1}{6},0,-\frac{1}{18},0,0,0\right)$$

and

$$M\left(b_{i,j}\right)=\left(\frac{1}{6},\frac{2}{9},0,\frac{2}{9},-\frac{2}{3},\frac{4}{9},\frac{4}{9},0,0,0,0,-\frac{1}{18},0,\frac{1}{6},0,-\frac{1}{18},-\frac{2}{9},\frac{1}{9},\frac{2}{9}\right).$$

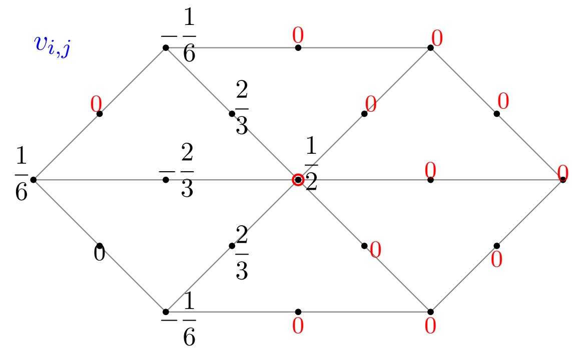

Figure 5.6: Mask v.

6. Use the masks

$$M\left(t^1_{i,j}\right) = \left(\frac{1}{6}, 0, 0, 0, -\frac{1}{3}, \frac{2}{3}, \frac{1}{3}, 0, 0, 0, 0, 0, 0, \frac{1}{12}, 0, -\frac{1}{4}, \frac{1}{3}, 0, 0\right),$$
$$M\left(t^2_{i,j}\right) = \left(\frac{1}{3}, 0, \frac{2}{3}, \frac{2}{3}, -1, \frac{1}{3}, 0, 0, 0, \frac{1}{4}, -\frac{1}{3}, -\frac{1}{12}, 0, \frac{1}{4}, 0, -\frac{1}{12}, 0, 0, 0\right),$$
$$M\left(t^3_{i,j}\right) = \left(\frac{5}{12}, \frac{1}{3}, 0, \frac{2}{3}, -1, \frac{1}{3}, 0, 0, \frac{1}{3}, -\frac{1}{12}, 0, -\frac{1}{6}, 0, \frac{1}{4}, 0, -\frac{1}{12}, 0, 0, 0\right),$$

for the domain points around $t_{i,j}$, and

$$M\left(b^1_{i,j}\right) = \left(\frac{1}{6}, 0, \frac{1}{3}, \frac{2}{3}, -\frac{1}{3}, 0, 0, 0, 0, 0, 0, \frac{1}{3}, -\frac{1}{4}, 0, \frac{1}{12}, 0, 0, 0, 0, 0\right),$$
$$M\left(b^2_{i,j}\right) = \left(\frac{1}{3}, 0, 0, \frac{1}{3}, -1, \frac{2}{3}, \frac{2}{3}, 0, 0, 0, 0, -\frac{1}{12}, 0, \frac{1}{4}, 0, -\frac{1}{12}, -\frac{1}{3}, \frac{1}{4}, 0\right),$$
$$M\left(b^3_{i,j}\right) = \left(\frac{5}{12}, \frac{1}{3}, 0, \frac{1}{3}, -1, \frac{2}{3}, 0, 0, 0, 0, 0, -\frac{1}{12}, 0, \frac{1}{4}, 0, -\frac{1}{6}, 0, -\frac{1}{12}, \frac{1}{3}\right),$$

for those around $b_{i,j}$.

Figure 5.6 shows the mask relative to vertex $v_{i,j}$. Note that the B-ordinate $c\,(v_{i,j})$ can be easily computed from the values of f at seven domain points in $H_{i,j}$:

$$c\,(v_{i,j}) = \frac{1}{6}\left(3f\,(v_{i,j}) - f\,(v_{i,j-1}) + f\,(v_{i-1,j-1}) - f\,(v_{i-1,j})\right) + \frac{2}{3}\left(f\left(e^{0,1}_{i,j-1}\right) - f\left(e^{1,1}_{i-1,j-1}\right) + f\left(e^{1,0}_{i-1,j}\right)\right).$$

In Figure 5.7 the masks corresponding to mid-points $e^{1,1}_{i,j}$ and $e^{1,0}_{i,j}$ are shown. The one corresponding to $e^{0,1}_{i,j}$ is the symmetrical of $M\left(e^{1,0}_{i,j}\right)$ with respect to the segment $[v_{i-1,j-1}, v_{i+1,j+1}]$.

This characteristic of the mid-point masks is also true for the x- and y-points. The hexagonal representations of $M\left(x^{1,0}_{i,j}\right)$ and $M\left(x^{-1,0}_{i,j}\right)$ show that they produce by symmetry those of $M\left(x^{0,1}_{i,j}\right)$ and $M\left(x^{0,-1}_{i,j}\right)$, respectively. No symmetries are involved in the case of $M\left(x^{1,1}_{i,j}\right)$ and $M\left(x^{-1,-1}_{i,j}\right)$. Moreover, no more than seven point evaluations are needed to compute the correspondig BB-coefficients. The case of the y-point masks is slightly different, since they are pairwise related by symmetry: $M\left(y^{-1,1}_{i,j}\right)$, $M\left(y^{-1,-2}_{i,j}\right)$ and $M\left(y^{2,1}_{i,j}\right)$ are obtained by symmetry from $M\left(y^{1,-1}_{i,j}\right)$, $M\left(y^{-2,-1}_{i,j}\right)$ and $M\left(y^{1,2}_{i,j}\right)$, respectively. Also in this case, the B-ordinates are computed from a maximum of seven point evaluations.

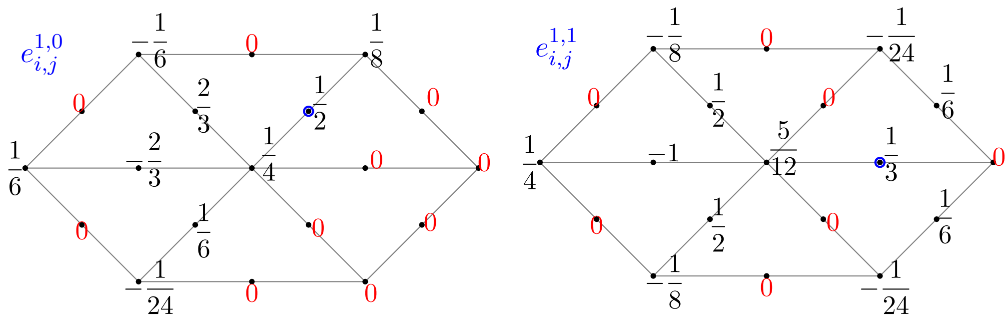

Figure 5.7: Mask e.

Finally, as regards the masks related to the t- and b-points, it should be noted that the latter are obtained from those of the t-points by symmetry with respect to $[v_{i-1,j-1}, v_{i+1,j+1}]$.

Once the masks have been defined, the smoothness and exactness of the quasi-interpolant defined from them must be proved.

Theorem 5.2.2. *The quasi-interpolating spline $\mathcal{Q}f$ is C^1 continuous.*

Proof. There are three types of edges in Δ_{PS}: edges that connect vertices with triangle split points, edges that connect triangle split points and edge split points and edges that connect vertices with edge split points. Therefore, we need to check the C^1 conditions across one edge of each kind.

Consider, for instance, the edge $\langle v_{i,j},\, b_{i,j}\rangle$ in the micro-triangle t_6^- of $B_{i,j}$. The C^1 conditions across this edge are

$$c\left(x_{i,j}^{1,0}\right)+c\left(x_{i,j}^{1,1}\right)-\frac{3}{2}c\left(y_{i,j}^{2,1}\right)-\frac{1}{2}c\left(v_{i,j}\right)=0 \quad \text{and} \quad c\left(t_{i,j}^{2}\right)+c\left(t_{i,j}^{3}\right)-\frac{3}{2}c\left(t_{i,j}\right)-\frac{1}{2}c\left(y_{i,j}^{2,1}\right)=0.$$

Regarding the remaining two types, they are $\left\langle b_{i,j},\, e_{i,j}^{1,1}\right\rangle$ are $\left\langle v_{i,j},\, e_{i,j}^{1,1}\right\rangle$. The C^1 conditions across them are

$$c\left(x_{i,j}^{1,1}\right)+c\left(x_{i+1,j+1}^{-1,-1}\right)-2c\left(e_{i,j}^{1,1}\right)=0, \qquad c\left(y_{i,j}^{2,1}\right)+c\left(y_{i+1,j+1}^{-1,-2}\right)-2c\left(t_{i,j}^{3}\right)=0,$$

and

$$c\left(y_{i,j}^{2,1}\right)+c\left(y_{i,j}^{1,2}\right)-2c\left(x_{i,j}^{1,1}\right)=0, \qquad c\left(t_{i,j}^{3}\right)+c\left(b_{i,j}^{3}\right)-2c\left(e_{i,j}^{1,1}\right)=0,$$

respectively. Direct substitution of the involved B-ordinates into the above conditions proves they are fulfilled. C^1 through the remaining micro-edges is proved in an analogous way. □

The next result states that the quasi-interpolation operator $\mathcal{Q}$ reproduces the linear space of quadratic polynomials.

Lemma 5.2.3. *For any $p \in \mathbb{P}_2$, it is satisfied that $\mathcal{Q}p = p$.*

Proof. It suffices to prove that $\mathcal{Q}\mathfrak{B}_{\beta,t} = \mathfrak{B}_{\beta,t}$, $|\beta| = 2$, for all micro-triangle in Δ_{PS}. We will give the proof only for $\beta = (2,0,0)$ and the micro-triangle t_1^+ of $T_{i,j}$. The results in the other cases are similarly proved.

The B-ordinates of $\mathfrak{B}_{(2,0,0),t_1^+}$ on t_1^+ are shown in Figure 5.8.

To compute the B-ordinates of $\mathcal{Q}\mathfrak{B}_{(2,0,0),t_1^+}$ on t_1^+, the values of $\mathfrak{B}_{(2,0,0),t_1^+}$ at the domain points in $\Xi_{i,j}$ are needed. They are listed below:

$$(1, 1/4, 1/4, 1, 9/4, 9/4, 1, 0, 0, 0, 1/4, 1, 9/4, 4, 4, 4, 9/4, 1, 1/4)\,.$$

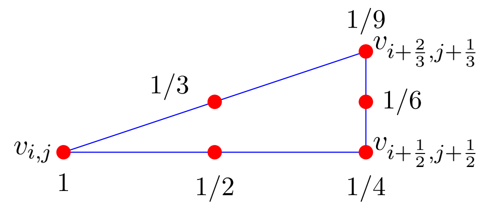

Figure 5.8: B-ordinates corresponding to the Bernstein polynomial $\mathfrak{B}_{\beta,t_1^+}$ relative to the micro-triangle t_1^+ of $T_{i,j}$.

The domain points relative to t_1^+ are $v_{i,j}$, $x_{i,j}^{1,1}$, $e_{i,j}^{1,1}$, $t_{i,j}^3$, $t_{i,j}$ and $y_{i,j}^{2,1}$, and their B-ordinates are easily computed from the masks given in Definition 5.2.1. The following results are obtained:

$$\begin{aligned}
c\left(v_{i,j}\right) &= M\left(v_{i,j}\right)\cdot\mathfrak{B}_{(2,0,0),t_1^+}\left(\Xi_{i,j}\right)=1, & c\left(x_{i,j}^{1,1}\right) &= M\left(x_{i,j}^{1,1}\right)\cdot\mathfrak{B}_{(2,0,0),t_1^+}\left(\Xi_{i,j}\right)=\frac{1}{2},\\
c\left(e_{i,j}^{1,1}\right) &= M\left(e_{i,j}^{1,1}\right)\cdot\mathfrak{B}_{(2,0,0),t_1^+}\left(\Xi_{i,j}\right)=\frac{1}{4}, & c\left(t_{i,j}^{3}\right) &= M\left(t_{i,j}^{3}\right)\cdot\mathfrak{B}_{(2,0,0),t_1^+}\left(\Xi_{i,j}\right)=\frac{1}{6},\\
c\left(t_{i,j}\right) &= M\left(t_{i,j}\right)\cdot\mathfrak{B}_{(2,0,0),t_1^+}\left(\Xi_{i,j}\right)=\frac{1}{9}, & c\left(y_{i,j}^{2,1}\right) &= M\left(y_{i,j}^{2,1}\right)\cdot\mathfrak{B}_{(2,0,0),t_1^+}\left(\Xi_{i,j}\right)=\frac{1}{3},
\end{aligned}$$

and the proof is complete in the indicated case.

□

Remark 5.2.4. *Using a symbolic computation software it is possible to show that the masks given in Definition 5.2.1 are the only ones that give rise to a quasi-interpolation operator exact on $\mathbb{P}_2$ that produces C^1 quadratic quasi-interpolants.*

The value of the uniform norm of $\mathcal{Q}$ is easily deduced taken into account that

$$\|\mathcal{Q}\|_\infty \le \max_{p\in\Xi_{i,j}} \|M(p)\|_1$$

and the l_1-norms of the masks in Definition 5.2.1:

$$\begin{aligned}
&\left\|M\left(v_{i,j}\right)\right\|_1 = 3,\\
&\left\|M\left(x_{i,j}^{1,1}\right)\right\|_1 = 6, \left\|M\left(x_{i,j}^{-1,-1}\right)\right\|_1 = \tfrac{5}{3}, \left\|M\left(x_{i,j}^{1,0}\right)\right\|_1 = \left\|M\left(x_{i,j}^{0,1}\right)\right\|_1 = \tfrac{9}{2}, \left\|M\left(x_{i,j}^{0,-1}\right)\right\|_1 = \left\|M\left(x_{i,j}^{-1,0}\right)\right\|_1 = \tfrac{3}{2},\\
&\left\|M\left(y_{i,j}^{1,-1}\right)\right\|_1 = \left\|M\left(y_{i,j}^{-1,1}\right)\right\|_1 = 3, \left\|M\left(y_{i,j}^{1,2}\right)\right\|_1 = \left\|M\left(y_{i,j}^{2,1}\right)\right\|_1 = 6, \left\|M\left(y_{i,j}^{-1,-2}\right)\right\|_1 = \left\|M\left(y_{i,j}^{-2,-1}\right)\right\|_1 = \tfrac{5}{3},\\
&\left\|M\left(e_{i,j}^{1,1}\right)\right\|_1 = \tfrac{11}{3}, \left\|M\left(e_{i,j}^{1,0}\right)\right\|_1 = \left\|M\left(e_{i,j}^{0,1}\right)\right\|_1 = \tfrac{11}{4},\\
&\left\|M\left(t_{i,j}\right)\right\|_1 = 3, \left\|M\left(t_{i,j}^{1}\right)\right\|_1 = \tfrac{13}{6}, \left\|M\left(t_{i,j}^{2}\right)\right\|_1 = 4, \left\|M\left(t_{i,j}^{3}\right)\right\|_1 = \tfrac{11}{3},\\
&\left\|M\left(b_{i,j}\right)\right\|_1 = 3, \left\|M\left(b_{i,j}^{1}\right)\right\|_1 = \tfrac{13}{6}, \left\|M\left(b_{i,j}^{2}\right)\right\|_1 = 4, \left\|M\left(b_{i,j}^{3}\right)\right\|_1 = \tfrac{11}{3},
\end{aligned}$$

Moreover, quasi-interpolation error estimates are found using a standard procedure.

Proposition 5.2.5. *The following results hold.*

1. *The uniform norm of Q is equal to 6.*

2. *There exists an absolute constant K such that for every $f\in C^{m+1}\left(\mathbb{R}^2\right)$, $0\le m\le 2$,*

$$\left\|D^\gamma\left(f-\mathcal{Q}f\right)\right\|_{\infty,T} \le K h^{m+1-|\gamma|}\left\|D^{m+1}f\right\|_{\infty,\Omega_T}, \tag{5.1}$$

for all $0\le|\gamma|\le 1$, $\gamma=(\gamma_1,\gamma_2)$, with Ω_T denoting the union of the triangles in Δ having a non-empty intersection with T.

5.3 Numerical tests

In order to illustrate the performance of the quasi-interpolating spline we have defined, we consider three test functions defined on the unit square:

$$\begin{aligned} f_1(x_1,x_2) &= \frac{3}{4}\exp\left(-\frac{(9x_1-2)^2}{4}-\frac{(9x_2-2)^2}{4}\right)+\frac{3}{4}\exp\left(-\frac{(9x_1+1)^2}{49}-\frac{9x_2+1}{10}\right) \\ &\quad +\frac{1}{2}\exp\left(-\frac{(9x_1-7)^2}{4}-\frac{(9x_2-3)^2}{4}\right)-\frac{1}{5}\exp\left(-(9x_1-4)^2-(9x_2-7)^2\right), \\ f_2(x_1,x_2) &= \frac{y}{2}\cos^4\left(4(x_1^2+x_2-1)\right). \end{aligned}$$

They are the Franke and Nielson functions [51, 52], respectively.

The quasi-interpolation error is estimated as

$$\max_{k,\ell=1,\ldots,400}\left|\mathcal{Q}f(x_k,y_\ell)-f(x_k,y_\ell)\right|,$$

where x_k and y_ℓ are equally spaced points in $[0,1]$. The numerical convergence order (NCO) is given by the rate

$$\mathrm{NCO} := \log\left(\frac{\mathtt{E}(h_2)}{\mathtt{E}(h_1)}\right)/\log\left(\frac{h_2}{h_1}\right),$$

where $\mathtt{E}(h)$ marks the estimated error associated with the step-length h.

Figure 5.9 shows the quasi-interpolant $\mathcal{Q}f$ together with the functions f_1 and f_2 for a step-length equals 0.00625.

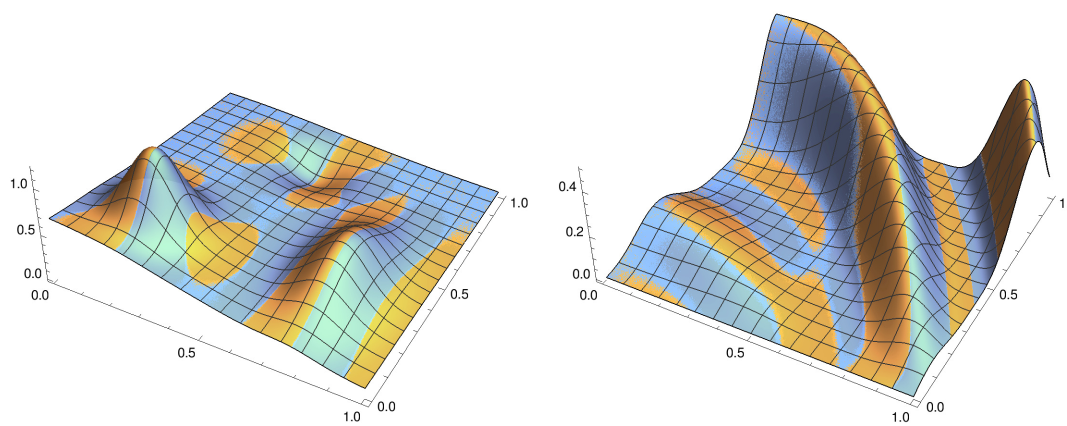

Figure 5.9: Functions f_1, f_2 (green) and their quasi-interpolant $\mathcal{Q}f$ (blue) for $h = 0.00625$, i.e., (left) f_1, (right) f_2.

The quasi-interpolation errors are estimated for different values of the step-length h and the NCO are calculated. The results are shown in Table 5.1. They confirm the theoretical ones.

5.4 Quasi-interpolation from point values at vertices

In [77] new approximating splines were constructed by application of a *preprocessing* to the quasi-interpolating splines defined in [75] from the values at vertices and midpoints: firstly, the values of the given function f at e-points are replaced by the ones obtained after one step of a subdivision algorithm suitable for type-1 triangulated data, and then the resulting values are used jointly with the values $f(v_{i,j})$ to get a quasi-interpolant whose BB-coefficients only involve values at the vertices.

	f_1		f_2	
n	estimated error	NCO	estimated error	NCO
20	1.42759×10^{-2}	–	1.58082×10^{-2}	–
40	1.78419×10^{-3}	3.00024	2.25332×10^{-3}	2.81055
80	2.18182×10^{-4}	3.03167	2.93772×10^{-4}	2.93928
160	2.71191×10^{-5}	3.00815	3.72658×10^{-5}	2.97877

Table 5.1: Errors and NCOs for the functions f_1 and f_2 with $h = 1/n$, $n = 20, 40, 80, 160$.

The aim of this section is similar, i.e. the construction of quasi-interpolants $\widetilde{\mathcal{Q}}f$ from values at the vertices, but without preprocessing the values of f at the midpoints. Only the values at the points in

$$\begin{aligned}\Theta_{i,j} =& \big(v_{i,j},\, v_{i+1,j+1},\, v_{i+1,j},\, v_{i,j-1},\, v_{i-1,j-1},\, v_{i-1,j},\, v_{i,j+1},\, v_{i+2,j+2},\, v_{i+2,j-1},\, v_{i+2,j},\\ & v_{i+1,j-1},\, v_{i,j-2},\, v_{i-1,j-2},\, v_{i-1,j-2},\, v_{i-2,j-1}, v_{i-2,j}, v_{i-1,j+1}, v_{i+1,j+2}, v_{i+1,j+2}\big)\,,\end{aligned}$$

will be used to define the BB-coefficients of the restriction of $\widetilde{\mathcal{Q}}f$ to each micro-triangle. The graphical representation of the nineteen points in $\Theta_{i,j}$ would result in an hexagonal structure: at the centre, the vertex $v_{i,j}$, surrounded by vertices $v_{i+k,j+\ell}$, $-1 \le k, \ell \le 1$, $k+\ell \ne 0$, which determine an hexagon; and the remaining twelve ones form a new hexagon. Now, for each domain point $p \in D_{i,j}$ we will look for a mask $\widetilde{M}$ such that its B-ordinate is computed as

$$\widetilde{c}(p) = \widetilde{M}\,(p) \cdot f\,(\Theta_{i,j}) = \sum_{\ell=1}^{19} \widetilde{M}\,(p)_\ell\, f\,(\Theta_{i,j})_\ell\,.$$

Similar notations are used as in Section 5.2. There we provided the unique C^1 quadratic quasi-interpolant exact in $\mathbb{P}_2$ whose BB-coefficients in the micro-triangles of each macro-triangle are linear combinations of values of the approximate function at vertices and midpoints of the containing hexagon. When only the values at the vertices of the function being approximated are known, imposing the required regularity and exactness does not result in a unique quasi-interpolant. In fact, using the symbolic computation facilities of the Mathematica software is tis possible to prove that there exist a 9-parametric family of masks that give rise to quasi-interpolants with the required characteristics. Similar properties to those of $\mathcal{Q}$ hold for the operator $\widetilde{\mathcal{Q}}$. Given f, the spline $\widetilde{\mathcal{Q}}f$ is C^1 continuous. Regarding the quasi-interpolation error, estimate (5.1) is applicable but a larger neighbourhood $\widetilde{\Omega}_T$ is involved.

In order to reduce the number of parameters, we will take into account the symmetries and patterns of zeros presented by the masks of Section 5.2. More precisely, we will first impose that the masks associated with the BB-coefficients of the domain points $x_{i,j}^{0,1}$, $x_{i,j}^{0,-1}$, $y_{i,j}^{-1,1}$, $y_{i,j}^{2,1}$, $y_{i,j}^{-2,-1}$, $e_{i,j}^{0,1}$, $b_{i,j}$, $b_{i,j}^1$, $b_{i,j}^2$ y $b_{i,j}^3$ are symmetric with respect to the segment defined by the vertices $v_{i-2,j-2}$ and $v_{i+2,j+2}$ of $x_{i,j}^{1,0}$, $x_{i,j}^{-1,0}$, $y_{i,j}^{1,-1}$, $y_{i,j}^{1,2}$, $y_{i,j}^{-1,-2}$, $e_{i,j}^{1,0}$, $t_{i,j}$, $t_{i,j}^1$, $t_{i,j}^2$ y $t_{i,j}^3$, respectively. Second, we require that the mask of $v_{i,j}$ be symmetric with respect to that segment. Furthermore, the entries in positions 2, 3, 7, 8, 9, 10, 18 and 19 of the masks of $v_{i,j}$, $x_{i,j}^{1,1}$, $x_{i,j}^{-1,-1}$, $x_{i,j}^{1,0}$, $y_{i,j}^{1,-1}$, $y_{i,j}^{1,2}$, $x_{i,j}^{0,-1}$ and $y_{i,j}^{-1,-2}$ are null.

The following result is also proved.

Proposition 5.4.1. *There exists a 3-parametric family of masks that satisfy the above requirements and provide C^1-continuous quasi-interpolants that reproduce polynomials of total degree two. If a, b and c denote the values of the first, second and third entries of the mask of $e_{i,j}^{1,1}$,* *then the vertex mask is*

$$\begin{aligned}\widetilde{M}\left(v_{i,j}\right) = \Big(&\frac{1}{2}(2a+10b+8c-3),0,0,\frac{1}{4}(5-4a-4b),5-16b-16c,\\ &\frac{1}{4}(5-4a-4b),0,0,0,0,0,\frac{1}{4}(5-16b-16c),\frac{1}{4}(4a+68b+64c-25),\\ &5-a-13b-12c,\frac{1}{4}(4a+68b+64c-25),\frac{1}{4}(5-16b-16c),0,0,0\Big).\end{aligned}$$

Those of $x-$points are obtained from

$$\begin{aligned}\widetilde{M}\left(x_{i,j}^{1,1}\right) &= \Big(2a+8b+8c-3,0,0,\frac{1}{2}(-4a-4b-4c+5),-24b-24c+7,\frac{1}{2}(-4a-4b-4c+5),\\ &\quad 0,0,0,0,0,\frac{1}{8}(-3)(16b+16c-5),2(a+13b+13c-5),\frac{1}{4}(-8a-80b-80c+33),\\ &\quad 2(a+13b+13c-5),\frac{1}{8}(-3)(16b+16c-5),0,0,0\Big),\\
\widetilde{M}\left(x_{i,j}^{-1,-1}\right) &= \Big(2b,0,0,2c,-8b-8c+3,2c,0,0,0,0,0,\frac{1}{8}(-16b-16c+5),\frac{1}{2}(16b+12c-5),\\ &\quad \frac{1}{4}(-24b-16c+7),\frac{1}{2}(16b+12c-5),\frac{1}{8}(-16b-16c+5),0,0,0\Big),\\
\widetilde{M}\left(x_{i,j}^{1,0}\right) &= \Big(\frac{1}{4}(6a+26b+24c-9),0,0,\frac{1}{8}(9-12a+12b+16c),-2(10b+10c-3),\\ &\quad \frac{1}{8}(21-12a-36b-32c),0,0,0,0,0,\frac{1}{2}(5-16b-16c),\frac{1}{8}(12a+196b+192c-73),\\ &\quad \frac{1}{8}(53-12a-132b-128c),\frac{1}{8}(12a+148b+144c-57),\frac{1}{8}(5-16b-16c),0,0,0\Big),\\
\widetilde{M}\left(x_{i,j}^{-1,0}\right) &= \Big(\frac{1}{4}(2a+14b+8c-3),0,0,\frac{1}{8}(11-4a-28b-16c),-4(3b+3c-1),\\ &\quad \frac{1}{8}(-4a+20b+32c-1),0,0,0,0,0,0,\frac{1}{8}(4a+76b+64c-27),\\ &\quad \frac{1}{8}(27-4a-76b-64c),\frac{1}{8}(4a+124b+112c-43),\frac{1}{8}(-3)(16b+16c-5),0,0,0\Big).\end{aligned}$$

$y-$points masks comme from

$$\begin{aligned}\widetilde{M}\left(y_{i,j}^{1,-1}\right) &= \Big(\frac{1}{2}(2a+10b+8c-3),0,0,\frac{1}{4}(1-4a+12b+16c),5-16b-16c,\\ &\quad \frac{1}{4}(9-4a-20b-16c),0,0,0,0,0,\frac{1}{2}(5-16b-16c),\frac{1}{12}(12a+252b+240c-91),\\ &\quad 5-a-13b-12c,\frac{1}{12}(12a+156b+144c-59),0,0,0,0\Big),\\
\widetilde{M}\left(y_{i,j}^{1,2}\right) &= (2a+8b+8c-3,0,0,3-2a-4b-4c,7-24b-24c,-2(a-1),0,0,0,0,0,\\ &\quad \frac{1}{4}(5-16b-16c),\frac{2}{3}(3a+36b+36c-14),\frac{1}{4}(33-8a-80b-80c),\\ &\quad \frac{2}{3}(3a+42b+42c-16),\frac{1}{2}(5-16b-16c),0,0,0\Big),\\
\widetilde{M}\left(y_{i,j}^{-1,-2}\right) &= \Big(2b,0,0,\frac{1}{2}(4b+8c-1),3-8b-8c,\frac{1}{2}(1-4b),0,0,0,0,0,\frac{1}{4}(5-16b-16c),\\ &\quad \frac{1}{6}(60b+48c-19),\frac{1}{4}(7-24b-16c),\frac{1}{6}(36b+24c-11),0,0,0,0\Big),\end{aligned}$$

and those e−points are given by

$$\begin{aligned}
\widetilde{M}\left(e_{i,j}^{1,1}\right) = \Big(& a, b, c, -a+3b+2c, \frac{1}{8}(-120b-112c+35), -a+3b+2c, c, 0, 0, 0, \\
& \frac{1}{16}(-16b-16c+5), -\frac{3}{16}(16b+16c-5), a+13b+13c-5, \frac{1}{8}(33-8a-80b-80c), \\
& a+13b+13c-5, -\frac{3}{16}(16b+16c-5), \frac{1}{16}(5-16b-16c), 0, 0\Big), \\
\widetilde{M}\left(e_{i,j}^{1,0}\right) = \Big(& \frac{1}{16}(8a+72b+80c-19), 0, \frac{1}{8}(2a+14b+8c-3), \frac{1}{16}(41-12a-84b-80c), \\
& \frac{1}{16}(5+4a-36b-48c), \frac{1}{4}(9-3a-21b-20c), 0, 0, 0, 0, \frac{1}{16}(11-4a-28b-16c), \\
& \frac{1}{16}(4a+12b-7), \frac{1}{8}(4a+60b+64c-23), \frac{1}{16}(53-12a-132b-128c), \\
& \frac{1}{16}(12a+148b+144c-57), \frac{1}{16}(5-16b-16c), 0, 0, 0\Big).
\end{aligned}$$

Finally, the t−points masks are

$$\begin{aligned}
\widetilde{M}\left(t_{i,j}\right) = \Big(& \frac{1}{12}(4a+12b+16c+1), \frac{2b}{3}, \frac{1}{3}(a+7b+8c-2), \frac{1}{18}(23-12a-36b-48c), \\
& \frac{1}{18}(6a-54b-48c+7), \frac{1}{9}(11-6a-18b-24c), \frac{1}{6}(1-4b), 0, 0, 0, \\
& \frac{1}{6}(7-2a-18b-16c), \frac{1}{36}(12a+60b+48c-29), \frac{1}{9}(3a+45b+48c-17), \\
& \frac{1}{12}(33-8a-80b-80c), \frac{2}{9}(3a+36b+36c-14), \frac{1}{12}(5-16b-16c), 0, 0, 0\Big), \\
\widetilde{M}\left(t_{i,j}^{1}\right) = \Big(& \frac{1}{2}(a+7b+8c-2), 0, 0, \frac{1}{4}(7-2a-18b-16c), \frac{1}{12}(11-36b-48c), \\
& \frac{1}{8}(13-4a-20b-16c), b, 0, 0, 0, 0, 0, \frac{1}{24}(12a+156b+144c-59), \\
& \frac{1}{2}(5-a-13b-12c), \frac{1}{12}(6a+90b+96c-35), \frac{1}{3}(1-3b-6c), \frac{1}{4}(1-4b), 0, 0\Big), \\
\widetilde{M}\left(t_{i,j}^{2}\right) = \Big(& \frac{1}{8}(4a+44b+48c-11), 0, \frac{1}{4}(2a+10b+8c-3), \frac{1}{2}(-2a-16b-16c+7), \\
& \frac{1}{24}(12a-36b-48c-7), \frac{1}{4}(-4a-24b-24c+11), 0, 0, 0, 0, \frac{1}{8}(-4a-20b-16c+9), \\
& \frac{1}{24}(12a+60b+48c-29), \frac{1}{6}(3a+45b+48c-17), \frac{1}{8}(-8a-80b-80c+33), \\
& \frac{1}{3}(3a+36b+36c-14), \frac{1}{8}(-16b-16c+5), 0, 0, 0\Big), \\
\widetilde{M}\left(t_{i,j}^{3}\right) = \Big(& a, b, \frac{1}{4}(4b+8c-1), \frac{1}{12}(-12a+60b+48c-7), \frac{1}{8}(35-120b-112c), \\
& \frac{1}{12}(7-12a+12b), \frac{1}{4}(1-4b), 0, 0, 0, \frac{1}{8}(5-16b-16c), \frac{1}{4}(5-16b-16c), \\
& \frac{1}{3}(3a+42b+42c-16), \frac{1}{8}(33-8a-80b-80c), \frac{1}{3}(3a+36b+36c-14), \\
& \frac{1}{8}(5-16b-16c), 0, 0, 0\Big).
\end{aligned}$$

Once all the conditions from the structure of the masks found in Section 5.2 are imposed when vertex and point values are known, it is possible to reduce the number of parameters.

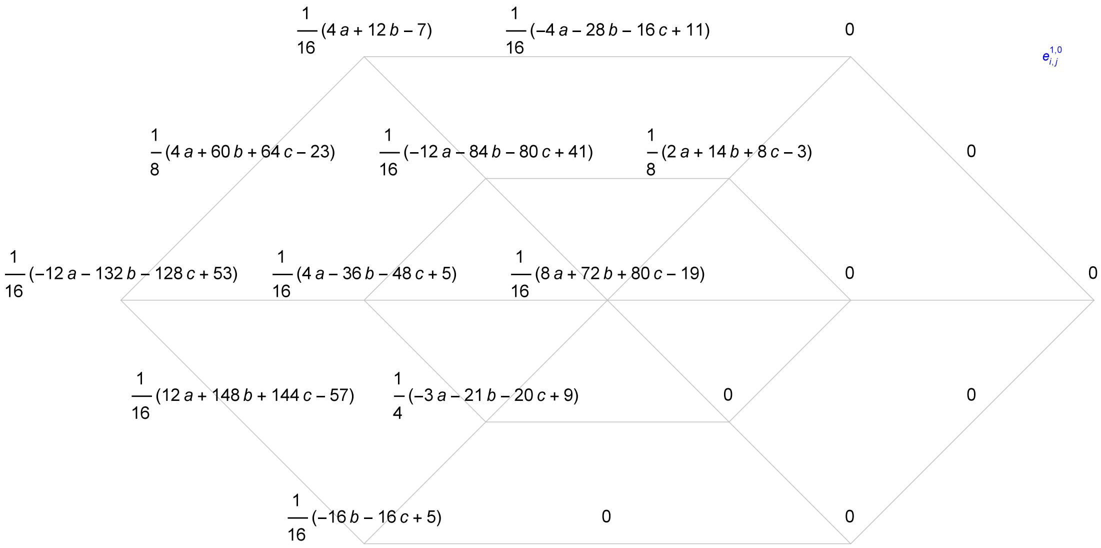

Figure 5.10: Mask of point $e_{i,j}^{1,0}$. It depends on the three parameters.

Note the mask of $e_{i,j}^{1,0}$ in Figure 5.10. A feature shared by all Section 5.2 masks is that the 13th and 15th entries are equal to zero. We therefore choose to impose these restrictions on the mask of $e_{i,j}^{1,0}$, and the foloowing conditions must be satisfied:

$$a + 15b + 16c = \frac{23}{4} \quad \text{and} \quad 3a + 37b + 36c = \frac{57}{4}.$$

Consequently,

$$b = \frac{3}{52}(7 - 4a) \quad \text{and} \quad c = \frac{1}{52}(1 + 8a).$$

Finally, these values are applied to the masks and the selection of the parameter a is carried out by minimizing the infinity norm of the associated quasi-interpolation operator, $\widetilde{\mathcal{Q}}_a$, which, after simplication, is the maximum of the following functions:

- $\dfrac{12\,|3a-2|}{13} + \dfrac{3\,|4a-7|}{26} + \dfrac{3\,|16a-15|}{104} + \dfrac{5}{8}.$
- $\dfrac{5\,|4a-7|}{52} + \dfrac{|16a-15|}{208} + \dfrac{3\,|16a+37|}{208} + \dfrac{5\,|7-4a|}{52} + \dfrac{|47-64a|}{208} + \dfrac{5}{16}.$
- $\dfrac{4\,|3a-2|}{39} + \dfrac{3\,|16a-15|}{52} + \dfrac{|18a+1|}{13} + \dfrac{|24a-29|}{13} + |2-2a| + \dfrac{|19-22a|}{13} + \dfrac{|29-24a|}{52}.$
- $\dfrac{15\,|16a-15|}{52} + \dfrac{|18a+1|}{13} + \dfrac{|24a-29|}{13} + \dfrac{|29-24a|}{52}.$
- $\dfrac{4\,|3a-2|}{13} + \dfrac{|8a-1|}{52} + \dfrac{3\,|16a-15|}{26} + \dfrac{|24a+23|}{52} + \dfrac{2\,|11-10a|}{13}.$
- $\dfrac{6\,|3a-2|}{13} + \dfrac{2\,|7a-9|}{13} + \dfrac{|8a-1|}{52} + \dfrac{3\,|16a-15|}{26} + \dfrac{|24a+23|}{52}.$
- $\dfrac{2\,|3a-2|}{13} + \dfrac{4\,|10a-11|}{13} + \dfrac{5\,|16a-15|}{104} + \dfrac{3\,|32a+9|}{104} + \dfrac{|7-4a|}{26} + \dfrac{|23-28a|}{26}.$
- $\dfrac{|3a-2|}{13} + \dfrac{3\,|4a-7|}{52} + \dfrac{|6a-17|}{78} + \dfrac{|8a-1|}{104} + \dfrac{|32a+35|}{104} + \dfrac{|2-3a|}{39} + \dfrac{|17-6a|}{26} + \dfrac{|1-8a|}{104} + \dfrac{1}{156}\,|-12a-5| + \dfrac{1}{24}.$

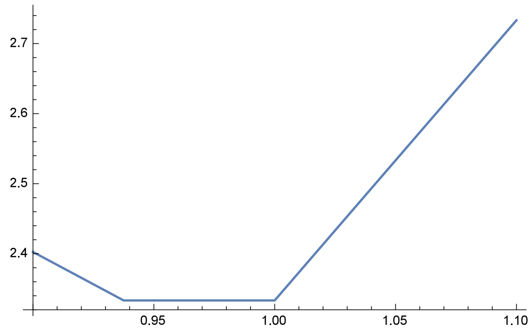

Figure 5.11: Plot of the objetive function.

- $\frac{2|2a+3|}{13}+\frac{8|3a-2|}{117}+\frac{|16a-15|}{156}+\frac{|32a+35|}{156}+\frac{|36a-37|}{234}+\frac{|288a-361|}{468}+\frac{|7-4a|}{26}+\frac{|1-8a|}{156}+\frac{|29-24a|}{156}+\frac{|61-72a|}{117}+\frac{|109-144a|}{234}+\frac{1}{36}.$
- $\frac{|2a+3|}{13}+\frac{10|3a-2|}{13}+\frac{3|4a-7|}{26}+\frac{|8a-1|}{13}+\frac{|16a-15|}{52}+\frac{|40a-31|}{52}.$
- $\frac{8|3a-2|}{13}+\frac{3|4a-7|}{26}+\frac{2|8a-1|}{13}+\frac{|16a-15|}{52}+\frac{|40a-31|}{52}.$
- $\frac{|3a-2|}{39}+\frac{|4a+19|}{26}+\frac{|16a-15|}{104}+\frac{|24a+23|}{104}+\frac{|36a-37|}{156}+\frac{|42a-67|}{78}+\frac{|2-3a|}{13}+\frac{|11-10a|}{26}+\frac{|29-24a|}{104}+\frac{|23-28a|}{52}+\frac{1}{24}.$
- $|a|+\frac{|2a+3|}{26}+\frac{4|3a-2|}{39}+\frac{3|4a-7|}{52}+\frac{|16a-15|}{26}+\frac{|136a-147|}{104}+\frac{|2-3a|}{39}+\frac{|29-24a|}{104}+\frac{|53-60a|}{39}+\frac{|77-96a|}{78}.$
- $|a|+\frac{3|4a-7|}{52}+\frac{|8a-1|}{26}+\frac{|16a-15|}{26}+\frac{|136a-147|}{104}+\frac{|29-24a|}{104}+\frac{|61-72a|}{26}.$

The objective function is convex, so that its absolute minimum is attained at least at a point. Its plot is shown in Figure 5.11. In fact, the minimum is reached at the points of the interval $\left[\frac{15}{16},1\right]$.

A priori, there is no privileged choice in this interval of the parameter value a, but inspection of the masks when $a=\frac{15}{16}$ allows us to observe that the number of zero entries in the masks is increased, which implies a lower computational cost. They are shown next.

5.5 Conclusion

In this chapter, we have introduced two kinds of quasi-interpolation schemes. Both kinds are generated by setting their B-ordinates to suitable combinations of the given data values, instead of being defined as linear combinations of a set of bivariate functions and they do not require derivative values. The first kind involves the values at the vertices and middle points of the original vertices. While, the second one is restricted to the values prescribed at the set of vertices. The presented schemes are C^1 continuous, and the numerical tests show that they yield the optimal approximation power.

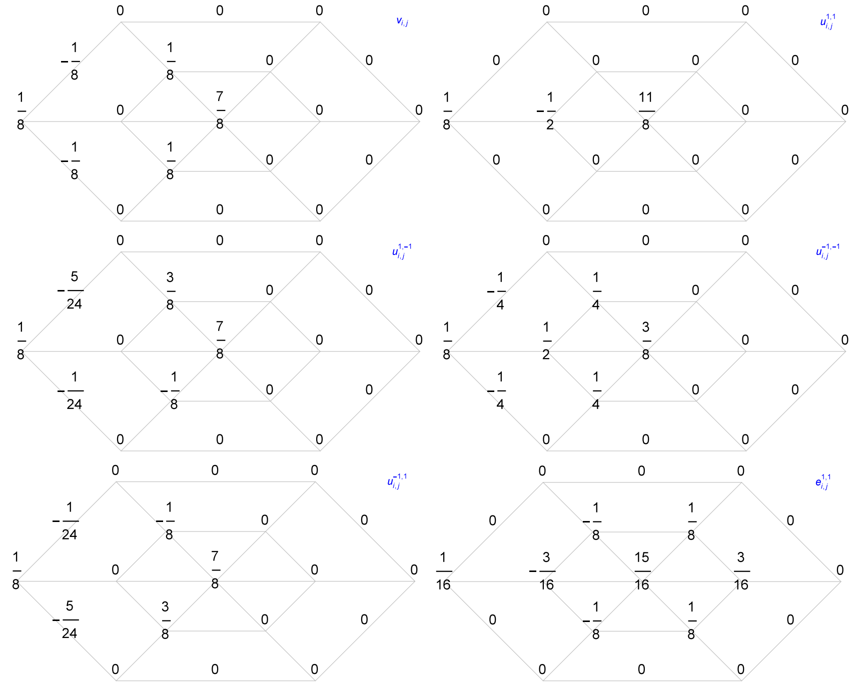

Figure 5.12: Hexagonal representations of masks.

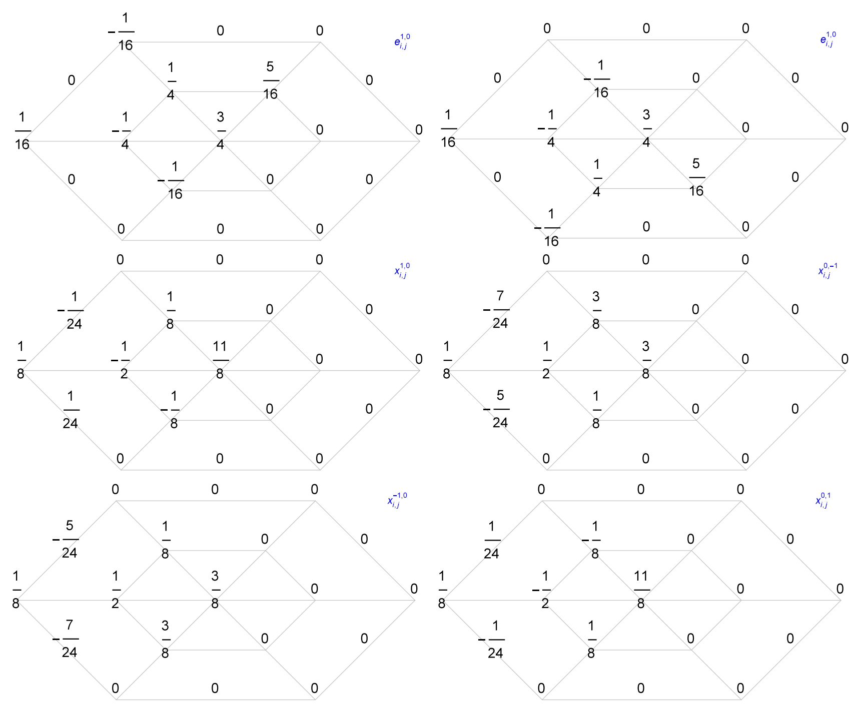

Figure 5.13: Hexagonal representations of masks (cont'd)

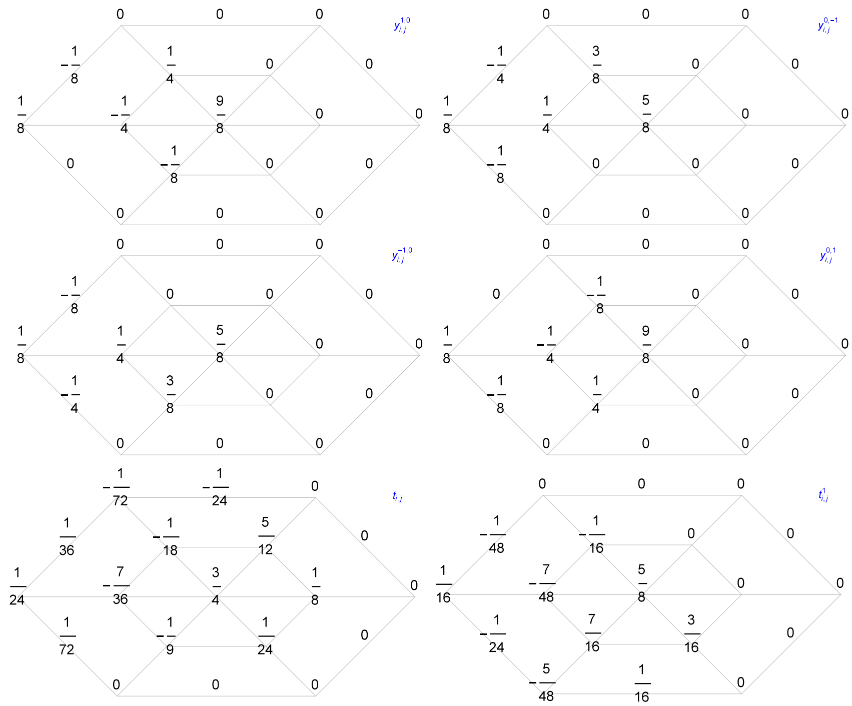

Figure 5.14: Hexagonal representations of masks (cont'd)

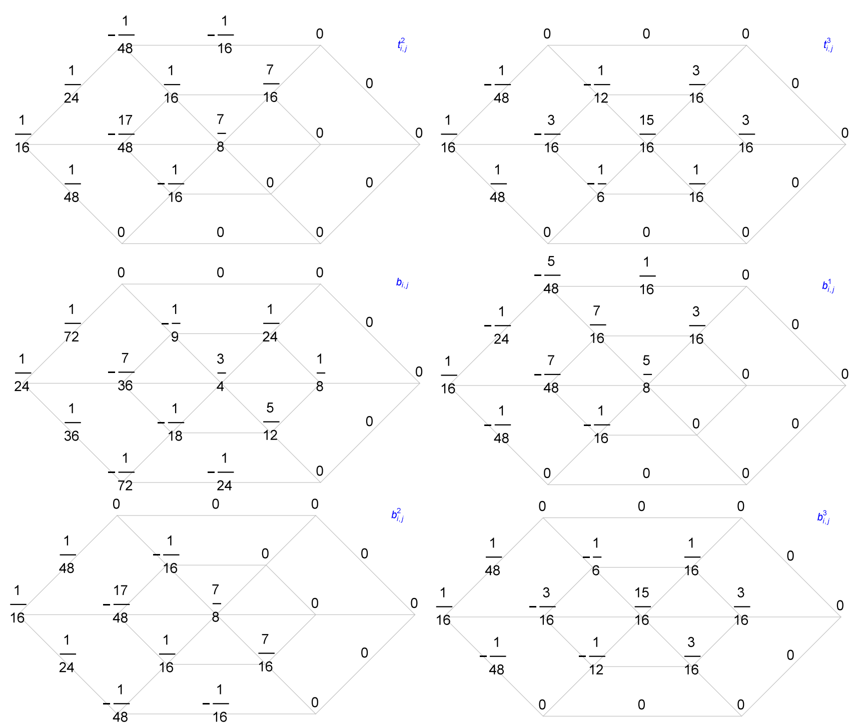

Figure 5.15: Hexagonal representations of masks (cont'd)

Chapter 6

Family of many knot spline spaces

Spline functions play an essential role in interpolating or approximating functions or data from their values or that of some of their derivatives at a given set of points. Generally, the calculation of the interpolant requires solving a system of equations, and in addition, in many cases only noisy data are available. Therefore, since its introduction in [1], spline quasi-interpolation has been an increasingly used method to obtain approximating splines efficiently and a low computational cost. The introduction of the de Boor-Cox recurrence formula to evaluate the B-splines from which the interpolant and quasi-interpolant can be expressed allowed extensive use of spline functions in multiple fields and made the B-splines a central tool in both approximation theory and applications.

Given a partition $X_n := \{x_i, 0 \leq i \leq n\}$ of an interval $I := [a, b]$ into sub-intervals $I_i := [x_i, x_{i+1}]$, $0 \leq i \leq n-1$, and real values f_i^j, $0 \leq i \leq n$, $0 \leq j \leq k-1$, $k \geq 2$, the Hermite spline interpolation problem consisting of finding a $\mathcal{C}^{k-1}$ piecewise poynomial function s of degree $2k-1$ such that $s^{(j)}(x_i) = f_i^j$ admits a unique solution. An explicit formula for the coefficients of the B-spline representation of s has been derived in [78], and a simpler proof based on blossoming has been given in [79, 80].

A refinement of the initial partition X_n is defined by taking an interior point ξ_i in each sub-interval I_i. It is the extension of Powell-Sabin split to the univariate case [22, 85]. With $\xi := \{\xi_i, 0 \leq i \leq n-1\}$, a Hermite spline interpolation problem in a spline space of degree $d \geq 2$ and class $\lfloor d/2 \rfloor$ on the refined partition $X_n^{\mathrm{ref}} := X_n \cup \xi$ will be stated and analyzed. As usual, $\lfloor \cdot \rfloor$ stands for the integer part of a real number. When $d = 2r+1$, the class $\mathcal{C}^{r+1}$ is imposed at the added points to get a super-spline space. The solution of the interpolation problem will be explicitly determined by means of a local construction. Since the spline space is characterized by an interpolation problem, a basis is obtained as dual of the basis of the dual space given by the interpolation functionals.

In this chapter, each spline is uniquely determined by its values and those of its derivatives up to the order $\lfloor d/2 \rfloor$ at each knot of the initial partition, and its values and those of its derivatives up to the order $\lfloor d/2 \rfloor - 2$ if d is even and $\lfloor d/2 \rfloor - 1$ otherwise at the additional split points.

The idea of adding a split knot was introduced firstly in [81] to deal with the quadratic case. Following the same approach, $\mathcal{C}^1$ quadratic and $\mathcal{C}^2$ cubic many knot spline interpolation with sharp parameters is studied in [82], and $\mathcal{C}^1$ cubic Hermite splines with minimal derivative oscillation are constructed in [83] and [84]. In all these works, the bases used do not necessarily benefit from the properties usually requested, such as the non-negativity of the basis functions and the fact of forming a partition of unity. Moreover, it is proved in [85] that a C^1 quadratic univariate spline on such a kind of refined partition is uniquely determined by the values of the spline and its first derivative at the knots of the initial partition, and that the data specified at each knot affect only the values of the spline on the sub-intervals sharing that particular knot.

Refinement of a given partition is widely used in multivariate approximation by splines. In fact, for constructing smooth splines with a low degree, a given partition is refined to get a number of smaller simplices [15, 18, 22]. For bivariate splines, Clough-Tocher split (into three sub-triangles) and Powell-Sabin split (into six sub-triangles) are commonly used divisions. For instance, a normalized B-spline representation for bivariate Powell-Sabin splines with higher degree and smoothness is discussed in [42, 26]. With the help of Marsden's identity, various families of smooth quasi-interpolation schemes involving values and/or derivatives of a given function have been constructed in [36]. This construction has been generalized to the multivariate case, and specialized to the one-dimensional case for quadratic splines [85]. The procedure used in constructing bivariate splines on Powell-Sabin and Clough-Tocher triangulations, based on the Bernstein-Bézier representation and blossoming inspires the study in this work, and stable bases consisting of non-negative compactly supported functions that form partitions of unity are defined through a geometrical approach for the family of super-spline spaces described above. General Marsden's identities are derived and used to define quasi-interpolating splines in those spaces.

Bearing in mind that for any spline space defined on an arbitrary partition of an interval it is possible to define a basis of B-splines from an extended partition, that the coefficients of the representation in this basis of any spline of this space can be expressed via polar forms and that it is also possible to construct quasi-interpolants of different types in a general way, it must be explained what is the interest in constructing a new basis, which is the main goal of this chapter along with its application to quasi-interpolation. Consider the case $d = 2r$. An extended partition to define a basis of B-splines to $S^r_{2r}\left(X^{\text{ref}}_n\right)$ is

$$\{x_0\,[2r+1]\,,\xi_0\,[r]\,,x_1\,[r]\,,\xi_1\,[r]\,,\ldots,x_{n-1}\,[r]\,,\xi_{n-1}\,[r]\,,x_n\,[2r+1]\}\,,$$

where the notation $p[\ell]$ is used to indicate that the point p is repeated $\ell \geq 2$ times. The multiplicity will be omitted when $\ell = 1$. Since the B-splines are defined from divided differences with $2r+2$ knots of the truncated power $(\cdot - x)^{2r}_+$, they are compactly supported piecewise polynomial functions of class $\mathcal{C}^r$ whose supports are made up of one, two or three micro-intervals induced by X^{ref}_n. More precisely, for each boundary value $x_0 = a$ and $x_n = b$ there are r boundary B-splines supported on on $[x_0, \xi_0]$ and $[\xi_{n-1}, x_n]$, respectively. The B-splines given by the knots $\{x_0\,[r+1]\,,\xi_0\,[r]\,,x_1\}$ and $\{x_{n-1},\xi_{n-1}\,[r]\,,x_n\,[r+1]\}$ are supported on $[x_0, x_1] = [x_0, \xi_1] \cup [\xi_1, x_1]$ and $[x_{n-1}, x_n] = [x_{n-1}, \xi_{n-1}] \cup [\xi_{n-1}, x_n]$, respectively. The supports of those associated with $\{x_i\,[r]\,,\xi_i\,[r]\,,x_{i+1}\,[2]\}$, $i = 0,\ldots,n-1$, are $[x_i, x_{i+1}] = [x_i, \xi_i] \cup [\xi_i, x_{i+1}]$. Finally, the remaining B-splines are defined from $\{x_i, \xi_i\,[r]\,,x_{i+1}\,[r]\,,\xi_{i+1}\}$ or $\{\xi_i, x_{i+1}\,[r]\,,\xi_{i+1}\,[r]\,,x_{i+2}\}$, $i = 0,\ldots,n-2$, so that their supports are equal to $[x_i, \xi_{i+1}]$ and $[\xi_i, x_{i+2}]$. A somewhat more complex situation arises in the case $d = 2r+1$ because the additional $\mathcal{C}^{r+1}$ continuity at breakpoints ξ_i, $i = 0,\ldots,n-1$, makes these points appear repeated $r-1$ times in the extended partition instead of r times.

Although the evaluation of any spline of the considered spaces can be performed by evaluating the involved B-splines by means of the Cox-de Boor's recursion formula [97], the construction of an alternative basis whose elements can be calculated explicitly would be useful if they enjoy properties similar to those of the B-splines. Moreover, these functions will have more uniform supports, in the sense that those of the boundary B-spline-like functions will consist of a single macro-interval and the remaining ones will have two.

Inserting additional knots is often used to incorporate shape parameters in order to construct approximating splines that preserve convexity or monotony to given data [81]. Shape-preserving properties for the spline spaces proposed in this work can be achieved by imposing conditions on the location of the new knots to achieve simpler results than those available when using spaces without split points. Inserting new knots is used also in the bivariate case to preserve convexity [86].

The proposed B-spline-like functions could be used in a natural way to define shape-preseving approximating splines.

6.1 Preliminaries

The construction of the bases that will be used to define quasi-interpolating splines makes extensive use of the Bernstein-Bézier representation and the notion of polar form or blossom.

Recall that $I = [a, b]$. Each point $x \in \mathbb{R}$ can be written as $x = (1-t)\,a + t\,b$, and the vector $(1-t, t)$ provides the barycentric coordinates of x with respect to I, from which the Bernstein polynomials of degree $d > 0$ relative to I are defined as

$$\mathfrak{B}^d_{\beta,\,I}(t) := \frac{d!}{\beta!}\,(1-t)^{\beta_1}\;t^{\beta_2},$$

where $t := \dfrac{x-a}{b-a}$ is the local variable, $\beta := (\beta_1, \beta_2)$, $\beta! := \beta_1!\beta_2!$ and $|\beta| := \beta_1 + \beta_2 = d$. They form a basis of the space $\mathbb{P}_d$ of polynomials of degree less than or equal to d.

For all $t \in \mathbb{R}$, it holds

$$\sum_{|\beta|=d} \mathfrak{B}^d_{\beta,\,I}(t) = 1,$$

and each Bernstein polynomial $\mathfrak{B}^d_{\beta,\,I}(t)$ is non-negative whenever $0 \le t \le 1$, i.e. when $x \in I$.

Moreover, for each $p_d \in \mathbb{P}_d$ there are coefficients $\{b_\beta\}_{|\beta|=d}$ such that

$$p_d\,(x) = \sum_{|\beta|=d} b_\beta\,\mathfrak{B}^d_{\beta,\,I}\,(t) := b_d\,(t)\,. \tag{6.1}$$

The restriction of p_d to I is a convex combination of the coefficients $\{b_\beta\}_{|\beta|=d}$. Equality (6.1) is said to be the Bernstein-Bézier (BB-) representation of p_d, and those coefficients are called BB-coefficients or Bézier (B-) ordinates of p_d with respect to I.

The smoothing conditions of two adjacent polynomial patches can be easily described in terms of BB-coefficients with respect to the intervals. Let $I_1 = [a, c]$ and $I_2 = [c, b]$ be two adjacent intervals, and let p_1 and p_2 be two polynomials of degree d defined on I_1 and I_2, respectively. Let $b_{1,\beta}$ and $b_{2,\beta}$ the BB-coefficients of p_1 and p_2, respectively. Assume that $\hat\tau := (\hat\tau_1, \hat\tau_2)$ are the barycentric coordinates of b with respect to I_1. Then, the piecewise function defined as p_1 on I_1 and p_2 on I_2 is of class $\mathcal{C}^r$ at c if, for $\beta_1 = 0, \ldots, r$, and $\beta_2 = n - r$, it holds

$$b_{2,\beta} \;=\; \sum_{|\alpha|=\beta_1} b_{1,\alpha+\beta_2 e_2}\mathfrak{B}^r_{\alpha,I_1}\,(\hat\tau)\,,$$

where $e_2 := (0, 1)$.

The smoothness conditions can be determined by using the De Casteljau's algorithm, that is, by making only convex linear combinations:

$$b_{2,\beta} = b^{[\beta_1]}_{1,(0,\beta_2)},$$

where

$$\begin{aligned} b^{[0]}_{1,\beta} &= b_{1,\beta},\ \text{for}\ \ |\beta| = n,\\ b^{[\ell]}_{1,\beta} &= \hat\tau_1\; b^{[\ell-1]}_{1,\beta+e_1} + \hat\tau_2\; b^{[\ell-1]}_{1,\beta+e_2}, \text{for}\ \ |\beta| = n-\ell,\ \text{and}\ \ell = 1, \ldots, d, \end{aligned}$$

with $e_1 := (1, 0)$.

Blossoming is the other tool to be extensively used through the manuscript. It allows to determine the BB-representation of a polynomial on an interval. If $p_d \in \mathbb{P}_d$ and $(1-\tau, \tau)$ are the barycentric coordinates relative to I, then its restriction to I can be written as

$$p_d\,(x) = \sum_{|\beta|=n} \mathbf{B}\,[p_d]\,(a\,[\beta_1]\,, b\,[\beta_2])\;\mathfrak{B}^d_{\beta,\,I}\,(\tau)\,,\;\; x \in I,$$

where the polar form $\mathbf{B}\,[p_d]$ of the polynomial p_d is the unique function provided by the following result [41]:

Theorem 6.1.1. *Given a nonnegative integer d, for each bivariate polynomial $p_d \in \mathbb{P}_d$ there exists a unique blossom or polar form $\mathbf{B}[p_d] : \mathbb{R}^d \to \mathbb{R}$ of p_d satisfying the following properties:*

- $\mathbf{B}[p_d]$ *is symmetric, i.e. for any permutation Π of integers $1, \ldots, d$ it holds*

$$\mathbf{B}\left[p_d\right](A_1, \ldots, A_d) \,=\, \mathbf{B}\left[p_d\right]\left(A_{\Pi(1)}, \ldots, A_{\Pi(d)}\right).$$

- $\mathbf{B}[p_d]$ *is multi-affine, i.e. for values a and b such that $a+b=1$ it is fulfilled that*

$$\mathbf{B}\left[p_d\right](A_1, a\,B + b\,C, \ldots, A_d) \,=\, a\,\mathbf{B}\left[p_d\right](A_1, B, \ldots, A_d) \,+\, b\,\mathbf{B}\left(p_d\right)(A_1, C, \cdots, A_d).$$

- $\mathbf{B}[p_d]$ *is diagonal,i.e. it holds*

$$\mathbf{B}\left[p_d\right](A, \ldots, A) \,=\, p_d\left(A\right).$$

We will write indistinctly $\mathbf{B}\left[p_d\right](A_1, \ldots, A_d)$ and $\mathbf{B}\left[p_d\right]\left(\tau^1, \ldots, \tau^d\right)$, where $\tau^k := \left(\tau_1^k, \tau_2^k\right)$ stands for the barycentric coordinates of A_k.

Also the De Casteljau's algorithm is used to calculate the blossom in a stable way. Once again, only convex combinations are produced:

$$\mathbf{B}\left[p_d\right]\left(\tau^1, \ldots, \tau^d\right) = b_{(0,0)}^{[d]},$$

where

$$\begin{aligned} b_\beta^{[0]} &= b_\beta, \text{ for } |\beta| = d, \\ b_\beta^{[r]} &= \tau_1^r\, b_{\beta+e_1}^{[r-1]} \,+\, \tau_2^r\, b_{\beta+e_2}^{[r-1]}, \text{ for } |\beta| = d-r, \text{ and } r = 1, \ldots, d. \end{aligned}$$

As an example, let $d=2$, $\tau^r := (\tau_1^r, \tau_2^r)$, $r = 1, 2$. Then, the blossom of the polynomial

$$b_2\left(t\right) = \, b_{2,0}\,\mathfrak{B}_{(2,0),\,I}^2\left(t\right) + b_{1,1}\,\mathfrak{B}_{(1,1),\,I}^2\left(t\right) + b_{0,2}\,\mathfrak{B}_{(0,2),\,I}^2\left(t\right), \quad t \in [0,\,1],$$

is computed as follows:

1. $b_{(2,0)}^{[0]} = b_{2,0}, \quad b_{(1,1)}^{[0]} = b_{1,1}, \quad b_{(0,2)}^{[0]} = b_{0,2}.$
2. $b_{(1,0)}^{[1]} = \tau_1^1 b_{(2,0)}^{[0]} + \tau_2^1 b_{(1,1)}^{[0]}, \quad b_{(0,1)}^{[1]} = \tau_1^1 b_{(1,1)}^{[0]} + \tau_2^1 b_{(0,2)}^{[0]}.$
3. Then,

$$\begin{aligned} \mathbf{B}\left[p_2\right]\left(\tau^1,\,\tau^2\right) &= \tau_1^2 b_{(1,0)}^{[1]} + \tau_2^2 b_{(0,1)}^{[1]} \\ &= \tau_1^2\left(\tau_1^1 b_{2,0} + \tau_2^1 b_{1,1}\right) + \tau_2^2\left(\tau_1^1 b_{1,1} + \tau_2^1 b_{0,2}\right) \\ &= \tau_1^1\tau_1^2 b_{2,0} + \left(\tau_1^1\tau_2^2 + \tau_1^2\tau_2^1\right) b_{1,1} + \tau_2^1\tau_2^2 b_{0,2}. \end{aligned}$$

Another very utility practical of polar forms is the computation of the BB-coefficients of the restriction of a polynomial p_d to a subinterval of I from the ones of p_d relative to I. For a subinterval $\widetilde{I} = [c_1, c_2]$ of I, with c_1 and c_2 having barycentric coordinates $\mu^i = (\mu_1^i,\, \mu_2^i)$, $i = 1, 2$, with respect to I, then the BB-coefficients $\widetilde{b}_\beta$ of p_d on $\widetilde{I}$ can be determined in the following form:

$$\widetilde{b}_\beta = \mathbf{B}\left[p_d\right]\left(\mu^1[\beta_1],\, \mu^2[\beta_2]\right), \; |\beta| = d. \tag{6.2}$$

6.2 A family of many knot spline spaces

Let X_n and X_n^{ref} be the subsets defined in the introduction, which define a partition of I and a refinement of it, respectively. The sub-intervals induced by X_n^{ref} are denoted by I^{ref}. For a given integer $r \geq 1$, we consider the two following spline spaces defined over the partition induced by X_n^{ref}:

$$S_{2r}^{r}\left(X_n^{\text{ref}}\right) := \left\{s \in \mathcal{C}^r(I) : s_{|I^{\text{ref}}} \in \mathbb{P}_{2r} \text{ for all } I^{\text{ref}}\right\}, \tag{6.3}$$

$$S_{2r+1}^{r,r+1}\left(X_n^{\text{ref}}\right) := \left\{s \in \mathcal{C}^r(I) : s_{|I^{\text{ref}}} \in \mathbb{P}_{2r+1} \text{ for all } I^{\text{ref}} \text{ and } s \in \mathcal{C}^{r+1}(\xi)\right\}. \tag{6.4}$$

Here, $\mathcal{C}^{r+1}(\xi)$ means that the polynomials on subintervals sharing a split point have common derivatives up to order $r+1$ at that split point. Splines $s_1 \in S_{2r}^{r}\left(X_n^{\text{ref}}\right)$ and $s_2 \in S_{2r+1}^{r,r+1}\left(X_n^{\text{ref}}\right)$ can be provided as solutions of the following Hermite interpolation problem.

Theorem 6.2.1. *Given values f_i^q, $0 \leq i \leq n$ and $0 \leq q \leq r$, and g_k^q, $0 \leq k \leq n-1$ and $0 \leq q \leq r-2$, there exists a unique spline $s_1 \in S_{2r}^{r}\left(X_n^{ref}\right)$ satisfying the interpolation conditions:*

$$s_1^{(q)}(x_i) = f_i^q, \quad \text{for } i = 0, \ldots, n, \ 0 \leq q \leq r, \tag{6.5a}$$

$$s_1^{(q)}(\xi_k) = g_k^q, \quad \text{for } k = 0, \ldots, n-1, \ 0 \leq q \leq r-2. \tag{6.5b}$$

Analogously, for values f_i^q, $0 \leq i \leq n$ and $0 \leq q \leq r$, and g_k^q, $0 \leq k \leq n-1$ and $0 \leq q \leq r-1$, there exists a unique spline $s_2 \in S_{2r+1}^{r,r+1}\left(X_n^{ref}\right)$ such that

$$s_2^{(q)}(x_i) = f_i^q, \quad \text{for } i = 0, \ldots, n, \ 0 \leq q \leq r, \tag{6.6a}$$

$$s_2^{(q)}(\xi_k) := g_k^q, \quad \text{for } k = 0, \ldots, n-1, \ 0 \leq q \leq r-1. \tag{6.6b}$$

Proof. Functions $s_1 \in S_{2r}^{r}\left(X_n^{\text{ref}}\right)$ and $s_2 \in S_{2r+1}^{r,r+1}\left(X_n^{\text{ref}}\right)$ satisfying respectively (6.5) and (6.6) will be determined via the Bernstein-Bézier representation.

Consider the interval $I_i := [x_i, x_{i+1}]$, that is divided into two sub-intervals $I_{i,1} := [x_i, \xi_i]$ and $I_{i,2} := [\xi_i, x_{i+1}]$. Let $b_{2r-s,s}^{i,1}$, and $b_{2r-s,s}^{i,2}$, $0 \leq s \leq 2r$, be the BB-coefficients of s_1 on $I_{i,1}$ and $I_{i,2}$, respectively. Thoses in $\mathfrak{D}_r^{\text{right}}(x_i) := \left\{b_{2r-s,s}^{i,1}, 0 \leq s \leq r\right\}$ and $\mathfrak{D}_r^{\text{left}}(x_{i+1}) := \left\{b_{2r-s,s}^{i,2}, r \leq s \leq 2r\right\}$ are provided by interpolation conditions at the knots x_i and x_{i+1} (6.5a), respectively (see Fig. 6.1).

Now, interpolation conditions (6.5b) at ξ_k allow to compute the BB-coefficients of s_1 in $\mathfrak{D}_{r-2}^{\text{left}}(\xi_i) := \left\{b_{2r-s,s}^{i,1}, r+2 \leq s \leq 2r\right\}$ and $\mathfrak{D}_{r-2}^{\text{right}}(\xi_i) := \left\{b_{2r-s,s}^{i,1}, 0 \leq s \leq r-2\right\}$.

Only the BB-coefficients $b_{r-1,r+1}^{i,1}$ and $b_{r+1,r-1}^{i,2}$ remain to be determined. They are obtained by imposing the C^r condition at the split point ξ_i. By assembling the splines constructed on intervals I_i, the unique spline $s_1 \in S_{2r}^{r}\left(\mathbf{I}_n^{ref}\right)$ solving the Hermite interpolation problem (6.5) results.

The same approach is used to prove the existence and uniqueness of s_2. In this case, its BB-coefficients in $\overline{\mathfrak{D}}_r^{\text{right}}(x_i) := \left\{b_{2r+1-s,s}^{i,1}, 0 \leq s \leq r\right\}$ and $\overline{\mathfrak{D}}_r^{\text{left}}(x_{i+1}) := \left\{b_{2r+1-s,s}^{i,2}, r+1 \leq s \leq 2r+1\right\}$ are determined from interpolation conditions (6.6a) at x_i and x_{i+1}, respectively, and those in $\overline{\mathfrak{D}}_{r-1}^{\text{left}}(\xi_i) := \left\{b_{2r+1-s,s}^{i,1}, r+2 \leq s \leq 2r+1\right\}$ and $\overline{\mathfrak{D}}_{r-1}^{\text{right}}(\xi_i) := \left\{b_{2r+1-s,s}^{i,2}, 0 \leq s \leq r-1\right\}$ are obtained by applying the interpolation conditions at ξ_i (6.6b) (see Fig. 6.2). The remaining two BB-coefficients are computed by imposing the C^{r+1} conditions at ξ_i. □

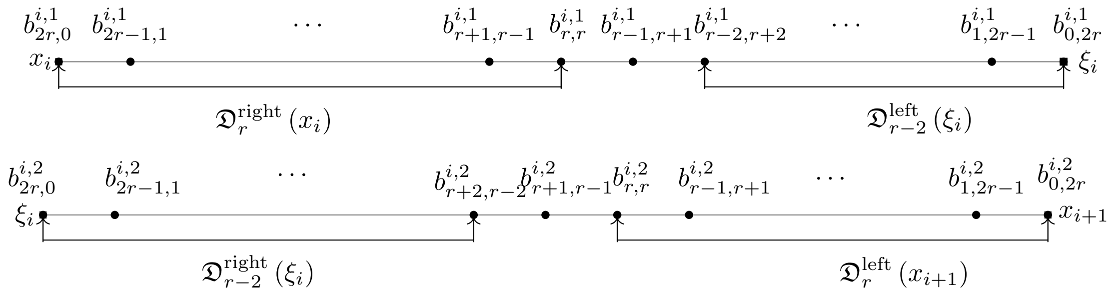

Figure 6.1: BB-coefficients of s_1 relative to the subintervals $[x_i, \xi_i]$ and $[\xi_i, x_{i+1}]$.

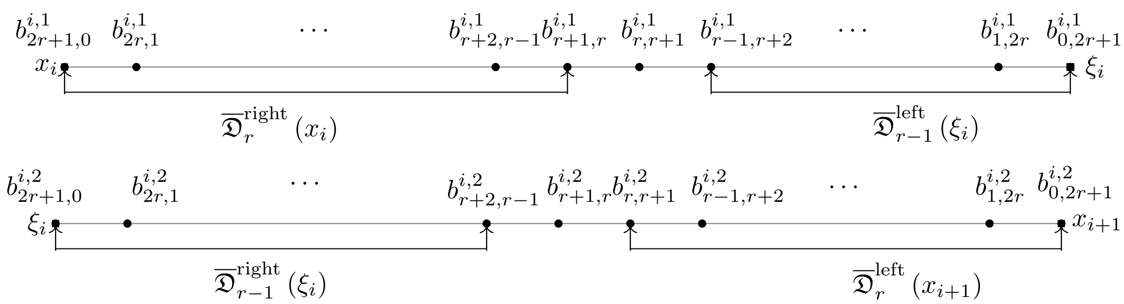

Figure 6.2: BB-coefficients of s_2 relative to the sub-intervals $[x_i, \xi_i]$ and $[\xi_i, x_{i+1}]$.

The dimensions of spaces $S^r_{2r}\left(X^{\text{ref}}_n\right)$ and $S^{r,r+1}_{2r+1}\left(X^{\text{ref}}_n\right)$ follow from Theorem 6.2.1.

Corollary 6.2.2. *It holds that* $\dim S^r_{2r}\left(X^{ref}_n\right) = (2n+1)r+1$ *and* $\dim S^{r,r+1}_{2r+1}\left(X^{ref}_n\right) = (2n+1)r+n+1$.

6.3 B-spline-like bases

To ensure an adequate representation of the functions in the spline space we will look for a basis formed by non-negative locally supported splines forming a partition of unity. For each knot x_i, $0 \le i \le n$, we will construct functions $\mathcal{B}^{\text{kn},i}_{\ell,m} \in S^r_{2r}\left(X^{\text{ref}}_n\right)$ (resp. $\mathcal{D}^{\text{kn},i}_{\ell,m} \in S^{r,r+1}_{2r+1}\left(X^{\text{ref}}_n\right)$), $\ell+m=r$, and for each split point ξ_k, $0 \le k \le n-1$, we will define basis functions $\mathcal{B}^{\text{sp},k}_{\ell,m} \in S^r_{2r}\left(X^{\text{ref}}_n\right)$, $\ell+m=r-2$ (resp. $\mathcal{D}^{\text{sp},k}_{\ell,m} \in S^{r,r+1}_{2r+1}\left(X^{\text{ref}}_n\right)$, $\ell+m=r-1$), so that any splines $s_1 \in S^r_{2r}\left(X^{\text{ref}}_n\right)$ and $s_2 \in S^{r,r+1}_{2r+1}\left(X^{\text{ref}}_n\right)$ can be written in the form

$$s_1 = \sum_{i=0}^{n} \sum_{\ell+m=r} c^{\text{kn},i}_{\ell,m}\, \mathcal{B}^{\text{kn},i}_{\ell,m} + \sum_{k=0}^{n-1} \sum_{\ell+m=r-2} c^{\text{sp},k}_{\ell,m}\, \mathcal{B}^{\text{sp},k}_{\ell,m},$$

$$s_2 = \sum_{i=0}^{n} \sum_{\ell+m=r} \tilde{c}^{\text{kn},i}_{\ell,m}\, \mathcal{D}^{\text{kn},i}_{\ell,m} + \sum_{k=0}^{n-1} \sum_{\ell+m=r-1} \tilde{c}^{\text{sp},k}_{\ell,m}\, \mathcal{D}^{\text{sp},k}_{\ell,m}.$$

These basis functions $\mathcal{B}^{\text{kn},i}_{\ell,m}$ and $\mathcal{D}^{\text{kn},i}_{\ell,m}$ (resp. $\mathcal{B}^{\text{sp},k}_{\ell,m}$ and $\mathcal{D}^{\text{sp},k}_{\ell,m}$) will be called B-splines with respect to the knots (resp. the split points).

The main tool to construct the B-splines is interpolation problem (6.5)-(6.6) by choosing f- and g-values that guarantee that the resulting functions will form a basis of the spline space, are non-negative and locally supported, and constitute a partition of unity.

6.3.1 A basis for $S_{2r}^{r}\left(X_n^{\mathbf{ref}}\right)$

Let x_i be an interior knot. Function $\mathcal{B}_{\ell,m}^{\mathrm{kn},i}$ will be constructed as the solution of a Hermite interpolation problem by specifying appropriate values f_i^q, $0 \le q \le r$, and g_k^q, $0 \le q \le r-2$. Regarding the f-values, let $\mathfrak{B}_{j,k}^{i}$, $j+k=r$, be the $r+1$ Bernstein polynomials of degree r relative to the interval $[S_{i,1}, S_{i,2}]$ given by

$$S_{i,1} := \frac{x_i + x_{i-1}}{2} \quad \text{and} \quad S_{i,2} := \frac{x_i + x_{i+1}}{2}. \tag{6.7}$$

Define

$$\alpha_{j,k}^{i,q} := \frac{\binom{2r}{q}}{\binom{r}{q}} \left(\frac{1}{2}\right)^q D_x^q\, \mathfrak{B}_{j,k}^{i}(x_i),\ \ 0 \le q \le r. \tag{6.8}$$

Definition 6.3.1 (B-splines for an interior knot)**.** *The B-spline $\mathcal{B}_{\ell,m}^{kn,i}$ associated with the interior point x_i is the unique solution of the Hermite spline interpolation problem (6.5) with the following data:*

- *$f_k^q = 0$ for all $k \neq i$, and $f_i^q = \alpha_{\ell,m}^{i,q}$, $0 \le q \le r$, with the α-values are given by (6.8).*
- *$g_k^q = 0$ for all $k \neq i-1, i$, $g_{i-1}^q = \gamma_{\ell,m}^{i-1,q}$ and $g_i^q = \gamma_{\ell,m}^{i,q}$,$0 \le q \le r-2$, where the values $\gamma_{\ell,m}^{i,q}$ are given next in (6.9).*

Let $b_{\ell,m}^{\mathrm{kn},i,1}$, $\ell+m=2r$, be the BB-coefficients of $\mathcal{B}_{\ell,m}^{\mathrm{kn},i}$ relative to the subinterval $[x_i, \xi_i]$.

Since $\mathcal{B}_{\ell,m}^{\mathrm{kn},i}$ is a $\mathcal{C}^r$ function at x_i, its BB-coefficients $b_{2r,0}^{\mathrm{kn},i,1}, \ldots, b_{r,r}^{\mathrm{kn},i,1}$ are completely determined by the values $\alpha_{j,k}^{i,q}$. Similarly, the BB-coefficients $b_{\ell,m}^{\mathrm{kn},i,2}$, $\ell+m=2r$, relative to the subinterval $[\xi_i, x_{i+1}]$ are determined by the interpolation conditions at x_{i+1}, and $b_{r,r}^{\mathrm{kn},i,2}, \ldots, b_{0,2r}^{\mathrm{kn},i,2}$ are all equal to zero (see Fig. 6.3). Let $p_{\ell,m}^{\mathrm{kn},i}$ be the polynomial of degree r defined on the interval $\left[\frac{x_i+\xi_i}{2}, \frac{x_{i+1}+\xi_i}{2}\right]$ having BB-coefficients $b_{r,r}^{\mathrm{kn},i,1}, 0, \ldots, 0$. Then, we define

$$\gamma_{\ell,m}^{q.i} := \frac{\binom{2r}{q}}{\binom{r}{q}} \left(\frac{1}{2}\right)^q D_x^q\, p_{\ell,m}^{\mathrm{kn},i}(\xi_i), \tag{6.9}$$

These values can be computed from the BB-coefficients obtained by subdivision of $p_{\ell,m}^{\mathrm{kn},i}$ by means of De Casteljau's algorithm (6.2).

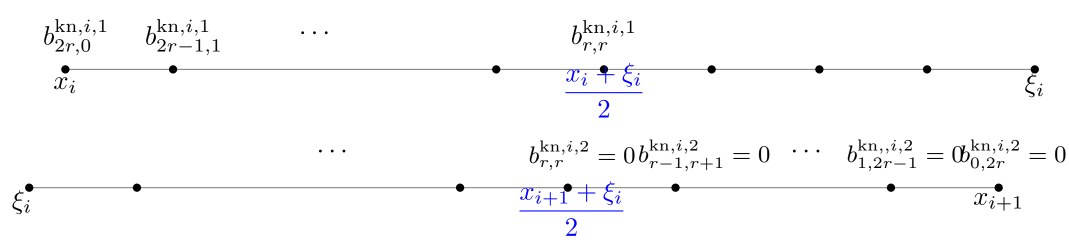

Figure 6.3: BB-coefficients of B-spline $\mathcal{B}_{\ell,m}^{\mathrm{kn},i}$ relative to the sub-intervals $[x_i, \xi_i]$ and $[\xi_i, x_{i+1}]$ for an interior point x_i.

Once the B-splines associated with the knots have been defined, it is time to define those corresponding to the split points. For each ξ_k, let $\mathfrak{B}^k_{\ell,m}$ the $r+1$ Bernstein polynomials of degree r defined on the segment $\left[\frac{x_k+\xi_k}{2}, \frac{x_{k+1}+\xi_k}{2}\right]$. For all $0 \le q \le r-2$, define

$$\beta^{k,q}_{i,j} := \frac{\binom{2r}{q}}{\binom{r}{q}} \left(\frac{1}{2}\right)^q D^q_x \, \mathfrak{B}^k_{r-1-i,\, r-1-j}(\xi_k). \tag{6.10}$$

Definition 6.3.2 (B-splines for a split point)**.** *The B-spline $\mathcal{B}^{sp,k}_{\ell,m}$ associated with the split point ξ_k is the unique solution of the Hermite spline interpolation problem (6.5) such that $f^q_i = 0$, $0 \le q \le r$, for all $i = 0, \ldots, n$, $g^q_i = 0$ when $i \ne k$, and $g^q_k = \beta^{k,q}_{\ell,m}$, $0 \le q \le r-2$.*

6.3.2 A basis for $S^{r,r+1}_{2r+1}\left(X^{\mathbf{ref}}_n\right)$

A similar method is used also in this case. For each interior knot x_i, define the

$$N_{i,1} := \frac{r\,x_i + (r+1)\,x_{i-1}}{2r+1} \text{ and } N_{i,2} := \frac{r\,x_i + (r+1)\,x_{i+1}}{2r+1}, \tag{6.11}$$

and consider the $r+1$ Bernstein polynomials of degree r defined on the segment W_i determined by $N_{i,1}$ and $N_{i,2}$. Then, for $0 \le a \le r$ set

$$\alpha^{i,a}_{j,k} := \frac{\binom{2r+1}{a}}{\binom{r}{a}} \left(\frac{r}{2r+1}\right)^a D^a_x \, \mathfrak{B}^i_{j,k}\left(x_i\right). \tag{6.12}$$

Definition 6.3.3 (B-splines for an interior knot)**.** *The B-spline $\mathcal{D}^{kn,i}_{\ell,m}$ associated with the interior point x_i is the unique solution of the following Hermite spline interpolation problem (6.6) with the following data:*

- *$f^a_k = 0$ for all $k \ne i$, and $f^a_i = \alpha^{i,a}_{\ell,m}$, $0 \le a \le r$, with the α-values given in (6.12).*
- *$g^a_k = 0$ for all $k \ne i-1, i$, $g^a_{i-1} = \gamma^{i-1,a}_{\ell,m}$ and $g^a_i = \gamma^{i,a}_{\ell,m}$,$0 \le a \le r-1$, where the values $\gamma^{i,a}_{\ell,m}$ are given next in (6.13).*

Let $b^{\mathrm{kn},i,1}_{\ell,m}$, $\ell+m = 2r+1$, be the BB-coefficients of $\mathcal{B}^{\mathrm{kn},i}_{\ell,m}$ relative to the subinterval $[x_i, \xi_i]$. Since $\mathcal{B}^{\mathrm{kn},i}_{\ell,m}$ is a $\mathcal{C}^r$ function at x_i, its BB-coefficients $b^{\mathrm{kn},i,1}_{2r+1,0}, \ldots, b^{\mathrm{kn},i,1}_{r+1,r}$ are completely determined by the α-values $\alpha^{i,a}_{j,k}$. Now, let $b^{\mathrm{kn},i,2}_{\ell,m}$, $\ell+m = 2r+1$, be the BB-coefficients of $\mathcal{B}^{\mathrm{kn},i}_{\ell,m}$ with respect to $[\xi_i, x_{i+1}]$. They are determined by the interpolation conditions at x_{i+1}, and $b^{\mathrm{kn},i,2}_{r,r+1}, \ldots, b^{\mathrm{kn},i,2}_{0,2r+1}$ are all equal to zero (see Fig. 6.4).

Let $p^{\mathrm{kn},i}_{\ell,m} \in \mathbb{P}_{2r+1}$ be the polynomial defined on the interval $\left[\frac{(r+1)\,x_i + r\,\xi_i}{2r+1}, \frac{r\,\xi_i + (r+1)\,x_{i+1}}{2r+1}\right]$ having BB-coefficients $b^{\mathrm{kn},i,1}_{r+1,r}, 0, \ldots, 0$. Then, we define

$$\gamma^{k,a}_{\ell,m} := \frac{\binom{2r+1}{a}}{\binom{r+1}{a}} \left(\frac{r+1}{2r+1}\right)^a D^a_x \, p(\xi_k). \tag{6.13}$$

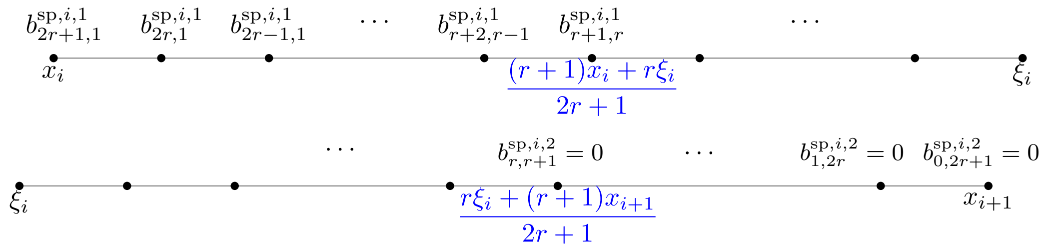

Figure 6.4: BB-coefficients of B-spline $\mathcal{B}^{\mathrm{sp},i}_{\ell,m}$ relative to the sub-intervals $[x_i, \xi_i]$ and $[\xi_i, x_{i+1}]$ for an interior point x_i.

Also in this case, the γ-values can be computed from the BB-coefficients obtained by subdivision of $p^{\mathrm{kn},i}_{\ell,m}$ by means of the De Casteljau's algorithm (6.2).

For each split point ξ_k, consider the $r+2$ Bernstein polynomials of degree $r+1$ defined on the segment $\left[\dfrac{(r+1)\,x_k + r\,\xi_k}{2r+1}, \dfrac{(r+1)\,x_{k+1} + r\,\xi_k}{2r+1}\right]$. For $0 \le a \le r-1$, define

$$\beta^{k,a}_{i,j} := \frac{\binom{2r+1}{a}}{\binom{r+1}{a}} \left(\frac{r+1}{2r+1}\right)^a D^a_x\, \mathfrak{B}^k_{r-i,\, r-j}\,(\xi_k)\,. \tag{6.14}$$

Definition 6.3.4 (B-splines for a split point)**.** *The B-spline $\mathcal{D}^{sp,k}_{\ell,m}$ associated with the split point ξ_k is the unique solution of the Hermite spline interpolation problem (6.6) such that $f^a_i = 0$, $0 \le a \le r$, for all $i = 0, \ldots, n$, $g^a_i = 0$ when $i \ne k$, and $g^a_k = \beta^{k,a}_{\ell,m}$, $0 \le a \le r-1$, where the β-values are given in (6.14).*

Figures 6.5 shows the quartic B-splines associated with the points $x_0 = 0$ and $x_n = 1$ of a partition of the interval $[0,1]$, as well as the B-splines relative to the point $1/2$. Figure 6.6 shows similar B-splines in the cubic case.

Remark 6.3.5. *Boundary B-splines basis for $S^r_{2r}\left(X^{ref}_n\right)$ and $S^{r,r+1}_{2r+1}\left(X^{ref}_n\right)$ are constructed according to the same procedure outlined in Subsections 6.3.1 and 6.3.2, respectively. For $S^r_{2r}\left(X^{ref}_n\right)$, the B-spline with respect to vertex x_0 (resp. x_n) is constructed according to the procedure in Subsection 6.3.1 with a particular choice of points in (6.7), namely $S_{0,1} = x_0$ and $S_{0,2} = \dfrac{x_0 + x_1}{2}$ (resp. $S_{n,1} = \dfrac{x_{n-1} + x_n}{2}$ and $S_{n,2} = x_n$). The same procedure is used for the B-splines in $S^{r,r+1}_{2r+1}\left(X^{ref}_n\right)$. Now, the boundary points in (6.11) are $N_{0,1} = x_0$ and $N_{n,2} = x_n$.*

6.4 Marsden's identity

Any B-spline $\mathcal{B}^{\mathrm{kn},i}_{\ell,m}$ and $\mathcal{D}^{\mathrm{kn},i}_{\ell,m}$, $\ell + m = r$, with respect to a knot x_i is related to some Bernstein polynomials of degree r, as shown in (6.8) and (6.12). Furthermore, the spline coefficients $c^{\mathrm{kn},i}_{\ell,m}$, $\ell + m = r$, corresponding to $\mathcal{B}^{\mathrm{kn},i}_{\ell,m}$ or $\mathcal{D}^{\mathrm{kn},i}_{\ell,m}$ can be considered as the BB- coefficientes of a polynomial of degree r defined over the interval $[S_{i,1}, S_{i,2}]$. This control polynomial with respect to the knot x_i is then defined as

$$T^r_i\,(x) := \sum_{\ell+m=r} c^{\mathrm{kn},i}_{\ell,m}\, \mathfrak{B}^r_{\ell,m}\,(x)\,,\ x \in [S_{i,1}, S_{i,2}]\,. \tag{6.15}$$

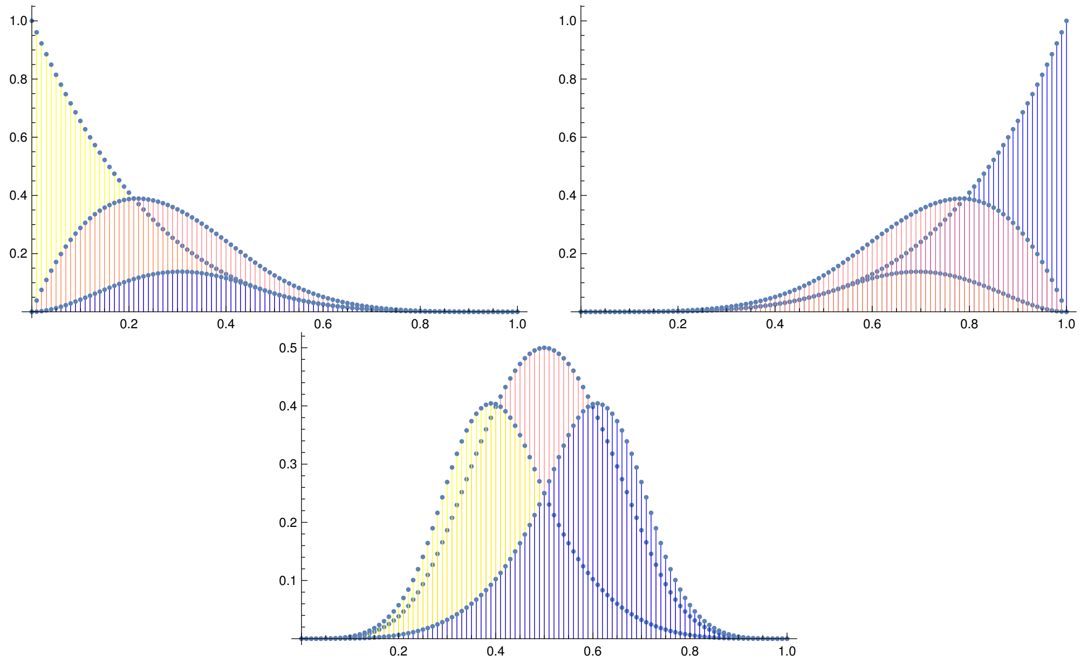

Figure 6.5: Quartic B-splines associated with the boundary points $x_0 = 0$ (top, left) and $x_n = 1$ (top, right), B-splines relative to the interior point 1/2 (bottom)

.

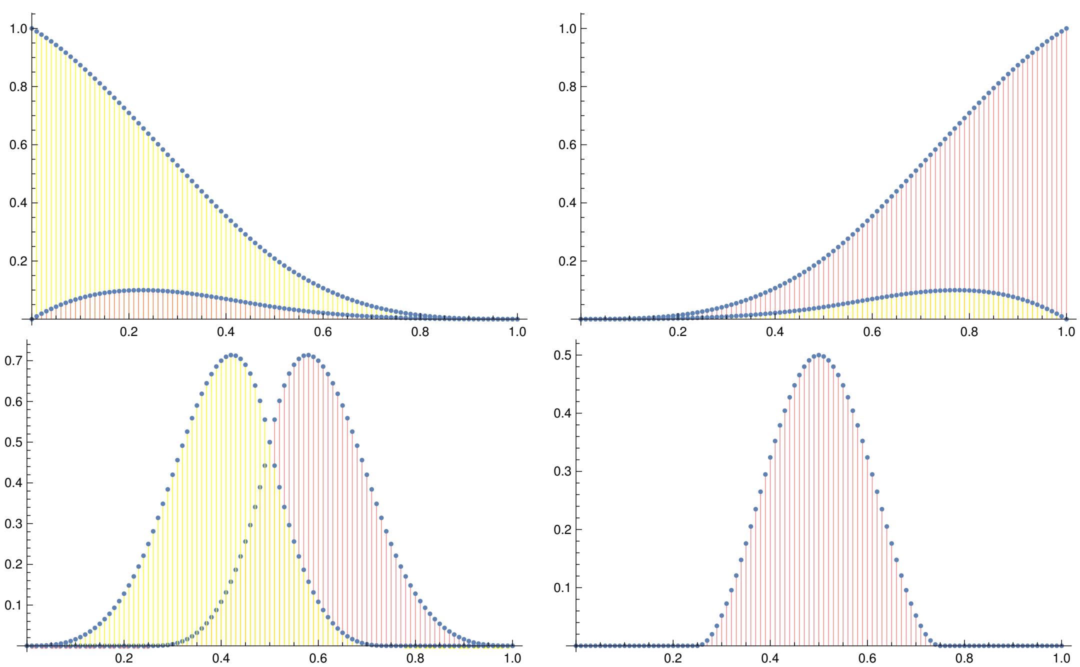

Figure 6.6: Cubic B-splines associated with the boundary points $x_0 = 0$ (top, left) and $x_n = 1$ (top, right), B-splines relative to the interior point 1/2 (bottom, left) and B-spline with respect to the split point 1/2 (bottom, right)

.

Taking into account the definitions given in (6.8) for $s \in S^r_{2r}$ and $0 \le a \le r$ it holds

$$\begin{aligned} D^a_x\, s\,(x_i) &= \sum_{\ell+m=r} c^{\mathrm{kn},i}_{\ell,m}\, \alpha^{i,a}_{\ell,m} \\ &= \frac{\binom{2r}{a}}{\binom{r}{a}} \left(\frac{1}{2}\right)^a \sum_{l+m=r} c^{\mathrm{kn},i}_{\ell,m}\, D^a_x\, \mathfrak{B}^{\mathrm{kn},i}_{\ell,m}(x_i) \\ &= \frac{\binom{2r}{a}}{\binom{r}{a}} \left(\frac{1}{2}\right)^a D^a_x\, T^r_i\,(x_i). \end{aligned} \tag{6.16}$$

Analogously, by (6.12), if $s \in S^{r,r+1}_{2r+1}$, then

$$D^a_x\, s\,(x_i) = \frac{\binom{2r+1}{a}}{\binom{r}{a}} \left(\frac{r}{2r+1}\right)^a D^a_x\, T^r_i\,(x_i)\,.$$

Since $s\,(x_i) = T^r_i\,(x_i)$ and $D_x\, s(x_i) = D_x\, T^r_i\,(x_i)$, we have the following result.

Theorem 6.4.1. *The curve of the control polynomial T^r_i is tangent to the curve of s at the vertex x_i.*

In order to get an overview of the definition of many knot B-splines-like defined here, the following result is first considered. The m-order directional derivative of a polynomial $p \in \mathbb{P}_d$ with respect to the unit barycentric directions $\delta_i,\ i = 1, \ldots, m$, related to the interval I can be briefly expressed as follows [41, 47]:

$$D^m_{\delta_1,\ldots,\delta_m}\, p\,(\tau) = \frac{d!}{(d-m)!}\, \mathbf{B}\,[p]\,(\tau[d-m], \delta_1, \ldots, \delta_m)\,. \tag{6.17}$$

If $b_{i,j},\ i + j\ = d$, denote the BB-coefficients of p, then

$$\mathbf{B}\,[p]\left(\tau^1, \ldots, \tau^d\right) = \sum_{i+j=d} b_{i,j} \sum_{\pi\in\,\Pi^d_{i,j}} \prod_{l=1}^{d} \tau^l_{\pi(l)}, \tag{6.18}$$

where $\Pi^d_{i,j}$ stands for the set of permutations of $(1[i], 2[j])$.

Theorem 6.4.2. *Let p_1 be a polynomial of degree d_1 defined on the interval $[x_1,\, x_2]$, and p_2 be a polynomial of degree d_2 and defined on the interval $[x_1,\, y_1]$, where $d_2 \le d_1$ and*

$$y_1 := (1-\theta)\, x_1 + \theta\, x_2,$$

where $\theta \in \mathbb{R}$.

Denote by $b_{i,j},\ i+j = d_1$, the BB-coefficients of p_1, and $d_{i,j},\ i+j = d_2$, those of p_2.. Then,

$$D^a_x\, p_1(x_1) = \frac{\binom{d_1}{a}}{\binom{d_2}{a}}\, \theta^a\, D^a_x\, p_2\,(x_i)\,, \tag{6.19}$$

for all $0 \le a \le \mu$ with $0 \le \mu \le d_2$ if and only if

$$b_{d_1-\mu+i,j}\ = d_{d_2-\mu+i,j}, \tag{6.20}$$

for all $(i, j) \in \mathbb{N}^2$ with $i + j\ = \mu$.

Proof. Let ρ and ϱ be the unit barycentric directions with respect to the intervals $[x_1,\, x_2]$ and $[x_1,\, y_1]$, respectively. In view of the definition of the intervals, it is clear that

$$\theta\, \varrho = \rho.$$

By (6.17), we have

$$D_x^a\, p_1\,(x_1) = \frac{d_1!}{(d_1-a)!}\, \mathbf{B}\,[p_1]\,(e_1[d_1-a],\, \rho[a])\,.$$

From the relation between ρ and ϱ, we deduce that

$$D_x^a\, p_2\,(x_1) = \frac{d_2!}{(d_2-a)!}\, \mathbf{B}\,[p_2]\,(e_1[d_2-a],\, \varrho[a]) = \frac{d_2!}{(d_2-a)!}\, \frac{1}{\theta^a}\, \mathbf{B}\,[p_2]\,(e_1[d_2-a],\, \rho[a])\,.$$

In light of (6.19), for all $0 \le a \le \mu$ it follows that

$$\begin{aligned} &\frac{d_1!}{(d_1-a)!}\, \mathbf{B}\,[p_1]\,(e_1[d_1-\mu],\, e_1[\mu-a],\, \rho[a]) \\ &= \frac{\binom{d_1}{a}}{\binom{d_2}{a}}\, \theta^a\, \frac{d_2!}{(d_2-a)!}\, \frac{1}{\theta^a}\, \mathbf{B}\,[p_2]\,(e_1[d_2-\mu],\, e_1[\mu-a],\, \rho[a])\,, \end{aligned}$$

then

$$\mathbf{B}\,[p_1]\,(e_1[d_1-\mu],\, e_1[\mu-a],\, \rho[a]) = \mathbf{B}\,[p_2]\,(e_1[d_2-\mu],\, e_1[\mu-a],\, \rho[a])\,,$$

and, by (6.18), for all $0 \le a \le \mu$ it holds

$$\sum_{i+j=\mu} b_{d_1-\mu+i,j} \sum_{\pi\in\Pi^{\mu}_{i,j}} \prod_{l=1}^{\mu-a} e_{1,\pi(l)} \prod_{l=\mu-a+1}^{\mu} \rho_{\pi(l)} = \sum_{i+j=\mu} d_{d_2-\mu+i,j} \sum_{\pi\in\Pi^{\mu}_{i,j}} \prod_{l=1}^{\mu-a} e_{1,\pi(l)} \prod_{l=\mu-a+1}^{\mu} \rho_{\pi(l)}.$$

There are $\mu+1$ linearly independent constraints that only involve the BB-coefficients $b_{d_1-\mu+i,j}$ and $d_{d_2-\mu+i,j}$, for $i+j=\mu$. Then, this linear system implies (6.20). □

Next result concerns the representation the splines in the spaces analysed above. It is the main tool to construct differential and integral quasi-interpolants.

Theorem 6.4.3 (Marsden's identity)**.** *Each splines $s_1 \in S^r_{2r}\left(X^{ref}_n\right)$ and $s_2 \in S^{r,r+1}_{2r+1}\left(X^{ref}_n\right)$ can be represented as*

$$s_1 = \sum_{i=0}^{n} \sum_{\ell+m=r} c^{kn,i}_{\ell,m}\, \mathcal{B}^{kn,i}_{\ell,m} + \sum_{k=0}^{n-1} \sum_{\ell+m=r-2} c^{sp,k}_{\ell,m}\, \mathcal{B}^{sp,k}_{\ell,m}, \tag{6.21}$$

$$s_2 = \sum_{i=0}^{n} \sum_{\ell+m=r} \tilde{c}^{kn,i}_{\ell,m}\, \mathcal{D}^{kn,i}_{\ell,m} + \sum_{k=0}^{n-1} \sum_{\ell+m=r-1} \tilde{c}^{sp,k}_{\ell,m}\, \mathcal{D}^{sp,k}_{\ell,m}, \tag{6.22}$$

where

$$\begin{aligned} c^{kn,i}_{\ell,m} &:= \mathbf{B}\left[s_{1|[x_i,\xi_i]}\right]\left(x_i[r],\, \hat{S}_{i,1}[\ell],\, \hat{S}_{i,2}[m]\right), \\ c^{sp,k}_{\ell,m} &:= \mathbf{B}\left[s_{1|[x_k,\xi_k]}\right](\xi_k[r],\, x_k[r-1-\ell],\, x_{k+1}[r-1-m])\,, \\ \tilde{c}^{kn,i}_{\ell,m} &:= \mathbf{B}\left[s_{2|[x_i,\xi_i]}\right]\left(x_i[r+1],\, \hat{N}_{i,1}[\ell],\, \hat{N}_{i,2}[m]\right), \\ \tilde{c}^{sp,k}_{\ell,m} &:= \mathbf{B}\left[s_{2|[x_k,\xi_k]}\right](\xi_k[r],\, x_k[r-\ell],\, x_{k+1}[r-m])\,, \end{aligned}$$

with $\hat{S}_{i,j} := 2\, S_{i,j} - x_i$ *and, for* $j = 1, 2$,

$$\hat{N}_{i,j} := \left(1 + \frac{r}{r+1}\right) N_{i,j} - \frac{r}{r+1} x_i,$$

being $S_{i,j}$ *and* $N_{i,j}$ *the points given in (6.7) and (6.11), respectively.*

Proof. Here, we give only the proof in the case where $s \in S_{2r}^r\left(X_n^{\text{ref}}\right)$. A similar approach can be followed in the other case. Let T_i^r be the control polynomial (6.15) of a spline $s \in S_{2r}^r\left(X_n^{\text{ref}}\right)$ at x_i. Then, by Theorem 6.4.2,

$$D_x^a\, s(x_i) = \frac{\binom{2r}{a}}{\binom{r}{a}} \left(\frac{1}{2}\right)^a D_x^a\, T_i^r(x_i),$$

for all $0 \le \mu \le r$ and $0 \le a \le \mu$, if and only if

$$b_{2r-\mu+i,j} = d_{r-\mu+i,j},$$

for all $(i, j) \in \mathbb{N}^2$ with $i + j = \mu$, where $b_{i,j}$, $i + j = 2r$, are the BB-coefficients of s, and $d_{i,j}$, $i + j = r$, are the BB-coefficients of T_i^r. This equivalent to the condition

$$\mathbf{B}\left[T_i^r\right]\left(\tau^1, \ldots, \tau^r\right) = \mathbf{B}\left[s_{1|[x_i,\xi_i]}\right]\left(e_1[r],\, \tau[r]\right) \tag{6.23}$$

for any set of barycentric coordinates $\tau^1, \ldots, \tau^r$. It is known that

$$c_{\ell,m}^{\text{kn},i} = \mathbf{B}\left[T_i^r\right]\left(S_{i,1}[\ell],\, S_{i,2}[m]\right) = \mathbf{B}\left[T^r_{i|[x_i,S_{i,2}]}\right]\left(\tau^{i,1}[\ell],\, e_2[m]\right),$$

where $S_{i,1} = \tau_1^{i,1}\, x_i + \tau_2^{i,1} S_{i,2}$, $\tau_1^{i,1} + \tau_1^{i,2} = 1$, and $S_{i,2} = 0\, x_i + S_{i,2}$. One can easily verify that

$$\hat{S}_{i,1} = \tau_1^{i,1}\, x_i + \tau_2^{i,1}\, x_{i+1} \text{ and } \hat{S}_{i,2} = 0\, x_i + x_{i+1}.$$

By (6.23), it follows that

$$\begin{aligned} c_{\ell,m}^{\text{kn},i} &= \mathbf{B}\left[T^r_{i|[x_i,S_{i,2}]}\right]\left(\tau^{i,1}[\ell],\, e_2[m]\right) = \mathbf{B}\left[s_{1|[x_i,x_{i+1}]}\right]\left(e_1[r],\, \tau^{i,1}[\ell],\, e_2[m]\right) \\ &= \mathbf{B}\left[s_{1|[x_i,x_{i+1}]}\right]\left(x_i[r],\, S_{i,1}[\ell],\, \hat{S}_{i,2}[m]\right) \end{aligned}$$

which concludes the proof. □

Regarding the points $\hat{S}_{i,1}$, $\hat{S}_{i,2}$, $\widehat{N}_{i,1}$ and $\widehat{N}_{i,2}$ involved in Theorem 6.4.3, note that by (6.7) and (6.11), we get

$$\hat{S}_{i,1} = 2S_{i,1} - x_i = x_{i-1} \quad \text{and} \quad \hat{S}_{i,2} = 2S_{i,2} - x_i = x_{i+1},$$

as well as

$$\hat{N}_{i,1} = \frac{2r+1}{r+1} N_{i,1} - \frac{r}{r+1} x_i = x_{i-1} \quad \text{and} \quad \hat{N}_{i,2} = \frac{2r+1}{r+1} N_{i,2} - \frac{r}{r+1} x_i = x_{i+1}.$$

For boundary knots, we have $S_{0,1} = x_0$ and $N_{n,2} = x_n$. Then, $\hat{S}_{0,1} = x_0$ and $\hat{N}_{n,2} = x_n$.

Next, we define points that will allow to express the monomial of the first degree in the bases of $S_{2r}^r\left(X_n^{\text{ref}}\right)$ and $S_{2r+1}^{r,r+1}\left(X_n^{\text{ref}}\right)$ as a direct application of Theorem 6.4.3. For $i = 0, \ldots, n$, $k = 0, \ldots, n-1$, $\ell + m = r - 2$,

$$P_{\ell,m}^{i,\text{even}} := \frac{\ell}{r} S_{i,1} + \frac{m}{r} S_{i,2}, \quad P_{\ell,m}^{i,\text{odd}} := \frac{\ell}{r} N_{i,1} + \frac{m}{r} N_{i,2}, \tag{6.24}$$

and, for $i=0,\dots,n$, $k=0,\dots,n-1$, $\ell+m=r-2$, $\ell^*+m^*=r-1$,

$$Q^{k,\text{even}}_{\ell,m} := \frac{r-1-\ell}{r}V_{k,1} + \frac{r-1-m}{r}V_{k,2}, \quad Q^{k,\text{odd}}_{\ell,m} := \frac{r-\ell^*}{r+1}\widetilde{V}_{k,1} + \frac{r-m^*}{r+1}\widetilde{V}_{k,2}, \tag{6.25}$$

where $S_{i,1}$, $S_{i,2}$, $N_{i,1}$ and $N_{i,2}$ are defined in (6.7) and (6.11),

$$V_{i,1} := \frac{x_i+\xi_i}{2}, V_{i,2} := \frac{x_{i+1}+\xi_i}{2}, \widetilde{V}_{i,1} := \frac{(r+1)\,x_i + r\,\xi_i}{2r+1} \text{ and } \widetilde{V}_{i,2} := \frac{(r+1)\,x_{i+1} + r\,\xi_i}{2r+1}.$$

Theorem 6.4.4. *Let $P^{i,even}_{\ell,m}$, $P^{i,odd}_{\ell,m}$, $Q^{k,even}_{\ell,m}$ and $Q^{k,odd}_{\ell,m}$ be the points defined in (6.24) and (6.25). Then,*

$$x = \sum_{i=0}^{n}\sum_{\ell+m=r} P^{i,even}_{\ell,m}\,\mathcal{B}^{kn,i}_{\ell,m}(x) + \sum_{k=0}^{n-1}\sum_{\ell+m=r-2} Q^{k,even}_{\ell,m}\,\mathcal{B}^{sp,k}_{\ell,m}(x), \tag{6.26}$$

$$x = \sum_{i=0}^{n}\sum_{\ell+m=r} P^{i,odd}_{\ell,m}\,\mathcal{D}^{kn,i}_{\ell,m}(x) + \sum_{k=0}^{n-1}\sum_{\ell+m=r-1} Q^{k,odd}_{\ell,m}\,\mathcal{D}^{sp,k}_{\ell,m}(x). \tag{6.27}$$

Proof. Let $s_1(x)=x$ be the spline in the left-hand side in (6.26). Applying Theorem 6.4.3, we can write

$$\begin{aligned} s_1 &= \sum_{i=0}^{n}\sum_{\ell+m=r} \mathbf{B}\left[s_{1|[x_i,\xi_i]}\right](x_i[r],\, x_{i-1}[\ell],\, x_{i+1}[m])\,\mathcal{B}^{\text{kn},i}_{\ell,m} \\ &\quad + \sum_{k=0}^{n-1}\sum_{\ell+m=r-2} \mathbf{B}\left[s_{1|[x_k,\xi_k]}\right](\xi_k[r],\, x_k[r-1-\ell],\, x_{k+1}[r-1-m])\,\mathcal{B}^{\text{sp},k}_{\ell,m} \end{aligned}$$

Using Proposition 6.5.1, and for $\ell+m=r$, we have

$$\begin{aligned} \mathbf{B}\left[s_{1|[x_i,\xi_i]}\right](x_i[r],\, x_{i-1}[\ell],\, x_{i+1}[m]) &= s_1(x_i) + \frac{1}{2r}\left(\ell\, D_{x_{i-1}-x_i}s_1(x_i) + m\, D_{x_{i+1}-x_i}s_1(x_i)\right), \\ &= x_i + \frac{1}{2r}\left(\ell(x_{i-1}-x_i) + m(x_{i+1}-x_i)\right), \\ &= \frac{1}{r}\left(\ell\frac{x_i+x_{i-1}}{2} + m\frac{x_i+x_{i+1}}{2}\right), \\ &= P^{i,\text{even}}_{\ell,m}. \end{aligned}$$

Similarly, we get the expression of the remind points. □

6.4.1 Some properties of the B-splines

The construction of the B-splines $\mathcal{B}^{\text{kn},i}_{\ell,m}$, $\mathcal{B}^{\text{sp},k}_{\ell,m}$, $\mathcal{D}^{\text{kn},i}_{\ell,m}$ and $\mathcal{D}^{\text{sp},k}_{\ell,m}$ shows that they are compactly supported functions. More precisely, $\mathcal{B}^{\text{kn},i}_{\ell,m}$ and $\mathcal{D}^{\text{kn},i}_{\ell,m}$ are supported on the interval $[x_{i-1},x_{i+1}]$, while the supports of $\mathcal{B}^{\text{sp},k}_{\ell,m}$ and $\mathcal{D}^{\text{sp},k}_{\ell,m}$ are the interval $[x_k,x_{k+1}]$.

As said before, an essential property in many fields is that the elements at the basis of the space of spline functions form a convex partition of unity. This property is stated and proved in the following two results.

Theorem 6.4.5. *It holds that*

$$1 = \sum_{i=0}^{n}\sum_{\ell+m=r}\mathcal{B}^{kn,i}_{\ell,m} + \sum_{k=0}^{n-1}\sum_{\ell+m=r-2}\mathcal{B}^{sp,k}_{\ell,m}. \tag{6.28}$$

and

$$1 = \sum_{i=0}^{n}\sum_{\ell+m=r}\mathcal{D}^{kn,i}_{\ell,m} + \sum_{k=0}^{n-1}\sum_{\ell+m=r-1}\mathcal{D}^{sp,k}_{\ell,m}. \tag{6.29}$$

Proof. As the constant 1 is an element of $S_{2r}^{r}\left(X_n^{\mathrm{ref}}\right)$ and $S_{2r+1}^{r,r+1}\left(X_n^{\mathrm{ref}}\right)$, by (6.21) it can be written as a linear combination of the basis in each space with coefficients given by the polar forms of its restrictions to the subintervals $[x_i, \xi_i]$ and $[\xi_i, x_{i+1}]$. Since the blossom of 1 is equal to one irrespectively of the arguments, all coefficients are equal to one. □

Theorem 6.4.6. *All the B-splines $\mathcal{B}_{\ell,m}^{kn,i}$, $\mathcal{B}_{\ell,m}^{sp,k}$, $\mathcal{D}_{\ell,m}^{kn,i}$ and $\mathcal{D}_{\ell,m}^{sp,k}$ are non-negative.*

Proof. It is enough to prove that the BB-coefficients of the B-splines are non-negative on a single interval $[x_i, x_{i+1}]$. For each B-spline $\mathcal{B}_{\ell,m}^{\mathrm{kn},i}$ with respect to the knot x_i, its BB-coefficients in $\mathfrak{D}_r^{\mathrm{right}}(x_i)$ can be seen after subdivision as BB-coefficients of a Bernstein polynomial defined on $[S_{i,1}, S_{i,2}]$. Note that the domain points associated with $\mathfrak{D}_r^{\mathrm{right}}(x_i)$ lie in $[S_{i,1}, S_{i,2}]$. Hence, the barycentric coordinates of these points with respect to $[S_{i,1}, S_{i,2}]$ are non-negative.

On the other hand, the BB-coefficients in the subset $\mathfrak{D}_r(\xi_i)$ given by the union without repetition of $\mathfrak{D}_r^{\mathrm{right}}(\xi_i)$ and $\mathfrak{D}_r^{\mathrm{left}}(\xi_i)$ can also be seen after subdivision as BB-coefficients of a polynomial of degree r defined on $\left[\dfrac{x_i+\xi_i}{2}, \dfrac{\xi_i+x_{i+1}}{2}\right]$. Let $b_{i,j}$, $i+j=r$, be the BB-coefficients of this polynomial. Only the BB-coefficient in $\mathfrak{D}_0^{\mathrm{right}}(\dfrac{x_i+\xi_i}{2}) = \mathfrak{D}_0^{\mathrm{left}}(\dfrac{x_i+\xi_i}{2})$, i.e. $b_{r,0} := b_{r,r}^{i,1}$, is non null (see Fig. 6.1). However, this non-zero BB-coefficient is uniquely derived from the values $\alpha_{\ell,m}^{i,q}$, which implies that all the BB-coefficients in $\mathfrak{D}_r(\xi_i)$ are also non-negative.

The BB-coefficients in $\mathfrak{D}_r(\xi_k)$ of B-spline $\mathcal{B}_{\ell,m}^{\mathrm{sp},k}$ can be seen after subdivision as BB-coefficients of the Bernstein basis $\mathfrak{B}_{r-1-i,r-1-j}^{k}$ of degree r defined on $\left[\dfrac{x_k+\xi_k}{2}, \dfrac{\xi_k+x_{k+1}}{2}\right]$, and

$$D_x^a \,\mathfrak{B}_{r-1-i,r-1-j}^{k}(x_{k+l}) = 0$$

for all $0 \le a \le r$ and $l = 0,1$, which implies that the BB-coefficients in $\mathfrak{D}_r^{\mathrm{left}}\left(\dfrac{x_k+\xi_k}{2}\right)$ and $\mathfrak{D}_r^{\mathrm{right}}\left(\dfrac{x_{k+1}+\xi_k}{2}\right)$ are all equal to zero.

From the non-negativity of the Bernstein polynomials on their domain interval, we conclude that the considered BB-coefficients are non-negative. □

6.5 Quasi-interpolation schemes

In this section, Marsden's identity will allow to introduce some methods for constructing quasi-interpolants of the form

$$\mathcal{Q}^r f := \sum_{i=0}^{n} \sum_{\ell+m=r} \mu_{\ell,m}^{\mathrm{kn},i}(f)\, \mathcal{B}_{\ell,m}^{\mathrm{kn},i} + \sum_{k=0}^{n-1} \sum_{\ell+m=r-2} \nu_{\ell,m}^{\mathrm{sp},k}(f)\, \mathcal{B}_{\ell,m}^{\mathrm{sp},k}, \tag{6.30}$$

$$\tilde{\mathcal{Q}}^r f := \sum_{i=0}^{n} \sum_{l+m=r} \tilde{\mu}_{\ell,m}^{\mathrm{kn},i}(f)\, \mathcal{D}_{\ell,m}^{\mathrm{kn},i} + \sum_{k=0}^{n-1} \sum_{\ell+m=r-1} \tilde{\nu}_{\ell,m}^{\mathrm{sp},k}(f)\, \mathcal{D}_{\ell,m}^{\mathrm{sp},k},$$

and satisfying $\mathcal{Q}^r p = p$ for all $p \in \mathbb{P}_{2r}$ and $\tilde{\mathcal{Q}}^r p = p$ for all $p \in \mathbb{P}_{2r+1}$, being $\mu_{\ell,m}^{\mathrm{kn},i}$, $\nu_{\ell,m}^{\mathrm{sp},k}$, $\tilde{\mu}_{\ell,m}^{\mathrm{kn},i}$ and $\tilde{\nu}_{\ell,m}^{\mathrm{sp},k}$ suitable linear functionals.

6.5.1 Differential quasi-interpolation operator

Firstly, we recall a result that shows a connection between blossoming and directional derivatives [47].

Proposition 6.5.1. *Let u, v_i, $i = 1, \ldots, \ell$, be some points in $\mathbb{R}$. For any polynomial $p \in \mathbb{P}_d$, we have*

$$\mathbf{B}\,[p]\,(u[d-\ell],\, v_1,\, \ldots,\, v_\ell) = \sum_{i=0}^{\ell} \frac{(d-\ell+i)!}{d!} \sum_{\substack{S\subseteq\{\delta_1 \cdots,\delta_\ell\} \\ |S|=\ell-i}} D_S p\,(u)\,,$$

where $\delta_i := v_i - u$.

From the functional defined as

$$\mathbf{N}\,[f]\,(u[d-\ell],\, v_1, \ldots,\, v_\ell) := \sum_{i=0}^{\ell} \frac{(d-\ell+i)!}{d!} \sum_{\substack{S\subseteq\{\delta_1 \cdots,\delta_\ell\} \\ |S|=\ell-i}} D_S f\,(u) \tag{6.31}$$

we define linear functionals providing quasi-interpolation operators.

Theorem 6.5.2. *Let us define*

$$\begin{aligned}
\mu_{\ell,m}^{kn,i}\,(f) &:= \mathbf{N}\,[f]\,(x_i[r],\, x_{i-1}[\ell],\, x_{i+1}[m])\,,\\
\nu_{\ell,m}^{sp,k}\,(f) &:= \mathbf{N}\,[f]\,(\xi_k[r],\, x_k[r-1-\ell],\, x_{k+1}[r-1-m])\,,\\
\widetilde{\mu}_{\ell,m}^{kn,i}\,(f) &:= \mathbf{N}\,[f]\,(x_i[r+1],\, x_{i-1}[\ell],\, x_{i+1}[m])\,,\\
\widetilde{\nu}_{\ell,m}^{sp,k}\,(f) &:= \mathbf{N}\,[f]\,(\xi_k[r],\, x_k[r-\ell],\, x_{k+1}[r-m])\,.
\end{aligned}$$

Then, the operators $\mathcal{Q}^r$ and $\tilde{\mathcal{Q}}^r$ defined by (6.30) are exact on $\mathbb{P}_{2r}$ and $\mathbb{P}_{2r+1}$, respectively.

Proof. From Proposition 6.5.1 and (6.31), it is easy to see that

$$\mathbf{N}\,[p]\,(x_i[r],\, x_{i-1}[\ell],\, x_{i+1}[m]) = \mathbf{B}\,[p]\,(x_i[r],\, x_{i-1}[\ell],\, x_{i+1}[m])$$

and

$$\mathbf{N}\,[p]\,(\xi_k[r],\, x_k[r-1-\ell],\, x_{k+1}[r-1-m]) = \mathbf{B}\,[p]\,(\xi_k[r],\, x_k[r-1-\ell],\, x_{k+1}[r-1-m])$$

for all $p \in \mathbb{P}_{2r}$. Applying Theorem 6.4.3, we get

$$\mathcal{Q}^r p = p, \text{ for all } p \in \mathbb{P}_{2r}.$$

The same approach is used to prove that the proposed operator is exact on $\mathbb{P}_{2r+1}$. □

6.5.2 Discrete quasi-interpolation operator

Polarization with constant coefficients can be used to obtain functions in the form of a linear combination of discrete values. According to [87, Section 8.7, p.17], the following polarization identity is obtained:

$$\mathbf{B}\,[p]\,(u_1,\, \ldots,\, u_d) \;=\; \frac{1}{d!} \sum_{\substack{S\subset\{1,\cdots,d\} \\ k=|S|}} (-1)^{d-k}\; k^d\, p\left(\tfrac{1}{k} \sum_{i\,\in\,S} u_i\right). \tag{6.32}$$

Let us define the operator

$$\mathbf{M}\,[f]\,(u_1,\, \ldots,\, u_d) \;=\; \frac{1}{d!} \sum_{\substack{S\subset\{1,\cdots,d\} \\ k=|S|}} (-1)^{d-k}\; k^d\, f\left(\tfrac{1}{k} \sum_{i\,\in\,S} u_i\right).$$

From Marsden's identity, we have the following result.

Theorem 6.5.3. *Let*

$$\begin{aligned}
\mu_{\ell,m}^{kn,i}(f) &:= \mathbf{M}[f](x_i[r],\, x_{i-1}[\ell],\, x_{i+1}[m]),\\
\nu_{\ell,m}^{sp,k}(f) &:= \mathbf{M}[f](\xi_k[r],\, x_k[r-1-\ell],\, x_{k+1}[r-1-m]),\\
\widetilde{\mu}_{\ell,m}^{kn,i}(f) &:= \mathbf{M}[f](x_i[r+1],\, x_{i-1}[\ell],\, x_{i+1}[m]),\\
\widetilde{\nu}_{\ell,m}^{sp,k}(f) &:= \mathbf{M}[f](\xi_k[r],\, x_k[r-\ell],\, x_{k+1}[r-m]).
\end{aligned}$$

Then, the operators $\mathcal{Q}^r$ and $\tilde{\mathcal{Q}}^r$ defined by (6.30) are exact on $\mathbb{P}_{2r}$ and $\mathbb{P}_{2r+1}$, respectively.

Proof. It is clear that

$$\mathbf{M}[p](x_i[r],\, x_{i-1}[\ell],\, x_{i+1}[m]) = \mathbf{B}[p](x_i[r],\, x_{i-1}[\ell],\, x_{i+1}[m])$$

and

$$\mathbf{M}[p](\xi_k[r], x_k[r-1-\ell],\, x_{k+1}[r-1-m]) = \mathbf{B}[p](\xi_k[r], x_k[r-1-\ell],\, x_{k+1}[r-1-m])$$

for all $p \in \mathbb{P}_{2r}$. Then, by applying Theorem 6.4.3, one can obtains

$$\mathcal{Q}^r p = p, \text{ for all } p \in \mathbb{P}_{2r}.$$

The same approach is used to prove that the operator $\tilde{\mathcal{Q}}^r$ is exact on $\mathbb{P}_{2r+1}$. ☐

6.6 Explicit examples of spline quasi-interpolants for $r = 1$

In this section, we provide discrete quasi-interpolation operators for $r = 1$ that reproduce $\mathbb{P}_2$ and $\mathbb{P}_3$. The linear functionals are defined by

$$\mu_{\ell,m}^{\mathrm{kn},i}(f) = \sum_{j=1}^{n_r} q_{j,\ell,m}^{\mathrm{kn},i}\, f\left(Z_{j,\ell,m}^{\mathrm{kn},i}\right), \quad \nu_{\ell,m}^{\mathrm{sp},k}(f) = \sum_{j=1}^{n_r} q_{j,\ell,m}^{\mathrm{sp},k}\, f\left(Z_{j,\ell,m}^{\mathrm{sp},k}\right) \tag{6.33}$$

and

$$\tilde{\mu}_{\ell,m}^{\mathrm{kn},i}(f) = \sum_{j=1}^{n_r} \tilde{q}_{j,\ell,m}^{\mathrm{kn},i}\, f\left(Z_{j,\ell,m}^{\mathrm{kn},i}\right), \quad \tilde{\nu}_{\ell,m}^{\mathrm{sp},k}(f) = \sum_{j=1}^{n_r} \tilde{q}_{j,\ell,m}^{\mathrm{sp},k}\, f\left(Z_{j,\ell,m}^{\mathrm{sp},k}\right), \tag{6.34}$$

where $q_{j,\ell,m}^{\mathrm{kn},i}$, $q_{j,\ell,m}^{\mathrm{sp},k}$, $\tilde{q}_{j,\ell,m}^{\mathrm{kn},i}$ and $\tilde{q}_{j,\ell,m}^{\mathrm{sp},k}$ are real coefficients, $Z_{j,\ell,m}^{\mathrm{kn},i}, Z_{j,\ell,m}^{\mathrm{sp},k} \in \mathbb{R}$ and $n_r \geq 1$.

6.6.1 Discrete spline quasi-interpolation operator associated with $S_2^1\left(X_n^{\mathbf{ref}}\right)$

When a uniform partition of step size h is considered, from (6.30) and (6.33) the following quasi-interpolation operator that reproduces $\mathbb{P}_2$, results:

$$\mathcal{Q}^1 f = \sum_{i=0}^{n} \sum_{\ell+m=1} \mu_{\ell,m}^{\mathrm{kn},i,1}(f)\, \mathcal{B}_{\ell,m}^{\mathrm{kn},i},$$

where

$$\begin{aligned}
\mu_{1,0}^{\mathrm{kn},i,1}(f) &= -\frac{1}{8} f\left(x_i - \frac{3h}{2}\right) + \frac{5}{4} f\left(x_i - \frac{h}{2}\right) - \frac{1}{8} f\left(x_i + \frac{h}{2}\right),\\
\mu_{0,1}^{\mathrm{kn},i,1}(f) &= -\frac{1}{8} f\left(x_i - \frac{h}{2}\right) + \frac{5}{4} f\left(x_i + \frac{h}{2}\right) - \frac{1}{8} f\left(x_i + \frac{3h}{2}\right).
\end{aligned}$$

Notice that these coefficients are the same as those in [88].

6.6.2 Discrete spline quasi-interpolation operator associated with $S_3^{1,2}\left(X_n^{\mathbf{ref}}\right)$

Now, we are looking for a discrete quasi-interpolation operator of the form (6.30) and (6.34) which reproduces $\mathbb{P}_3$, i.e.

$$\tilde{\mathcal{Q}}^1 f := \sum_{i=0}^{n} \sum_{\ell+m=1} \widetilde{\mu}_{\ell,m}^{\mathrm{kn},i,1}(f)\, \mathcal{B}_{\ell,m}^{\mathrm{kn},i} + \sum_{k=0}^{n-1} \tilde{\nu}_k^{\mathrm{sp},k,1}(f)\mathcal{B}_{\ell,m}^{\,\mathrm{sp},k},$$

and $\tilde{\mathcal{Q}}^1 p = p$ for all $p \in \mathbb{P}_3$. In this case, the following coefficients are obtained:

$$\begin{aligned}
\tilde{\mu}_{1,0}^{\mathrm{kn},i,1}\,(f) &= \frac{1}{6} f\left(x_i - \frac{3h}{2}\right) - \frac{7}{9} f\left(x_i - h\right) + \frac{5}{3} f\left(x_i - \frac{h}{2}\right) - \frac{1}{18} f\left(x_i + \frac{h}{2}\right),\\
\tilde{\mu}_{0,1}^{\mathrm{kn},i,1}\,(f) &= \frac{1}{6} f\left(x_i + \frac{3h}{2}\right) - \frac{7}{9} f\left(x_i + h\right) + \frac{5}{3} f\left(x_i + \frac{h}{2}\right) - \frac{1}{18} f\left(x_i - \frac{h}{2}\right),\\
\tilde{\nu}_k^{\mathrm{sp},k,1}(f) &= f\left(\xi_k\right).
\end{aligned}$$

6.7 Conclusion

We have defined and analyzed a family of many knot spline spaces with smoothness $\lfloor d/2 \rfloor$ and degree d. They are defined on a refined partition, obtained by inserting a split knot in each interval. We have provided B-spline-like bases for these spaces when $d = 2r$ and $d = 2r + 1$. Also, Marsden's identities have been established and used to construct various families of quasi-interpolation operators having optimal approximation orders.

Chapter 7

On C^2 cubic quasi-interpolating splines and their computation by subdivision via blossoming

Given a partition $X_n := \{x_i : a = x_0 < x_1 < \cdots < x_n = b\}$ of a bounded interval $I := [a, b]$, $C^2(I)$-continuous cubic splines can be constructed by decomposing each interval $I_i := [x_i, x_{i+1}]$, $0 \le i \le n-1$, into three micro-intervals after inserting two new knots [89]. More recently, the same idea has been used in [82, 90] to addressing the problem of Hermite interpolation with cubic splines of class C^2. In both papers, the constructed spline is expressed in each subinterval I_i in terms of function and derivative values up to order two at the knots x_i and x_{i+1}. The spline is written as a linear combination of a set of basis functions. In [82], the considered basis is a classical Hermite basis, which means that the basis functions are not all non-negative. While, the authors in [90] have been provided a strategy to construct normalized B-splines-like basis, i.e., the basis function form a partition of unity, are compactly supported and are all non-negative. These properties ensure both numerical stability and local control of the constructed spline. This strategy is somewhat complicated and may be seen as a special case of the approach used in this chapter.

We consider a space of C^1 continuous cubic splines on a sample-refined partition with C^2 super-smoothness conditions at the set of split points recently introduced in [91]. Also, a general framework of quasi-interpolation methods based on the cubic B-splines has been developed in [91]. The provided quasi-interpolating splines are C^1 continuous on I, and C^2 at the set of split points. The main goal here is to provide a recipe that will enforce the C^2 smoothness conditions at the set of vertices, and later, on the whole domain. Thus, we develop a subdivision rule by blossoming which provides the coefficients of the B-spline-like representation on a finer partition (simple-split) written as convex combinations of the B-spline-like coefficients on the former partition (twice-split). The convexity property is useful because it allows to get a stable computation and makes the subdivision geometrically intuitive. By means of the derived subdivision rule, we can provide a C^2 quasi-interpolating spline defined on the twice-refined partition like those splines in [82, 90] but with small set of functional data.

This chapter can be divided into two parts. Firstly, we have reduced the computational cost, by considering a simple refinement of X_n obtained by introducing a single split point in each element of X_n. Then, a reduced space of C^2 cubic splines is defined from function values and first derivative values at the grid points and from function values at the inserted split points. In summary, full smoothness is preserved and the number of degree freedom is reduced, so that the computational cost diminish. In the second part, we construct a novel normalized B-spline-like representation for C^2-continuous cubic spline space defined on an initial partition refined by inserting two new points inside each sub-interval. The basis functions are non-negative, compactly supported, forming a convex partition of unity and that are geometrically constructed. With the help of the control polynomial theory introduced herein, a Marsden identity is derived, from which several families of super-convergent quasi-interpolation operators are defined.

7.1 Reduced C^2 cubic splines space

In what follows, we start from a space of C^1 cubic splines and then a recipe to achieve C^2 regularity on an arbitrary partition is given.

7.1.1 C^1 cubic splines

Let $\widetilde{X}_n$ be the refinement of X_n obtained by inserting in I_i a split point ξ_i. We focus on the subspace $S_3^{1,2}\left(\widetilde{X}_n\right)$ of $S_3^1\left(\widetilde{X}_n\right)$ resulting when C^2 smoothness at the inserted knots [91] is required, i.e.

$$S_3^{1,2}\left(\widetilde{X}_n\right) := \left\{s \in S_3^1\left(\widetilde{X}_n\right) : s \in C^2\left(\xi\right)\right\},$$

where $\xi := \{\xi_i\}_{i=1}^{n-1}$ is the set of the inserted split points. A spline $s \in S_3^{1,2}\left(\widetilde{X}_n\right)$ can be uniquely characterized by specifying two particular values for each knot of X_n, and another one for each interval induced by X_n.

Theorem 7.1.1. *Given values f_i, and $f_{i,x}$, $0 \le i \le n$, and g_i, $0 \le i \le n-1$, there exists a unique spline $s \in S_3^{1,2}\left(\widetilde{X}_n\right)$ such that*

$$s(x_i) = f_i, \quad s'(x_i) = f_{i,x} \tag{7.1}$$

for every knot x_i of X_n and

$$\mathcal{B}\left[s_{|[x_i,\xi_i]}\right]\left(\xi_i\left[3\right]\right) = g_i \tag{7.2}$$

for every interval I_i.

Proof. It suffices to show how the B-ordinates of the solution $s \in S_3^{1,2}\left(\widetilde{X}_n\right)$ of this non standard interpolation problem are obtained for all macro-interval I_i.

On each of the two micro-intervals $J_{i,1} := [x_i, \xi_i]$ and $J_{i,2} := [\xi_i, x_{i+1}]$ the spline s is a polynomial of degree 3, which can be represented from its B-ordinates. They are shown in Figure 7.1.

The B-ordinates d_0, d_1, d_2 and d_3 indicated by ($\bullet$) are provided by the values of the spline and its first derivative at knots x_i and x_{i+1} (7.1).

The interpolation condition (7.2) at ξ_i allows to compute the B-ordinate d_4 indicated by ($\blacktriangle$). The remaining B-ordinates d_5 and d_6, indicated by ($\circ$), are computed from C^2 smoothness at ξ_i. More precisely, they are given as follows

$$d_5 := \tau_{i,1}d_1 + \tau_{i,2}d_4, \qquad d_6 := \tau_{i,1}d_4 + \tau_{i,2}d_2,$$

where $\tau_{i,1}$ and $\tau_{i,2} = 1 - \tau_{i,1}$ are the barycentric coordinates of ξ_i with respect to I_i. $\square$

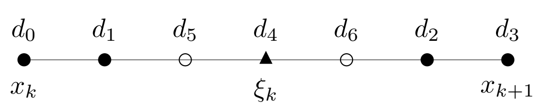

Figure 7.1: A schematic representation of the domain points involved in Theorem 7.1.1.

Having proved the unisolvency of the interpolation problem, we consider how to represent its unique solution. To do so, we construct B-spline-like functions (B-splines for short) $\mathcal{D}^{\mathrm{kn}}_{i,(l,m)}$ and $\mathcal{D}^{\mathrm{sp}}_{k}$ in order to express any spline $s \in S_3^{1,2}\left(\widetilde{X}_n\right)$ is the form

$$s = \sum_{i=0}^{n} \sum_{l+m=1} c^{\mathrm{kn}}_{i,(\ell,m)}\, \mathcal{D}^{\mathrm{kn}}_{i,(l,m)} + \sum_{k=0}^{n-1} c^{\mathrm{sp}}_{k}\, \mathcal{D}^{\mathrm{sp}}_{k}. \tag{7.3}$$

We now show how to construct suitable B-splines $\mathcal{D}^{\mathrm{kn}}_{i,(l,m)}$ and $\mathcal{D}^{\mathrm{sp}}_{k}$ for the knot x_i and the interval I_k, respectively. The construction used herein is entirely based on the choice of a single interval $W_i := [W_{i,1}, W_{i,2}]$ for every knot x_i in X_n. It must contain x_i and some specific points in a neighbourhood of x_i, namely

$$P_{i,1} := \frac{2}{3}x_i + \frac{1}{3}\xi_{i-1} \quad \text{and} \quad P_{i,2} := \frac{2}{3}x_i + \frac{1}{3}\xi_i.$$

Equipped with W_i we introduce four parameters associated with x_i. Let $\left(\alpha^0_{i,(1,0)},\, \alpha^0_{i,(0,1)}\right)$ be the barycentric coordinates of x_i with respect to W_i. This is the unique duplet satisfying

$$\alpha^0_{i,(1,0)} W_{i,1} + \alpha^0_{i,(0,1)} W_{i,2} = x_i, \quad \alpha^0_{i,(1,0)} + \alpha^0_{i,(0,1)} = 1.$$

Furthermore, let $\left(\alpha^1_{i,(1,0)},\, \alpha^1_{i,(0,1)}\right)$ be the directional barycentric coordinates of the vector $\overrightarrow{x}$ with respect to W_i. This is the unique duplet satisfying

$$\alpha^1_{i,(1,0)} W_{i,1} + \alpha^1_{i,(0,1)} W_{i,2} = 1, \quad \alpha^1_{i,(1,0)} + \alpha^1_{i,(0,1)} = 0.$$

We define the B-spline basis for $S_3^{1,2}\left(\widetilde{X}_n\right)$ in terms of conditions (7.1) and (7.2) provided in Theorem 7.1.1. The definition of the B-splines $\mathcal{D}^{\mathrm{kn}}_{i,(\ell,m)}$, $\ell + m = 1$, corresponding to the knot x_i are based on $\alpha^0_{i,(\ell,m)}$ and $\alpha^1_{i,(\ell,m)}$: at x_i we set

$$\mathcal{D}^{\mathrm{kn}}_{i,(\ell,m)}(x_i) = \alpha^0_{i,(\ell,m)}, \quad \left(\mathcal{D}^{\mathrm{kn}}_{i,(\ell,m)}\right)'(x_i) = \alpha^1_{i,(\ell,m)},$$

and

$$\mathcal{D}^{\mathrm{kn}}_{i,(\ell,m)}(x_j) = 0, \quad \left(\mathcal{D}^{\mathrm{kn}}_{i,(\ell,m)}\right)'(x_j) = 0$$

at any knot x_j of X_n different from x_i. Moreover, if $\tau_{i,1}$ and $\tau_{i,2}$ are convex weights such that $\xi_i = \tau_{i,1}x_i + \tau_{i,2}x_{i+1}$, then we set the values in condition (7.2) to zero except

$$\mathcal{B}\left[\mathcal{D}^{\mathrm{kn}}_{i,(\ell,m)}\right](\xi_i[3]) = \tau^2_{i,1}\left(\alpha^0_{i,(\ell,m)} + \alpha^1_{i,(\ell,m)}\,\frac{\xi_i - x_i}{3}\right)$$

and

$$\mathcal{B}\left[\mathcal{D}^{\mathrm{kn}}_{i,(\ell,m)}\right](\xi_{i-1}[3]) = \tau^2_{i-1,2}\left(\alpha^0_{i,(\ell,m)} + \alpha^1_{i,(\ell,m)}\,\frac{\xi_{i-1} - x_i}{3}\right).$$

Similarly, we define the B-spline $\mathcal{D}^{\mathrm{sp}}_{k}$ corresponding to I_k by the setting all values in (7.1) and (7.2) to zero, except the following one:

$$\mathcal{B}\left[\mathcal{D}^{\mathrm{sp}}_{k}\right](\xi_k[3]) = 2\tau_{k,1}\tau_{k,2}.$$

Once constructed the B-splines as solutions of the corresponding interpolation problems, one needs to give the explicit expressions of coefficients $c^{\mathrm{kn}}_{i,(\ell,m)}$ and c^{sp}_{k} in the BB-representation

(7.3) of $s \in S_3^{1,2}\left(\widetilde{X}_n\right)$. This is achieved by means of polar forms of restrictions of s to specific intervals of X_n. To be precise, for any interval J_i of X_n with an end-point at x_i, it holds

$$c^{\mathrm{kn}}_{i,(\ell,m)} = \mathcal{B}\left[s_{|J_i}\right](x_i[2],\, x_{i-1}[\ell],\, x_{i+1}[m])\,. \tag{7.4}$$

Note that the above blossom value can be evaluated in terms of s and its first derivative at the knot x_i, namely

$$\mathcal{B}\left[s_{|J_i}\right](x_i\,[2]\,,\, x_{i+1}) = s\,(x_i)\, +\, \frac{2}{3}s'\,(x_i)\,(x_{i+1} - x_i)\,,$$

This confirms that the value of $c^{\mathrm{kn}}_{i,(\ell,m)}$ is independent of the choice of J_i. Regarding the coefficient c^{sp}_k corresponding to I_k, it is satisfied that

$$c^{\mathrm{sp}}_k = \mathcal{B}\left[s_{|J_k}\right](x_k,\, x_{k+1},\, \xi_k)\,. \tag{7.5}$$

To understand the super-smoothness condition C^2 at the vertices in X_n for C^1 cubic splines that we will explore later, we now review the Bernstein-Bézier representation of s restricted to an interval induced by X_n. Let $J_{i,1} = [x_i,\, \xi_i]$ be the left sub-interval of I_i. The blossom value giving the B-ordinate of $s_{|J_{i,1}}$ corresponding to the knot x_i is given by

$$\mathcal{B}\left[s_{|J_{i,1}}\right](x_i\,[3]) = \sum_{\ell+m=1} \alpha^0_{i,(\ell,m)}\, c^{\mathrm{kn}}_{i,(\ell,m)}.$$

The B-ordinate associated with the domain point $\frac{2}{3}x_i + \frac{1}{3}\xi_i$ is equal to

$$\mathcal{B}\left[s_{|J_{i,1}}\right](x_i\,[2]\,,\, \xi_i) = \sum_{\ell+m=1}\left(\alpha^0_{i,(\ell,m)} + \alpha^1_{i,(\ell,m)}\frac{\xi_i - x_i}{3}\right) c^{\mathrm{kn}}_{i,(\ell,m)}. \tag{7.6}$$

Note that the weights in (7.6) are the barycentric coordinates of the $\dfrac{2}{3}x_i + \dfrac{1}{3}\xi_i$ with respect to W_i.

Furthermore, the B-ordinate corresponding to the split point ξ_i is

$$\mathcal{B}\left[s_{|J_{i,1}}\right](\xi_i[3]) = \tau^2_{i,1}\mathcal{B}\left[s_{|J_{i,1}}\right](x_i,\, \xi_i\,[2]) + \tau^2_{i,2}\mathcal{B}\left[s_{|J_{i,2}}\right](x_{i+1},\, \xi_i\,[2]) + 2\tau_{i,1}\tau_{i,2}\, c^{\mathrm{sp}}_k,$$

where $J_{i,2} = [\xi_i,\, x_{i+1}]$.

The B-ordinate corresponding to the domain point $\frac{1}{3}x_i + \frac{2}{3}\xi_i$ is a convex combination of certain B-ordinates associated with the domain points $\frac{2}{3}x_i + \frac{1}{3}\xi_i$ and ξ_i. Indeed, it is given by

$$\mathcal{B}\left[s_{|J_{i,1}}\right](x_i,\, \xi_i\,[2]) = \tau_{i,1}\mathcal{B}\left[s_{|J_{i,1}}\right](x_i\,[2]\,,\, \xi_i) + \tau_{i,2}c^{\mathrm{sp}}_i.$$

Remark 7.1.2. *Boundary B-splines-like basis for $S_3^{1,2}$ are constructed according to the same procedure outlined for interior points. The B-spline-like with respect to vertex $a = x_0$ (resp. $b = x_n$) is constructed with a particular choice of the interval W_0 (resp. W_n). Namely, W_0 must contains $P_{0,1} = x_0$ and $P_{0,2} = \dfrac{2}{3}x_0 + \dfrac{1}{3}\xi_0$. The interval W_n also must contain $P_{n,1} = \frac{2}{3}x_n + \frac{1}{3}\xi_{n-1}$ and $P_{n,2} = x_n$.*

7.1.2 Recipe to achieve C^2 smoothness at the set of vertices

Consider a linear operator $\mathcal{Q}$ of the form

$$\mathcal{Q}f := \sum_{i=0}^{n}\sum_{\ell+m=1} \psi^{\mathrm{kn}}_{i,(\ell,m)}\,(f)\; \mathcal{D}^{\mathrm{kn}}_{i,(\ell,m)} + \sum_{k=0}^{n-1} \psi^{\mathrm{sp}}_k\,(f)\; \mathcal{D}^{\mathrm{sp}}_k, \tag{7.7}$$

which associates with a given function f a spline in $S_3^{1,2}\left(\widetilde{X}_n\right)$. It is based on the choice of linear functionals $\psi_{i,(\ell,m)}^{\mathrm{kn}}$ and ψ_k^{sp} corresponding to vertices and intervals, respecively. Motivated by (7.4) and (7.5), we consider the linear functionals $\psi_{i,(\ell,m)}^{\mathrm{kn}}$ and ψ_k^{sp} given by

$$\psi_{i,(\ell,m)}^{\mathrm{kn}}(f) = \mathcal{B}\left[\mathcal{I}_{i,(\ell,m)}^{\mathrm{kn}} f\right](x_i[2], x_{i-1}[\ell], x_{i+1}[m]),$$
$$\psi_k^{\mathrm{sp}}(f) = \mathcal{B}\left[\mathcal{I}_k^{\mathrm{sp}} f\right](x_k, x_{k+1}, \xi_k),$$

for some linear operators $\mathcal{I}_{i,(\ell,m)}^{\mathrm{kn}}$ and $\mathcal{I}_k^{\mathrm{sp}}$ that map a function f to cubic polynomials $\mathcal{I}_{i,(\ell,m)}^{\mathrm{kn}} f$ and $\mathcal{I}_k^{\mathrm{sp}} f$.

In what follows, we provide an approach that enables us to get C^2 smoothness at the vertices in X_n. We start by observing from (7.4) and (7.7) that

$$\mathcal{B}\left[\mathcal{I}_{i,(\ell,m)}^{\mathrm{kn}} f_{|J_{i,1}}\right](x_i[2], x_{i-1}[\ell], x_{i+1}[m]) = \mathcal{B}\left[\mathcal{Q} f_{|J_{i,1}}\right](x_i[2], x_{i-1}[\ell], x_{i+1}[m]),$$
$$\mathcal{B}\left[\mathcal{I}_k^{\mathrm{sp}} f_{|J_{k,1}}\right](x_k, x_{k+1}, \xi_k) = \mathcal{B}\left[\mathcal{Q} f_{|J_{k,1}}\right](x_k, x_{k+1}, \xi_k).$$

As the following result shows, C^2 smoothness can be achieved by specifying a cubic polynomial that *connect* the local operators acting in the closest neighbourhood of the knot.

Theorem 7.1.3. *Let $\mathcal{Q}f$ be defined by (7.7), and let x_i be a knot of X_n. Assume that there exists a polynomial $p \in \mathbb{P}_3$ such that the following requirements are met:*

- *The operator $\mathcal{I}_{i,(\ell,m)}^{kn}$, $\ell + m = 1$, corresponding to x_i satisfies*

$$\mathcal{I}_{i,(\ell,m)}^{kn} f(x_i) = p(x_i), \quad \left(\mathcal{I}_{i,(\ell,m)}^{kn} f\right)'(x_i) = p'(x_i). \tag{7.8}$$

- *The operators $\mathcal{I}_{i-1}^{sp}$ and $\mathcal{I}_i^{sp}$ corresponding to the intervals I_{i-1} and I_i with an end-point at x_i satisfy the conditions*

$$\mathcal{B}\left[\mathcal{I}_{i-1}^{sp} f\right](x_i, x_{i-1}, \xi_{i-1}) = \mathcal{B}[p](x_i, x_{i-1}, \xi_{i-1}) \text{ and } \mathcal{B}\left[\mathcal{I}_i^{sp} f\right](x_i, x_{i+1}, \xi_i) = \mathcal{B}[p](x_i, x_{i+1}, \xi_i). \tag{7.9}$$

Then, $\mathcal{Q}f$ is C^2-continuous at x_i.

Proof. We need to prove that $(\mathcal{Q}f)''(x_i) = p''(x_i)$. Recall that,

$$\begin{aligned} D_{\xi_i - x_i}^2 \mathcal{Q} f_{|J_{i,1}}(x_i) &= 6\,\mathcal{B}\left[\mathcal{Q} f_{|J_{i,1}}\right](x_i, (\xi_i - x_i)[2]) \\ &= 6\left(-2\mathcal{B}\left[\mathcal{Q} f_{|J_{i,1}}\right](x_i[2], \xi_i) + \mathcal{B}\left[\mathcal{Q} f_{|J_{i,1}}\right](x_i, \xi_i[2]) + \mathcal{B}\left[\mathcal{Q} f_{|J_{i,1}}\right](x_i[3])\right). \end{aligned}$$

More precisely, we need to prove that

$$D_{\xi_i - x_i}^2 \mathcal{Q} f_{|J_{i,1}}(x_i) = 6\left(-2\mathcal{B}[p](x_i[2], \xi_i) + \mathcal{B}[p](x_i, \xi_i[2]) + \mathcal{B}[p](x_i[3])\right)$$

where the blossom values of p are all independent of $J_{i,1}$. To his end, we consider the blossom values

$$\mathcal{B}\left[\mathcal{Q} f_{|J_{i,1}}\right](x_i[2], \xi_i) \text{ and } \mathcal{B}\left[\mathcal{Q} f_{|J_{i,1}}\right](x_i, \xi_i[2])$$

which will help us to express the second order derivative of $\mathcal{Q} f_{|J_{i,1}}$ at x_i.

- The blossom value $\mathcal{B}\left[\mathcal{Q} f_{|J_{i,1}}\right](x_i[2], \xi_i)$ is the B-ordinate of $\mathcal{Q} f_{|J_{i,1}}$ on $J_{i,1}$ corresponding to the domain point $\frac{2}{3}x_i + \frac{1}{3}\xi_i$ (7.6), i.e.

$$\mathcal{B}\left[\mathcal{Q} f_{|J_{i,1}}\right](x_i[2], \xi_i) = \sum_{\ell+m=1}\left(\alpha_{i,(\ell,m)}^0 + \alpha_{i,(\ell,m)}^1 \frac{\xi_i - x_i}{3}\right)\mathcal{B}\left[\mathcal{I}_{i,(\ell,m)}^{\mathrm{kn}} f\right](x_i[2], x_{i-1}[\ell], x_{i+1}[m]).$$

The weights $\alpha^0_{i,(\ell,m)} + \frac{1}{3}\alpha^1_{i,(\ell,m)}(\xi_i - x_i)$ are the barycentric coordinates of the point $\frac{2}{3}x_i + \frac{1}{3}\xi_i$ with respect to W_i, which implies that they are also the barycentric coordinates of the point ξ_i with respect to the interval $[x_{i-1},\, x_{i+1}]$. Hence, throughout multi-affinity of the blossom and by (7.8), one can obtains

$$\mathcal{B}\left[\mathcal{Q}f_{|J_{i,1}}\right](x_i[2],\, \xi_i) = \mathcal{B}\left[\mathcal{I}^{\mathrm{kn}}_{i,(\ell,m)} f\right](x_i[2],\, \xi_i) = \mathcal{B}\,[p]\,(x_i[2],\, \xi_i)\,.$$

- Considering the B-ordinate of $\mathcal{Q}f_{|J_{i,1}}$ corresponding to the domain point $\frac{1}{3}x_i + \frac{2}{3}\xi_i$, it holds

$$\mathcal{B}\left[\mathcal{Q}f_{|J_{i,1}}\right](x_i,\, \xi_i[2]) = \tau_{i,1}\mathcal{B}\left[\mathcal{Q}f_{|J_{i,1}}\right](x_i[2],\, \xi_i) + \tau_{i,2}\mathcal{B}\left[\mathcal{Q}f_{|J_{i,1}}\right](x_i,\, x_{i+1},\, \xi_i)\,.$$

From (7.9), we get

$$\begin{aligned}\mathcal{B}\left[\mathcal{Q}f_{|J_{i,1}}\right](x_i,\, \xi_i[2]) &= \tau_{i,1}\mathcal{B}\,[p]\,(x_i[2],\, \xi_i) + \tau_{i,2}\mathcal{B}\,[p]\,(x_i,\, x_{i+1},\, \xi_i)\\ &= \mathcal{B}\,[p]\,(x_i,\, \xi_i[2])\,,\end{aligned}$$

This confirms that $(\mathcal{Q}f)''\,(x_i) = p''(x_i)$.

□

Next, we provide a recipe to choose the operators $\mathcal{I}^{\mathrm{kn}}_{i,(\ell,m)}$ and $\mathcal{I}^{\mathrm{sp}}_k$ in such a way that the conditions in Theorem 7.1.3 are fulfilled.

Let $\mathcal{Q}f$ be defined by (7.7).

- For every knot x_i, take $\mathcal{I}^{\mathrm{kn}}_{i,(\ell,m)} f = \mathcal{I}^{\mathrm{kn}}_i f$, $\ell + m = 1$.
- Take $\mathcal{I}^{\mathrm{sp}}_k f = \mathcal{I}^{\mathrm{kn}}_k f$, where $\mathcal{I}^{\mathrm{kn}}_k f$ is associated with x_k, which is an end-point of I_k.

These choices ensure that $\mathcal{Q}f \in S^2_3\left(\widetilde{X}_n\right)$.

Finally, we proved that with an appropriate choice of certain interpolation operators the C^1 cubic splines space defined on a refined partition are C^2 everywhere.

7.1.3 Numerical results

This section provides some numerical results to illustrate the performance of the above quasi-interpolation operators. To this end, we will use the test functions

$$\begin{aligned}f_1(x) &= \frac{3}{4}e^{-2(9x-2)^2} - \frac{1}{5}e^{-(9x-7)^2-(9x-4)^2} + \frac{1}{2}e^{-(9x-7)^2-\frac{1}{4}(9x-3)^2} + \frac{3}{4}e^{\frac{1}{10}(-9x-1)-\frac{1}{49}(9x+1)^2},\\ f_2(x) &= \frac{1}{2}x\cos^4\left(4\left(x^2+x-1\right)\right),\end{aligned}$$

whose plots appear in Figure 7.10. Let us consider the interval $I = [0, 1]$. The tests are carried out for a sequence of uniform mesh X_n associated with the break-points $x_i = ih$, $i = 0, \ldots, n$, where $h = \frac{1}{n}$. The inserted split points are chosen as the middle points of the macro-intervals, i.e., $\xi_i = \left(i + \frac{1}{2}\right)h$, $i = 0, \ldots, n-1$.

For each $i = 0, \ldots, n$, we choose $\mathcal{I}^{\mathrm{kn}}_i$ as Lagrange interpolation operator. More precisely, $\mathcal{I}^{\mathrm{kn}}_i f\,(y)$ is the Lagrangian interpolation polynomial of f at points x_{i-1}, x_i, ξ_i and x_{i+1}. From this choice, the linear functionals $\psi^{\mathrm{kn}}_{i,(\ell,m)}$ and ψ^{sp}_k will be given by the following expressions:

$$\begin{aligned}\psi^{\mathrm{kn}}_{i,(1,0)} f &= \frac{1}{18}\left(f\left(h\left(i-1\right)\right) + 30f\left(hi\right) + 3f\left(h\left(i+1\right)\right)\right) - 16f\left(h\left(i+\frac{1}{2}\right)\right)\right),\\ \psi^{\mathrm{kn}}_{i,(0,1)}\left(f\right) &= \frac{1}{18}\left(-f\left(h\left(i-1\right)\right) + 6ff\left(hi\right) - 3f\left(h\left(i+1\right)\right)\right) + 16f\left(h\left(i+\frac{1}{2}\right)\right)\right),\\ \psi^{\mathrm{sp}}_k\left(f\right) &= \frac{1}{6}\left(-f\left(hk\right) - f\left(h\left(k+1\right)\right) + 8f\left(h\left(k+\frac{1}{2}\right)\right)\right).\end{aligned}$$

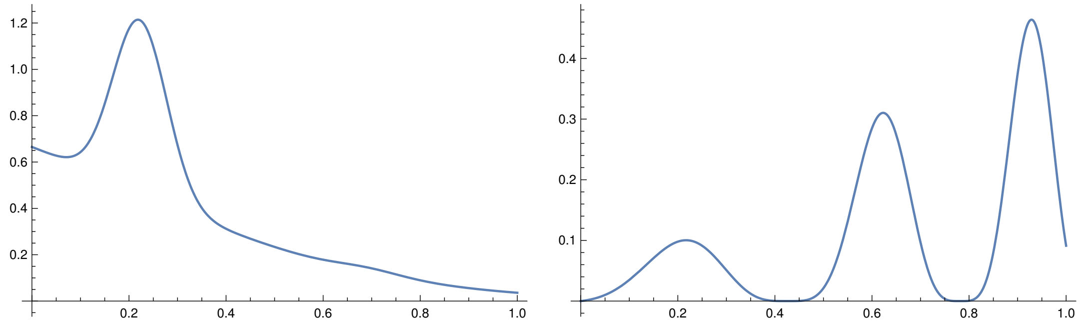

Figure 7.2: Plots of tests functions: f_1 (left) and f_2 (right).

The boundary functionals are given as follows:

$$\psi_{0,(1,0)}^{\text{kn}} f = f(x_0),$$
$$\psi_{0,(0,1)}^{\text{kn}}(f) = 2f\left(\frac{h}{2}\right) + \frac{2}{9}f\left(\frac{3h}{2}\right) - f(h) - \frac{1}{9}2f(0),$$
$$\psi_0^{\text{sp}}(f) = \frac{1}{6}\left(8f\left(\frac{h}{2}\right) - f(h) - f(0)\right).$$

And

$$\psi_{0,(1,0)}^{\text{kn}} f = -f(h(n-1)) - \frac{2}{9}f(hn) + 2f\left(h\left(n-\frac{1}{2}\right)\right) + \frac{2}{9}f\left(h\left(n-\frac{3}{2}\right)\right),$$
$$\psi_{n,(0,1)}^{\text{kn}}(f) = f(hn),$$
$$\psi_{n-1}^{\text{sp}}(f) = \frac{1}{6}\left(-f(h(n-1)) - f(hn) + 8f\left(h\left(n-\frac{1}{2}\right)\right)\right).$$

The quasi-interpolation error is estimated as

$$\mathcal{E}_n(f) = \max_{0\le\ell\le 200} |\mathcal{Q}f(z_\ell) - f(z_\ell)|, \tag{7.10}$$

where z_ℓ, $\ell = 0,\ldots,200$, are equally spaced points in I. The estimated numerical convergence order (NCO) is given by the rate

$$NCO := \frac{\log\left(\frac{\mathcal{E}_{n_1}}{\mathcal{E}_{n_2}}\right)}{\log\left(\frac{n_2}{n_1}\right)}.$$

n	$\mathcal{E}_n(f_1)$	NCO	$\mathcal{E}_n(f_2)$	NCO
16	$9.1296537835926 \times 10^{-4}$	$--$	$1.260787334071 \times 10^{-3}$	$--$
32	$6.1127061602148 \times 10^{-5}$	3.900677028041	$8.145770956876 \times 10^{-5}$	3.952129887220
64	$3.7983549236761 \times 10^{-6}$	4.008364593575	$5.299660586700 \times 10^{-6}$	3.942079377867
128	$1.9959603911938 \times 10^{-7}$	4.250219722727	$3.515981562213 \times 10^{-7}$	3.913900556044
256	$1.5928529425907 \times 10^{-8}$	3.647398107630	$2.129053828850 \times 10^{-8}$	4.045643174010

Table 7.1: Estimated errors for functions f_1 and f_2, and NCOs with different values of n.

In Table 7.1, the estimated quasi-interpolation errors and NCOs for functions f_1 and f_2 are shown.

7.1.4 Spline spaces on twice-refined partitions

In the previous section a C^2 cubic quasi-interpolant on a refinement $\widetilde{X}_n$ of the initial partition X_n by adding an additional knot at each macro-interval has been defined. That quasi-interpolant is written in terms of B-spline-like functions $\mathcal{D}^{\mathrm{kn}}_{i,(\ell,m)}$, $0 \le i \le n$, $\ell{+}m = 1$, and $\mathcal{D}^{\mathrm{sp}}_k$, $0 \le k \le n{-}1$. The computation of such a spline by refinement of the original refined partition, while retaining the cubic precision, is considered in this section. For this purpose, we consider a refinement $\widetilde{X}_{n,2}$ of the refined partition $\widetilde{X}_{n,1} := \widetilde{X}_n$. Each micro–interval $\widetilde{I}_i$ induced by $\widetilde{X}_{n,1}$ is decomposed into two sub-intervals by inserting points $\xi_{i,1}$ and $\xi_{i,2}$ into $\widetilde{I}_{i,1} := [x_i,\, \xi_i]$ and $\widetilde{I}_{i,2} := [\xi_i,\, x_{i+1}]$, respectively. For the sake of simplicity, we note by x_i^{old} and $x_i^{\mathrm{new}} = \xi_i$ the old knots in X_n and the inserted split points in $\widetilde{X}_{n,1}$, which means that the new chosen points are the inserted split points in the first refinement. A schematic representation of the two levels of refinement is depicted in Figure 7.3.

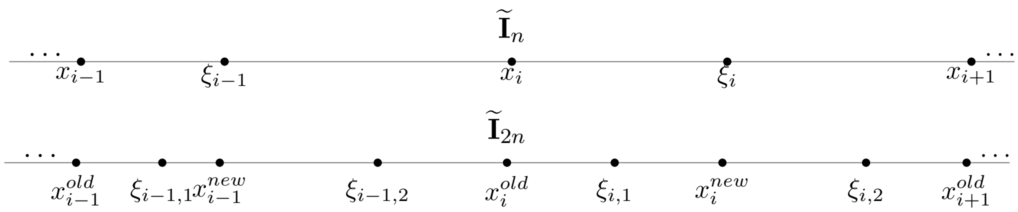

Figure 7.3: A schematic representation for the first (top) and second refinement (bottom) levels.

The spline space $S^2_3\left(\widetilde{X}_{n,1}\right)$ is considered since we are interested in refining C^2 cubic functions, namely the quasi-interpolants constructed in the previous section. The space $S^2_3\left(\widetilde{X}_{n,2}\right)$ is also involved. A spline $s \in S^2_3\left(\widetilde{X}_{n,1}\right)$ is also an element of the finer space $S^2_3\left(\widetilde{X}_{n,2}\right)$, and we look for expressing the coefficients in (7.3) associated with second level partition $\widetilde{X}_{n,2}$ in terms of those corresponding to the first level refinement $\widetilde{X}_{n,1}$.

Le us suppose that the spline $s \in S^2_3\left(\widetilde{X}_{n,2}\right)$ is expressed as

$$s = \sum_{i=0}^{n} \sum_{\ell+m=1} c^{\mathrm{kn,\,old}}_{i,(\ell,m)}\, \mathcal{D}^{\mathrm{kn,\,old}}_{i,(\ell,m)} + \sum_{i=0}^{n} \sum_{\ell+m=1} c^{\mathrm{kn,\,new}}_{i,(\ell,m)}\, \mathcal{D}^{\mathrm{kn,\,new}}_{i,(\ell,m)} + \sum_{k=0}^{n-1} \left(c^{\mathrm{sp},1}_k\, \mathcal{D}^{\mathrm{sp},1}_k + c^{\mathrm{sp},2}_k\, \mathcal{D}^{\mathrm{sp},2}_k \right), \tag{7.11}$$

where $c^{\mathrm{kn,\,old}}_{i,(\ell,m)}$, $c^{\mathrm{kn,\,new}}_{i,(\ell,m)}$, $c^{\mathrm{sp},1}_k$ and $c^{\mathrm{sp},2}_k$ are the coefficients associated with points x_i^{old}, x_i^{new}, $\xi_{k,1}$ and $\xi_{k,2}$, respectively.

We will start by providing the expressions of the spline coefficients associated with a uniform partition, where the inserted split points in each level are the mid-points. Later on, we will prove subdivision rules for the case of non-uniform partitions.

7.1.4.1 Subdivision rules for uniform partitions

Consider the uniform case, with $x_i = a + ih$, $i = 0, \ldots, n$, h being the step-size. In this case, the inserted split points in the first level are $\xi_i = \frac{1}{2}\,(x_i + x_{i+1})$, and those corresponding to the second level refinement are $\xi_{i,1} = \frac{3}{4}x_i + \frac{1}{4}x_{i+1}$ and $\xi_{i,2} = \frac{1}{4}x_i + \frac{3}{4}x_{i+1}$.

The following results show the relationship between old and new coefficients for vertices.

Proposition 7.1.4. *The coefficients $c^{kn,old}_{i,(\ell,m)}$, $\ell + m = 1$, corresponding to the knot x_i^{old} are expressed as*

$$c^{kn,\ old}_{i,(1,0)} = \frac{3}{4} c^{kn}_{i,(1,0)} + \frac{1}{4} c^{kn}_{i,(0,1)}, \qquad c^{kn,\ old}_{i,(0,1)} = \frac{1}{4} c^{kn}_{i,(1,0)} + \frac{3}{4} c^{kn}_{i,(0,1)}.$$

Proof. Note that $x_i^{\text{new}} = \xi_i = \frac{3}{4}x_i + \frac{1}{4}x_{i+2}$. Then, using the multi-affinity of blossoms and (7.4), we have

$$\begin{aligned}
c_{i,(1,0)}^{\text{kn, old}} &= \mathcal{B}[s]\left(x_i^{\text{old}}[2], x_{i-1}^{\text{new}}\right) \\
&= \mathcal{B}[s]\left(x_i[2], \frac{3}{4}x_{i-1} + \frac{1}{4}x_{i+1}\right) \\
&= \frac{3}{4}\mathcal{B}[s](x_i[2], x_{i-1}) + \frac{1}{4}\mathcal{B}[s](x_i[2], x_{i+1}),
\end{aligned}$$

and,

$$\begin{aligned}
c_{i,(0,1)}^{\text{kn, old}} &= \mathcal{B}[s]\left(x_i^{\text{old}}[2], x_{i+1}^{\text{new}}\right) \\
&= \mathcal{B}[s]\left(x_i[2], \frac{1}{4}x_{i-1} + \frac{3}{4}x_{i+1}\right) \\
&= \frac{1}{4}\mathcal{B}[s](x_i[2], x_{i-1}) + \frac{3}{4}\mathcal{B}[s](x_i[2], x_{i+1}),
\end{aligned}$$

The proof is complete. □

Proposition 7.1.5. *The coefficients $c_{i,(\ell,m)}^{kn,new}$, $\ell + m = 1$, corresponding to the knot x_i^{new} are expressed as*

$$c_{i,(1,0)}^{kn,\ new} = \frac{1}{8}c_{i,(1,0)}^{kn} + \frac{3}{8}c_{i,(0,1)}^{kn} + \frac{1}{2}c_i^{sp}, \qquad c_{i,(0,1)}^{kn,\ new} = \frac{3}{8}c_{i+1,(1,0)}^{kn} + \frac{1}{8}c_{i+1,(0,1)}^{kn} + \frac{1}{2}c_i^{sp}.$$

Proof. Again, we use the multi-affinity of blossoms and (7.4)-(7.5) to get

$$\begin{aligned}
c_{i,(1,0)}^{\text{kn, new}} &= \mathcal{B}[s]\left(x_i^{\text{new}}[2], x_i^{\text{old}}\right) \\
&= \frac{1}{2}\mathcal{B}[s]\left(x_i^{\text{new}}, x_i^{\text{old}}[2]\right) + \frac{1}{2}\mathcal{B}[s]\left(x_i^{\text{new}}, x_i^{\text{old}}, x_{i+1}^{\text{old}}\right) \\
&= \frac{1}{2}\left(\frac{1}{4}\mathcal{B}[s](x_i[2], x_{i-1}) + \frac{3}{4}\mathcal{B}[s](x_i[2], x_{i+1})\right) + \frac{1}{2}\mathcal{B}[s](\xi_i, x_i, x_{i+1}).
\end{aligned}$$

The same technique is used to get the expression of $c_{i,(0,1)}^{\text{kn, new}}$. □

Similar results are given next for split points.

Proposition 7.1.6. *The coefficients $c_i^{sp,1}$ and $c_i^{sp,2}$ associated with the split points $\xi_{i,1}$ and $\xi_{i,2}$, respectively, are given by*

$$c_i^{sp,1} = \frac{3}{16}c_{i,(1,0)}^{kn} + \frac{9}{16}c_{i,(0,1)}^{kn} + \frac{1}{4}c_i^{sp}, \qquad c_i^{sp,2} = \frac{9}{16}c_{i+1,(1,0)}^{kn} + \frac{3}{16}c_{i+1,(0,1)}^{kn} + \frac{1}{4}c_i^{sp}.$$

Proof. Using (7.5), we can write

$$c_i^{\text{sp},1} = \mathcal{B}[s]\left(\xi_{i,1}, x_i^{\text{old}}, x_i^{\text{new}}\right).$$

By definition, $\xi_{i,1} = \frac{1}{2}x_i^{\text{old}} + \frac{1}{2}x_i^{\text{new}}$ and

$$x_i^{\text{new}} = \frac{1}{2}x_i^{\text{old}} + \frac{1}{2}x_{i+1}^{\text{old}} = \frac{1}{4}x_{i-1}^{\text{old}} + \frac{3}{4}x_{i+1}^{\text{old}}.$$

Then, by multi-affinity of blossoms, we have

$$c_i^{\text{sp},1} = \frac{1}{2}\mathcal{B}[s]\left(x_i^{\text{old}}[2], x_i^{\text{new}}\right) + \frac{1}{2}\mathcal{B}[s]\left(x_i^{\text{old}}, x_i^{\text{new}}[2]\right).$$

Taking into account that

$$\begin{aligned}
\mathcal{B}\,[s]\left(x_i^{\text{old}}[2],\, x_i^{\text{new}}\right) &= \frac{1}{4}\mathcal{B}\,[s]\left(x_i^{\text{old}}[2],\, x_{i-1}^{\text{old}}\right) + \frac{3}{4}\mathcal{B}\,[s]\left(x_i^{\text{old}}[2],\, x_{i+1}^{\text{old}}\right)\\
&= \frac{1}{4}c_{i,(1,0)}^{\text{kn}} + \frac{3}{4}c_{i,(0,1)}^{\text{kn}}
\end{aligned}$$

and

$$\begin{aligned}
\mathcal{B}\,[s]\left(x_i^{\text{old}},\, x_i^{\text{new}}[2]\right) &= \frac{1}{2}\mathcal{B}\,[s]\left(x_i^{\text{old}}[2],\, x_i^{\text{new}}\right) + \frac{1}{2}\mathcal{B}\,[s]\left(x_i^{\text{old}},\, x_{i+1}^{\text{old}},\, x_i^{\text{new}}\right)\\
&= \frac{1}{8}c_{i,(1,0)}^{\text{kn}} + \frac{3}{8}c_{i,(0,1)}^{\text{kn}} + \frac{1}{4}c_i^{\text{sp}},
\end{aligned}$$

the claim follows for $c_i^{\text{sp},1}$. The same approach is used to prove the expression for $c_i^{\text{sp},2}$. □

7.1.4.2 Subdivision rules for non-uniform partition

Now, we consider the case of non-uniform partitions. Let

$$\mathbb{B}_i^n[a,b,c] = \binom{n}{i}\frac{(b-c)^i(c-a)^{n-i}}{(b-a)^n}$$

be the ith Bernstein basis function of degree n in Cartesian coordinates with respect to $[a,b]$. The following results are obtained.

- Subdivision rules for the coefficients associated with the set of old vertices: for $\ell+m=1$,

$$\begin{aligned}
c_{i,(\ell,m)}^{\text{kn, old}} &= \mathcal{B}[s]\left(x_i^{\text{old}}\,[r+1]\,, x_{i-1}^{\text{new}}\,[\ell]\,,\, x_i^{\text{new}}\,[m]\right),\\
&= \sum_{j=0}^{l}\sum_{k=0}^{m}\mathbb{B}_j^{\ell}\left[x_{i-1}^{\text{old}}, x_{i+1}^{\text{old}}, x_{i-1}^{\text{new}}\right]\,\mathbb{B}_k^{m}\left[x_{i-1}^{\text{old}}, x_{i+1}^{\text{old}}, x_i^{\text{new}}\right]\times\\
&\qquad \mathcal{B}\,[s]\left(x_i^{\text{old}}\,[r+1]\,, x_{i-1}^{\text{old}}\,[j+k]\,,\, x_{i+1}^{\text{old}}\,[r-j-k]\right),\\
&= \sum_{j=0}^{l}\sum_{k=0}^{m}\mathbb{B}_j^{\ell}\left[x_{i-1}^{\text{old}}, x_{i+1}^{\text{old}}, x_{i-1}^{\text{new}}\right]\,\mathbb{B}_k^{m}\left[x_{i-1}^{\text{old}}, x_{i+1}^{\text{old}}, x_i^{\text{new}}\right]\,c_{i,(j+k,r-j-k)}^{\text{kn}}.
\end{aligned}$$

- Subdivision rules for the coefficients associated with the set of new vertices:

  - For $\ell=1$ and $m=0$,

$$\begin{aligned}
c_{i,(1,0)}^{\text{kn, new}} &= \mathcal{B}\,[s]\left(x_i^{\text{new}}\,[2]\,, x_i^{\text{old}}\right),\\
&= \mathbb{B}_0^1\left[x_i^{\text{old}}, x_{i+1}^{\text{old}}, x_i^{\text{new}}\right]\mathcal{B}\,[s]\left(x_i^{\text{new}}, x_i^{\text{old}}\,[2]\right)\\
&+ \mathbb{B}_1^1\left[x_i^{\text{old}}, x_{i+1}^{\text{old}}, x_i^{\text{new}}\right]\mathcal{B}\,[s]\left(x_i^{\text{new}}, x_i^{\text{old}},\, x_{i+1}^{\text{old}}\right),\\
&= \mathbb{B}_0^1\left[x_i^{\text{old}}, x_{i+1}^{\text{old}}, x_i^{\text{new}}\right]\sum_{j=0}^{1}\mathbb{B}_j^1\left[x_{i-1}^{\text{old}}, x_{i+1}^{\text{old}}, x_i^{\text{new}}\right]c_{i,(j,1-j)}^{\text{kn}}\\
&+ \mathbb{B}_1^1\left[x_i^{\text{old}}, x_{i+1}^{\text{old}}, x_i^{\text{new}}\right]c_i^{\text{sp}}.
\end{aligned}$$

– For $\ell = 0$ and $m = 1$,

$$\begin{aligned} c_{i,(0,1)}^{\text{kn, new}} &= \mathcal{B}[s]\left(x_i^{\text{new}}[2], x_{i+1}^{\text{old}}\right), \\ &= \mathbb{B}_0^1\left[x_i^{\text{old}}, x_{i+1}^{\text{old}}, x_i^{\text{new}}\right] c_i^{\text{sp}} \\ &+ \mathbb{B}_1^1\left[x_i^{\text{old}}, x_{i+1}^{\text{old}}, x_i^{\text{new}}\right] \sum_{j=0}^{1} \mathbb{B}_j^1\left[x_i^{\text{old}}, x_{i+2}^{\text{old}}, x_i^{\text{new}}\right] c_{i+1,(j,1-j)}^{\text{kn}}. \end{aligned}$$

- Subdivision rules for the coefficients associated with the set of split points (we consider only the subdivision rule associated with $\xi_{i,1}$, the case of $\xi_{i,2}$ being similar): it holds

$$\begin{aligned} c_i^{\text{sp},1} &= \mathcal{B}[s]\left(\xi_{i,1}, x_i^{\text{old}}, x_i^{\text{new}}\right), \\ &= \sum_{j=0}^{1} \mathbb{B}_j^1\left[x_i^{\text{old}}, x_i^{\text{new}}, \xi_{i,1}\right] \mathcal{B}[s]\left(x_i^{\text{old}}[1+j], x_i^{\text{new}}[2-j]\right), \\ &= \mathbb{B}_0^1\left[x_i^{\text{old}}, x_i^{\text{new}}, \xi_{i,1}\right] \Xi_1 + \mathbb{B}_1^1\left[x_i^{\text{old}}, x_i^{\text{new}}, \xi_{i,1}\right] \Xi_2, \end{aligned}$$

where

$$\Xi_1 := \mathbb{B}_0^1\left[x_i^{\text{old}}, x_{i+1}^{\text{old}}, x_i^{\text{new}}\right] c_i^{\text{sp}} + \mathbb{B}_1^1\left[x_i^{\text{old}}, x_{i+1}^{\text{old}}, x_i^{\text{new}}\right] \sum_{q=0}^{1} \mathbb{B}_q^1\left[x_{i-1}^{\text{old}}, x_{i+1}^{\text{old}}, x_i^{\text{new}}\right] c_{i,(q,1-q)}^{\text{kn}}$$

and

$$\Xi_2 := \sum_{q=0}^{1} \mathbb{B}_q^1\left[x_{i-1}^{\text{old}}, x_{i+1}^{\text{old}}, x_i^{\text{new}}\right] c_{i,(q,1-q)}^{\text{kn}}.$$

7.1.5 Numerical examples

Define the control points as

$$\mathbf{c}_{i,(1,0)}^{\text{kn}} := \left(W_{i,1}, c_{i,(1,0)}^{\text{kn}}\right), \quad \mathbf{c}_{i,(0,1)}^{\text{kn}} := \left(W_{i,2}, c_{i,(0,1)}^{\text{kn}}\right), \quad \mathbf{c}_k^{\text{sp}} := \left(\xi_k, c_k^{\text{sp}}\right).$$

Consider the curve associated with the function $f_3(x) = \sin(5\pi x)$. Its plot is shown in Figure 7.4 (left). Figures 7.5 and 7.6 show an example of the polygon of control associated with the set of control points with different level of refinement.

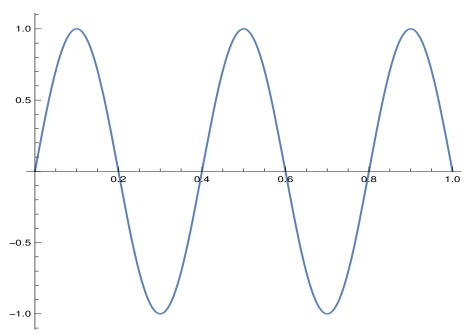

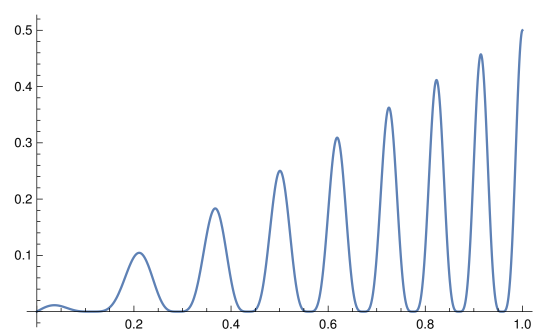

Figure 7.4: Plots of f_3 and f_4 (from left to right).

Thus, we consider the polygon control depicted in Figure 7.4 (right) associated with the function $f_4(x) = \dfrac{1}{2} x \cos\left(4\pi\left(x^2 + x - 1\right)\right)^4$. Figure 7.6 shows the control polygons associated with several levels of refinement.

After applying one or more subdivision steps, the sequence of approximate control polygons converges to the original one.

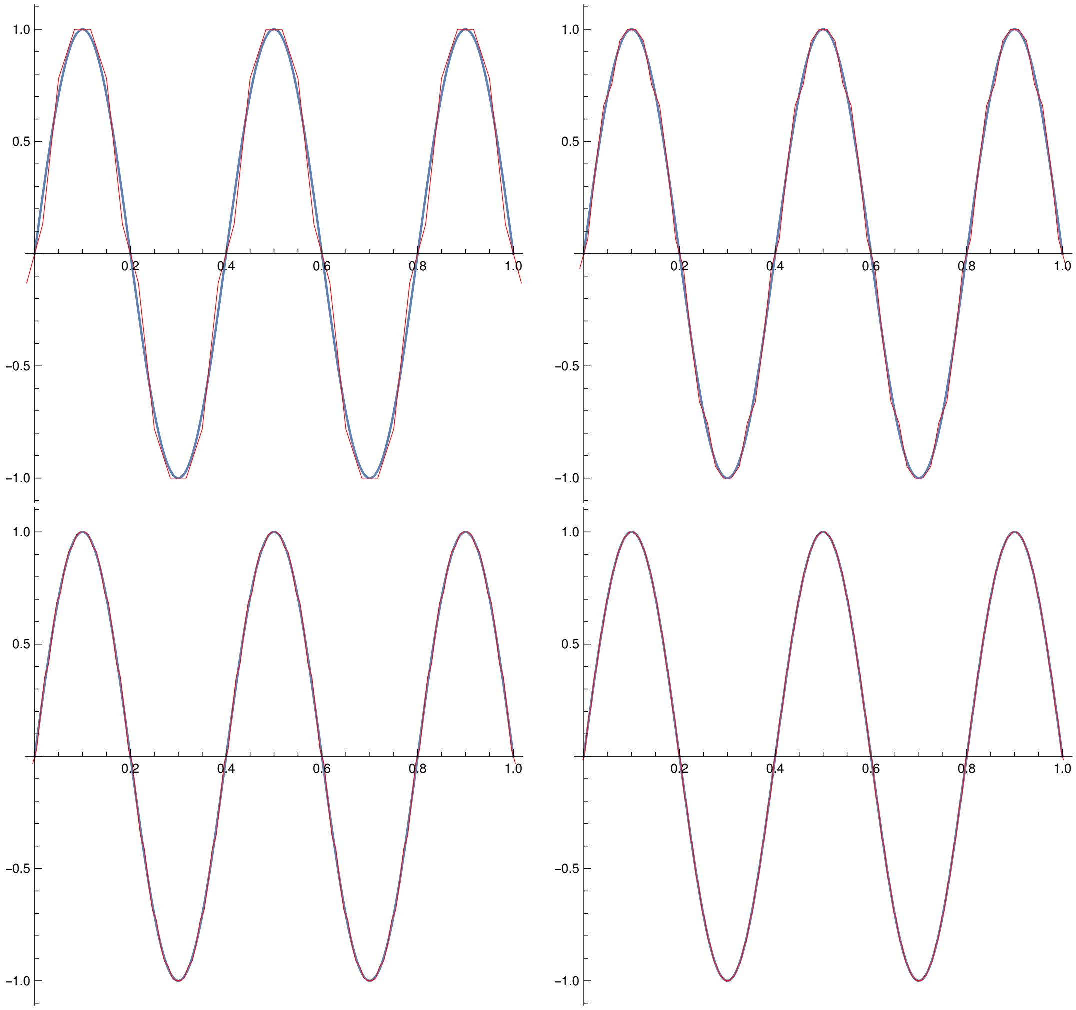

Figure 7.5: From top to bottom and from left to right, plots of control polygons given by levels X_{10}, X_{20}, X_{40} and X_{80} in red color and the original one in blue color.

7.2 A new approach to deal with C^2 cubic splines and its application to super-convergent quasi-interpolation

As shown in [82], C^2-continuous cubic splines on a partition endowed with a specific refinement are obtained if all values and derivative values up to order 2 at the break-points of the initial partition are given. More specifically, to get globally C^2 cubic splines, the initial partition should be refined by inserting two new knots inside each sub-interval induced by the primary partition (for the general case, see [89]).

The idea of introducing a split knot was introduced for the first time by L. L. Schumaker in [81] to address the case of quadratic splines. Adopting the same procedure, C. Manni in [94] has investigated interpolation by means of C^1 quadratic and C^2 cubic many-knots splines with shape parameters. More recently, the same idea has been used in [82, 90] when addressing the problem of Hermite interpolation with C^2 cubic splines with the aid of blossoming. Unfortunately, the strategies outlined in those last papers have some drawbacks. In fact, the B-spline bases constructed in [82] are non-positives, while the strategy developed in [90] is somewhat complicated, which may be seen as a special case of the approach that will be proposed here.

As mentioned above, in this section we consider a refinement of the initial partition by inserting two split knots inside each initial sub-interval and define a space of C^2 cubic splines.

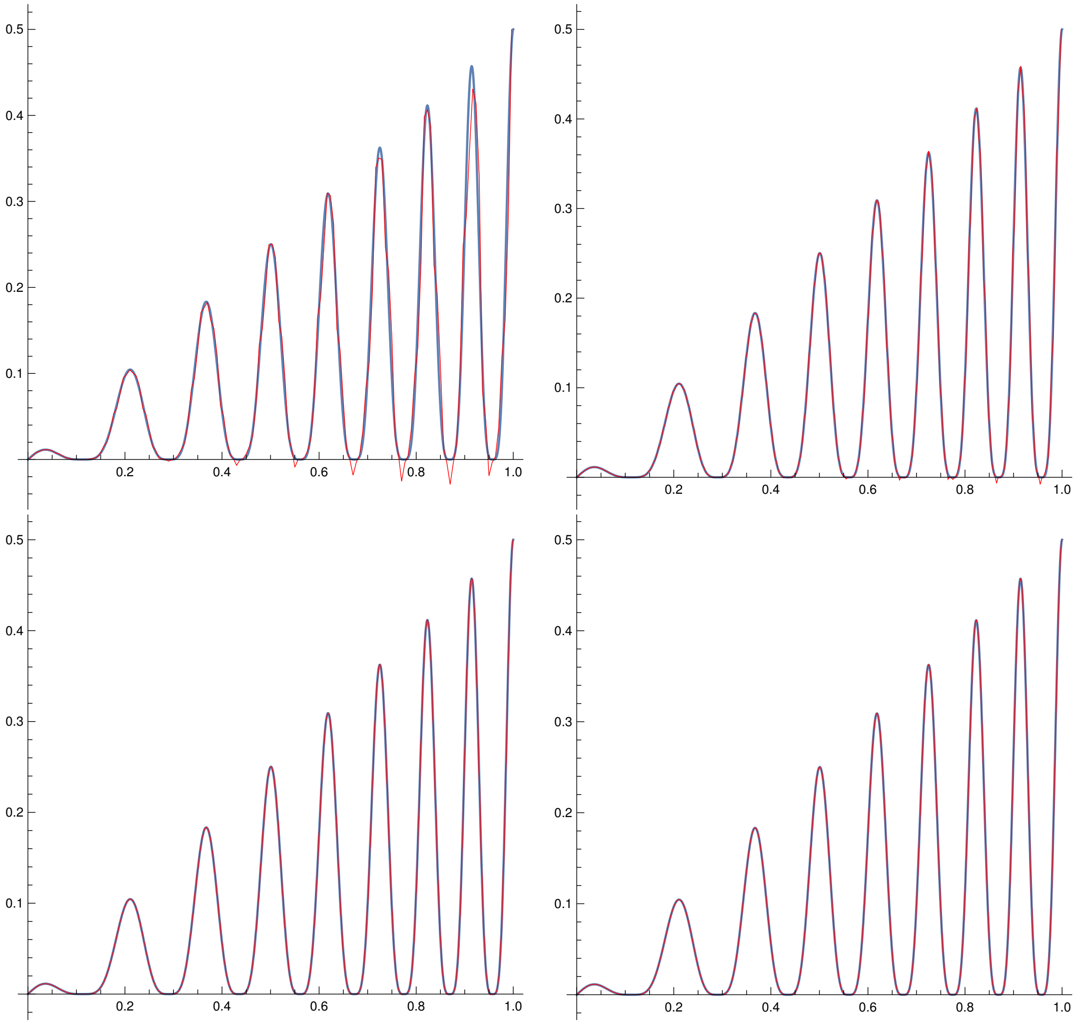

Figure 7.6: From top to bottom and from left to right, plots of control polygons given by levels X_{50}, X_{100}, X_{200} and X_{400} in red color and the original one in blue color.

Every spline in this space is uniquely determined by its value and that of its derivatives up to order 2 at each knot of the initial partition. Since the C^2 cubic spline space is characterized by an interpolation problem, then a B-spline basis is constructed by defining its basis functions as duals of the interpolation functionals. This will be done in a completely geometric form in order to get compactly supported non-negative B-spline functions forming a convex partition of unity.

The solution of a Hermite interpolation problem in this space gives rise to a many knot spline, which can be considered as a differential quasi-interpolant. Therefore, the notion of control polynomial allows us to obtain a Marsden identity from which we define quasi-interpolants that reproduce the cubic polynomials.

Super-convergence is a phenomenon that appears when the order of convergence at some particular points is higher than the order of convergence over the whole domain of definition [92, 93, 96]. Super-convergence is an advantageous theoretical property that can be exploited successfully in practice. The theory of control polynomials used here allows to define a family of super-convergent quasi-interpolation operators.

7.2.1 A space of C^2 many-knot splines

For a given $n \geq 2$, let $X_n := \{x_0 < x_1 < \ldots < x_n\}$ be a subset of knots providing a partition of I into subintervals $I_i := [x_i, x_{i+1}]$, $0 \leq i \leq n-1$. A refinement X_n^{ref} of the initial partition X_n is defined by inserting two split points $\xi_{i,1} = \frac{1}{3}(2x_i + x_{i+1})$ and $\xi_{i,2} = \frac{1}{3}(x_i + 2x_{i+1})$ in each macro-element I_i that define the micro-intervals $I_{i,1} := [x_i, \xi_{i,1}]$, $I_{i,2} := [\xi_{i,1}, \xi_{i,2}]$ and $I_{i,3} := [\xi_{i,2}, x_{i+1}]$.

Here, we focus on the spline space

$$S_3^2\left(X_n^{\text{ref}}\right) := \left\{s \in C^2(I) : s_{|I_{i,j}} \in \mathbb{P}_3,\ j = 1,2,3,\ 0 \leq i \leq n-1\right\}.$$

A spline $s \in S_3^2\left(X_n^{\text{ref}}\right)$ can be uniquely characterized by three specific values at each knot x_i (see [89]).

Theorem 7.2.1. *Given values $f_{i,0}$, $f_{i,1}$, $f_{i,2}$, $0 \leq i \leq n$, there exists a unique spline $s \in S_3^2\left(X_n^{ref}\right)$ such that*

$$s(x_i) = f_{i,0}, \quad s'(x_i) = f_{i,1}, \quad s''(x_i) = f_{i,2}, \tag{7.12}$$

Figure 7.7 shows a graphical representation relative to Theorem 7.2.1. The B-ordinates of s corresponding to x_i and its neighboring domain points depicted by dark bullets ($\bullet$) are computed from interpolation conditions (7.12). The remaining B-ordinates are determined from the C^2 smoothness conditions at the inserted split points.

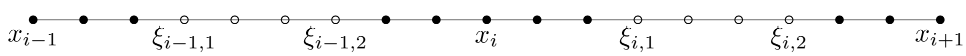

Figure 7.7: Schematic representation of domain points corresponding to the BB-representation of a C^2 cubic spline. The points depicted by ($\bullet$) represent the degree of freedom, while, the points represented by ($\circ$) mark the B-ordinates computed from imposed C^2 smoothness at the inserted split points.

In what follows, we will look for a normalized representation of the spline $s \in S_3^2\left(X_n^{\text{ref}}\right)$ of the form

$$s(x) = \sum_{i=0}^{n} \sum_{|\alpha|=2} c_{i,\alpha}\, \mathcal{B}_{i,\alpha}(x), \tag{7.13}$$

in which the basis functions $\mathcal{B}_{i,\alpha}$ are non-negative, have a local supports and form partition of unity.

7.2.1.1 Construction of normalized B-spline-like representation

This subsection is devoted to construct suitable B-spline-like functions $\mathcal{B}_{i,\alpha}$, $i = 0, \ldots, n$, $|\alpha| = 2$, for which (7.13) holds of a spline $s \in S_3^2\left(X_n^{\text{ref}}\right)$.

The construction used herein is entirely geometric. For every break-point x_i, $0 \leq i \leq n$, define

$$W_{i,1} := \frac{4}{3}\xi_{i-1,2} - \frac{1}{3}x_i, \quad W_{i,2} := \frac{4}{3}\xi_{i,1} - \frac{1}{3}x_i, \tag{7.14}$$

and the interval $W_i := [W_{i,1}, W_{i,2}]$. From W_i we introduce nine parameters relative to x_i. Let $\mathfrak{B}^2_{W_i,\alpha}$, $|\alpha| = 2$, denote the Bernstein polynomials of degree 2 with respect to W_i, and define, for $0 \leq j \leq 2$ and a given integer $m \geq 3$, the values

$$\gamma_{i,\alpha}^j := \frac{\binom{j}{m}}{\binom{j}{2}} \left(\frac{2}{m}\right)^j D^j\, \mathfrak{B}^2_{W_i,\alpha}(x_i). \tag{7.15}$$

The B-spline for $S_3^2\left(X_n^{\text{ref}}\right)$ are defined in terms of conditions (7.12) provided in Theorem 7.2.1. The construction of the B-splines $\mathcal{B}_{i,\alpha}$, $|\alpha| = 2$, corresponding to the break-point x_i is based entirely on parameters $\gamma_{i,\alpha}^j$, $0 \leq j \leq 2$, $|\alpha| = 2$. Indeed, $\mathcal{B}_{i,\alpha}$ is the unique function in $S_3^2\left(X_n^{\text{ref}}\right)$ such that

$$\mathcal{B}_{i,\alpha}(x_i) = \gamma_{i,\alpha}^0, \quad \mathcal{B}'_{i,\alpha}(x_i) = \gamma_{i,\alpha}^1, \quad \mathcal{B}''_{i,\alpha}(x_i) = \gamma_{i,\alpha}^2,$$

and $\mathcal{B}_{i,\alpha}(x_\ell) = \mathcal{B}'_{i,\alpha}(x_\ell) = \mathcal{B}''_{i,\alpha}(x_\ell) = 0$ at any knot x_ℓ different from x_i.

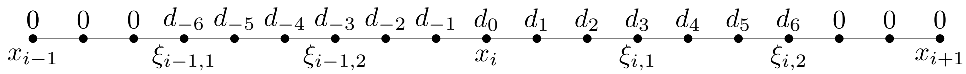

Figure 7.8: B-ordinates of the B-spline $\mathcal{B}_{i,\alpha}$ associated with the break-point x_i.

A schematic representation of the B-ordinates corresponding to the B-spline $\mathcal{B}_{i,\alpha}$ associated with the break-point x_i of X_n is depicted in Figure 7.8. By definition, the B-ordinates at the domain points in a neighbourhood of x_{i-1} and x_{i+1} are equal to zero. Because of C^2 smoothness at x_i, B-ordinates d_{-2}, d_{-1}, d_0, d_1 and d_2 are completely determined by the value $\gamma_{i,\alpha}^j$. They are given explicitly as follows:

$$d_0 = \gamma_{i,\alpha}^0, \quad d_1 = \gamma_{i,\alpha}^0 + \gamma_{i,\alpha}^1 \frac{\xi_{i,1} - x_i}{3}, \quad d_2 = \gamma_{i,\alpha}^0 + 2\gamma_{i,\alpha}^1 \frac{\xi_{i,1} - x_i}{3} + \gamma_{i,\alpha}^2 \frac{(\xi_{i,1} - x_i)^2}{6},$$
$$d_{-1} = \gamma_{i,\alpha}^0 + \gamma_{i,\alpha}^1 \frac{\xi_{i-1,2} - x_i}{3}, \quad d_{-2} = \gamma_{i,\alpha}^0 + 2\gamma_{i,\alpha}^1 \frac{\xi_{i-1,2} - x_i}{3} + \gamma_{i,\alpha}^2 \frac{(\xi_{i-1,2} - x_i)^2}{6}.$$

The B-spline $\mathcal{B}_{i,\alpha}$ is C^2-continuous at $\xi_{i-1,1}$, $\xi_{i-1,2}$, $\xi_{i,1}$ and $\xi_{i,2}$, then

$$d_3 = \frac{1}{6}\left(7d_2 - 2d_1\right), \; d_4 = \frac{1}{3}\left(4d_2 - 2d_1\right), \; d_5 = \frac{1}{3}\left(2d_2 - d_1\right), \; d_6 = \frac{1}{6}\left(2d_2 - d_1\right)$$
$$d_{-3} = \frac{1}{6}\left(7d_{-2} - 2d_{-1}\right), \; d_{-4} = \frac{1}{3}\left(4d_{-2} - 2d_{-1}\right), \; d_{-5} = \frac{1}{3}\left(2d_{-2} - d_{-1}\right), \; d_{-6} = \frac{1}{6}\left(2d_{-2} - d_{-1}\right)$$

Remark 7.2.2. *Boundary B-spline-like functions for $S_3^2\left(X_n^{ref}\right)$ are constructed according to the same procedure highlighted in Subsection (7.2.1.1), with a particular choice of points in* (7.14)*, namely $W_{0,1} := x_0$ (resp. $W_{n,2} := x_n$).*

Figure 7.9 shows the graphs of the vertex B-spline-like functions for interior and boundaries vertices.

7.2.1.2 Properties of B-splines

In many practical applications, especially in the area of computer aided geometric design, bases that are non-negative, locally supported and form a partition of unity are desired. In what follows, we are going to prove that the B-splines constructed here accomplish these properties.

Property 7.2.3. *The B-splines $\mathcal{B}_{i,\alpha}$, $i = 0, \ldots, n$, $|\alpha| = 2$, form a partition of unity, i.e.,*

$$1 = \sum_{i=0}^{n} \sum_{|\alpha|=2} \mathcal{B}_{i,\alpha}.$$

Proof. It follows from the definition of the B-splines that only three basis functions have function and derivative values at x_i that are not all zero. Moreover, the Bernstein polynomials in (7.15) form a partition of unity on W_i. Then, it claims that:

$$\sum_{|\alpha|=2} \gamma_{i,\alpha}^0 = 1, \quad \sum_{|\alpha|=2} \gamma_{i,\alpha}^1 = \sum_{|\alpha|=2} \gamma_{i,\alpha}^2 = 0. \tag{7.16}$$

The proof is completed by considering interpolation problem (7.12) and (7.16). $\square$

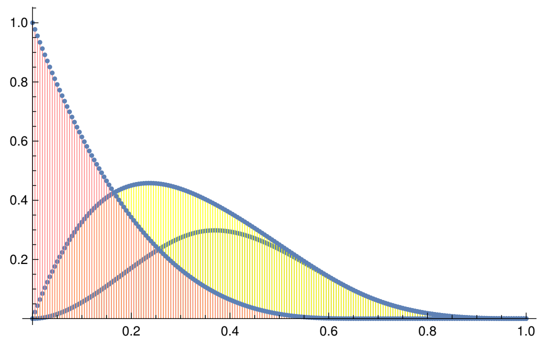

(a) B-spline-like functions with respect to vertex x_0.

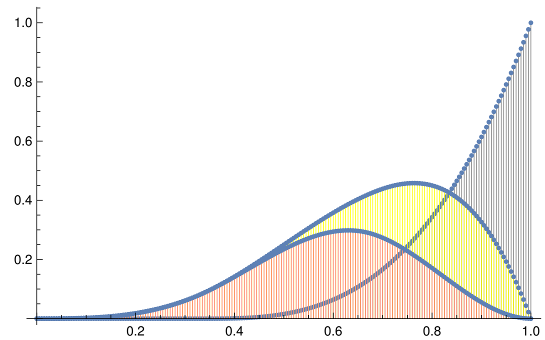

(b) B-spline-like functions with respect to vertex x_n.

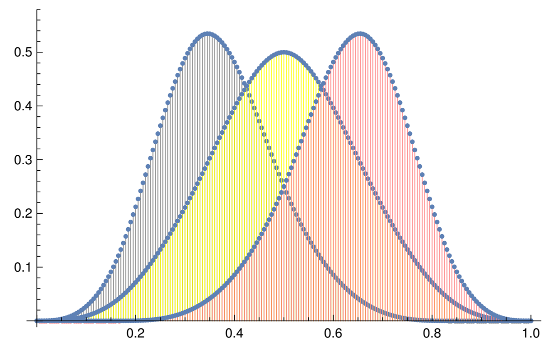

(c) B-spline-like functions with respect to an interior vertex.

Figure 7.9: Knot B-spline-like functions for interior and boundaries knots.

Property 7.2.4. *The B-splines $\mathcal{B}_{i,\alpha}$, are non-negative.*

Proof. It suffices to prove that the B-ordinates of $\mathcal{B}_{i,\alpha}$ are all non-negative. Let

$$u := \frac{\xi_{i,1} - x_i}{|\xi_{i,1} - x_i|}.$$

A quadratic polynomial p defined on the interval $[P_1, P_2]$, where,

$$P_1 = x_i, \quad P_2 = \frac{1}{3}x_i + \frac{2}{3}\xi_{i,1},$$

has B-ordinates d_0, d_1 and d_2, if and only if

$$\begin{aligned} p(x_i) = \mathcal{B}_{i,\alpha}(x_i) &= d_0 \\ \frac{1}{2}\frac{2}{3}D_u p(x_i) = \frac{1}{3}D_u\mathcal{B}_{i,\alpha}(x_i) &= \frac{d_1 - d_0}{|\xi_{i,1} - x_i|} \\ \frac{1}{2}\left(\frac{2}{3}\right)^2 D_u^2 p(x_i) = \frac{1}{6}D_u^2\mathcal{B}_{i,\alpha}(x_i) &= \frac{d_0 - 2d_1 + d_2}{|\xi_{i,1} - x_i|}. \end{aligned}$$

From (7.15) it follows that p must be equal to a certain Bernstein polynomial of degree 2 with respect to W_i.

Since P_1, P_2 can be written as

$$P_1 = x_i, \quad P_2 = \frac{1}{2}x_i + \frac{1}{2}W_{i,2}.$$

It follows that P_1 and P_2 are situated inside W_i. Which means that the barycentric coordinates of P_1 and P_2 with respect to W_i are non-negative. Let $\sigma^1 = (\sigma_1^1, \sigma_2^1)$, $\sigma^2 = (\sigma_1^2, \sigma_2^2)$ be the barycentric coordinates of P_1 and P_2 with respect to W_i, respectively. Then, we get,

$$d_0 = \mathbf{B}[p]\left(\sigma^1, \sigma^1\right), \quad d_1 = \mathbf{B}[p]\left(\sigma^1, \sigma^2\right), \quad d_2 = \mathbf{B}[p]\left(\sigma^2, \sigma^2\right).$$

By multi-affinity of blossoms, we obtain that:

$$d_6 = \frac{1}{6}(2d_2 - d_1) = \frac{1}{6}\mathbf{B}[p]\left(2\sigma^2 - \sigma^1, \sigma^2\right),$$

the barycentric coordinates $(2\sigma^2 - \sigma^1)$ correspond to the point $W_{i,2}$, since

$$W_{i,2} = \frac{4}{3}\xi_{i,1} - \frac{1}{3}x_i = 2P_2 - P_1.$$

Then, it follows that $2d_2 - d_1 \geq 0$, therefore, $d_3, d_4, d_5 \geq 0$. □

Any B-spline-like $\mathcal{B}_{i,\alpha}$ with respect to a knot x_i is related to a Bernstein basis polynomials of degree 2. Furthermore, the spline coefficients $c_{i,\alpha}$, $|\alpha| = 2$, corresponding to $\mathcal{B}_{i,\alpha}$ are considered as the B-ordinates of a polynomial of degree 2 defined on the interval W_i. This polynomial function is called control polynomial with respect to the break-point x_i and is defined as

$$T_i(x) := \sum_{|\alpha|=2} c_{i,\alpha}\, \mathfrak{B}^2_{W_i,\alpha}(x), \quad x \in W_i. \tag{7.17}$$

Property 7.2.5. *T_i is tangent to the spline $s \in S_3^2\left(X_n^{ref}\right)$ at x_i.*

Proof. For $s \in S_3^2\left(X_n^{\text{ref}}\right)$, and $a = 0, 1$, it holds

$$s^{(j)}(x_i) = \sum_{|\alpha|=2} c_{i,\alpha}\, \gamma^j_{i,\alpha} = \sum_{|\alpha|=2} c_{i,\alpha}\, D^j \mathfrak{B}^2_{W_i,\alpha}(x) = T_i^{(j)}(x_i),$$

and the proof is complete. □

7.2.1.3 B-splines representation

This subsection aims to derive the coefficients of (7.13) for an interpolation spline.

Suppose that $s \in S_3^2\left(X_n^{\text{ref}}\right)$ is determined by the Hermite interpolation problem (7.12). The evaluation of $s^{(j)}$, $0 \leq j \leq 2$, at x_i yields the linear system

$$\begin{pmatrix} \gamma^0_{i,(2,0)} & \gamma^0_{i,(1,1)} & \gamma^0_{i,(0,2)} \\ \gamma^1_{i,(2,0)} & \gamma^1_{i,(1,1)} & \gamma^1_{i,(0,2)} \\ \gamma^2_{i,(2,0)} & \gamma^2_{i,(1,1)} & \gamma^2_{i,(0,2)} \end{pmatrix} \begin{pmatrix} c_{i,(2,0)} \\ c_{i,(1,1)} \\ c_{i,(0,2)} \end{pmatrix} = \begin{pmatrix} f_{i,0} \\ f_{i,1} \\ f_{i,2} \end{pmatrix}.$$

The definition of the parameters $\gamma^j_{i,\alpha}$ in (7.15) includes the values and derivative values of Bernstein basis polynomials. Since they are linear independent, the solution of the linear system is then unique. It is given by

$$\begin{aligned}
c_{i,(2,0)} &= f_{i,0} + f_{i,1}\left(W_{i,1} - x_i\right) + \frac{m}{4(m-1)} f_{i,2}\left(W_{i,1} - x_i\right)^2 \\
c_{i,(1,1)} &= f_{i,0} + \frac{1}{2} f_{i,1}\left(W_{i,1} + W_{i,2} - 2x_i\right) + \frac{m}{4(m-1)} f_{i,2}\left(W_{i,1} - x_i\right)\left(W_{i,2} - x_i\right) \\
c_{i,(0,2)} &= f_{i,0} + f_{i,1}\left(W_{i,2} - x_i\right) + \frac{m}{4(m-1)} f_{i,2}\left(W_{i,2} - x_i\right)^2.
\end{aligned}$$

We can simplify the expressions of the coefficients $c_{i,\alpha}$. Define $h_{i-1} = x_i - x_{i-1}$, $h_i = x_{i+1} - x_i$, then, one can obtains

$$\begin{aligned}
c_{i,(2,0)} &= f_{i,0} + \frac{4}{81}h_{i-1}\left(-9f_{i,1} + \frac{m}{m-1}h_{i-1}f_{i,2}\right)\\
c_{i,(1,1)} &= f_{i,0} + \frac{2}{9}f_{i,1}\left(h_i - h_{i-1}\right) - \frac{4m}{81(m-1)}h_{i-1}h_if_{i,2}\\
c_{i,(0,2)} &= f_{i,0} + \frac{4}{81}h_i\left(9f_{i,1} + \frac{m}{m-1}h_if_{i,2}\right)
\end{aligned}$$

.

Each cubic spline $s \in S_3^2\left(X_n^{\mathrm{ref}}\right)$ can be uniquely expressed in the form (7.13). Thus, in the Bernstein-Bézier representation of a polynomial p, the coefficients $c_{i,\alpha}$ of s can be expressed in terms of polar form values of a polynomial obtained by restricting s to a specific sub-interval.

Proposition 7.2.6. *For $m = 3$, let $s \in S_3^2\left(X_n^{ref}\right)$. Denote by $s_{|[x_i,\xi_{i,1}]}$ the restriction of s to the interval $[x_i, \xi_{i,1}]$. Then, the coefficients $c_{i,\alpha}$ in the B-splines representation (7.13) of s can be expressed as*

$$\begin{aligned}
&c_{i,(2,0)} = \mathbf{B}\left[s_{|[x_i,\xi_{i,1}]}\right]\left(x_i, \tilde{W}_{i,1}, \tilde{W}_{i,1}\right), \quad c_{i,(1,1)} = \mathbf{B}\left[s_{|[x_i,\xi_{i,1}]}\right]\left(x_i, \tilde{W}_{i,1}, \tilde{W}_{i,2}\right),\\
&c_{i,(0,2)} = \mathbf{B}\left[s_{|[x_i,\xi_{i,1}]}\right]\left(x_i, \tilde{W}_{i,2}, \tilde{W}_{i,2}\right),
\end{aligned}$$

where $\tilde{W}_{i,1} = \frac{3}{2}W_{i,1} - \frac{1}{2}x_i$ and $\tilde{W}_{i,2} = \frac{3}{2}W_{i,2} - \frac{1}{2}x_i$.

Proof. The values of the above blossoms are expressed in terms of the function values and derivative values up to order 2 of s at x_i as,

$$\begin{aligned}
&\mathbf{B}\left[s_{|[x_i,\xi_{i,1}]}\right]\left(x_i, \tilde{W}_{i,1}, \tilde{W}_{i,1}\right)\\
&= \mathbf{B}\left[s_{|[x_i,\xi_{i,1}]}\right]\left(x_i, \frac{3}{2}W_{i,1} - \frac{1}{2}x_i, \frac{3}{2}W_{i,1} - \frac{1}{2}x_i\right)\\
&= \mathbf{B}\left[s_{|[x_i,\xi_{i,1}]}\right]\left(x_i, \frac{3}{2}\left(W_{i,1} - x_i\right) + x_i, \frac{3}{2}\left(W_{i,1} - x_i\right) + x_i\right)\\
&= \frac{9}{4}\mathbf{B}\left[s_{|[x_i,\xi_{i,1}]}\right]\left(x_i, W_{i,1} - x_i, W_{i,1} - x_i\right) + 3\mathbf{B}\left[s_{|[x_i,\xi_{i,1}]}\right]\left(x_i, W_{i,1} - x_i, x_i\right)\\
&+ \mathbf{B}\left[s_{|[x_i,\xi_{i,1}]}\right]\left(x_i, x_i, x_i\right)\\
&= \frac{3}{8}D^2_{W_{i,1}-x_i}s(x_i) + D_{W_{i,1}-x_i}s(x_i) + s(x_i).
\end{aligned}$$

Which concludes the proof. □

Every spline $s \in S_3^2\left(X_n^{\mathrm{ref}}\right)$ can be compactly expressed as

$$s(x) := \sum_{i=0}^{n}\sum_{|\alpha|=2}\mathbf{B}\left[s_{|[x_i,\xi_{i,1}]}\right]\left(x_i[1], \tilde{W}_{i,1}[\alpha_1], \tilde{W}_{i,2}[\alpha_2]\right)\mathcal{B}_{i,\alpha}(x). \tag{7.18}$$

7.2.2 Super-convergent quasi-interpolation operators

In what follows, we aim to construct some super-convergent quasi-interpolation operators that map an element of the linear space of polynomials of degree less or equal to $m \geq 3$ to an element of $S_3^2\left(X_n^{\mathrm{ref}}\right)$.

Define

$$Q_{i,\ell} = \frac{m}{2}W_{i,\ell} + (1-\frac{m}{2})x_i, \quad \ell = 1,2,$$

for all $m \geq 3$. Then, we have the following result.

Theorem 7.2.7. *Let m be an integer ≥ 3. Let $\mathcal{Q}_m\, p$ be a quasi-interpolation operator of the form*

$$\mathcal{Q}_m\, p(x) := \sum_{i=0}^{n} \sum_{|\alpha|=2} \mathbf{B}\,[p]\,(x_i[m-2], Q_{i,1}[\alpha_1],\, Q_{i,2}[\alpha_2])\; \mathcal{B}_{i,\alpha}(x). \tag{7.19}$$

It holds $\mathcal{Q}_m\, p \in S_3^2\left(X_n^{ref}\right)$ for all $p \in \mathbb{P}_m$. Moreover,

$$\mathcal{Q}_3\, p = p, \quad \textit{for all } p \in \mathbb{P}_3.$$

Proof. We will prove that:

$$D^j\, \mathcal{Q}_m\, p(x_i) \;=\; D^j\, p(x_i), \quad i = 0,\ldots,n, \quad 0 \leq j \leq 2, \quad \text{for all } p \in \mathbb{P}_m.$$

We have

$$\mathcal{Q}_m\, p(x_i) = \sum_{|\alpha|=2} \mathbf{B}\,[p]\,(x_i[m-2], Q_{i,1}[\alpha_1],\, Q_{i,2}[\alpha_2])\; \mathcal{B}_{i,\alpha}(x_i).$$

Define

$$q_{x_i}(x) := \sum_{|\alpha|=2} \mathbf{B}\,[p]\,(x_i[m-2], Q_{i,1}[\alpha_1],\, Q_{i,2}[\alpha_2])\; \mathcal{B}_{i,\alpha}(x).$$

Then,

$$D^j q_{x_i}(x) = \left(\frac{2}{m}\right)^j \frac{\binom{j}{m}}{\binom{j}{2}} \sum_{|\alpha|=2} \mathbf{B}\,[p]\,(x_i[m-2], Q_{i,1}[\alpha_1],\, Q_{i,2}[\alpha_2])\; \mathfrak{B}^2_{W_i,\alpha}(x).$$

Using Proposition 1.3.1, we define

$$\tilde{q}(x) := \mathbf{B}\,[p]\left(x_i[m-2], \left(\frac{m}{2}x + \left(1-\frac{m}{2}\right)x_i\right)[2]\right),$$

$\tilde{q}(x)$ written in W_i as follows,

$$\begin{aligned}\tilde{q}(x) &= \sum_{|\alpha|=2} \mathbf{B}\,[\tilde{q}]\,(W_{i,1}[\alpha_1],\, W_{i,2}[\alpha_2])\; \mathfrak{B}^2_{W_i,\alpha}(x)\\ &= \sum_{|\alpha|=2} \mathbf{B}\,[p]\,(x_i[m-2], Q_{i,1}[\alpha_1],\, Q_{i,2}[\alpha_2])\; \mathfrak{B}^2_{W_i,\alpha}(x).\end{aligned}$$

Therefore,

$$D^j p(x_i) = \left(\frac{2}{m}\right)^j \frac{\binom{j}{m}}{\binom{j}{2}} D^j \tilde{q}(x_i) = D^j q_{x_i}(x_i) = D^j\, \mathcal{Q}_m\, p(x_i),$$

which completes the proof. □

Remark 7.2.8. *Note the fact that to get the expression of $\tilde{W}_{i,\ell}$, $\ell = 1,2$, it suffices to choose $m = 3$.*

Error estimate of super-convergent quasi-interpolation operators

Consider a function f in $C^4([a,b])$. The operators $\mathcal{Q}_m$, $m \geq 3$, reproduce the linear space of polynomial function of degree less than or equal to three, then, it follows that, there exist a non-negative constant C, independent of m, such that

$$\|\mathcal{Q}_m^{(k)} f - f^{(k)}\|_{\infty,\,[a,b]} \leq C\,\bar{h}^{4-k}\,\|f^{(4-k)}\|_{\infty,\,[a,b]},$$

where, $\|.\|_{\infty,\,[a,b]}$ stands for the infinity norm on the interval $[a,\ b]$, and $\bar{h} = \max\limits_i h_i$ is the maximum step size in X_n.

The following result claims the super-convergence of $\mathcal{Q}_m$, $m \geq 3$, at the break-points of X_n.

Proposition 7.2.9. *For all $i = 0, \ldots, n$, and for any function f in $C^{m+1}([a,b])$, there hold*

$$|\mathcal{Q}_m^{(k)} f(x_i) - f^{(k)}(x_i)| = \mathcal{O}\left(\bar{h}^{m+1-k}\right), \quad k = 0, 1, 2.$$

7.2.3 Various family of super-convergent quasi-interpolation operators

This section aims to define such quasi-interpolants of the form

$$\mathcal{Q}_m f := \sum_{i=0}^{n} \sum_{|\alpha|=2} \mu_{i,\alpha}^m(f)\ \mathcal{B}_{i,\alpha}(x). \tag{7.20}$$

where $\mu_{i,\alpha}^m$ is a linear functional such that

$$\mathcal{Q}_m f \in S_3^2\left(X_n^{\mathrm{ref}}\right) \quad \text{for all } f \in \mathbb{P}_m, \quad m \geq 3. \tag{7.21}$$

Differential quasi-interpolation operator

Let u, v, w be three points in $\mathbb{R}$. Consider a polynomial $p \in \mathbb{P}_m$, $m \geq 2$. By using (1.3), we have

$$\mathbf{B}[p](u[m-2], v[1], w[1]) = p(u) + \frac{1}{m}\left(D_{v-u}p(u) + D_{w-u}p(u)\right) + \frac{1}{m(m-1)} D^2_{(v-u)(w-u)}p(u).$$

From the functional defined as

$$\mathbf{N}[f](u[m-2], v[1], w[1]) = f(u) + \frac{1}{m}\left(D_{v-u}f(u) + D_{w-u}f(u)\right) + \frac{1}{m(m-1)} D^2_{(v-u)(w-u)}f(u)$$

we define linear functionals providing differential quasi-interpolation operator.

Theorem 7.2.10. *Define*

$$\mu_{i,\alpha}^m(f) = \mathbf{N}[f](x_i[m-2], Q_{i,1}[\alpha_1], Q_{i,2}[\alpha_2]). \tag{7.22}$$

Then, the operator $\mathcal{Q}_m$ defined by (7.20), satisfies (7.21).

Proof. It is enough to notice that

$$\mathbf{N}[p](x_i[m-2], Q_{i,1}[\alpha_1], Q_{i,2}[\alpha_2]) = \mathbf{B}[p](x_i[m-2], Q_{i,1}[\alpha_1], Q_{i,2}[\alpha_2]), \quad \text{for all} \quad p \in \mathbb{P}_m, \quad m \geq 3.$$

□

Quasi-interpolation based on point values

In order to construct a super-convergent discrete quasi-interpolation operator based on point values, it suffices to take $m+1$ distinct points in the support of $\mathcal{B}_{i,\alpha}$, $i=0,\ldots,n$, $\alpha=(\alpha_1,\,\alpha_2)$ $|\alpha|=2$.

Let $t^m_{i,\alpha,k}$, $k=0,\ldots,m$ be $m+1$ distinct points in $\mathbb{R}$. Then, there exist a Lagrange basis $\left\{L^m_{i,\alpha,0},\ldots,\,L^m_{i,\alpha,m}\right\}$ such that $L^m_{i,\alpha,k}\left(t^m_{i,\alpha,j}\right)=\delta_{k,j}$, $j,k=0,\ldots,m$, and $\delta_{k,j}$ stands for Kronecker's delta. The polynomial

$$\mathcal{I}_m\left(f\right):=\sum_{k=0}^{m} f\left(t^m_{i,\alpha,k}\right)L^m_{i,\alpha,k} \tag{7.23}$$

interpolates f at the points $t^m_{i,\alpha,k}$, $k=0,\ldots,m$. In the following theorem, we give an explicit formula of the coefficients $\mu^m_{i,\alpha}\left(f\right)$ in terms of $f\left(t^m_{i,\alpha,k}\right)$.

Theorem 7.2.11. *Consider,* $t^m_{i,(2,0),k}=\beta^m_{i,(2,0),k}Q_{i,1}+\left(1-\beta^m_{i,(2,0),k}\right)x_i$, $t^m_{i,(1,1),k}=\beta^m_{i,(1,1),k}Q_{i,1}+\left(1-\beta^m_{i,(1,1),k}\right)Q_{i,2}$, $t^m_{i,(0,2),k}=\beta^m_{i,(0,2),k}Q_{i,2}+\left(1-\beta^m_{i,(0,2),k}\right)x_i$, $i=1,\ldots,n$, $k=0,\ldots,m$. *Then, the quasi-interpolation operator* $\mathcal{Q}_m$ *defined by* (7.20) *with*

$$\mu^m_{i,\alpha}\left(f\right)=\sum_{k=0}^{m} q^m_{i,\alpha,k}\,f\left(t^m_{i,\alpha,k}\right) \tag{7.24}$$

satisfies (7.21)*, if and only if*

$$q^m_{i,(2,0),k}=\frac{1}{m}\frac{\sum_{\substack{s_1,s_2=0\\ s1\neq s2\neq k}}^{m}\left(1-\beta^m_{i,(2,0),s_1}\right)\left(1-\beta^m_{i,(2,0),s_2}\right)\prod_{\substack{n=0\\ n\neq s_1,s_2,k}}^{m}-\beta^m_{i,(2,0),n}}{\prod_{\substack{j=0\\ j\neq k}}^{m}\left(\beta^m_{i,(2,0),k}-\beta^m_{i,(2,0),j}\right)}$$

$$q^m_{i,(1,1),k}=\frac{1}{m(m-1)}\frac{\sum_{\substack{s_1,s_2=0\\ s1\neq s2\neq k}}^{m}\left(1-\beta^m_{i,(1,1),s_1}\right)-\beta^m_{i,(1,1),s_2}\prod_{\substack{n=0\\ n\neq s_1,s_2,k}}^{m}\left(\bar{\beta}_i-\beta^m_{i,(1,1),n}\right)}{\prod_{\substack{j=0\\ j\neq k}}^{m}\left(\beta^m_{i,(1,1),k}-\beta^m_{i,(1,1),j}\right)}$$

$$q^m_{i,(0,2),k}=\frac{1}{m}\frac{\sum_{\substack{s_1,s_2=0\\ s1\neq s2\neq k}}^{m}\left(1-\beta^m_{i,(0,2),s_1}\right)\left(1-\beta^m_{i,(0,2),s_2}\right)\prod_{\substack{n=0\\ n\neq s_1,s_2,k}}^{m}-\beta^m_{i,(0,2),n}}{\prod_{\substack{j=0\\ j\neq k}}^{m}\left(\beta^m_{i,(0,2),k}-\beta^m_{i,(0,2),j}\right)},$$

where, $x_i=\bar{\beta}_iQ_{i,1}+(1-\bar{\beta}_i)Q_{i,2}$.

Proof. According to (7.19), we have

$$\begin{aligned}\mu^m_{i,\alpha}\left(f\right)&=\mathbf{B}\left[\mathcal{I}_m\left(f\right)\right]\left(x_i[m-2],Q_{i,1}[\alpha_1],Q_{i,2}[\alpha_2]\right),\\ &=\sum_{k=0}^{m} f\left(t^m_{i,\alpha,k}\right)\mathbf{B}\left[L^m_{i,\alpha,k}\right]\left(x_i[m-2],Q_{i,1}[\alpha_1],Q_{i,2}[\alpha_2]\right).\end{aligned}$$

Then, $q^m_{i,\alpha,k}=\mathbf{B}\left[L^m_{i,\alpha,k}\right]\left(x_i[m-2],Q_{i,1}[\alpha_1],Q_{i,2}[\alpha_2]\right)$.

By using Proposition 1.3.1, we can get the values of $q^m_{i,\alpha,k}$, $k=0,\ldots,m$, and the proof is complete. ☐

In what follows, we provide an example of discrete quasi-interpolation operators based on evaluated points for a uniform partition.

$$\mu^3_{0,(2,0)}(f) = f(x_0),$$
$$\mu^3_{0,(1,1)}(f) = \frac{2}{9}f(h_0+x_0) + 2f\left(\frac{1}{3}(h_0+3x_0)\right) - f\left(\frac{1}{3}(2(h_0+x_0)+x_0)\right) - \frac{2}{9}f(x_0),$$
$$\mu^3_{0,(0,2)}(f) = -\frac{2}{9}f(h_0+x_0) + \frac{2}{3}f\left(\frac{1}{3}(h_0+3x_0)\right) + \frac{2}{3}f\left(\frac{1}{3}(2(h_0+x_0)+x_0)\right) - \frac{1}{9}f(x_0),$$

and

$$\mu^3_{i,(2,0)}(f) = \frac{4}{27}f(x_{i-1}) + \frac{47}{27}f(x_i) - \frac{32}{27}f\left(\frac{x_i+x_{i+1}}{2}\right) + \frac{8}{27}f(x_{i+1}),$$
$$\mu^3_{i,(1,1)}(f) = \frac{-2}{27}f(x_{i-1}) + \frac{31}{27}f(x_i) - \frac{2}{27}f(x_{i+1}),$$
$$\mu^3_{i,(0,2)}(f) = -\frac{1}{27}f(x_i) + \frac{32}{27}f\left(\frac{x_i+x_{i+1}}{2}\right) - \frac{4}{27}f(x_{i+1}).$$

Remark 7.2.12. *The coefficients of the functional $\mu^m_{n,\alpha}$ associated with the boundary knot x_n are symmetric to those associated with x_0.*

Discrete quasi-interpolation operator based on polarization

Polarization with constant coefficients can be used to obtain functions in the form of combination of discrete values (for more details see [91] and references therein). The polarization formula is given as follows,

$$\mathbf{B}[p](u_1,\ldots,u_m) = \frac{1}{m!}\sum_{\substack{S\subset\{1,\ldots,m\}\\ k=|S|}} (-1)^{m-k}\,k^m\,p\left(\frac{1}{k}\sum_{i\in S}u_i\right).$$

Let us consider the operator

$$\mathbf{M}[f](u_1,\ldots,u_m) = \frac{1}{m!}\sum_{\substack{S\subset\{1,\ldots,m\}\\ k=|S|}} (-1)^{m-k}\,k^m\,f\left(\frac{1}{k}\sum_{i\in S}u_i\right)$$

from Marsden's identity, we have the following result.

Theorem 7.2.13. *Let,*

$$\mu^m_{i,\alpha}(f) = \mathbf{M}[f](x_i[m-2],\,Q_{i,1}[\alpha_1],\,Q_{i,2}[\alpha_2]). \tag{7.25}$$

Then, the operator $\mathcal{Q}_m$ defined by (7.20) satisfies (7.21).

7.2.4 Numerical tests

This section provides some numerical results to illustrate the performance of the above quasi-interpolation operators. To this end, we will test its performance using the functions

$$f_1(x) = \frac{3}{4}e^{-2(9x-2)^2} - \frac{1}{5}e^{-(9x-7)^2-(9x-4)^2} + \frac{1}{2}e^{-(9x-7)^2-\frac{1}{4}(9x-3)^2} + \frac{3}{4}e^{\frac{1}{10}(-9x-1)-\frac{1}{49}(9x+1)^2},$$

$$f_2(x) = e^{-x}\sin(5\pi x),$$

and,

$$f_3(x) = \frac{1}{2}x\cos^4\left(4\left(x^2+x-1\right)\right)$$

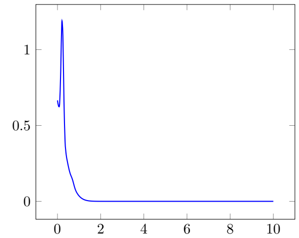

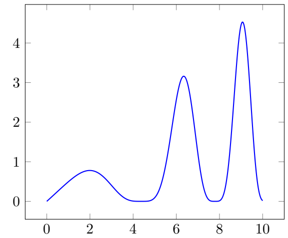

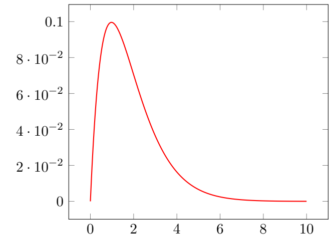

Figure 7.10: Plots of the tests functions: f_1 (left), f_2 (middle) and f_3 (right).

whose plots appear in Figure 7.10.

Let us consider the interval $I = [0,\ 1]$. The tests are carried out for a sequence of uniform mesh $\mathfrak{I}_n$ associated with the break-points ih, $i = 0, \ldots, n$, where $h = \frac{1}{n}$.

The quasi-interpolation error is estimated as

$$\mathcal{E}_{m,n} := \max_{0 \le \ell \le 200} |\mathcal{Q}_m f(x_\ell) - f(x_\ell)|, \quad m = 3, 4, 5, 6.$$

where x_ℓ, $\ell = 0, \ldots, 200$, are equally spaced points in $[0,\ 1]$. $\mathcal{E}_{df,m,n}$, $\mathcal{E}_{di,m,n}$, $\mathcal{E}_{dp,m,n}$ mark the estimated error $\mathcal{E}_{m,n}$ for the differential quasi-interpolant (7.22), the discrete quasi-interpolant (7.24) and the discrete quasi-interpolant based on polarization (7.25), respectively. The numerical convergence order (NCO) is given by the rate

$$NCO := \frac{\log\left(\frac{\mathcal{E}_{m,n_1}}{\mathcal{E}_{m,n_2}}\right)}{\log\left(\frac{n_2}{n_1}\right)}.$$

The estimated errors of differential quasi-interpolant (7.22) and NCOs for the functions f_1, f_2 and f_3 are shown in Table 7.2. They confirm the theoretical results. In Table 7.3, we illustrate

n	$\mathcal{E}_{df,3,n}(f_1)$	$\mathcal{E}_{df,3,n}(f_2)$	$\mathcal{E}_{df,3,n}(f_3)$	$NCO(f_1)$	$NCO(f_2)$	$NCO(f_3)$
10	3.5239×10^{-3}	1.2861×10^{-3}	5.5739×10^{-3}	$--$	$--$	$--$
20	2.8618×10^{-4}	9.5743×10^{-5}	4.0099×10^{-4}	3.6222	3.7477	3.7970
30	7.1933×10^{-5}	1.9565×10^{-5}	8.9648×10^{-5}	3.4056	3.9163	3.6946
40	2.3741×10^{-5}	6.2143×10^{-6}	3.2991×10^{-5}	3.8533	3.9866	3.4748
50	9.7510×10^{-6}	2.5611×10^{-6}	1.3853×10^{-5}	3.9876	3.9723	3.8884
60	5.0067×10^{-6}	1.2503×10^{-6}	6.6813×10^{-6}	3.6560	3.9325	3.9998
70	2.7104×10^{-6}	6.6895×10^{-7}	3.7777×10^{-6}	3.9809	4.05763	3.6989
80	1.6092×10^{-6}	3.9255×10^{-7}	2.1791×10^{-6}	3.9044	3.9919	4.1202
90	9.0493×10^{-7}	2.4106×10^{-7}	1.3219×10^{-6}	4.8874	4.1396	4.2438
100	6.6818×10^{-7}	1.6277×10^{-7}	9.2262×10^{-7}	2.8786	3.7273	3.4132

Table 7.2: Estimated errors of the differential Q.I. (7.22) for the functions f_1, f_2 and f_3 and NCOs with $n = 10\ell$, $\ell = 1, \ldots, 10$.

the estimated errors of discrete quasi-interpolant (7.24) and NCOs for the functions f_1, f_2 and f_3.

In Tables 7.4, 7.5 and 7.6, we list the resulting errors and NCOs for the approximation of the functions f_1, f_2 and f_3, respectively, by using the discrete spline quasi-interpolant based on polarization (7.25) for different values of m.

Tables 7.4, 7.5 and 7.6 show that the numerical convergence orders are in good agreement with the theoretical ones.

n	$\mathcal{E}_{di,3,n}(f_1)$	$\mathcal{E}_{di,3,n}(f_3)$	$\mathcal{E}_{di,3,n}(f_2)$	$NCO(f_1)$	$NCO(f_3)$	$NCO(f_2)$
10	1.8646×10^{-2}	2.9778×10^{-2}	5.2251×10^{-3}	$--$	$--$	$--$
20	1.1630×10^{-3}	1.9875×10^{-3}	3.2841×10^{-4}	4.0030	3.9052	3.9918
30	2.3050×10^{-4}	3.9273×10^{-4}	7.0841×10^{-5}	3.9916	3.9991	3.7828
40	8.5906×10^{-5}	1.2000×10^{-4}	2.0878×10^{-5}	3.4308	4.1211	4.2468
50	3.3864×10^{-5}	4.5507×10^{-5}	8.1204×10^{-6}	4.1717	4.3454	4.2319
60	1.7205×10^{-5}	2.4659×10^{-5}	4.1315×10^{-6}	3.7140	3.3605	3.7062
70	9.5539×10^{-6}	1.3593×10^{-5}	2.2698×10^{-6}	3.8160	3.8634	3.8856
80	5.3656×10^{-6}	7.3688×10^{-6}	1.3000×10^{-6}	4.3206	4.5859	4.1737
90	3.1927×10^{-6}	4.9837×10^{-6}	8.6994×10^{-7}	4.4074	3.3203	3.4104
100	1.4655×10^{-6}	2.0231×10^{-6}	3.4588×10^{-7}	7.3906	8.5565	8.7539

Table 7.3: Estimated errors of the discret Q.I. (7.24) for the functions f_1, f_2 and f_3 and NCOs with $n = 10\ell$, $\ell = 1, \ldots, 10$.

n	$\mathcal{E}_{dp,3,n}(f_1)$	$\mathcal{E}_{dp,4,n}(f_1)$	$\mathcal{E}_{dp,5,n}(f_1)$	$NCO\mathcal{E}_{dp,3,n}(f_1)$	$NCO\mathcal{E}_{dp,4,n}(f_1)$	$NCO\mathcal{E}_{dp,5,n}(f_1)$
10	4.2245×10^{-3}	6.3612×10^{-3}	1.9123×10^{-3}	$--$	$--$	$--$
20	3.6695×10^{-4}	1.4630×10^{-4}	5.1646×10^{-5}	3.2213	5.4423	5.2105
30	7.9143×10^{-5}	1.3716×10^{-5}	6.0072×10^{-6}	3.7832	5.8379	5.3061
40	2.5806×10^{-5}	2.4968×10^{-6}	1.1658×10^{-6}	3.8953	5.9216	5.6989
50	1.0717×10^{-5}	6.6135×10^{-7}	3.1758×10^{-7}	3.9380	5.9535	5.8280
60	5.2073×10^{-6}	2.2273×10^{-7}	1.0855×10^{-7}	3.9589	5.9692	5.8880
70	2.8234×10^{-6}	8.8626×10^{-8}	4.3575×10^{-8}	3.9708	5.9781	5.9210
80	1.6598×10^{-6}	3.9862×10^{-8}	1.9710×10^{-8}	3.9781	5.9836	5.9412
90	1.0383×10^{-6}	1.9692×10^{-8}	9.7747×10^{-9}	3.9830	5.9872	5.9545
100	6.8222×10^{-7}	1.0476×10^{-8}	5.2145×10^{-9}	3.9864	5.9898	5.9638

Table 7.4: Estimated errors of the discret Q.I. (7.25) for the functions f_1 and NCOs with $n = 10\ell$, $\ell = 1, \ldots, 10$, and $m = 3, 4, 5$.

n	$\mathcal{E}_{dp,3,n}(f_2)$	$\mathcal{E}_{dp,4,n}(f_2)$	$\mathcal{E}_{dp,5,n}(f_2)$	$NCO\mathcal{E}_{dp,3,n}(f_2)$	$NCO\mathcal{E}_{dp,4,n}(f_2)$	$NCO\mathcal{E}_{dp,5,n}(f_2)$
10	2.1886×10^{-3}	5.6590×10^{-4}	2.3397×10^{-4}	$--$	$--$	$--$
20	1.4931×10^{-4}	9.3265×10^{-6}	4.4871×10^{-6}	3.8735	5.9230	5.7043
30	2.9963×10^{-5}	8.2685×10^{-7}	4.0812×10^{-7}	3.9610	5.9758	5.9127
40	9.5327×10^{-6}	1.4766×10^{-7}	7.3529×10^{-8}	3.9809	5.9880	5.9575
50	3.9145×10^{-6}	3.8771×10^{-8}	1.9384×10^{-8}	3.9886	5.9929	5.9747
60	1.8904×10^{-6}	1.2995×10^{-8}	6.5114×10^{-9}	3.9924	5.9952	5.9832
70	1.0212×10^{-6}	5.1563×10^{-9}	2.5870×10^{-9}	3.9946	5.9966	5.9881
80	5.9895×10^{-7}	2.3149×10^{-9}	1.1624×10^{-9}	3.9959	5.9974	5.9911
90	3.7406×10^{-7}	1.1421×10^{-9}	5.7384×10^{-10}	3.9968	5.9980	5.9931
100	2.4548×10^{-7}	6.0708×10^{-10}	3.0514×10^{-10}	3.9975	5.9984	5.9945

Table 7.5: Estimated errors of the discret Q.I. (7.25) for the functions f_2 and NCOs with $n = 10\ell$, $\ell = 1, \ldots, 10$, and $m = 3, 4, 5$.

7.3 Conclusion

In this chapter, we have shown that the space of C^2 cubic splines can be defined on a partition endowed with a split that divides each interval into just two sub-intervals instead of three sub-intervals. This is carried out by providing a recipe. The reduced C^2 cubic space obtained in this paper have the same order of convergence as those spaces introduced in [82, 90]. Moreover,

n	$\mathcal{E}_{dp,3,n}(f_3)$	$\mathcal{E}_{dp,4,n}(f_3)$	$\mathcal{E}_{dp,5,n}(f_3)$	$NCO\mathcal{E}_{dp,3,n}(f_3)$	$NCO\mathcal{E}_{dp,4,n}(f_3)$	$NCO\mathcal{E}_{dp,5,n}(f_3)$
10	2.8071×10^{-3}	5.8048×10^{-3}	2.3020×10^{-3}	$--$	$--$	$--$
20	2.0400×10^{-4}	1.5420×10^{-4}	4.6572×10^{-5}	3.7824	5.2343	5.6272
30	4.4729×10^{-5}	1.4793×10^{-5}	6.1440×10^{-6}	3.7426	5.7812	4.9955
40	1.5111×10^{-5}	2.7143×10^{-6}	1.2327×10^{-6}	3.7722	5.8940	5.5833
50	6.3742×10^{-6}	7.2158×10^{-7}	3.4059×10^{-7}	3.8682	5.9372	5.7645
60	3.1227×10^{-6}	2.4349×10^{-7}	1.1728×10^{-7}	3.9136	5.9584	5.8473
70	1.7015×10^{-6}	9.7005×10^{-8}	4.7288×10^{-8}	3.9388	5.9703	5.8925
80	1.0035×10^{-6}	4.3664×10^{-8}	2.1450×10^{-8}	3.9544	5.9778	5.9201
90	6.2909×10^{-7}	2.1582×10^{-8}	1.0658×10^{-8}	3.9647	5.9827	5.9383
100	4.1397×10^{-7}	1.1486×10^{-8}	5.6935×10^{-9}	3.9718	5.9862	5.9508

Table 7.6: Estimated errors of the discret Q.I. (7.25) for the functions f_3 and NCOs with $n = 10\ell$, $\ell = 1, \ldots, 10$, and $m = 3, 4, 5$.

it has the same order of smoothness.

Also, we dealt with the space of C^2-continuous cubic splines defined on a partition endowed with a specific refinement. We have also constructed a B-spline basis, having the usual properties required for its use in CAGD, and developed a theory of control polynomials which is used to establish a Marsden identity, from which various families of super-convergent quasi-interpolation operators have been defined.

Conclusion and perspectives

At the end of this Ph.D. thesis, we should look both forward and backward. Indeed, some results have been obtained, but many questions remain. We start by outlining the contributions presented in this thesis and then briefly discuss possible future research lines.

Overview of the contributions

We review the principal outcomes of this thesis.

Full C^2 smoothness. We have characterized the geometry of Powell-Sabin triangulations that allows to define bivariate quartic splines of class C^2. We have proved that a C^2 spline space can be achieved in a general case, if the considered triangulation is divided by mixed refinement which involves both Powell-Sabin 6-split and modified Morgan-Scott 10-split.

Quasi-interpolantion. Families of quasi-interpolation operators yielding the optimal approximation power for both quartic and sextic over Powell-Sabin 6-split are derived. They are constructed with the help of Marsden's identities that are established from a more explicit version of the control polynomials introduced some years ago in the literature. Moreover, an algorithm is proposed to define the Powell–Sabin triangles with a small area and diameter needed to construct a normalized basis.

In general, it can be stated that the construction of quasi-interpolation by blossoming is not only elegant, but also very efficient, especially when the data to be approximated is randomly arranged. The blossom can also be used to develop quasi-interpolants with parameters that can be used to preserve the shape or simply to optimize the norms of the quasi-interpolants.

Gaussian rules on Powell-Sabin 6-split. It has been proved that any Gaussian quadrature formula exact on the space of quadratic polynomials defined on a triangle T endowed with a C-refinement integrates also the functions in the space of C^1 quadratic splines defined on T. This extends the existing results, where the inner split point Z had to lie on a very specific subset of the T. Now Z can be freely chosen inside T.

Explicit quasi-interpolation schemes on 6-split. Tow kinds of quasi-interpolation schemes are provided. Both kinds are expressed in Bernstein-Bézier form. They are generated by setting their B-ordinates to suitable combinations of the given data values, instead of being defined as linear combinations of a set of bivariate functions and they do not require derivative values. The first kind involves the values at the vertices and middle points of the original vertices, and the second one is restricted to use the values prescribed at the set of vertices. The provided schemes are of class C^1, and they yield the optimal approximation power.

Univariate case. Inspiring from bivariate Powell-Sabin case, we have provided:

- Stable bases consisting of non-negative compactly supported functions that form partitions of unity are defined through a geometrical approach for the family of super-spline spaces described above. General Marsden's identities are derived and used to define quasi-interpolating splines in those spaces.
- A recipe to achieve a space of C^2 cubic splines defined on a partition endowed with a split that divides each interval into just two sub-intervals instead of three sub-intervals.
- A novel normalized B-spline-like representation for C^2-continuous cubic spline space defined on an initial partition refined by inserting two new points inside each sub-interval. With the help of the control polynomial theory introduced herein, a Marsden identity is derived, from which several families of super-convergent quasi-interpolation operators are defined.

Future research suggestions

Some suggestions for further research that are not addressed in this thesis are outlined.

Reduced C^2 quartic splines on mixed macro-structure. It has been proved that under certain geometrical conditions regarding the triangle and edge split-points associated with an arbitrary triangulation of a polygonal domain Ω, the space of $C^2(\Omega)$ continuous quartic splines can be achieved on Powell-Sabin 6-split and a modified Morgan-Scott 10-split. Unfortunately, one single kind of refinement cannot be used when dealing with a general triangulation. Therefore, it will be desirable to give a geometrical construction of a B-spline-like basis for the space of quartic splines that can be defined over this sub-triangulation in order to get a normalized B-spline-like representation, whose coefficients will be expressed in terms of polar forms.

Application of explicit quasi-interpolation schemes defined on 6-split in dealing with Digital Elevation Models in engineering. In engineering, when dealing with a set of large data, in particular Digital Elevation Models, it will be better use explicit quasi-interpolation schemes. Namely, the spline schemes should be generated by setting their B-ordinates to suitable combinations of the given data values instead of constructing a set of appropriate basis functions.

Construction of explicit quasi-interpolation schemes defined on Clough-Tocher 3-split.

List of Figures

List of Tables

Bibliography

[1] I. J. Schoenberg, Contributions to the problem of approximation of equidistant data by analytic functions. Part A. on the problem of smoothing or graduation. A first class of analytic approximation formulae. Quarterly of Applied Mathematics, 4 (1946), 45–99.

[2] I. J. Schoenberg, Contributions to the problem of approximation of equidistant data by analytic functions. Part B. On the problem of osculatory interpolation. A second class of analytic approximation formulae, Quarterly of Applied Mathematics, 4 (1946), 112–141.

[3] C. De Boor, A Practical Guide to Splines, Applied Mathematical Sciences, Springer-Verlag, 27, 1978.

[4] M. J. Lai, L.L. Schumaker, Spline Functions on Triangulations, Cambridge University Press, Cambridge, 2007.

[5] C. Manni, Lower bounds on the dimension of bivariate spline spaces and generic triangulations. In T. Lyche and L.L. Schumaker, editors, Mathematical Methods in Computer Aided Geometric Design II, pages 401–412. Academic Press, 1992.

[6] L.L. Schumaker, Lower bounds for the dimension of spaces of piecewise polynomials in two variables. In W. Schempp and K. Zeller, editors, Multivariate Approximation Theory, pages 396–412. Brikhauser Verlag, 1979.

[7] L.L. Schumaker, Bounds on the dimension of spaces of multivariate piecewise polynomials. Rocky Mt. J. Math., 14 (1984), 251–264.

[8] D.J. Ripmeester, Upper bounds on the dimension of bivariate spline spaces and duality in the plane. In M. Dæhlen, T. Lyche, and L.L. Schumaker, editors, Mathematical Methods for Curves and Surfaces, pages 455–466. Vanderbilt University Press, 1995.

[9] P. Alfeld, L. L. Schumaker, The dimension of bivariate spline spaces of smoothness r for degree $geq4r + 1$, Constr. Approx. 3 (1) (1987) 189–197.

[10] P. Alfeld, L. L. Schumaker, On the dimension of bivariate spline spaces of smoothness r and degree $= 3r + 1$, Numer. Math. 57 (1) (1990) 651–661.

[11] D. Hong, Spaces of bivariate spline functions over triangulation, Approx. Theory Appl., 7 (1991), 56–75.

[12] C. Manni, On the dimension of bivariate spline spaces on generalized quasi-cross-cut partitions, J. Approx. Theory, 69 (1992), 141–155.

[13] G. Farin, Dimensions of spline spaces over un-constricted triangulations. J. Comput. Appl. Math., 192 (2006), 320–327.

[14] A. Ženíšek, A general theorem on triangular finite $C^{(m)}$-elements, Revue française d'automatique, informatique, recherche opérationnelle. Analyse numérique 8(R2) (1974) 119–127.

[15] R.W. Clough, J.L. Tocher, Finite element stiffness matrices for analysis of plates in bending, in: Proceedings of the Conference on Matrix Methods in Structural Mechanics, Wright-Patterson A. F. B., OH, 1965.

[16] P. Percell, On cubic and quartic Clough-Tocher finite elements, SIAM J Numer Anal 13(1) (1976) 100–103.

[17] M. Bartoň, J. Kosinka, Gaussian quadrature for C^1 cubic Clough-Tocher macro-triangles, J Comput Appl Math 351 (2019) 6–13.

[18] M. Powell, M. Sabin, Piecewise quadratic approximations on triangles, ACM Trans. Math. Softw. 3 (1977) 316–325.

[19] A. Lamnii, M. Lamnii, H. Mraoui, A normalized basis for condensed C^1 Powell-Sabin-12 splines, Comput. Aided Geom. Design 34 (2015) 5–20.

[20] A. Worsey, B. Piper, A trivariate Powell-Sabin interpolant, Comput. Aided Geom. Design, 5 (1988), 177–186.

[21] C. Bangert, H. Prautzsch, A geometric criterion for the convexity of Powell-Sabin interpolants and its multivariate generalization, Comput. Aided Geom. Design, 16 (1999), 529–538.

[22] T. Sorokina, A. Worsey, A multivariate Powell-Sabin interpolant, Adv. Comput. Math, 29 (2008), 71–89.

[23] P. Dierckx, On calculating normalized Powell-Sabin B-splines, Comput. Aided Geom. Design 15 (1997) 61–78.

[24] M. Lamnii, H. Mraoui, A. Tijini, A. Zidna, A normalized basis for C^1 cubic super spline space on Powell-Sabin triangulation, Math. and Comput. in Simul. 99 (2014) 108–124.

[25] H. Speleers, A normalized basis for quintic Powell-Sabin splines, Comput. Aided Geom. Design 27 (2010) 438–457.

[26] H. Speleers, Construction of normalized B-splines for a family of smooth spline spaces over Powell-Sabin triangulations, Constr. Approx. 37 (2013) 41–72.

[27] H. Speleers, A new B-spline representation for cubic splines over Powell-Sabin triangulations, Comput. Aided Geom. Design 37 (2015) 42–56.

[28] J. Grošelj, M. Krajnc, C^1 cubic splines on Powell-Sabin triangulations, Appl. Math. and Comput. 272 (2016) 114–126.

[29] J. Grošelj, H. Speleers, Construction and analysis of cubic Powell-Sabin B-splines, Comput. Aided Geom. Design 57 (2017) 1–22.

[30] M. J. Lai, On C^2 quintic spline functions over triangulations of Powell–Sabin's type, J. Comput. Appl. Math. 73 (1996) 135–155.

[31] M. Lamnii, H. Mraoui, A. Tijini, Construction of quintic Powell-Sabin spline quasi-interpolants based on blossoming, Journal of Comput. and Appl. Math. 250 (2013) 190–209.

[32] J. Grošelj, M. Krajnc, Quartic splines on Powell-Sabin triangulations, Comput. Aided Geom. Design 49 (2016) 1–16.

[33] M. Lamnii, H. Mraoui, A. Tijini, Raising the approximation order of multivariate quasi-interpolants, BIT Numer. Math. 54 (2014) 749–761.

[34] C. Manni, P. Sablonnière, Quadratic spline quasi-interpolants on Powell-Sabin partitions, Adv. Comput. Math. 26 (2007) 283–304.

[35] D. Sbibih, A. Serghini, A. Tijini, Polar forms and quadratic spline quasi-interpolants on Powell Sabin partitions, Appl. Numer. Math. 59 (2009) 938–958.

[36] H. Speleers, A family of smooth quasi-interpolants defined over Powell–Sabin triangulations, Constr. Approx. 41, 297–324 (2015)

[37] C. Allouch, D. Sbibih, P. Sablonniere, A collocation method for the numerical solution of a two dimensional integral equation using a quadratic spline quasi-interpolant, Numer. Algorithms, 62 (2013), 445–468.

[38] D. Barrera, F. El Mokhtari, D. Sbibih, Two methods based on bivariate spline quasi-interpolants for solving Fredholm integral equations, Appl. Numer. Math., 127 (2018), 78–94.

[39] D. Jinyuan, Quadrature formulas of quasi-interpolation type for singular integrals with Hilbert kernel, Approx. Theory, 93 (1998), 231–257.

[40] S. Eddargani, A. Lamnii, M. Lamnii, D. Sbibih, A. Zidna, Algebraic hyperbolic spline quasi-interpolants and applications, Journal of Computational and Applied Mathematics, 347 (2019), 196–209.

[41] L. Ramshaw, Blossoming: a connect-the-dots approach to splines, Tech. Rep. 19, Digital Systems Research Center (1987).

[42] J. Grošelj, A normalized representation of super splines of arbitrary degree on Powell-Sabin triangles, BIT Numer Math 56 (2016) 1257–1280.

[43] H. Speleers, C. Manni, F. Pelosi, M. L. Sampoli, Isogeometric analysis with Powell–Sabin splines for advection–diffusion–reaction problems, Comput. Methods Appl. Mech. Engrg. 221–222 (2012) 132–148.

[44] P. C. Hammer and A. H. Stroud, Numerical integration over simplexes. Mathematical tables and other aids to computation. 10(55):137-139, 1956.

[45] M. Bartoň, J. Kosinka, On numerical quadrature for $\mathcal{C}^1$ quadratic Powell-Sabin 6-split macro-triangles, Journal of Computational and Applied Mathematics 349 (2019) 239–250.

[46] W. Boehm, A. Müller, On de Casteljau's algorithm, Comput. Aided Geom. Design, 16 (1999), 587–605.

[47] H. Seidel, An introduction to polar forms, IEEE Comput. Graph. Appl. 13 (1993), 38–46.

[48] P. Dierckx J. Maes, E. Vanraes and A. Bultheel, On the stability of normalized powell-sabin b-splines, J. Comput. Appl. Math., 170 (2004), 181–196.

[49] K. C. Chung, T. H. Yao, On a lattices admitting unique Lagrange interpolation, SIAM J. Numer. Math. Anal, 14 (1977), 735–743.

[50] C. Manni, P. Sablonnière, Piecewise quadratic approximations on triangles, ACM Trans. Math. Softw, 3 (1977), 316–325.

[51] F. Franke, Scattered data interpolation: tests of some methods, Math. Comp, 38 (1982), 181–200.

[52] G. M. Nielson, A first order blending method for triangles based upon cubic interpolation, Int. J. Numer. Meth. Engng, 15 (1978), 308–318.

[53] H. Speleers, A normalized basis for quintic Powell-Sabin splines, Comput Aided Geom D, 27 (2010) 438–457.

[54] P. Percell, On cubic and quartic Clough-Tocher finite elements, SIAM J Numer Anal 13(1) (1976) 100–103.

[55] M. Lamnii, H. Mraoui, A. Tijini, A. Zidna, A normalized basis for C^1 cubic super spline space on Powell-Sabin triangulations, Math Comput Simulat 99 (2015) 108–124.

[56] S. K. Chen, H. W. Liu, A bivariate C^1 cubic super spline space on Powell-Sabin triangulation, Comput Math Appl 56 (2008) 1395–1401.

[57] D. Sbibih, A. Serghini, A. Tijini, C^1 quadratic and C^2 quartic macro-elements on a modified Morgan-Scott triangulation, Mediterr J Math 10 (2013) 1273–1292.

[58] J. Grošelj, M. Krajnc, Interpolation with C^2 quartic macro-elements based on 10-splits, J Comput Appl Math, 362 (2019) 143–160.

[59] J. Grošelj, M. Knez, A B-spline basis for C^1 quadratic splines on triangulations with a 10-split, J Comput Appl Math, 343, (2018), Pages 413–427.

[60] Remogna, S. Bivariate C^2 cubic spline quasi-interpolants on uniform Powell-Sabin triangulations of a rectangular domain. *Advances in Computational Mathematics.* **2012**, *36*, 39–65.

[61] Speleers, H.; Dierckx, P.; Vandewalle, S. Powell-Sabin splines with boundary conditions for polygonal and non-polygonal domains, J. Comput. Appl. Math., 206(1), (2007), 55–72.

[62] Vanraes, E.; Dierckx, P.; Bultheel, A. *On the choice of the PS-triangles. Technical Report 353, Dept. of Computer Science.* K.U. Leuven, 2003.

[63] B. Grünbaum, G. C. Shephard, Ceva, Menelaus and the Area Principle, Mathematics Magazine 68(4) (1995) 254–268. doi:10.2307/2690569

[64] J. B. Hogendijk, Al-Mutaman ibn Hūd, 11th century king of Saragossa and brilliant mathematician, Historia Mathematica 22 (1995) 1–18.

[65] C. Micchelli, The fundamental theorem of algebra for mono-splines with multiplicities, in: Lineare Operatoren und Approximation, 1972, pp. 419–430.

[66] C.A. Micchelli, A. Pinkus, Moment theory for weak Chebyshev systems with applications to mono-splines, quadrature formulae and best one-sided l^1 approximation by spline functions with fixed knots, SIAM J. Math. Anal. 8 (1977) 206–230.

[67] A. H. Stroud, Approximate calculation of multiple integrals. Prentice-Hall, 1971.

[68] P. C. Hammer and A. H. Stroud, Numerical integration over simplexes. Mathematical tables and other aids to computation. 10(55):137-139, 1956.

[69] G. Nürnberger, C. Rössl, H.-P. Seidel, F. Zeilfelder. Quasi-Interpolation by quadratic piecewise polynomials in three variables, J. Computer Aided Geometric Design 22 (2005) 221–249.

[70] C. Rössl, F. Zeilfelder, G. Nürnberger, H. P. Seidel, Reconstruction of volume data with quadratic super splines. In: van Wijk, J., Moorhead, R., Turk, G. (Eds.), Transactions on Visualization and Computer Graphics. IEEE Computer Society, (2004), pp. 397–409.

[71] T. Sorokina, F. Zeilfelder, Optimal quasi-interpolation by quadratic C^1 splines on four-directional meshes. In: Chui, C., et al. (Eds.), Approximation Theory, vol. XI. Gatlinburg 2004. Nashboro Press, Brentwood, TN, (2005), pp. 423–438.

[72] T. Sorokina, F. Zeilfelder, Local Quasi-Interpolation by cubic C^1 splines on type-6 tetrahedral partitions, IMA J. Numerical Analysis 27 (2007) 74–101.

[73] T. Sorokina, F. Zeilfelder, An explicit quasi-interpolation scheme based on C^1 quartic splines on type-1 triangulations, Computer Aided Geometric Design 25 (2008) 1–13.

[74] T. Sorokina, F. Zeilfelder, Optimal quasi-interpolation by quadratic C^1 splines on four-directional meshes. In: C. Chui et al. (Eds.), Approximation Theory, vol. XI, Gatlinburg 2004, Nashboro Press, Brentwood, 2005, pp. 423–438.

[75] D. Barrera, C. Dagnino, M.J. Ibáñez, S. Remogna, Quasi-interpolation by C^1 quartic splines on type-1 triangulations, J. of Comput. and Appl. Maths. 349 (2019) 225–238.

[76] D. Barrera, C. Dagnino, M.J. Ibáñez, S. Remogna, Point and differential C^1 quasi-interpolation on three direction meshes, J. of Comput. and Appl. Maths. 354 (2019) 373–389.

[77] D. Barrera, C. Conti, C. Dagnino, M. J. Ibáñez, S. Remogna, C^1-Quartic Butterfly-spline interpolation on type-1 triangulations. In: G. E. Fasshauer, M. Neamtu, L. L. Schumaker (Eds.), Approximation Theory XVI, Nashville, TN, USA, May 19–22, 2019. Springer Proceedings in Mathematics & Statistics, vol. 336, 2021, pp. 11–26.

[78] M. S. Mummy, Hermite interpolation with B-splines, Comput. Aided Geom. Design 6(2) (1989) 177–179.

[79] H.-P. Seidel, On Hermite interpolation with B-splines, Comput. Aided Geom. Design 8(6) (1991) 439–441.

[80] H.-P. Seidel, Polar forms for geometrically continuous spline curves of arbitrary degree, ACM Trans. Graph. 12(1) (1993) 1–34.

[81] L.L. Schumaker, On shape preserving quadratic spline interpolation, SIAM J Numer Anal 20(4) (1983) 854–864.

[82] A. Lamnii, M. Lamnii, F. Oumellal, Computation of Hermite interpolation in terms of B-spline basis using polar forms, Mathematics and Computers in Simulation 134 (2017) 17–27.

[83] A. M. Bica, Fitting data using optimal Hermite type cubic interpolating splines, Applied Mathematics Letters 25 (2012) 2047–2051.

[84] X. Han, X. Guo, Cubic Hermite interpolation with minimal derivative oscillation, Journal of Computational and Applied Mathematics 331 (2018) 82–87.

[85] H. Speleers, Multivariate normalized Powell-Sabin B-splines and quasi-interpolants, Computer Aided Geometric Design 30 (2013) 2–19.

[86] J.M. Carnicer, T.N.T. Goodman, J.M. Peña, Convexity preserving scattered data interpolation using Powell-Sabin elements, Computer Aided Geometric Design 26 (2009) 779–796.

[87] L. Ramshaw, Blossoms are polar forms, Computer Aided Geometric Design 4 (1989) 323–358.

[88] P. Sablonnière, A quadrature formula associated with a univariate spline quasi-interpolant, BIT Numerical Mathematics 47 (2007) 825–837.

[89] W. Dahmen, T.N.T. Goodman, C.A. Micchelli, Compactly supported fundamental functions for spline interpolation. Numer. Math. 52 (1988) 639–664.

[90] A. Rahouti, A. Serghini, A. Tijini, Construction of superconvergent quasi-interpolants using new normalized C^2 cubic B-splines, Mathematics and Computers in Simulation 178 (2020) 603–624.

[91] D. Barrera, S. Eddargani, A. Lamnii, A novel B-spline basis for a family of many knot spline spaces and its application to quasi-interpolation, Journal of Comput. and Appl. Math., https://doi.org/10.1016/j.cam.2021.113761.

[92] A. Boujraf · D. Sbibih · M. Tahrichi · A. Tijini, A superconvergent cubic spline quasi-interpolant and application, Afr. Mat. (2015) 26:1531–1547.

[93] A. Boujraf, M. Tahrichi, A. Tijini, C^1 Super-convergent quasi-interpolation based on polar forms, Mathematics and Computers in Simulation 118 (2015) 102–115.

[94] C. Manni, On shape preserving C^2 Hermite interpolation, BIT 41 (1) (2001) 127–148.

[95] K. Strom, Splines, Polynomials and Polar Forms, Vol. 165 de Research Report, Department of Informatics, University of Oslo, February 1992.

[96] D. Sbibih, A. Serghini, A. Tijini, A. Zidna, Superconvergent C^1 cubic spline quasi-interpolants on Powell-Sabin partitions, BIT Numer Math (2015) 55, 797–821.

[97] L.L. Schumaker, On shape preserving quadratic spline interpolation, SIAM J Numer Anal 20(4) (1983) 854–864.

[98] S. K. Chen, H. W. Liu, A bivariate C^1 cubic super spline space on Powell-Sabin triangulation, Comp. and Math. with Appl 56 (2008) 1395–1401